



State of Wildfires 2023-24

Authors:

Matthew W. Jones^{1,*}, Douglas I. Kelley^{2,*}, Chantelle A. Burton^{3,*}, Francesca Di Giuseppe^{4,*},
Maria Lucia F. Barbosa^{5,6}, Esther Brambleby¹, Andrew J. Hartley³, Anna Lombardi⁷, Guilherme
Mataveli^{8,1}, Joe R. McNorton⁴, Fiona R. Spuler⁹, Jakob B. Wessel^{10,11}, John T. Abatzoglou¹²,
Liana O. Anderson¹³, Niels Andela¹⁴, Sally Archibald¹⁵, Dolores Armenteras¹⁶, Eleanor Burke³,
Rachel Carmenta¹⁷, Emilio Chuvieco¹⁸, Hamish Clarke¹⁹, Stefan H. Doerr²⁰, Paulo M.
Fernandes²¹, Louis Giglio²², Douglas S. Hamilton²³, Stijn Hantson²⁴, Sarah Harris²⁵, Piyush
Jain²⁶, Crystal A. Kolden²⁷, Tiina Kurvits²⁸, Seppe Lampe²⁹, Sarah Meier³⁰, Stacey New³, Mark
Parrington³¹, Morgane M. G. Perron³², Yuquan Qu^{33,34}, Natasha S. Ribeiro³⁵, Bambang H.
Saharjo³⁶, Jesus San-Miguel-Ayanz³⁷, Jacquelyn K. Shuman³⁸, Veerachai Tanpipat³⁹, Guido
R. van der Werf⁴⁰, Sander Veraverbeke^{33,1}, Gavriil Xanthopoulos⁴¹

Institutions:

1. Tyndall Centre for Climate Change Research, School of Environmental Sciences, University of East Anglia, Norwich Research Park, Norwich, UK, NR4 7TJ
2. Hydro-climate risks, UK Centre for Ecology & Hydrology, Wallingford OX10 8BB, U.K.
3. Hadley Centre, Met Office, Fitzroy Road, Exeter, UK, EX1 3PB
4. Earth System Modelling Section, Forecast Department, European Centre for Medium-range Weather Forecast, Shinfield Park, Reading RG29AX, United Kingdom
5. Department of Remote Sensing, National Institute for Space Research, Avenida dos Astronautas, 1758. Jd. Granja - São José dos Campos - São Paulo, Brazil , 12227-010
6. Natural Sciences Center, Federal University of São Carlos, Rodovia Lauri Simões de Barros, km 12 - SP-189 - Aracaçu, Buri - São Paulo, Brazil, 18290-000
7. Climate Intelligence, Research Department, European Centre for Medium-range Weather Forecast, Shinfield Road, Reading, UK, RG29AX
8. Earth Observation and Geoinformatics Division, National Institute for Space Research, Avenida dos Astronautas, 1758. Jd. Granja - São José dos Campos - São Paulo, Brazil , 12227-010
9. Department of Meteorology, University of Reading, University of Reading, Earley Gate, Whiteknights Rd, Reading RG6 6ET
10. Department of Mathematics and Statistics, University of Exeter, Harrison Building, University of Exeter, North Park Road, Exeter, UK
11. The Alan Turing Institute, British Library, 96 Euston Road, London, UK
12. School of Engineering, University of California, Merced, 5200 N Lake Rd, Merced, CA, 95343, USA
13. Cemaden/MCTI, Estrada Doutor Altino Bondensan, 500 - Distrito de Eugênio de Melo, São José dos Campos - São Paulo, Brazil
14. BeZero Carbon, 25 Christopher Street, London, UK, EC2A 2BS
15. School of Animal Plant and Environmental Sciences, University of Witwatersrand Johannesburg, University Corner, Braamfontein, Johannesburg
16. Landscape Ecology and Ecosystem Modelling Group, Faculty of Sciences, Department of Biology, Universidad Nacional de Colombia, Cra. 30 # 45-03, Bogotá D.C., CP 111321, Colombia
17. Tyndall Centre for Climate Change Research, School of Global Development, University of East Anglia, Norwich Research Park, Norwich, UK, NR4 7TJ
18. Department of Geology, Geography and the Environment, Universidad de Alcalá, Colegios, 2 - 28801 Alcalá de Henares
19. FLARE Wildfire Research, School of Agriculture, Food and Ecosystem Sciences, University of Melbourne, Grattan St, Parkville, Australia, 3010
20. Centre for Wildfire Research, Swansea University , Singleton Park Swansea SA2 8PP Wales, UK
21. ForestWISE—Collaborative Laboratory for Integrated Forest & Fire Management, Centre for the Research and Technology of Agro-Environmental and Biological Sciences, Universidade de Trás-os-Montes e Alto Douro, Quinta de Prados, Vila Real, Portugal, 5000-801
22. Department of Geographical Sciences, University of Maryland, College Park, MD 20742
23. Marine, Earth and Atmospheric Science , North Carolina State University, Raleigh, North Carolina, USA, 27695
24. Program in Earth System Sciences, Faculty of Natural Sciences, Universidad del Rosario, Bogotá, Colombia



- 59 25. Fire Risk, Research and Community Preparedness, Country Fire Authority, Burwood East, Victoria, Australia
60 26. Northern Forestry Centre, Canadian Forest Service, Natural Resources Canada, 5320 122 St NW,
61 Edmonton, AB T6H 3S5, Canada
62 27. Wildfire Resilience Center, School of Engineering, University of California, Merced, 5200 N Lake Rd, Merced,
63 CA, 95343, USA
64 28. GRID-Arendal, P.O Box 183, N-4802, Arendal, NORWAY
65 29. Department of Water and Climate, Vrije Universiteit Brussel, Pleinlaan 2, 1050 Brussel, Belgium
66 30. Land, Environment, Economics and Policy Institute, Department of Economics, University of Exeter, Rennes
67 Drive, Exeter, United Kingdom, EX4 4ST
68 31. Atmospheric Composition Section, Research Department, European Centre for Medium-range Weather
69 Forecast, Robert-Schuman-Platz 3, 53175 Bonn, Germany
70 32. UMR 6539 CNRS/IRD/Ifremer/LEMAR, Institut Universitaire Européen de la Mer, University of Brest, F-29280
71 Plouzané, France
72 33. Department of Earth Sciences, Faculty of Science, Vrije Universiteit Amsterdam, De Boelelaan 1105, 1081
73 HV Amsterdam, Netherlands
74 34. Institute of Bio- and Geosciences: Agrosphere (IBG-3), Forschungszentrum Jülich, Wilhelm-Johnen-Straße,
75 52428 Jülich, Germany
76 35. Faculty of Agronomy and Forest Engineering, Eduardo Mondlane University, 3453 Avenida Julius Nyerere,
77 Maputo, Mozambique
78 36. Faculty of Forestry, Bogor Agricultural University, Kampus Ipb Darmaga, Bogor
79 37. European Commission Joint Research Center, European Commission, Rue du Champ de Mars 21, 1050
80 Brussels, Belgium
81 38. NASA Ames Research Center, PO Box 1 Moffett Field, CA 94035-1000
82 39. Upper ASEAN Wildland Fire Special Research Unit (WFSRU), Forestry Research Center, Faculty of Forestry,
83 Kasetsart University, 5th Floor, 72nd Anniversary of Faculty Forestry Building
84 40. Wageningen University, Droevendaalsesteeg 3, 6708PB Wageningen
85 41. Forest Fire Laboratory, Institute of Mediterranean Forest Ecosystems, Hellenic Agricultural Organization
86 (DIMITRA), Terma Alkmanos, Ilisia, 11528, Athens, Greece

87
88 ★ These authors contributed equally to this work.

89
90 Correspondence to:
91 matthew.w.jones@uea.ac.uk
92 doukel@ceh.ac.uk
93 chantelle.burton@metoffice.gov.uk
94 Francesca.DiGiuseppe@ecmwf.int
95

96 **Key words:** Wildfire, Extreme Fire, Attribution, Climate Change

97

98 Abstract

99

100 Climate change is increasing the frequency and intensity of wildfires globally, with significant
101 impacts on society and the environment. However, our understanding of the global distribution
102 of extreme fires remains skewed, primarily influenced by media coverage and regional
103 research concentration. This inaugural State of Wildfires report systematically analyses fire
104 activity worldwide, identifying extreme events from the March 2023-February 2024 fire season.
105 We assess the causes, predictability, and attribution of these events to climate change and
106 land use, and forecast future risks under different climate scenarios. During the 2023-24 fire
107 season, 3.9 million km² burned globally, slightly below the average of previous seasons, but
108 fire carbon (C) emissions were 16% above average, totaling 2.4 Pg C. This was driven by
109 record emissions in Canadian boreal forests (over 9 times the average) and dampened by
110 reduced activity in African savannahs. Notable events included record-breaking wildfire extent
111 and emissions in Canada, the largest recorded wildfire in the European Union (Greece),
112 drought-driven fires in western Amazonia and northern parts of South America, and deadly
113 fires in Hawai'i (100 deaths) and Chile (131 deaths). Over 232,000 people were evacuated in
114 Canada alone, highlighting the severity of human impact. Our analyses revealed that multiple
115 drivers were needed to cause areas of extreme fire activity. In Canada and Greece a



116 combination of high fire weather and an abundance of dry fuels increased the probability of
117 fires by 4.5-fold and 1.9-4.1-fold, respectively, whereas fuel load and direct human
118 suppression often modulated areas with anomalous burned area. The fire season in Canada
119 was predictable three months in advance based on the fire weather index, whereas events in
120 Greece and Amazonia had shorter predictability horizons. Formal attribution analyses
121 indicated that the probability of extreme events has increased significantly due to
122 anthropogenic climate change, with a 2.9-3.6-fold increase in likelihood of high fire weather in
123 Canada and a 20.0-28.5-fold increase in Amazonia. By the end of the century, events of similar
124 magnitude are projected to occur 2.22-9.58 times more frequently in Canada under high
125 emission scenarios. Without mitigation, regions like Western Amazonia could see up to a 2.9-
126 fold increase in extreme fire events. For the 2024-25 fire season, seasonal forecasts highlight
127 moderate positive anomalies in fire weather for parts of western Canada and South America,
128 but no clear signal for extreme anomalies is present in the forecast. This report represents our
129 first annual effort to catalogue extreme wildfire events, explain their occurrence, and predict
130 future risks. By consolidating state-of-the-art wildfire science and delivering key insights
131 relevant to policymakers, disaster management services, firefighting agencies, and land
132 managers, we aim to enhance society's resilience to wildfires and promote advances in
133 preparedness, mitigation, and adaptation.
134

135 **Short Summary**

136
137 This inaugural State of Wildfires report catalogues extreme fires of the 2023-24 fire season.
138 For key events, we analyse their predictability and drivers and attribute them to climate change
139 and land use. We provide a seasonal outlook and decadal projections. Key anomalies
140 occurred in Canada, Greece, and western Amazonia, with other high-impact events
141 catalogued worldwide. Climate change significantly increased the likelihood of extreme fires,
142 and mitigation is required to lessen future risk.

143 **1 Introduction**

144

145 **1.1 Background**

146

147 The potential for wildfires is growing under climate change, with increases in the frequency
148 and intensity of drought and periods of fire-favourable weather driving reductions in vegetation
149 (fuel) moisture and priming landscapes to burn more regularly, severely, and intensely (Jones
150 et al., 2022; UNEP, 2022a; Abatzoglou et al., 2019). Additionally, human activities and land
151 use change can contribute to or exacerbate the risk of extreme fires, especially in tropical
152 forests where people are the primary cause of ignition and forest degradation (Lapola et al.,
153 2023). Recent years have been marked by a series of extreme wildfire events spanning the
154 globe, with record levels of burned area (BA) occurring in the 2019-2020 Australian "Black
155 Summer" bushfires (Abram et al., 2021) and a series of high-ranking wildfire seasons
156 occurring in quick succession in the western US (2020 and 2021; Higuera & Abatzoglou,
157 2020), Siberia (2020 and 2021; Zheng et al., 2023), Europe (2022; European Commission
158 Joint Research Centre, 2023) and South America (2019, 2020; Kelley et al., 2021; Ferreira
159 Barbosa et al., 2022; Silveira et al., 2020). The 2023-24 fire season was marked by
160 unprecedented wildfire extent and emissions in Canada, deadly fast-moving fires in Hawaii
161 and Chile, the largest individual wildfires on record in the European Union and Canada,
162 widespread fires in northwestern South America including parts of Amazonia such as Brazil,
163 Bolivia, Colombia, and Venezuela (Mataveli et al., 2024; Kolden et al., 2024; European
164 Commission EU Science Hub, 2023).

165

166 The prominence of recent extreme wildfires and wildfire seasons notably contrasts with overall
167 trends in the area burned by fires globally. Due mostly to a reduction in the global savannahs



168 tied to landscape fragmentation and changing rainfall patterns, global BA has fallen since the
169 beginning of this century by around one-quarter (Andela et al., 2017; Jones et al., 2022; Chen
170 et al., 2024). Critically, this decline in fire extent masks major shifts in the distribution of fires
171 globally, with regions such as eastern Siberia and the western US and Canada experiencing
172 a more than 40% increase in BA since 2000 (Jones et al., 2022) and regions such as southeast
173 Australia also showing significant increases over longer periods (Canadell et al., 2021).
174 Likewise, there have been shifts in the global distribution of BA and fire carbon (C) emissions
175 from non-forests to forests globally and from the tropics to the extratropics (Kelley et al., 2019).
176 Hence, focussing on global aggregated BA extent underplays the scale and magnitude of
177 changes in wildfire activity and impact on regional levels. An increase in forest and peatland
178 burning is particularly concerning due to the rich ecosystem services that these regions
179 provide, including C storage and biodiversity (UNEP, 2022b). The intensification of fire
180 regimes in environments that are less fire-adapted is significant, as these ecosystems are
181 expected to be least resilient to such changes (Grau-Andrés et al., 2024).

182
183 The extreme wildfire events of recent years have significantly impacted society and
184 ecosystems across the globe. Since 1990, wildfire disasters have directly killed or injured at
185 least ~18,000 people, a conservative measure based on incomplete records and reporting
186 biased to the global Northern countries (updated from Jones et al., 2022; Centre for Research
187 on the Epidemiology of Disasters, 2024). In 2023, 232,000 people were evacuated due to
188 wildfires in Canada alone (Jain et al., 2024; Kolden et al., 2024). Also since 1990, fires are
189 estimated to have caused on the order of 10 million premature deaths globally through
190 degraded air quality (Johnston et al., 2012). Degraded air quality related to fires is experienced
191 most strongly in the tropics (Pai et al., 2022) and often disproportionately affects traditional
192 communities with poor public services or means of protection (Carmenta et al., 2021). Yet,
193 images of North America, including the infamous Wall Street, blanketed in smoke during the
194 2023 fire season highlight the global nature of this problem.

195
196 As anthropogenic emissions of CO₂ remain persistently high, the world's natural C sinks in
197 forests, peatlands and other ecosystems are increasingly pivotal to moderating increases in
198 atmospheric CO₂ concentration and are often relied upon for delivering national plans for
199 reaching Net Zero (Smith et al., 2023) and offering sites for nature based solutions (NBS). Yet,
200 massive wildfire emissions from boreal forests and soils in Siberia and Canada across the
201 years 2020, 2021, and 2023 amount to over 1 billion tonnes of C, a gross flux comparable in
202 magnitude to annual CO₂ emissions from fossil fuel combustion in India, the EU27 or the USA
203 (Friedlingstein et al., 2023; Zheng et al., 2023). Ecosystem function is also impacted by
204 extreme wildfires through widespread mortality of forest stands that undermine the
205 regenerative capacity of forests (Nolan et al., 2021a) and the habitats of many endemic
206 species being degraded in biodiversity hotspots (Ward et al., 2020). Not only are these
207 emissions high, but they may represent a change in the fire-C cycle from sink to source,
208 undermining assumptions about post-fire regrowth offsetting fire emissions. The lands and
209 territories of traditional communities and Indigenous Peoples are degraded and transformed
210 through wildfires, raising climate justice issues (Garnett et al., 2018; Barlow et al., 2018;
211 Lapola et al., 2023). Further, conflating distinct fire types has also stigmatised *intentional*
212 small-scale intergenerational managed fire use and led to prohibitive fire governance that
213 affects local communities (Carmenta et al., 2021; Barlow et al., 2020).

214
215 Mitigating and adapting to increases in wildfire potential are growing priorities of policymakers
216 and involve coordination with many other stakeholders. National and international disaster
217 management centres are seeking to enhance predictive capacity, while fire management
218 agencies are expanding or re-allocating their resources to rapidly suppress fires to avoid them
219 becoming too large, fast or intense. A number of international organisations such as the UN
220 Environment Programme (UNEP, 2022a), the World Bank (2020, 2024), and the Organisation
221 for Economic Co-operation and Development (OECD, 2023) and a range of other inter- or
222 non- governmental organisations are producing reports that consolidate evidence on the



223 changing risk of extreme fires and identify best practices for mitigating their impacts, including
224 through land management and urban/rural planning. Many land managers are developing and
225 implementing approaches such as fuel reduction, a process subject to permit systems issued
226 by regional fire management agencies in some countries (Fernandes and Botelho, 2003;
227 Stephens et al., 2012; Moreira et al., 2020; Chuvieco et al., 2023). Wildfire response agencies
228 are exploring innovative approaches to detecting and responding to fires, and there is rising
229 interest in the prospect of integrated fire management around the world (Food and Agriculture
230 Organization of the United Nations, 2024). Operators of C market projects and forest carbon-
231 conservation initiatives, such as REDD+ are particularly wary of the risks that wildfires present
232 to the permanence of C offsets, seen as a key tool for achieving Net Zero emissions (Barlow
233 et al., 2012; Smith et al., 2023).

234
235 Amidst extreme wildfires and wildfire seasons, stakeholders increasingly turn to scientists for
236 answers to pressing questions that naturally arise. How extreme was this fire event in a
237 historical context? Is climate change to blame? Will we see more wildfires like this in the
238 future? Did land management exacerbate or ameliorate the problem? Can we predict events
239 like this in future to improve early warning? What is the role of climate policy in reducing risk
240 of extreme wildfires in future?

241
242 While observational, statistical, and modelling tools for assessing extreme wildfire drivers and
243 predicting wildfire occurrence are advancing rapidly, their application to studying extreme
244 wildfire seasons or events on timescales relevant to public and political interest remains
245 limited. The State of Wildfires report embodies a structure for routinely cataloguing extreme
246 wildfire events at annual frequency and explaining their occurrence and relation to climate
247 change. We incorporate recent advances in disentangling the drivers of fire to fuel dryness,
248 fuel load, and weather, and ignition and suppression factors, and by applying these methods
249 in conjunction with models of global change we quantify the change in likelihood of the past
250 year's events under climate and land use changes. Observable fire metrics (e.g. burned area)
251 are the target variable of our causal inference and attribution work, which thereby advances
252 on more common climate attribution studies that attribute change in fire-favourable
253 meteorological conditions to climate change. Overall, this report capitalises on recent
254 advances in the study of extreme fire events and seasons to provide timely information about
255 shifting fire regimes and their causes. The findings of the report are relevant to policymakers,
256 the media, and the wider public.

257
258 Due to the diversity of environmental settings in which fires occur and the range of ecological,
259 economic, or societal impacts caused by fires, defining an extreme fire or an extreme fire
260 season remains inherently challenging. To date, extreme fires have commonly been defined
261 by their BA extent, by their feedback on the global climate compared to climatological data
262 and on large-scale ecosystem changes and by their socio-economic impact. While an extreme
263 fire event may result in significant anomalies against historical Earth Observations in the same
264 study region, the scientific community currently seeks to apply a more comprehensive
265 definition of extreme fire, including its impacts on societies, fire-prone regions and on
266 downwind society and ecosystems.

267 268 **1.2 Objectives of this Report**

269
270 This inaugural edition of the State of Wildfires report aims to stimulate development of tools
271 for understanding and predicting extreme fires and to deliver actionable information to policy
272 and practice stakeholders and society. In this edition we:

- 273
274 1. Regionally identify extreme individual wildfires or extreme wildfire seasons of the
275 period since March 2023, and place them in context of recent trends.



- 276 2. Shortlist a selective number of extremes (extreme individual wildfires or extreme
277 wildfire seasons) with notable impacts on society or the environment, which we term
278 the ‘focal events’ in this report.
- 279 3. Diagnose the contributions of fuel dryness, fuel load, ignitions and suppression to the
280 occurrence of each focal event.
- 281 4. Assess the capacity of operational predictive systems to predict each focal event.
- 282 5. Attribute each focal event to anthropogenic factors including climate change and land
283 use.
- 284 6. Provide an outlook on the probability of extreme events in the coming fire season.
- 285 7. Project future changes in the probability of each focal event under future climate
286 scenarios.

287
288 The State of Wildfires report will be an annually recurring report that can harness and adopt
289 new methodologies brought forward by the global community of fire scientists between
290 publications.

291
292 To achieve our objectives, we integrate a variety of advanced methods developed in recent
293 years. For instance, we identify anomalies in past fire seasons using both regional BA and
294 emissions records and a global dataset of individual fires (Giglio et al., 2018; van der Werf et
295 al., 2017; Andela et al., 2019). This dual approach enables us to detect not only regional
296 anomalies but also individual fires that are exceptionally large or fast-moving. Additionally, we
297 leverage the latest advances in fire risk forecasting on seasonal to sub-seasonal timescales
298 provided by the ECMWF. Furthermore, we employ two state-of-the-art machine learning
299 techniques (Kelley et al., 2019; McNorton et al., 2024) to pinpoint the causes of the extreme
300 fire events of 2023-24. We also apply multiple attribution methods to quantify the influence of
301 climate change and land use change on these extreme events (e.g. Kelley et al., 2019, 2021;
302 Burton, Lampe, et al., 2023). Fire is an inherently stochastic process, and any attempt to
303 assess its causes needs to account for uncertainty. The strength of our approach in this report
304 is in employing different techniques to address the complex questions of how unusual the fires
305 of the last season were, and what the drivers might have been. By using multiple tools to
306 measure different fire metrics and identify the factors driving fires, and by using different
307 techniques to attribute their causes to climate and human influences, we can either build up a
308 solid body of evidence or highlight aspects of extreme fires in recent years that we do not yet
309 understand. While the tools are diverse, they address the questions from different angles,
310 giving us a robust way to assess predictability or quantify uncertainty in their results - also vital
311 components in building confidence in the statements made in this report. We demonstrate the
312 range of tools we have available to tackle these important questions now, and highlight gaps
313 where we still need to develop the research further. The combination of these diverse
314 techniques marks a significant step toward the regular and comprehensive assessment of
315 past and future extreme wildfire events.

316
317 Over the coming years and decades, we aim to develop and apply the tools presented in this
318 report in near-real time, thus enhancing our capacity to transfer key insights to decision-
319 makers at the time they most need it. Ultimately, this report serves as a vehicle that
320 consolidates the novel advances and efforts of the fire science community to provide relevant
321 information to stakeholders, enabling society to adapt to emerging fire extremes.

322 **2 Methods**

323 324 **2.1 Extreme Wildfire Events of 2023-24**

325
326 We catalogued the extreme regional wildfire events or annual fire seasons in the period March
327 2023-February 2024 based on a combination of anomalies evident in Earth Observations
328 (**Section 2.1.1**), as well as expert assessment of wildfires that severely impacted people or



329 the environment (**Section 2.1.4**). This approach deliberately represents a broad definition of
330 extreme wildfire events by allowing our expert panel to flexibly integrate diverse forms of
331 wildfire impacts into their regional assessments of extreme wildfire events. In so doing, we
332 allow for the fact that it is challenging to define a consistent threshold for ‘extreme’ fires given
333 the diversity in the characteristics and impacts of fire across the many fire regimes (e.g.
334 Archibald et al., 2009; Cunningham et al. 2024). Metrics such as BA and emissions are a good
335 proxy for impact in some cases, yet they cannot fully account for the diverse relationships
336 between fire, ecosystems, people and societal values. Hence our broad definition of “extreme
337 fire” allows nuanced measures of fire impacts to be captured (e.g. fire severity or challenges
338 to suppression; Keeley 2009) and careful consideration of the complex interplay between
339 wildfire and the various forms of fire intentionally applied by humans and serving multiple
340 purposes. It also allows for elaboration of the links between wildfire and the various values
341 that benefit or are burdened by it, including ecosystem services, biodiversity, Indigenous
342 cultural values and biocultural landscapes, heritage, recreation, social capital, the built
343 environment, tourism, agriculture and other industries, and human health and wellbeing.
344

345 **2.1.1 Earth Observations of Fire**

346 **2.1.1.1 Input Datasets**

347
348
349 We assembled observations of global daily burned area (BA) for the period March 2001-
350 February 2024 from NASA’s MODIS BA product (MCD64A1, collection 6.1) at 500m resolution
351 (Giglio et al., 2018, 2021). We also produced a global record of individual fires for the period
352 March 2001-February 2024 by updating the Global Fire Atlas (Andela et al., 2019; Andela and
353 Jones, 2023) through February 2024, driven by the 500m MODIS BA data. The Global Fire
354 Atlas algorithm clusters burned cells into individual fires, tracks their daily progression, and
355 logs attributes such as fire size and mean daily rate of growth. Our updates are provided at
356 Andela and Jones (2023).
357

358 In addition, we gathered estimates of fire carbon (C) emissions for the period March 2023-
359 February 2024 from two models driven by Earth Observations of active fires or burned area:
360 firstly, the Global Fire Assimilation System (GFAS) product, provided operationally by the
361 Copernicus Atmospheric Services (AMS) at 0.1 degree spatial resolution and daily temporal
362 resolution (Kaiser et al., 2012; European Centre for Medium-Range Weather Forecasts,
363 2024), and; secondly, the Global Fire Emissions Database (GFED; version 4.1s) product at
364 0.25 degree spatial resolution and daily temporal resolution (van der Werf et al., 2017). GFAS
365 is driven by the fire radiative power (FRP) retrievals in the MODIS active fire product
366 MCD14A1 and biome-level relationships between FRP and biomass consumed based on
367 GFED3 (Kaiser et al., 2012). For the 1997-2016 period, GFED4s is driven by MODIS BA data
368 (MCD64A1 collection 5) supplemented with small fire BA based on MODIS active fire data,
369 and a model for biomass productivity and fuel consumption (van der Werf et al., 2017). For
370 the post-2016 period, emissions are based on active fire detections scaled to emissions using
371 pixel-based scaling factors derived from the 2003-2016 overlapping period.
372

373 We note that the MODIS MCD64A1 BA data used in various facets of our analyses are known
374 to be conservative due to the limitations to detecting small fires based on surface spectral
375 changes at 500m resolution. Recent work has shown that including detections of small active
376 fires increases global BA estimates by 93% (Chen et al., 2023). However, variability and trends
377 in regional BA totals using datasets that include small fires do not differ significantly from the
378 variability and trends present in the MODIS MCD64A1 BA data (Chen et al., 2023). In this
379 report, regional BA and fire C emissions totals are conservative and the context of missing
380 small fires must be considered when interpreting the threshold values of the upper quantiles
381 of the fire size distribution from the Global Fire Atlas. Nonetheless, there is consistency in our



382 approach across years such that anomalies are robust with respect to prior observations, and
 383 our focus on more extreme fires renders smaller fires obsolete in most of our analyses.
 384

385 **2.1.1.2 Regional Burned Area, Carbon Emissions and Fire Count Totals**

386
 387 We calculated regional totals of BA and C emissions based on a variety of regional layers
 388 defined in **Table 1**. The regional layers represent a range of biogeographical boundaries (e.g.
 389 biomes), geopolitical boundaries (e.g. countries), and values used in scientific reports (e.g. by
 390 the Intergovernmental Panel on Climate Change; IPCC). We calculated monthly totals of BA
 391 and fire C emissions for each region by aggregating monthly BA and daily C emissions data,
 392 summing the data from the input datasets both spatially and temporally as required. In the
 393 case of fire C emissions, we also calculated the mean estimate of fire C emissions from
 394 GFED4.1s and GFAS, regionally.
 395

396 We adopt a March-February definition of the global fire season (e.g. the latest global fire
 397 season spans March 2023-February 2024). Due to an annual lull in the global fire calendar in
 398 the boreal spring months, fire season BA totals are least sensitive to the shifts in fire season
 399 cutoffs of 1-2 months if the fire season centres on spring (Boschetti and Roy, 2008). This
 400 makes the global fire season centred on spring a pragmatic option for the study of interannual
 401 variability or trends in fire extent (Boschetti and Roy, 2008). The period March-February is
 402 specifically oriented at the end of the austral fire season and before widespread fires have
 403 begun in the boreal extratropics. The regions where this global definition of the fire season is
 404 most problematic are: northern hemisphere South America, Southeast Asia, and Central
 405 America (Giglio et al., 2013).
 406

407 In addition, we calculated totals of regional fire counts for each global fire season based on
 408 the number of individual fire ignition points present within each region, using ignition point
 409 vectors from the Global Fire Atlas. The resolution of the MODIS data supplied to the Global
 410 Fire Atlas algorithm is 500 m and hence fires that are smaller in scale are omitted. Regional
 411 or national systems may record greater fire counts due to the inclusion of smaller fires.
 412

413 **Table 1:** Regional layers to which global Earth Observations were disaggregated and used to
 414 define regions with extreme wildfire seasons or extreme individual wildfire attributes. Regional
 415 layers are available from Jones et al. (2024).

| Layer | Short Form | Source | Notes |
|--|----------------------|---------------------------------------|---|
| Biomes | NA | Olson et al. (2001) | |
| Continents | NA | ArcGIS Hub (2024) | |
| Continental Biomes | NA | See above | Spatial intersect of biomes and continents. |
| Countries | NA | EU Eurostat (2020) | |
| UC Davis Global Administrative Areas (GADM) Level 1 | GADM-L1 | UC Davis (2022) | First sub-national administrative level, such as states of the US or provinces of China. Version 4.1. |
| Intergovernmental Panel on Climate Change <i>Sixth Assessment Report (AR6) Working Group I (WGI) Reference Regions</i> | IPCC AR6 WGI Regions | IPCC (2021); SantanderMetGroup (2021) | |
| Global C Project <i>Regional C</i> | RECCAP2 | Ciais et al. (2022) | |



| | | | |
|--|---------------------|-------------------------------|--|
| <i>Cycle Assessment and Processes (RECCAP2)</i> Reference Regions | Regions | | |
| Global Fire Emissions Database (GFED) Basis Regions | GFED4.1s Regions | van der Werf et al. (2006) | |

416

417

418 **2.1.2 Identifying Extreme Fire Seasons and Events from Earth Observations**

419

420 **2.1.2.1 Regions with Extreme Wildfire Seasons**

421

422 Anomalies in BA, fire C emissions, and fire counts in the latest global fire season (March 2023-
 423 February 2024) were calculated in several ways:

424

- 425 I. as relative anomalies (expressed in %) from the annual mean during all previous
 426 March-February periods since 2001;
- 427 II. as standardised anomalies (standard deviations) from the annual mean during all
 428 previous March-February periods since 2001;
- 429 III. as a rank amongst all March-February periods since 2001 (2003 for C emissions),
 430 March 2023-February 2024 inclusive, and;

431

432 In this report, anomalies in fire C emissions are reported based on the two-model mean
 433 estimate from GFED4.1s and GFAS, however anomalies based on the GFED4.1s or GFAS
 434 estimates individually are also available via Jones et al. (2024).

435

436 We identified regions in which the latest fire season was potentially classifiable as ‘extreme’
 437 based on the rank of BA, C emissions and fire count amongst all fire seasons. For visualisation
 438 purposes, we identified regions in which the latest fire season ranked in the top 5 of all annual
 439 fire seasons on record (see [Section 3.1](#)). The BA data for the period March 2001-February
 440 2024 includes 23 fire seasons, while the C emissions data for the period March 2003-February
 441 2024 includes 21 fire seasons. Hence, a top-5 ranking translates approximately to a fire
 442 season in the upper quartile of those on record. While a high-ranking BA or C emissions is
 443 indicative of an extreme fire season, we reiterate that our regional experts play a crucial role
 444 in defining a broader range of events that could be considered extreme.

445

446 We further characterised the onset, peak, and cessation of anomalous monthly BA in March
 447 2023-February 2024. First, we identified the month of the event’s peak as the maximum
 448 difference between monthly BA values in March 2023-February 2024 and the climatological
 449 mean monthly values from the prior March-February periods. Thereafter, the event’s onset
 450 and cessation were defined as the bounds of consecutive months with above-average BA
 451 prior to and following the peak (relative to the monthly climatology).

452

453 **2.1.2.2 Regions with Extreme Individual Wildfire Attributes**

454

455 We identified regions in which large or fast-moving fires occurred in the latest fire season
 456 based on records of individual fires from the Global Fire Atlas. For each region (**Table 1**) and
 457 year, we estimated the size of the largest fire, the daily rate of growth of the fire that spread
 458 most rapidly, the size of the 95th percentile fire, and the daily rate of growth of the 95th
 459 percentile fire. In the Global Fire Atlas, the daily rate of growth for any given fire is determined
 460 by calculating the average daily rate of growth at which the fire advanced across all its
 461 constituent cells. This includes cells burned by the head, flank, and backfire. This method



462 produces lower spread rates than if the calculation were based solely on the cells burned by
463 the head fire.

464

465 Anomalies in each fire attribute were calculated using the same metrics as for BA (see *i-iii*
466 above), and we identified regions in which the latest fire season featured fires with potentially
467 extreme attributes based on the rank of BA and fire C emissions amongst all fire seasons.

468

469 **2.1.3 Updating Regional Trends in Burned Area and Carbon Emissions**

470

471 To place recent extremes in the context of fire trends of the past two decades, we update our
472 regional analyses of trends in annual BA from those published by Jones et al. (2022). In
473 contrast to Jones et al. (2022), we present trends that align more closely with global fire
474 seasons, spanning the period March 2001-February 2024 rather than trends over calendar
475 years. We quantified trends using the Theil-Sen slope estimator. The Theil-Sen approach is
476 useful when data may contain outliers or be non-normally distributed, as it calculates the
477 median of all possible pairwise slopes between data points. This makes it less sensitive to
478 outliers than a standard least squares regression slope. Changes were then assessed by
479 multiplying by the trends (unit year⁻¹) by the number of fire seasons in the period March 2001-
480 February 2024 (23 fire seasons). Relative changes were calculated as the absolute changes
481 divided by the mean annual BA during the period, which is a more conservative approach than
482 adopting the BA total in the first fire season as the denominator. The significance of the slopes
483 estimated by the Theil-Sen method was evaluated using the Mann-Kendall test, with a
484 confidence level set at 95%. The Mann-Kendall test assesses whether there is a statistically
485 significant trend in the series of data. This test does not require the data to follow any specific
486 distribution and is robust against outliers.

487

488 In addition to reporting trends in *total* BA, we also present trends in *forest* BA as these regularly
489 diverge from total BA trends (see **Section 3.1**). Forest BA is calculated as described in Section
490 **2.1.1.2** but after isolating burned cells in areas with tree cover exceeding 30% in NASA's
491 annual MODIS MOD44B collection 6.0 Continuous Vegetation Field product (250 m) (DiMiceli
492 et al., 2015). The 30% threshold is widely used amongst studies of forest cover change (e.g.
493 Li et al., 2017; Cunningham et al., 2020; Sexton et al., 2016).

494

495 **2.1.4 Expert Consultation**

496

497 We assembled a panel of regional experts (two from each continent, **Table 2**), to contribute to
498 the identification, description, and characterisation of extreme wildfire seasons or impactful
499 events in the latest fire season. A key role of the expert panel was to catalogue regional events
500 that significantly impacted society or the environment but which may not have been detected
501 by Earth-observing satellites due to issues such as scale, short duration, timing of overpass,
502 and cloud or canopy cover. This includes (but is not limited to) wildfires that impacted society
503 by causing fatalities, evacuations, displacement (e.g. homelessness), direct structure or
504 infrastructure loss or damage, degradation of air or water quality, loss of livelihood, cultural
505 practice or other ways of life, and loss of economic productivity. This definition also includes
506 (but is not limited to) wildfires that impact the environment via disturbance to vulnerable
507 ecosystems, biodiverse areas, or ecosystem services such as C storage. This approach
508 recognises that Earth Observations do not provide a complete record of all impactful fires. We
509 do not define ubiquitous quantitative thresholds of impact by any of the measures outlined
510 above, but rather invite in-region experts to identify events that triggered impacts that were
511 sufficient in magnitude to infiltrate public and political discourse. The sources of information
512 available for cataloguing regional events include national/regional fire records, fire service
513 reports, disaster management reports, news reports, and social media.

514



515 A second key role of our expert panel was to describe and contextualise the impacts of the
 516 fire seasons highlighted as extreme by Earth Observations or regional assessment (see
 517 **Section 3.1**). This includes the discussion of anomalies that rank highly in Earth Observations
 518 but nonetheless did not have major impacts in regions. Metrics such as percentage difference
 519 from the mean and standard deviations from the mean were also used by the expert panel to
 520 further characterise the magnitude of anomalies in regional BA, fire C emissions, fire counts
 521 and individual fire properties.

522
 523
 524 **Table 2:** Experts contributing to the identification of extreme events and characterisation of
 525 the global fire season during March 2023-February 2024.

| Region | Expert | Country of Organisation / Nationality | Professional Background(s) | Others Consulted |
|---------------|----------------------|---------------------------------------|---|--|
| Africa | Natasha Ribeiro | Mozambique | Research | Robert Ang'ila, Karatina University; Kebonyethata Dintwe, Botswana University; John Mendelsohn, Okavango Research Institute; Ronald Heath, Forestry South Africa; Helen De Klerk, Stellenbosch University |
| | Sally Archibald | South Africa | Research | |
| Asia | Bambang Saharjo | Indonesia | Research, Litigation | |
| | Veerachai Tanpipat | Thailand | Research, Fire Control and Management Instructor and Consultant | |
| Europe | Paulo Fernandes | Portugal | Research | Davide Ascoli, University of Turin, IT; Hellenic Agricultural Organization "DIMITRA"; Institute of Mediterranean Forest Ecosystems; Niall MacLennan, Scottish Fire and Rescue Service |
| | Stefan Doerr | UK / Germany | Research | |
| | Gavriil Xanthopoulos | Greece | Research | |
| North America | Crystal Kolden | USA | Research, Firefighting | |
| | Jacquelyn Shuman | USA | Research | |
| | Piyush Jain | Canada | Research | |
| Oceania | Hamish Clarke | Australia | Research, Environmental Management | Grant Pearce, Fire and Emergency NZ; Simeon Telfer, SA Country Fire Service; Agnes Kristina, Department of Fire and Emergency Services; Russell Stephens Peacock, QLD Fire and Emergency Services; Chris Collins, Tasmania Fire Service; David Field, NSW Rural |
| | Sarah Harris | Australia | Research, Emergency Management | |



| Region | Expert | Country of Organisation / Nationality | Professional Background(s) | Others Consulted |
|---------------|-------------------|---------------------------------------|--|--|
| Africa | Natasha Ribeiro | Mozambique | Research | Robert Ang'ila, Karatina University; Kebonyethata Dintwe, Botswana University; John Mendelsohn, Okavango Research Institute; Ronald Heath, Forestry South Africa; Helen De Klerk, Stellenbosch University Fire Service. |
| | Sally Archibald | South Africa | Research | |
| | | | | |
| South America | Dolors Armenteras | Colombia | Research | The Chico Mendes Institute for Biodiversity Conservation (ICMbio), Brazil, Santarém Office |
| | Liana Anderson | Brazil | Research, Disaster risk reduction strategies | |

526

527 **2.1.5 Bespoke Analysis: Air Quality Impacts in Canada**

528

529 Media and grey literature reports highlighted that wildfires in Canada during 2023 led to
 530 extreme degradation of air quality across North America (see **Section 3.1.3.4**). We evaluated
 531 air quality impacts of Canadian wildfire emissions in 2023 in the context of the previous 20
 532 years using PM_{2.5} surface concentrations from the CAMS reanalysis of global atmospheric
 533 composition (Inness et al., 2019). The CAMS reanalysis provides a 3-dimensional time-
 534 consistent dataset of atmospheric composition including aerosols, chemical species and
 535 greenhouse gases for the period 2003-2023). Estimated wildfire emissions for the reanalysis
 536 are provided by the GFAS v1.2 (Kaiser et al., 2012), based on fire radiative power
 537 observations from the Terra and Aqua MODIS instruments, in addition to inventories of
 538 anthropogenic and biogenic emissions, and natural emissions (such as desert dust). While
 539 the reanalysis PM_{2.5} includes contributions from all emissions sources, the most extreme
 540 values are strongly correlated with the estimated fire emissions. The extreme annual PM_{2.5}
 541 surface concentrations are calculated as the 95th, 97th and 99th percentiles of the daily
 542 maximum concentrations for each year in the reanalysis, and presented as the area-weighted
 543 average for Canada.

544

545 **2.2 Shortlisting of Focal Events**

546

547 In later sections of this report, we apply various models to understand the causes and
 548 predictability of a selection of extreme wildfire seasons or events during March 2023-February
 549 2024, to attribute the roles of climate change and land use change, and project the future
 550 likelihood of events of a similar magnitude under various climate change scenarios (see
 551 Methods below). We limited the number of analyses to three globally prominent focal events
 552 of the 2023-24 global fire season in this report because our models are not currently
 553 operational products and must be trained and optimised regionally, which is time-consuming.

554

555 Our models are structured and parameterised to predict anomalies in regional BA or fire count,
 556 meaning that they can only be applied to events that feature in Earth Observations. In addition,
 557 the models have not yet been applied to study fire C emissions or wildfires with extreme
 558 attributes, and so we restrict their application to regions with anomalous BA in the latest fire
 559 season. In discussion with our expert panel, we prioritised the three events studied in this



560 report by weighing up the anomalies in Earth Observations during the latest fire season as
561 well as the impacts that these extremes had on people and the environment. The focal events
562 are notable for their international significance, attracting attention from the media and
563 policymakers both within and beyond their region.
564

565 **2.3 Diagnosing Drivers and Predictability**

566

567 **2.3.1 Assessing Predictability of Extremes across Time Scales**

568

569 We evaluated the time frame over which extreme events could have been forecasted using
570 existing forecasting products that produce the Canadian Fire Weather Index (FWI) as outputs
571 (van Wagner, 1987). Developed by the Canadian Forest Service as part of the Canadian
572 Forest Fire Danger Rating System (van Wagner, 1987), the FWI comprises various
573 components that consider the influence of dead fuel moisture and wind on fire ignition and
574 spread behaviour, with 2m temperature, 10m wind speed, precipitation, and 2m relative
575 humidity as prerequisite variables. The FWI specifically combines three fuel moisture codes
576 representing vegetation moisture state at different layers in the forest floor, as well as a spread
577 index influenced by fuel moisture state and wind speed (van Wagner, 1987). A higher FWI
578 indicates fire weather conditions more conducive to wildfires in environments with sufficient
579 fuel load. Owing to its original design for use in forest ecosystems, the FWI is especially useful
580 for predicting the likelihood and severity of extreme events in ecosystems where weather is
581 the primary limitation to fire (i.e. those mainly limited by moisture or temperature); its accuracy
582 in forecasting BA in fuel-limited ecosystems is more limited (Carvalho et al., 2008; Bedia et
583 al., 2015; Abatzoglou et al., 2018; Jones et al., 2022). Its applications encompass early
584 warning systems, pre-suppression and suppression planning, prescribed burn planning and
585 effectively alerting authorities and the public to abnormal fire danger conditions. FWI is
586 extensively used in operational global information platforms such as the European Forest Fire
587 Information System (EFFIS; <https://forest-fire.emergency.copernicus.eu/>, last access: 2 June
588 2024) and the Global Wildfire Information System (GWIS; <https://gwis.jrc.ec.europa.eu/>, last
589 access: 2 June 2024), and the Canadian Wildland Fire Information System (CWFIS;
590 <http://cwfis.cfs.nrcan.gc.ca/>, last access: 2 June 2024).

591

592 In addition to well established fire danger forecasts with lead times of a few days, skilful
593 predictions of fire danger can be made on sub-seasonal to seasonal time scale (S2S) for
594 Mediterranean Europe (Bedia et al., 2015), United States (Roads et al., 2010) and Asia
595 (Spessa et al., 2015). Drought and fire weather conditions throughout the world have been
596 found to correlate with large scale climate patterns such as the El Niño Southern Oscillation
597 (ENSO) (Field et al., 2016; Chen et al., 2017), the Indian Ocean Dipole (Cai et al., 2009) and
598 other climate modes such as the Atlantic Multidecadal Oscillation and the Pacific Decadal
599 Oscillation implying predictability of fire-favourable weather conditions for various seasons and
600 regions (Aragão et al., 2018; Turco et al., 2018). Following the concept of seamless (Wetterhall
601 et al., 2018) prediction of fire weather on S2S timescales after Di Giuseppe et al. (2020), Di
602 Giuseppe et al. (2024) and Dowdy (2020), we collated FWI data from reanalyses and forecasts
603 designed to operate on S2S lead times of 10 days to 7 months. Specifically, the FWI is derived
604 from the operational monitoring provided by ERA5-land (Muñoz-Sabater et al., 2021), the
605 forecasts from the operational high-resolution ECMWF weather system, and the seasonal
606 predictions from the ECMWF's long-range forecasting system, SEAS5 (Johnson et al., 2019;
607 Di Giuseppe et al., 2020; Di Giuseppe et al., 2024). The predictions are compared to recorded
608 peaks in fire activity, both in terms of burned areas and active fires as observed by the MODIS
609 satellites. These prediction systems vary in spatial and temporal resolutions. Short to medium-
610 range FWI forecasts (up to 10 days) are available daily at a resolution of 9 km, while the FWI
611 seasonal forecast is available monthly at a resolution of approximately 25 km, however
612 seasonal skill is limited to 2-3 months in normal conditions (Di Giuseppe et al., 2024).
613



614 Predictability is assessed qualitatively by visually examining how extreme FWI was as a
615 precursor of the event, replicating the use of this indicator by fire agencies during the fire
616 season. Most fire agencies would have local information on fuel conditions and would be able
617 to interpret FWI values in an educated manner, thus reducing intervention on high FWI values
618 in fuel conditions that are not hazardous. This fuel consideration would not be included in a
619 validation of the FWI using traditional skill scores, as these would be dominated by false
620 alarms. We retain that FWI is an index representing flammability and cannot fairly be validated
621 against fire activities.

623 **2.3.2 Identifying Key Drivers of Focal Events**

625 **2.3.2.1 Overview**

626
627 We used two modelling systems with similar fire predictors to diagnose the direct drivers of
628 each focal event that was shortlisted: the Probability of Fire (PoF) model (McNorton et al.,
629 2024) and the Controls on Fire (ConFire) attribution framework (Kelley et al., 2019; Kelley et
630 al., 2021). The PoF model diagnoses the drivers of active fire (AF) observations from the
631 MODIS MCD14ML active fire product (collection 6.1; 1 km resolution; Giglio et al., 2016; NASA
632 FIRMS, 2020) using Shapley values (Lundberg and Lee, 2017), while ConFire diagnoses
633 drivers of BA from the MODIS MCD64A1 BA product (collection 6.1; 500 m resolution; Giglio
634 et al., 2018) regridded to 0.5°. Fires flagged as low confidence in the AF product were not
635 used. Although AF and BA have been used widely in global and regional scientific studies,
636 there are substantial differences between the two products (Roy et al., 2008; Di Giuseppe et
637 al., 2021; Chuvieco et al., 2019) and the strength of the relationship between them can vary
638 regionally (van der Werf et al., 2017; Hantson et al., 2013). Our use of two observational fire
639 products and two distinct model approaches provides a way to account for inherent
640 uncertainties in the definition of the fire events and the uncertainties in the methodologies.

641
642 Both methods use a number of predictors (we refer to the single variables as the drivers) of
643 AF or BA. The drivers are grouped into four main categories (we refer to grouped drivers as
644 the controls): weather; fuel abundance; fuel moisture, and; other drivers for PoF and human
645 drivers for ConFire (see **Table 3**). PoF drivers in “Other” include ignition and suppression
646 efforts as well as the residual error between forecast and observed fire activity. Grouping the
647 set of drivers between the four identified controls—weather, fuel moisture, fuel load, and
648 ignitions—is not always straightforward, as fuel moisture and weather variables are strongly
649 correlated, and fuel load is also related to weather conditions. Hence, some drivers can be
650 associated with more than one control. The categorisation stems mostly from the way the
651 driving datasets have been obtained and their underlying resolutions. We have also
652 considered the traditional approach of assessing fire weather in isolation within most fire
653 danger assessment metrics. We believe that grouping these metrics under the umbrella term
654 ‘control weather’ offers a concise way to reference the drivers of the Fire Weather Index
655 (Matthews, 2009). Despite this, it is important to note that the techniques employed ensure
656 contribution from specific variables cannot be double counted between categories. Both
657 ConFire and PoF are also capable of quantifying the contribution of individual drivers (Kelley
658 et al., 2019; McNorton et al., 2024). However, we will focus our analysis on the impact of the
659 controls.

660
661 The selected weather parameters are consistent with each other and are available at a base
662 resolution of 9 km. Land cover maps are available at a higher resolution of 1 km. Additionally,
663 fuel load is constrained by external (to the weather model) observations from the ESA CCI
664 above ground biomass product and satellite inversion estimates of net ecosystem exchange
665 of C, while the fuel moisture is parameterized using land surface parameters constrained by
666 the weather variables.

667



668 **2.3.2.2 Drivers and Controls Used in Fire Event Analysis**

669
670 For our assessment of the contribution of weather and fuel moisture to the anomalous events
671 we take several predictors from ERA5-Land (9 km resolution; Muñoz-Sabater et al., 2021),
672 specifically variables that are known to correlate with AF or BA (Bistinas et al., 2014; Haas et
673 al., 2022; Haas et al., 2022). The drivers considered for each control are listed in **Table 3**. For
674 the weather component in isolation, we use 2m temperature, 2m dewpoint temperature, 10m
675 wind speed and daily total precipitation (note that these are the prerequisite variables used in
676 the formulation of the FWI; van Wagner, 1987). We use a fuel characteristic model to estimate
677 the fuel load and fuel moisture components following McNorton and Di Giuseppe (2024), with
678 model estimates of fuel moisture constrained by estimates of leaf area index (LAI) from the
679 ECMWF's Integrated Forecast System (IFS) and model estimates of fuel loads constrained
680 by aboveground biomass estimates from the ESA Climate Change Initiative (CCI; Santoro and
681 Cartus, 2021) and net ecosystem exchange estimates from the Copernicus Atmosphere
682 Monitoring Service (CAMS; Agustí-Panareda et al., 2019). Additional predictors regarding fuel
683 load and state include vegetation cover and type (**Table 3**). Proxies for ignition and
684 suppression controls, placed within the "Other" set of controls, are more challenging to
685 establish. Currently, we use population density, urban fraction, cropland fraction, pasture
686 fraction, lightning, orography (**Table 3**). For consistency all variables are interpolated to 9 km
687 resolution. See "**Modelling frameworks**" in the **Extended Methods Supplement** for a
688 detailed description. PoF accurately captures the spatiotemporal patterns of fire activity in
689 Canada and Western Amazonia and effectively identifies areas of high fire danger in
690 Alexandroupolis, Greece. However, it underestimates the severity of fire events in that area.
691 See "**Evaluation**" in the **Extended Methods Supplement** for detailed evaluation.

692
693



694 **Table 3:** Drivers of fire and their parent control group included in the event fire analyses using
 695 ConFire and PoF. Drivers are individual explanatory variables, which are grouped into
 696 weather, fuel load, fuel moisture, and other controls. ** The 'Other' category includes proxies
 697 for ignition and suppression controls plus the missed prediction. +ive or -ive under "ConFire
 698 controls" describes if a driver increases or decreases BA in ConFire.

| Driver | POF control | ConFire controls | Frequency | Time Period | Source | Reference |
|---|--------------------|------------------------------------|-----------|------------------------|--------------------------|------------------------------|
| 2m Temperature | Weather | Weather +ive | Daily | Jan 2014-NRT | ERA5-Land | Muñoz-Sabater et al. 2021 |
| 2m Dewpoint Temperature | Weather | Weather -ive | Daily | Jan 2014-NRT | ERA5-Land | Muñoz-Sabater et al. 2021 |
| 10m Wind Speed+ | Weather | Not used | Daily | Jan 2014-NRT | ERA5-Land | Muñoz-Sabater et al. 2021 |
| Precipitation | Weather | Weather -ive | Daily | Jan 2014-NRT | ERA5-Land | Muñoz-Sabater et al. 2021 |
| Live Leaf Fuel Load | Fuel Load | Not used | Daily | 2014- 2020 | Fuel Model | McNorton et al. 2024a |
| Live Wood Fuel Load | Fuel Load | Not used | Daily | 2014- 2020 | Fuel Model | McNorton et al. 2024a |
| Dead Foliage Fuel Load | Fuel Load | Not used | Daily | 2014- 2020 | Fuel Model | McNorton et al. 2024a |
| Dead Wood Fuel Load | Fuel Load | Not used | Daily | 2014- 2020 | Fuel Model | McNorton et al. 2024a |
| Mean & Max Vegetation Optical Depth (VOD) of the last 12 months | Not used | Fuel Load +ive | Monthly | 2014-NRT | Satellite (SMOS) | Wigneron et al 2021 |
| Vegetation Optical Depth (VOD) | Moisture | Moisture -ive | Monthly | 2014-NRT | Satellite (SMOS) | Wigneron et al 2021 |
| Low Vegetation (LAI) | Fuel Load/Moisture | Not used | Monthly | 2002-2020 climatology | Satellite (multi-sensor) | Boussetta et al., 2021 |
| High Vegetation (LAI) | Fuel Load/Moisture | Not used | Monthly | 2002-2020 climatology | Satellite (multi-sensor) | Boussetta et al., 2021 |
| Live Fuel Moisture Content | Fuel Moisture | Fuel Moisture -ive | Daily | 2014-NRT | Fuel Model | McNorton et al. 2024a |
| Dead Fuel Moisture Content | Fuel Moisture | Fuel Moisture -ive | Daily | 2014-NRT | Fuel Model | McNorton et al. 2024a |
| Snow cover | Fuel Moisture | Snow -ive | Daily | 2014-NRT | ERA5-Land | Muñoz-Sabater et al. 2021 |
| Pasture | Not used | Ignitions +ive Suppression -ive | Annual | 2014-2023 | HYDE | Klein Goldewijk et al., 2011 |
| Cropland | Not used | Ignitions +ive Suppression -ive | Annual | 2014-2023 | HYDE | Klein Goldewijk et al., 2011 |
| Urban population | Not used | Ignitions +ive Suppression -ive | Annual | 2014-2023 | HYDE | Klein Goldewijk et al., 2011 |
| Rural populations | Not used | Ignitions +ive Suppression -ive | Annual | 2014-2023 | HYDE | Klein Goldewijk et al., 2011 |
| Lightning | Not used | Ignitions +ive | Monthly | 2000- 2020 climatology | LIS/OTD | Cecil et al., 2014 |
| Type of Vegetation | Other** | Not used | Fixed | Jan 2014-NRT | ECLand | Boussetta et al., 2021 |
| Urban Fraction | Other** | Not used | Fixed | Jan 2014-NRT | ECLand | McNorton et al. 2023 |
| Orography | Other** | Not used | Fixed | Jan 2014-NRT | ECLand | Boussetta et al., 2021 |

699
 700



701 **2.3.2.3 Analysis of Fire Drivers**

702
703 The PoF system uses gradient-boosted decision trees from the XGBoost library on detected
704 AF (McNorton et al., 2024). The training iteratively adds decision trees to an ensemble of
705 models to correct for errors made by previous iterations, resulting in a computationally efficient
706 optimization (Chen and Guestrin, 2016). The system training uses a classifier approach which
707 defines a positive hit as an AF detection within the grid cell on a given day. The driver
708 attribution is performed using the SHapley Additive exPlanations (SHAP) method taken from
709 the SHAP library (Lundberg and Lee, 2017). These are then combined to provide overall
710 attribution to one of the four controls for AF predictions.

711
712 ConFire is an evidence-based uncertainty attribution framework that uses Bayesian Inference
713 to evaluate the likelihood of different control strengths and their influence on observed BA.
714 Rather than produce a single number output at a given location/time, ConFire produces a
715 probability distribution based on relationships found between driving data input into a simple
716 semi-empirical process-representation fire model, and BA observations. ConFire's
717 hierarchical design permits each variable representing a fire driver to contribute to multiple
718 controls (weather, fuel moisture, fuel abundance, or others) simultaneously. ConFire operates
719 on a monthly time step and all drivers are aggregated to monthly daily means using the FLAME
720 system (Barbosa, 2024). Each control operates as an optimised weighted linear combination
721 of its respective drivers. The influence of each control is then represented using a logistic
722 function, with BA calculated as the product of the four controls. Bayesian inference is used to
723 optimise the weighted contribution of drivers to each control, as well as the manner in which
724 each control affects BA. ConFire also includes a stochasticity term that represents the inherent
725 unpredictability in fire occurrence and resultant BA which can occur under similar bioclimatic
726 conditions (Kelley et al., 2021). We use the mean logit transformed BA distance between
727 distributions with (equation 8 in supplement) and without (equation 7 in supplement) this
728 stochasticity term provides a measure of uncertainty that has not been captured within the
729 drivers considered. See **“Modelling frameworks” in the Extended Methods Supplement**
730 for a detailed description.

731
732 The model is trained and ran between 2014-2023, the common period of all driving datasets.
733 The model is trained on 50% of BA before being run in a predictive model for the full dataset.
734 We also perform a separate run, training on all data from 2014-2018 and evaluating against
735 2019-2023 following the protocol outlined in Barbosa (2024). This evaluation protocol aims to
736 test the ConFire model's ability to accurately represent the range of uncertainties and generate
737 observed distributions through its probabilistic framework. This tells us that the framework can
738 capture and reflect inherent uncertainties in fire processes during optimization. The model
739 consistently captures observations within its uncertainty range across all regions, strongly
740 aligning with real-world data and effectively representing BA anomalies and the stochastic
741 nature of fire in our regions. However, it consistently exhibits a low bias, often underestimating
742 BA, particularly in high-burn regions like deforestation areas in Western Amazonia and
743 northern Canada. It can also capture the anomalies in BA, particularly in 2023, though it
744 sometimes underestimates the anomaly's magnitude when not using stochasticity. Therefore
745 the size of BA anomalies may be underestimated. See **“Evaluation” in the Extended**
746 **Methods Supplement** for detailed evaluation.

747

748 **2.4 Attribution to Global Change**

749

750 **2.4.1 Role of Global Change Factors**

751

752 In addition to direct drivers of fire events as outlined in the previous section (e.g. weather, fuel,
753 moisture, ignition and suppression), fires are also influenced by global change factors such as
754 climate and land-use change which vary over longer timescales. Since the pre-industrial era,



755 global mean temperature has increased by nearly 1.3°C (Betts et al., 2023; Forster et al.,
756 2023), with regional temperatures even higher in some areas, providing additional potential
757 for fuel drying and facilitating fire ignition and propagation. Climate change has also resulted
758 in altered precipitation patterns, with total rainfall and dry season length increasing or
759 decreasing variably across regions (Polade et al., 2014; Swain et al., 2018; IPCC, 2023a).
760 Meanwhile, changes to fuel load and ignition rates are driven by climate change and
761 anthropogenic land-use, with varying effects regionally (Finney et al., 2018; Romps, 2019).
762 For example, in fuel-limited savannah biomes land-use change can drive more fragmented
763 fuel loads and a reduction in fire (or an increase in fire resulting from land abandonment),
764 whereas in forest ecosystems fragmentation provides more potential for ignition and leads to
765 increases in fire occurrence (Andela et al., 2017; Rosan et al., 2022).
766

767 **2.4.2 Overview of Attribution Approaches**

768

769 In this report, we apply different modelling techniques with consistent meteorological and fire
770 observations to attribute (i) regional changes in the probability of high fire weather to
771 anthropogenic forcing (**Section 2.4.3**) and (ii) changes in monthly BA to total climate forcing,
772 socio-economic change, and all forcing (**Section 2.4.4**), specifically targeting our focal regions
773 in both cases. Our analyses require separate approaches to attributing change to each of
774 these global change factors. Our attribution to *anthropogenic forcing* explicitly targets the
775 changes driven by anthropogenic emissions from greenhouse gases and land-use change,
776 following the IPCC WGI definition (Hegerl et al., 2009; Mengel et al., 2021). We prescribe
777 these emissions in a model to specifically isolate human forcing from natural variability
778 (**Section 2.4.3**). Our attribution to *total climate forcing* considers changes driven by climate
779 change since the pre-industrial period, including both anthropogenic forcing and natural
780 variability in line with the IPCC WGII definition of climate change impact attribution (IPCC,
781 2023b; IPCC 2023c). This involves comparing simulations driven with historical reanalysis to
782 a detrended counterfactual simulation with the historical warming signal removed (with both
783 simulations including historical transient land-use change) and therefore only the impacts of
784 climate change are attributed, not distinguishing between anthropogenic or natural causes
785 (Mengel et al., 2021; Burton, Lampe et al., 2023). Our attribution to *socio-economic factors* is
786 applied via the same set of simulations as our attribution to *total climate forcing*. The role of
787 socio-economic factors is isolated by comparing the early industrial period to the late industrial
788 period in the counterfactual scenario, in which only land-use and population density are
789 allowed to change (Burton, Lampe et al., 2023). Finally, *all forcing* compares the early
790 industrial period in the counterfactual scenario to the last industrial period in the factual
791 scenario, which gives the net effect of all forcings combined. These are summarised in the
792 **Table 4** below.

793
794
795



796 **Table 4:** Summary of the attribution approaches used in this report.

| Term | Definition | Experiments compared | Framework | Application |
|--|---|---|---|------------------------------|
| Event attribution for fire weather | | | | |
| Anthropogenic Forcing | Change in fire weather driven by anthropogenic emissions from greenhouse gases, land-use change and aerosols. As per (Ciavarella et al., 2018; Li et al., 2021) | ALL: natural forcing plus human emissions NAT: Natural-only forcing from solar variability and volcanoes | HadGEM3-A attribution ensemble. 0.5 degree resolution | Fire weather (FWI) |
| Impacts attribution for burned area | | | | |
| Total climate forcing | Changes in BA due to climate change, irrespective of the cause of warming. As per (Mengel et al., 2021 and Frieler et al., 2024) | Factual (2003-2019): present-day climate (driven by GSWP3-W5E5 reanalysis), CO ₂ , land-use and population Counterfactual (2003-2019): De-trended historical climate (warming signal removed), CO ₂ fixed at 1901 value, present-day land-use and population | ISIMIP3a impact attribution. 0.5 degree resolution | FireMIP ensemble and ConFire |
| Socio-economic factors | Changes in BA due to land-use and population change. As per (Burton, Lampe et al., 2023) | Counterfactual (1901-1917): Warming trend removed, fixed 1901 CO ₂ , limited land use and population change Counterfactual (2003-2019): Warming trend removed, fixed 1901 CO ₂ , present-day land use and population | ISIMIP3a impact attribution | FireMIP ensemble and ConFire |
| All forcing | Changes in BA due to climate, land-use and population change. As per (Burton, Lampe et al., 2023) | Counterfactual (1901-1917): Warming trend removed, fixed 1901 CO ₂ , limited land use and population change Factual (2003-2019): Historical climate driven by reanalysis | ISIMIP3a impact attribution | FireMIP ensemble |

797

798 The tools described here enable us to assess the influence of climate and socio-economic
 799 forcing on fire from 3 different perspectives. We use FWI to assess how the probability of
 800 experiencing meteorological conditions conducive to high (>90th percentile) fire danger has
 801 changed as a result of anthropogenic forcing. As climate change has a direct impact on fire
 802 weather, this approach enables us to isolate its effects without confounding factors of land-
 803 use change and ignitions, and tells us how a fire might develop once ignited. We use ConFIRE
 804 to model high (>90th percentile) BA and its uncertainty as a result of climate change and socio-
 805 economic factors, which other fire models are unable to capture well. We use an ensemble of
 806 7 fire models from FireMIP to put these specific extreme events into the context of changes in
 807 global median BA resulting from climate change and socio-economics in the recent present-
 808 day period. The fire model ensemble takes into account biogeochemical feedbacks between
 809 fire, climate, land-use and vegetation as a result of altered forcing across the 7 Dynamic Global
 810 Vegetation Models (DGVMs). Each of these methods is described in more detail below.

811 **2.4.3 Attributing Change in Likelihood of Fire Weather to Anthropogenic Forcing**

812 We use an established approach to attribute change in probability of high (>90th percentile)
 813 fire weather conditions to anthropogenic forcing. The approach uses estimates of FWI, as
 814 used in previous studies from the World Weather Attribution (Barnes et al., 2023), using
 815 outputs from the HadGEM3-A large ensemble (Christidis et al., 2013; Ciavarella et al., 2018).
 816 It follows the approach introduced by Stott et al. (2004) for attributing extreme weather events,



817 and it has been employed in other attribution studies targeting fire weather, such as Li et al.
818 (2021).

819

820 As outlined in **Section 2.3.1**, the FWI is used operationally and in research contexts to rate
821 fire danger based on meteorological conditions. Due to the availability of model output
822 variables we use maximum daily temperature at 1.5 m as a proxy for noon values, total daily
823 precipitation, mean daily relative humidity at 1.5 m, and mean daily wind speed at 10 m,
824 following Perry et al. (2022). We calculate the daily FWI for the month of 2023-24 peak BA
825 anomaly for each focus region, using the same month and region for validation over the
826 historical timeseries (1960-2013) (**Supplementary Figures S41-S43**).

827

828 We validate and bias-correct the model estimates of high FWI for the period 1960-2013 by
829 comparing a 15-member HadGEM3-A ensemble with ERA5 reanalysis data (C3S, 2024)
830 representing “observed” FWI. The 0.25 degree resolution observed FWI from ERA5 was
831 coarsened by linear interpolation (calculated by extending the gradient of the closest two
832 points) to match the 0.5 degree model grid. We compare the timeseries of individual
833 components of the FWI (**Figure S40**), and the distribution of the modelled and observed FWI
834 (**Supplementary Figures S41-S43**), and apply a simple linear regression to find the bias
835 correction required for the 2023 model output. Before bias-correction, the modelled FWI is
836 generally higher than the observed FWI, and some regions (e.g. Greece) require a larger
837 correction than others. The correction adjusts the trend and absolute value while maintaining
838 variability, and the model successfully reproduces the observed distribution after applying the
839 correction in each region (see **Extended Methods and Evaluation Supplement**).

840

841 For the events occurring in the 2023-24 fire season, we calculate the FWI from the HadGEM3-
842 A model simulations comprising 2 experiments of 525 members each, one driven by all
843 forcings including historical greenhouse gas emissions, aerosols, zonal-mean ozone
844 concentrations, land-use change and natural forcing (ALL), and a second counterfactual
845 simulation with natural-only forcing from solar variability and volcanic emissions, and 1850
846 land-use (NAT). By applying the bias correction from the previous step, and comparing the
847 fire weather in the two simulations to the 2023 observed FWI from ERA5, we calculate the
848 change in probability of high (>90th percentile) fire weather due to anthropogenic forcing.

849 **2.4.4 Attributing Change in Regional BA to Total Climate Forcing, Socio-economic** 850 **Factors and All Forcing**

851

852 **2.4.4.1 Monthly High Burned Area**

853

854 We use the ConFire attribution framework to attribute high (>95th percentile for Canada and
855 Western Amazonia and >90th percentile for Greece) BA in the month of peak anomaly to total
856 climate forcing and socio-economic factors using the ISIMIP3a protocol (see **Table 5**). We
857 used 90th percentile for Greece as using the 95th would restrict our analysis to just three grid
858 cells, and our uncertainty ranges are too large to make a clear statement on such a small
859 subset of data.

860

861 We trained ConFire on observed monthly BA from MODIS MCD64A1 during 2003-2019 at
862 0.5° across the entire region. For model training, we drive ConFire with GSWP3-W5E5
863 forcings provided at a 0.5° spatial resolution by ISIMIP3a, as outlined in **Table 5**. The land
864 surface information (tree cover and non-tree vegetated cover) is derived from the JULES-ES
865 model’s ISIMIP configuration described by Mathison et al. (2023) driven by ISIMIP3a GSWP3-
866 W5E5 forcings. This model includes dynamic vegetation, i.e. changing vegetation cover in
867 response to climate variables, growth, plant competition and mortality. So as not to double
868 count the impact of fire, we turn the interactive vegetation-fire model off. The bias in this land
869 surface information is adjusted to the MODIS Vegetation Continuous Fields collection 6.1



870 remote sensed data for <60°N DiMiceli et al. (2022) and collection 6 for <60°N DiMiceli et al.
871 (2015) using a trend-preserving empirical quantile mapping bias adjustment method
872 implemented with the ibicus software package Spuler et al. (2024). The bias adjustment
873 method calibrates a mapping between the empirical cumulative distribution function of each
874 surface cover type at each grid cell derived from the JULES-ES model output and the
875 corresponding quantiles in the MODIS remote sensed data at this grid cell over the reference
876 period (2003-2019). This method significantly reduces the model bias in the JULES-ES output
877 over the historical period for most regions and variables, ensuring accurate mean and
878 distribution shapes while preserving trends between historical and future periods (**Figure**
879 **S22**). See “**Data and Data Processing**” in **Extended Methods Supplement** for details.

880
881
882 ConFire was run in predictive mode on a monthly timestep and with a similar structure to that
883 used in **Section 2.3.2.3**, with variables representing specific drivers grouped into controls as
884 listed in **Table 5**. However, the specific driving variables used differed to **Section 2.3.2.3** due
885 to the selection of variables available in the forcing data. Specifically, fuel load controls were
886 represented by total vegetation cover and tree cover as drivers; fuel moisture controls were
887 represented by mean consecutive dry days within each month, the fraction of dry days within
888 the month, daily mean precipitation, mean and maximum monthly temperature, mean and
889 maximum VPD as drivers; ignition controls were represented by climatological lightning,
890 pasture, crop and population density as drivers; and suppression controls were represented
891 by pasture, crop and population density drivers. The Bayesian Inference procedure used here
892 is useful when using correlated drivers, which are accounted for in the weights given to driver
893 contributions (Gelman et al., 2013; Kelley et al., 2023). ConFire simulations presented here
894 were performed on all data, with the three experiments outlined under “simulation framework”.

895
896 For each of the experiments detailed above, we output the probability distribution BA for the
897 cells with the top 5% burned fractions for Canada and Western Amazonia, and 10% burned
898 fractions for Greece, to target the most extreme levels of burning.

899
900 To determine the impact of total climate forcing and socioeconomic factors on the increased
901 BA during our focal events, we conducted a paired sampling of monthly burned areas in our
902 target month(s) throughout the test period. This involved comparing the factual and
903 counterfactual scenarios for total climate forcing, as well as the counterfactual and early
904 industrial scenarios for socioeconomic factors (see **Table 5**). As there is no climate influence
905 in the Early Industrial simulation, we first adjusted the target event (a monthly regional BA
906 value) to that expected without climate change. For this adjustment, we find the percentile of
907 the observed BA in the factual and find the BA at the same percentile in the counterfactual.
908 We used paired samples to account for the uncertainty in the underlying mechanisms
909 relating our drivers to burned area, which would co-vary between experiments as per Kelley
910 et al. (2021). In total, we took 200 samples over the 17 years of each simulation, resulting in
911 3400 pairs.

912
913 The likelihood was then simply determined by the number of ensemble members in the
914 factual scenario that predicted greater BA than the counterfactual for total climate forcing, or
915 the counterfactual predicting greater BA than the early industrial scenario for socioeconomic
916 factors. The relative increase in BA extent is the BA in factual over counterfactual (total
917 climate forcing) or counterfactual over early industrial (socioeconomic).

918
919 As per, **Section 2.3.2.3** we evaluated the model using the procedure outline in Barbosa
920 (2024). We do a separate training on 50% of the data between 2003-2011 and evaluation on
921 2012-2019. The framework using ISIMIP3a reanalysis data outperforms its near-real-time
922 counterpart in **Section 2.3.2.3** at simulating burned areas, effectively representing high
923 burned areas and extremes across all regions. It shows a high probability of observations in



924 areas with extreme fires, indicating reliability for attribution analysis. Further details of the
 925 method can be found in supplement **Extended Methods and Evaluation Supplement**.

926
 927
 928

929 **Table 5:** Explanatory variables used for attributing extreme BA (**Section 2.4.4**) and decadal
 930 outlook (**Section 2.5.2**). The explanatory variables are forcing data from the Inter-Sectoral
 931 Impact Model Intercomparison Project (ISIMIP) protocols ISIMIP3a and ISIMIP3b (Frieler et
 932 al., 2024). +ive or -ive under “Controls” describes if a driver increases or decreases BA.

| Variable | Control s | Construction | Source | Reference |
|-----------------------------|-------------------------------------|--|--|--|
| Max. consecutive dry days | Moisture +ive | Monthly max of running count of days since rainfall > 0.1mm/m | Based on precipitation from ISIMIP3a/3b | Frieler et al. (2024) |
| No. dry days | Moisture +ive | fractional no. days of rainfall < 0.1mm/m | Based on precipitation from ISIMIP3a/3b | Frieler et al. (2024) |
| Maximum monthly temperature | Moisture +ive | maximum of maximum daily temperature within the month | Daily temperature approximated as ISIMIP3a/3b daily mean temperature + 0.5xdaily temperature range | Frieler et al. (2024) |
| Mean monthly temperature | Moisture +ive | | ISIMIP3a/3b | Frieler et al. (2024) |
| Mean monthly VPD | Moisture +ive | mean of daily values constructed from specific humidity, surface pressure and max. temperature | ISIMIP3a/3b | Frieler et al. (2024); Barbosa (2024) |
| Maximum monthly VPD | Moisture +ive | max of daily values | ISIMIP3a/3b | Frieler et al. (2024); Barbosa (2024) |
| Tree Cover | Moisture -ive & Fuel +ive | JULES-ISIMIP annual mean tree cover bias-corrected to VCF vs JULES-ISIMIP3a factual interpolated to monthly from annual values | JULES-ES-ISIMIP VCF | DiMiceli et al. (2017); Adzhar et al. (2022); Mathison et al. (2023) |
| Total vegetation cover | Fuel +ive | tree cover plus none-tree vegetated cover simulated by JULES and bias-corrected as above | JULES-ES-ISIMIP VCF | DiMiceli et al. (2017); Adzhar et al. (2022); Mathison et al. (2023) |
| Lightning | Ignitions +ive | Climatology | LIS taken from ISIMIP3a | Kelley et al. (2014); Frieler et al. (2024) |
| Cropland | Ignitions +ive/ Suppression -ive | Interpolated from annual to monthly | ISIMIP3a/3b | Frieler et al. (2024)) |
| Pasture | Ignitions +ive/ Suppression -ive | Interpolated from annual to monthly | ISIMIP3a/3b | Frieler et al. (2024) |
| Population Density | Ignitions +ive/ Suppression -ive | Interpolated from annual to monthly | ISIMIP3a/3b | Frieler et al. (2024) |

933
 934
 935

2.4.4.2 Monthly Median Burned Area

936 Finally, we report changes in present-day monthly median BA to total climate forcing, socio-
 937 economic factors and all forcings using a novel attribution method developed using state-of-
 938 the-art global fire models from the Fire Model Intercomparison Project (FireMIP) (Burton,
 939 Lampe et al., 2023). This employs the same ISIMIP3a simulation framework outlined above,



940 with 7 fire-enabled DGVMs (see **Table S1**) for the period 1901-2019 for the factual and
941 counterfactual experiments. For clarity, ConFire was not used in this element of our attribution
942 approaches; rather, the native fire modelling scheme of each fire-enabled DGVM was
943 employed. Model fire schemes are described in Burton, Lampe et al. (2023).

944 We assess the recent period 2003-2019 in the historical simulation against the counterfactual
945 simulation to find how BA has changed in response to total climate forcing. To attribute
946 changes in BA to socioeconomic factors, the early industrial period (1901-1917) is compared
947 to the recent period (2003-2019) in the counterfactual only simulation. To assess the impact
948 of all forcings the early industrial period in the counterfactual is compared to the recent period
949 in the factual simulation.

950
951 A weighted ensemble of the monthly outputs of BA, based on regional performance against
952 observational data from GFED5 and FireCCI is used for the analysis. Due to large differences
953 in absolute values of BA between the GFED5 and FireCCI observational datasets and across
954 the models, the weightings in the ensemble are based on model capability to capture relative
955 anomalies present in the observational datasets on a regional basis, and all changes are
956 reported as relative anomalies. We focus on the change in monthly median BA, as the fire
957 models underpredict the high tails of the distribution. The weighted models are randomly
958 resampled to generate uncertainty estimates for each region. The method and results are
959 reported in full for all 43 IPCC AR6 regions in Burton, Lampe et al. (2023), and in the current
960 report we select the IPCC regions that align most closely with our focus regions defined in
961 **Section 3.2**.

963 **2.5 Seasonal and Decadal Outlook**

965 **2.5.1 Seasonal Forecasts**

966
967 Among the modes of variability in the climate system most relevant to wildfire activity *globally*
968 is the El Niño-Southern Oscillation (ENSO) (Chen et al., 2017; Mariani et al., 2016; Fuller and
969 Murphy, 2006; Cardil et al., 2023). ENSO is a complex, naturally occurring climate
970 phenomenon characterised by fluctuations in sea surface temperatures and atmospheric
971 pressure across the Pacific Ocean. ENSO has far-reaching consequences generating dry
972 conditions in vast parts of South and Central America, the mediterranean and African savanna.
973 It also exacerbates dry conditions on the west coasts of continents such as California in the
974 United States, southern Europe, and parts of Australia, which can become more susceptible
975 to fires. The geographic areas with such fire favourable teleconnections differ by ENSO phase
976 (Chen et al., 2017).

977
978 Another phenomenon demonstrably linked to global fire activity is the Indian Ocean Dipole
979 (IOD), which occurs in the Indian Ocean and is characterised by differences in sea surface
980 temperatures (SST) between its western and eastern parts. The IOD has a notable influence
981 on weather patterns in various regions of the Southern Hemisphere, particularly affecting the
982 southern and eastern parts of Australia (Harris and Lucas, 2019). Positive IOD events typically
983 lead to reduced rainfall in these areas, resulting in drier-than-normal conditions. However,
984 there is still ongoing debate regarding the direct influence of the IOD on Australian fires, as
985 the signal is often obscured by changes in land management practices (Harris and Lucas,
986 2019).

987
988 ENSO and the IOD have a planetary scale influence on weather anomalies through
989 teleconnections. Other atmospheric modes of variability in the Southern, Northern hemisphere
990 and in the arctic regions can also have strong influence on the seasonal trend of regional
991 burned areas. For example, **Figure S1** shows the climate modes with strongest influence on
992 burned areas globally.



993
994 The large uncertainties in the analysis highlights that there are few regions in the world where
995 it is possible to establish statistically significant teleconnection between burned areas and
996 atmospheric modes. Hence, we utilised the Copernicus Climate Change Service (C3S) multi-
997 model seasonal prediction system to evaluate large-scale climate modes with most proven
998 links to variation in fire activity: ENSO and IOD. The C3S multimodel incorporates forecasts
999 from several prominent meteorological agencies, including the ECMWF, UK Met Office,
1000 Météo-France, German Weather Service (DWD), Euro-Mediterranean Center on Climate
1001 Change (CMCC), US National Weather Service's National Centers for Environmental
1002 Prediction (NCEP), Japan Meteorological Agency (JMA), and Environment and Climate
1003 Change Canada (ECCC). This multi-model system aids in defining the expected evolution of
1004 these two modes of variability. These indices, calculated as Sea Surface Temperature (SST)
1005 anomalies over the ocean, offer a succinct means of understanding the expected strengths of
1006 atmospheric modes of variability in the coming months.

1007
1008 To look more closely at the impact that these two modes might have in landscape flammability
1009 we use seasonal outlooks of the Fire Weather Index (FWI) using one of the models from the
1010 aforementioned multi-model system, ECMWF-System 5. Leveraging seasonal predictions for
1011 the FWI we generated probabilities of exceedance using a 51-member forecast ensemble and
1012 a 24-year model climatological distribution (derived from a 25-member ensemble re-forecast)
1013 covering the period 1993-2016. The probability of exceedance is determined based on the
1014 proportion of forecast members meeting two anomaly criteria at any given geographical point.
1015 We consider the 75th percentile indicative of moderate anomalous conditions and the 95th
1016 percentile indicative of extreme anomalous conditions over a month for the next season.

1018 2.5.2 Decadal Projections of Burned Area

1019
1020 In order to project future changes in BA, we utilised the same modelling approach detailed in
1021 **Section 2.4.4.1**, following a similar protocol to UNEP et al. (2022). We drive the model with
1022 ISIMIP3a and bias-corrected JULES-ES data. For predictive mode, we used bias-corrected
1023 GCM model outputs from ISIMIP3b. ISIMIP3b provides four sets of driving data for 5 bias-
1024 corrected models, including historical data up to 2014 and future scenarios from 2015-2100
1025 (SSP126, SSP370, and SSP585). Each SSP represents future socio-economic pathways and
1026 includes GHG emissions that feed each of the 5 GCMS: GFDL-ESM4 (Held et al., 2019),
1027 IPSL-CM6A-LR (Boucher et al., 2020), MPI-ESM1-2-HR (Mauritsen et al., 2019), MRI-ESM2-
1028 0 (Yukimoto et al., 2019), and UKESM1-0-LL (Tang et al., 2019; Sellar et al., 2019). As part
1029 of ISIMIP3b, each GCM is bias-corrected as described in Lange (2019).

1030 At present, future projections (aligned with shared socio-economic pathways; SSPs) for land
1031 use and population density forcing were not available for ISIMIP3b, so we only considered the
1032 climate's influence on fire distribution and intensity as well as available fuel from vegetation
1033 cover, and not changes in ignitions or land use. We used JULES-ES land cover outputs as
1034 per the previous section, but with JULES driven by each scenario-GCM combination in turn.
1035 This was then bias-corrected in the same mapping procedure as **Section 2.4.4.1**, based on
1036 biases between JULES-ES driven by ISIMIP3a and VCF observations to keep consistent with
1037 GCM bias-correcting procedures. This mapping was subsequently applied to the surface
1038 information outputs from JULES-ES driven by historical (1994-2014) and future (2015-2099)
1039 model runs. To preserve the trend in the vegetation cover over the future periods, additive
1040 detrending of the mean was applied. The results in **Section 3.5.3** are for the months June-
1041 August for Canada, July-September for Greece and August-October for Western Amazonia,
1042 corresponding to those regions' fire seasons today. See "**Data and Data Processing**" in
1043 **Extended Methods Supplement** for details.

1044 Our approach provides a probability distribution representing the uncertainty in future
1045 emissions, climate, and vegetation responses for each scenario and year in the period 2010-



1046 2100. For the first 4 years (2010-2014), we joined the historical experiment to each SSP in
1047 turn.

1048 For Western Amazonia, we additionally tested a 1-in-100 event under 2010-2020 climate,
1049 defined as the BA at the 99th percentile ConFires distribution. We then calculated decadal
1050 average likelihoods of the regions' event each decade up to 2100. Return times are simply
1051 1/likelihood. The change in likelihood of an event occurring (of a given return time) was
1052 calculated relative to the ISIMIP3b 2010-2020 baseline period.

1053 We also calculated the integrated probability of a return of the 2023 Canadian event within the
1054 expected lifespan of an individual. According to UN population statistics, the average life
1055 expectancy of a Canadian citizen born today is 83 years (United Nations Population Division,
1056 2022). In order to cover the 7-year period after 2100, we extrapolated the annual trend in
1057 probabilities. The integrated probability therefore is calculated as the product of the annual
1058 probability of not seeing a fire event like 2023, for each year between 2023 and 2106.

1059 3 Results

1060

1061 3.1 Extreme Wildfire Events of 2023-24

1062

1063 3.1.1 Highlights

1064

1065 • **Global:** A total of 3.9 million km² burned globally during the 2023-24 fire season,
1066 slightly below the average of previous seasons (4.0 million km²) and ranking 13th since
1067 2001. Despite the lower BA, fire C emissions were 16% above average, totaling 2.4
1068 Pg C, ranking 7th highest since 2003. Global C emissions were pushed up by record
1069 emissions in Canadian boreal forests and pulled down by below-average fire activity
1070 in the African savannahs (the largest contributor to global mean annual totals). If global
1071 savannah fire emissions had been in line with their average in 2023-24, global fire C
1072 emissions would have been the highest on record.

1073

1074 • **North America:** Record fire activity in Canada's boreal forests, with BA reaching six
1075 times the average and fire C emissions over nine times the average, contributing
1076 significantly to global C emissions. Canada experienced extreme and widespread fires,
1077 with over 150,000 km² burned, prompting evacuations of 232,000 people and eight
1078 firefighters lost their lives. The United States saw generally below-average fire activity,
1079 but the Lahaina wildfire in Maui, Hawai'i, resulted in 100 civilian deaths, destroyed
1080 2,000 homes, and displaced 10,000 people. Texas recorded its largest ever single fire,
1081 which destroyed 130 homes, killed two civilians, and caused significant livestock
1082 losses. Mexico faced its highest BA in the last decade due to ongoing drought
1083 conditions, with 10,000 km² burned.

1084

1085 • **South America:** South America experienced somewhat below-average fire extent
1086 overall, but notable exceptions included significant anomalies in the northern and
1087 western regions, linked to extended drought and heatwave conditions. In Brazil's
1088 Amazonas state, fire counts reached record highs due to historic drought, severely
1089 impacting air quality in Manaus and leading to deforestation and habitat loss. In Chile,
1090 the Valparaíso wildfire in February 2024 resulted in at least 131 deaths and widespread
1091 property destruction, highlighting severe societal impacts. Fires in Bolivia's La Paz and
1092 Beni departments and Peru's Loreto region caused significant environmental damage
1093 including loss of protected forest and biodiversity, and disruption of indigenous
1094 communities' livelihoods.

1095



- 1096
- 1097
- 1098
- 1099
- 1100
- 1101
- 1102
- 1103
- 1104
- 1105
- 1106
- 1107
- 1108
- 1109
- 1110
- 1111
- 1112
- 1113
- 1114
- 1115
- 1116
- 1117
- 1118
- 1119
- 1120
- 1121
- 1122
- 1123
- 1124
- 1125
- 1126
- 1127
- **Europe:** Low wildfire extent in general, however the Alexandroupolis fire in Greece set a new EU record for individual fire size. Individual fires in Greece, Spain, Italy, Portugal, France, and Scotland led to large-scale evacuations, significant suppression costs, disruption of water supplies, damage to infrastructure or agricultural lands, impacts on tourism and local economies, destruction of properties, or loss of life.
 - **Oceania:** Above-average fire activity in northern Australia's savannahs, grasslands, and shrublands was linked to fuel growth from three years of La Niña. Although less impactful than the 2019-20 Black Summer fires, wildfires near Perth resulted in five homes lost and several injuries. The Tara and Mount Isa fires in Queensland destroyed 65 homes and claimed two lives. In Victoria, fires destroyed over 40 homes and injured five firefighters. In New South Wales, forest fires caused widespread smoke-related damages.
 - **Asia:** The 2023-24 fire season in Asia saw generally low fire activity, with central Asia experiencing below-average burned areas. Lao PDR, Thailand, and Vietnam had high fire counts amidst heatwave conditions and a possible uptick in agricultural fire use, leading to severe regional haze and air quality issues. In Mongolia's Dornod Aimag province, wildfires burned large parts of the Daurian steppe and required extensive firefighting efforts to stop fires from crossing into Russia. Additionally, wildfires in Russia's southern borders, including Tyumenskaya, Omskaya, and Amurskaya Oblasts, caused evacuations, property damage, and at least one fatality.
 - **Africa:** Low wildfire extent in general with BA 13% below average in the African grassland, savannah, and shrubland biome. However, extreme fires in Northern Africa, particularly Algeria and Tunisia, prompted significant emergency responses including assistance from the EU. In Algeria, wildfires occurring in temperatures around 50°C resulted in 34 deaths and over 1,500 evacuations, with over 8,000 personnel deployed to combat the fires. Tunisia faced similar challenges with strong winds exacerbating wildfires, leading to evacuations in the northwestern region. In coastal South Africa, fires in the Western Cape caused structure damage and evacuations.

1128 **3.1.2 Global Perspective from Earth Observations**

1129

1130 **3.1.2.1 Extreme Fire Seasons Evident in Earth Observations**

1131

1132 According to the MODIS BA product, 3.9 million km² burned globally during the 2023-24 global
1133 fire season (March 2023-February 2024), slightly below the average of previous fire seasons
1134 (4.0 million km²) and overall ranking 13th of all fire seasons since 2001 (Jones et al., 2024).
1135 Despite this, fire C emissions were 16% above average at 2.4 Pg C during the 2023-24 global
1136 fire season, which ranks 7th amongst all fire seasons since 2003 (based on annual averages
1137 of GFED4.1s and GFAS estimates; see methods; Jones et al., 2024).

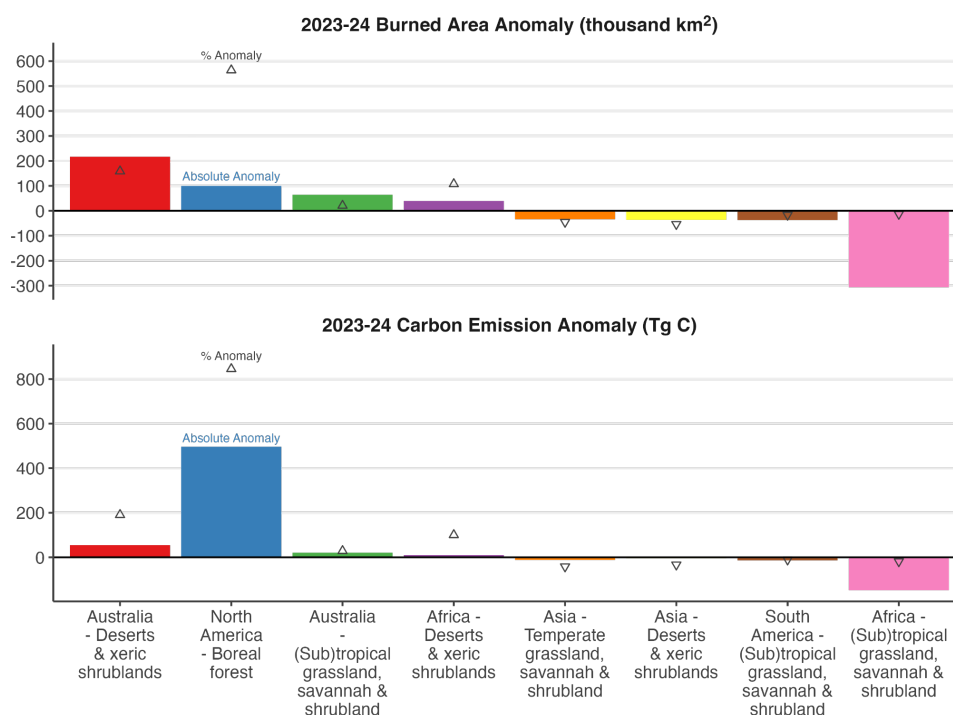
1138

1139 Stark regional contrasts in the anomalies in BA, fire C emissions and individual fire properties
1140 are visible in the Earth Observations on various regional scales (**Figure 1, Figure 2, Figure**
1141 **3**). **Figure 1** shows the strongest BA and fire C emissions anomalies of 2023-24 at continental
1142 biome scale versus previous fire seasons. BA was around 300 thousand km² (13%) below
1143 the average of previous fire seasons in the African grassland, savannah and shrubland biome,
1144 which is the largest contributor to global mean annual BA totals. BA was below average in the
1145 South American grassland, savannah and shrubland biome in 2023-24 and in Asian non-forest
1146 biomes. The global pattern of lower BA in savannah-like systems in 2023-24 was not observed
1147 in Australia, where several non-forest biomes experienced well above-average BA.

1148



1149 The North American boreal forests experienced a record-breaking fire season, with BA
 1150 reaching six times the average since 2001 and fire C emissions reaching over nine times the
 1151 average since 2003 (**Figure 1**; Jones et al., 2024). This strong regional signal primarily
 1152 explains the above-average global C emissions total of 2023-24, with the high rates of fire
 1153 emissions per unit area in boreal forests aggregating to override the reduced emissions totals
 1154 in African and South American savannahs. Record levels of fire C emissions were seen also
 1155 across the global pan-boreal forest biome, with fire C emissions surpassing the pan-boreal
 1156 record set in 2021 by more than 60%. This is despite a below-average fire season for BA and
 1157 fire C emissions in boreal Asia during 2023-24, in contrast to the 2021-22 fire season when
 1158 there was a synchronous peak in BA in both the Eurasian and North American boreal regions
 1159 (Zheng et al., 2021). According to the Global Fire Atlas, new records for individual fire size
 1160 and rate of spread were also set in the North American boreal forests during 2023-24, while
 1161 the upper 5% of fires ranked by size and rate of growth in 2023-24 were in the top 2 and 3
 1162 years on record since 2002, respectively.
 1163



1164 **Figure 1:** Anomalies in BA and C (C) emissions for selected continental biomes in the 2023-
 1165 24 global fire season (March 2023-February 2024), versus the average of prior fire seasons
 1166 since 2001. The selected regions all contribute at least 0.1% towards global mean annual BA
 1167 and experienced BA anomalies of over $\pm 30,000$ km² in the 2023-24 global fire season. Relative
 1168 changes (%) are also marked by triangular symbols and can be read on the same scale as
 1169 the absolute values.
 1170

1171
 1172
 1173 Anomalies in the African (sub-)tropical grasslands, savannahs and shrublands strongly drive
 1174 inter-annual variability in global fire C emissions because this biome contributes on average
 1175 58% towards total global BA and 40% towards total global fire C emissions. If fire C emissions
 1176 from African (sub-)tropical grasslands, savannahs and shrublands had been around average



1177 fire season in 2023-24, then global fire C emissions would have been the greatest of any fire
1178 season on record since 2003.

1179
1180 Elsewhere at the biome scale, BA extent was in the top three years on record in the South
1181 American broadleaf and mixed forests, the African xeric shrublands, and Australian xeric
1182 shrublands, and the Australian (sub-)tropical grasslands, savannahs and shrublands (**Figure**
1183 **1**). In contrast, BA or fire C emissions were the lowest on record in the European temperate
1184 broadleaf and mixed forests and Asian xeric shrublands, and in the bottom three years on
1185 record in the African savannahs, Asian montane grasslands and shrublands, and European
1186 tropical grasslands and shrublands.

1187
1188 On national levels, the most prominent global anomaly of the 2023-24 fire season occurred in
1189 Canada where BA reached six times the average of previous fire seasons and fire C emissions
1190 reached nine times the average of previous fire seasons. Across the Canadian provinces and
1191 territories, the highest BA or fire C emissions on record were observed in Northwest
1192 Territories, British Columbia, Alberta, and Quebec while Yukon, New Brunswick, and Ontario
1193 also experienced high-ranking years (**Figure 2, Figure 3**). The positive BA anomalies in
1194 Canada were visible in the MODIS BA dataset from as early as April 2023 in most provinces
1195 and persisted throughout summer through to October and even through to December 2023
1196 and January 2024 in British Columbia and Alberta (**Figure S2**). Peak anomalies were
1197 observed in Eastern Canada in June 2023, arriving later in western Canada (August-
1198 September). Data on individual fire characteristics from the Global Fire Atlas further reveals
1199 new record fire counts in many Canadian provinces, and high-ranking anomalies in fire count
1200 and daily rate of growth across Canada, as well as new records for fire size and rate of spread
1201 in provinces of both eastern and western Canada (**Figure 4; Jones et al., 2024**). **Section**
1202 **3.1.3.4** discusses the unprecedented Canadian fire season of 2023-24 in greater detail,
1203 including its impacts and regional context.

1204
1205 A second prominent regional feature of the 2023-24 global fire season, visible in Earth
1206 observations, is a cluster of administrative regions with positive BA and C emissions
1207 anomalies in the north and west of tropical South America (**Figure 2, Figure 3**). Bolivia,
1208 Guyana, Suriname and French Guiana, Honduras, Nicaragua and Belize all experienced a
1209 high-ranking fire season at national level in 2023-24. In addition, BA or fire emissions were
1210 ranked in the top three years in western parts of Amazonia including in Amazonas state of
1211 Brazil, the Loreto department of Peru, and the La Paz and Beni departments of Bolivia.
1212 Anomalies in the western Amazon spanned June 2023-January 2024, peaking in August-
1213 October 2023. In the north of South America, high-ranking fire seasons were seen in
1214 Venezuela, various subdivisions of Guyana, Suriname, and French Guiana, and in Amapá
1215 State in Brazil. The anomalies in northern South America spanned May 2023-February 2024,
1216 peaking in November 2023-February 2024 (**Figure S2**). The Global Fire Atlas data suggest
1217 that South American anomalies in BA during the 2023-24 fire season were principally driven
1218 by a large number of fires, whereas anomalies in fire size or rate of growth were uncommon
1219 in most of South America (**Figure 4**). **Section 3.1.3.6** discusses the 2023-24 fire season of
1220 tropical South America and its impacts and regional context in greater detail.

1221
1222 Several parts of South and Southeast Asia experienced high-ranking anomalies in BA or fire
1223 C emissions during the 2023-24 fire season, including various neighbouring administrative
1224 zones of Lao People's Democratic Republic (PDR), Thailand and Vietnam. The temporal peak
1225 of these anomalies was broadly in March-May 2023. Data on individual fire characteristics
1226 indicates that high-ranking fire counts, rather than anomalies in fire size, were the primary
1227 driver of the regional BA anomalies (**Figure 4**). **Section 3.1.3.2** discusses these anomalies
1228 and their impacts in greater detail.

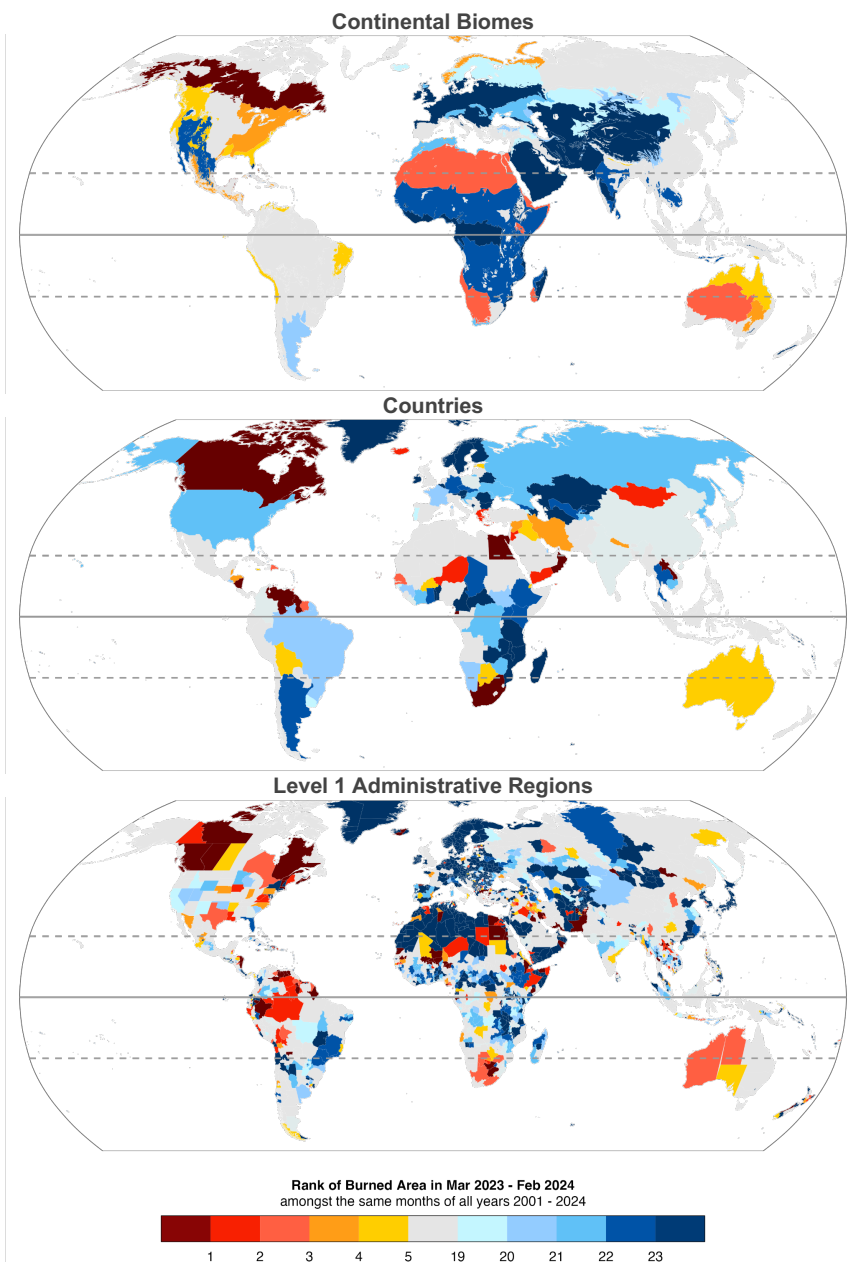
1229
1230 The anomalies observed in xeric biomes of Oceania are also apparent as high-ranking BA or
1231 C emissions in the 2023-24 fire season in western parts of Australia, particularly in Western



1232 Australia and the Northern Territory (**Figure 2, Figure 3**). Fires tended to affect more remote
1233 areas and so the impacts on society were muted in comparison to the Black Summer events
1234 affecting southeast Australia in 2019-20 (Abram et al., 2021); however, **Section 3.1.3.5**
1235 discusses some notable exceptions.
1236
1237 Other regional pockets of high-ranking BA anomalies or C emissions anomalies were
1238 observed in various dry zones of Africa and the Middle East, including the Sahel, Northern
1239 Africa and the Horn of Africa, Southern Africa (specifically South Africa and Botswana where
1240 three good rainfall years have resulted in grass fuel accumulation), parts of Iran, Iraq, parts of
1241 the Levant region, and parts of the Arabian Peninsula (**Figure 2, Figure 3**). Although various
1242 aspects of the fire season ranked highly in these regions, they are also fuel-limited with a
1243 generally a low baseline for BA and fire C emissions and the wildfire season. Nonetheless,
1244 regionally impactful wildfires were reported for Algeria, Tunisia and Morocco as well as coastal
1245 regions of South Africa and in Pakistan and are discussed further in **Section 3.1.3.1** and
1246 **Section 3.1.3.2**.
1247
1248



1249
1250



1251
1252

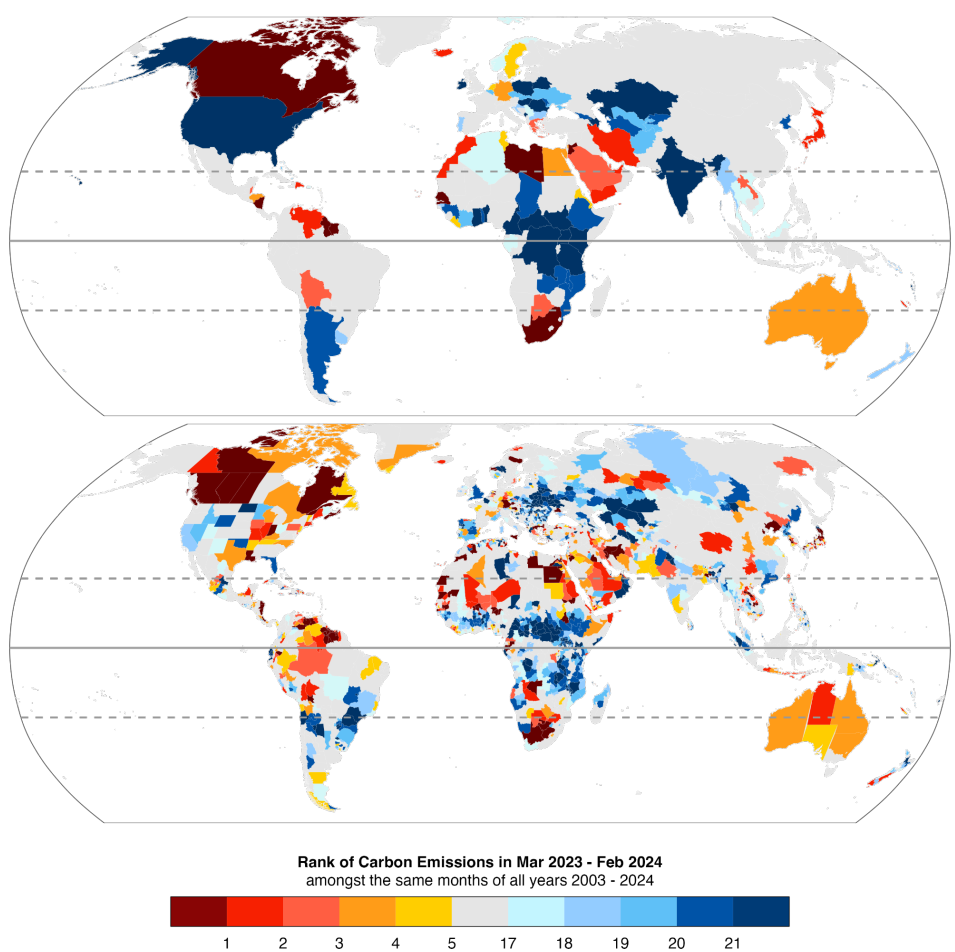
1253
1254

1255
1256

1257 **Figure 2:** Ranks of BA during March 2023–February 2024 versus previous March–February
1258 periods ($n = 23$ global fire seasons) for three regional layers: **(top panel)** continental biomes;
1259 **(middle panel)** countries, and; **(bottom panel)** states or provinces. Results for regions with
1260 high-ranking (top 5 years) or low-ranking (bottom 5 years) events are highlighted. The timing
1261 of BA anomalies is shown in **Supplementary Figure 2**.
1262



1263

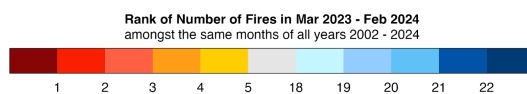
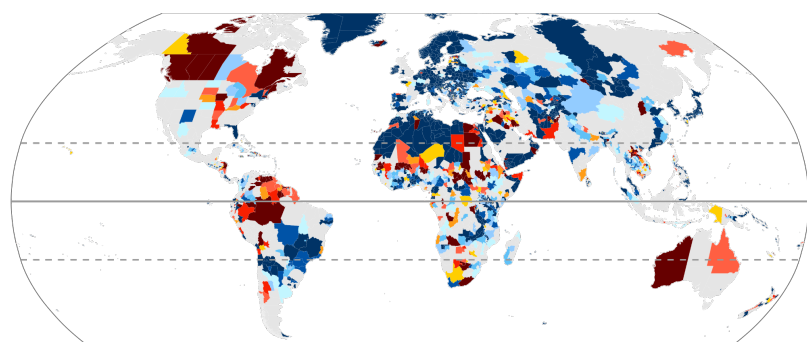


1264
1265
1266
1267
1268
1269
1270

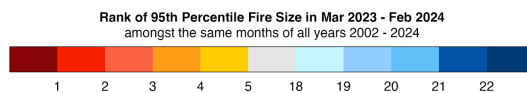
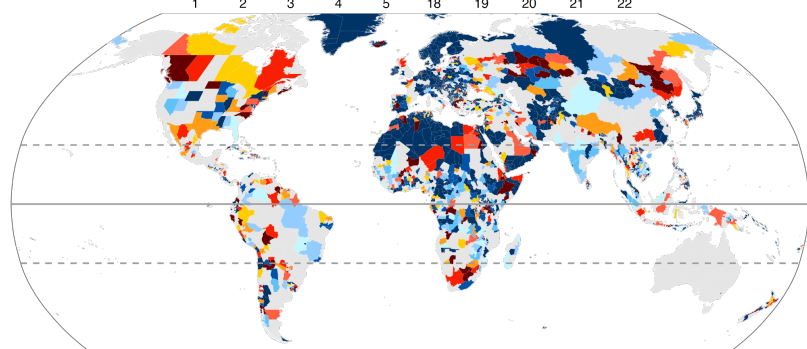
Figure 3: Rank of fire C emissions during March 2023-February 2024 versus all March-January periods since 2003 ($n = 21$ global fire seasons), at the scales of **(top panel)** countries and **(bottom panel)** level 1 administrative regions. We consider C emissions estimates from two products (GFAS and GFED), first calculating the mean emissions value from the two products, then ranking the values.



1271



1272



1273

1274

1275

1276

1277

1278

Figure 4: Ranks of **(top panel)** fire count, **(middle panel)** 95th percentile fire size, and **(bottom panel)** 95th percentile daily rate of growth during March 2023–February 2024 versus all March–February periods since 2002, at the scale of states or provinces (GADM administrative level 1 regions).



1279 **3.1.2.2 Extreme Individual Fires in Earth Observations**

1280

1281 The Global Fire Atlas (GFA) is one of several products tracking daily fire progression and
1282 identifying individual fires at global scale based on moderate resolution satellite data (Andela
1283 et al., 2019; Laurent et al., 2018; Artés et al., 2019). The product uses the MODIS BA product
1284 and the smallest unit of disaggregation is 500m and the shortest timestep on which the
1285 expansion of a fire can be observed is daily. The Global Fire Atlas is expected to represent
1286 the dynamics of large fires better than small, fast-moving fires.

1287

1288 The GFA represents some of the most impactful individual fire events in 2023-24 with varying
1289 skill (**Table 6; Figure S3, Figure S4, Figure S5**). For example, the Alexandroupolis fire that
1290 occurred in the decentralised administration of Macedonia and Thrace, Greece, in late August
1291 was captured reasonably well. The GFA identifies two fires that ignited on 19th August and
1292 merged to form one contiguous burned unit with an area of approximately 900 km². Alignment
1293 of the fire's timing, size and perimeter with high-resolution satellite imagery (**Figure S3**) and
1294 detailed reports (Xanthopoulos et al., 2024) suggest an overall reliable representation of this
1295 event. The impacts of this fire are discussed in detail below in **Section 3.1.3.3**. Notably,
1296 observations from the Visible Infrared Imaging Radiometer Suite (VIIRS) sensor, which
1297 features higher resolution and higher overpass frequency, did not improve the characterisation
1298 of this particular event (**Figure S3**).

1299

1300 A deadly fire near Valparaíso, Chile, is also captured with reasonable skill in the GFA (**Figure**
1301 **S4**). Around 90 km² was burned, with the fire skirting the city of Placilla de Peñuelas and
1302 encroaching upon Viña del Mar and Quilpué (**Section 3.1.3.6**). The timing, extent and
1303 perimeter of the fire as recorded by the GFA compares well with those reported by other
1304 sources (**Table 6**).

1305

1306 Among the largest fires to occur in Canada during 2023-24 happened near the La Grande
1307 Reservoir in Quebec, Canada. According to both the Global Fire Atlas and a separate NASA
1308 fire tracking product based on the VIIRS sensor, the fire's extent was around 11 thousand
1309 km², whereas the National BA Composite (NBAC; Skakun et al. 2022) shows a slightly lower
1310 extent nearer 10 thousand km². The timing of the fire also showed high correspondence across
1311 the products.

1312

1313 The Lahaina wildfire in Maui, Hawai'i, is an example of an event that was captured poorly by
1314 the GFA. Issues relating to the small scale of this fire relative to the resolution of the MODIS
1315 BA data are evident in **Figure S4**. As the MODIS BA algorithm is focussed on the detection of
1316 wildland fire, its effectiveness in tracking fires at the wildland-urban interface is limited. In this
1317 case, burned areas were not detected in cells in urban areas or at the wildland-urban interface,
1318 and hence the size of the fire was under-estimated significantly (**Table 6**). The timing of the
1319 fire on vegetation land adjacent Lahaina was compatible with reference reports.

1320

1321 Another example of the challenges of defining individual fire extent and applying global
1322 algorithms to do so comes from Western Australia (**Figure S5**). Two fires recorded by the
1323 Department of Fire and Emergency Services, Western Australia (the Great Sandy Desert and
1324 Anna Plains fires) totalled 57 thousand km² in extent. In the Global Fire Atlas, the burned cells
1325 detected by MODIS were instead dissected into 53 separate fires with the largest unit burning
1326 560 km². The date ranges were also rather different with the first record of fires logged in
1327 agency data one month later than in the Global Fire Atlas and the final record logged one
1328 month earlier.

1329

1330



1331 **Table 6:** Representation of selected individual fire events in the MODIS BA product (Giglio et
 1332 al., 2018) and Global Fire Atlas (Andela et al., 2019).

| Event | GFA Fire Size (km ²) | GFA Dates | Reported Area (km ²) (Reference) | Dates (Reference) | Reference | Comment |
|--|----------------------------------|--------------------------|--|--------------------------|--|---|
| Alexandroupolis Wildfire, Greece | 892 | 19/08/2023 to 30/08/2023 | 930 | 19/08/2023 to 31/08/2023 | Xanthopoulos et al. (2024) | Good characterisation of the event, with two fires merging in the date range and ultimate fire size comparable to reference. |
| Fire near La Grande Reservoir, Quebec, Canada | 10,725 | 29/05/2023 to 23/07/2023 | 11,400 (VIIRS) 9,694 (NBAC) | 01/06/2023 to 23/07/2023 | NASA Earth Observatory (2023; VIIRS); Jain et al. (2024; NBAC) | Reasonable characterisation of the fire's extent and timing. |
| Valparaiso Wildfire, Chile | 91.54 | 31/01/2024 to 10/02/2024 | 85 | 02/02/2024 to 05/02/2024 | NASA Earth Observatory (2024); Copernicus Emergency Management Service (2023a) | Good characterisation of the scale of the event and its perimeters at various wildland-urban interfaces, versus reference data. |
| Lahaina Wildfire, Maui, Hawaii | 1.50 | 08/08/2023 to 12/08/2023 | 8.49 | 08/08/2023 to 09/08/2023 | Fire Safety Research Institute (2024) | MODIS data has coarse spatial resolution relative to scale of event. Spread into urban areas not captured. |
| Western Australia (Great Sandy Desert and Anna Plains fires) | 45,544 | 31/08/2023 to 28/11/2023 | 56,561 | 27/09/2023 to 01/11/2023 | Department of Fire and Emergency Services, Western Australia (Shapefile for the Great Sandy Desert and Anna Plains fires; Agnes Kristina, pers. comm.) | GFA splits this event into 53 fires; we report their total combined area. Largest individual fire area in GFA was 760 km ² (ignited 06/09/2023). Great Sandy Desert and Anna Plains fires merged on 25th October 2023. |

1333

1334

1335 **3.1.3 Year in Review by Continent**

1336

1337 **3.1.3.1 Africa**

1338

1339 South Africa and Botswana experienced higher than average BA and fire size (**Figure 2**,
 1340 **Figure 4**) in 2023-24, linked to three consecutive years of above-average rainfall that
 1341 increased grassy fuel loads in the arid (fuel-limited) savannas and grasslands. This has
 1342 potentially been exacerbated by a lack of prescribed burning and active fire suppression in the
 1343 privately held land and conservancies in the region, that likewise would have resulted in fuel
 1344 build-up (*Atlas of Namibia*, 2021). The socio-economic impacts of these large fires were
 1345 minimal (extensive grassland fires linked to high rain years are expected due to periodic 7-20
 1346 year wet-dry cycles in these ecosystems). However, some farmers in western Botswana



1347 reported increased livestock losses from predators such as lion, wild dog and hyena, with the
1348 reduced vegetation cover after the fires driving predators to shift from wildlife prey to livestock.
1349

1350 In East Africa, the area burned was extremely low in 2023-24 due to the 2020-2023 triple la
1351 Nina experienced in this region, which causes droughts in East Africa (while increasing rainfall
1352 in southern Africa). This multi-year drought meant that there were no grass fuels to burn and
1353 reduced the likelihood of spread of accidental ignitions in many of the East African rangelands.
1354 However, the extreme fire weather enabled fires to burn through upland forests, which are not
1355 normally flammable. The Aberdare Forest, in Nyeri county Kenya had a fire incident on the
1356 17th of Feb 2023 that destroyed over 160 km², and was attributed to the dry conditions (*Citizen
1357 Digital*, 2023). This also occurred at a time when the country was undergoing a heatwave.
1358 This highlights the different responses of grassland and forest vegetation to the same climate
1359 conditions.

1360
1361 The 2023 heatwave in North Africa exacerbated fire behaviour in the region (*Al Jazeera*,
1362 2023a). Algeria recorded significant fires in the latter half of July, facilitated by high
1363 temperatures that reached upwards of 48°C (*Al Jazeera*, 2023b). Over 8,000 personnel,
1364 including firefighters and the military, were deployed to combat rapidly spreading fires across
1365 15 provinces (*South African Broadcasting Corporation*, 2023a). These efforts were critical in
1366 managing fires that forced over 1,500 people from their homes (*euronews*, 2023). Despite
1367 these efforts, the wildfires claimed the lives of at least 34 individuals, including 10 soldiers (*Al
1368 Jazeera*, 2023b).

1369
1370 Neighbouring Tunisia also faced wildfire outbreaks, exacerbated by strong winds that carried
1371 fires across the national border from Algeria, leading to the closure of two border crossings
1372 (*Reuters*, 2023a). The Tunisian wildfires prompted evacuations in the north-western region of
1373 Tabarka, affecting at least 300 people and extending firefighting efforts to Bizerte, Siliana, and
1374 Beja (Sullivan and Tondo, *The Guardian*, 2023). Resources such as firefighting aircraft and
1375 personnel were sent from EU nations to help tackle the fires, despite the challenging
1376 conditions imposed by near-record temperatures of 49°C (Gauldie, *AirMed&Rescue*, 2024).
1377 In August, forest fires in mountainous regions of Morocco were also fanned by strong winds
1378 and facilitated by protracted hot spring and summer temperatures (Erraji, *Morocco World
1379 News*, 2023; Copernicus Climate Change Service, 2024a).

1380
1381 During December 2023-January 2024, the Western Cape of South Africa experienced
1382 wildfires related to prolonged hot and windy conditions, causing substantial damage and
1383 prompting widespread evacuations. In the Overstrand local municipality, which includes
1384 coastal towns like Pringle Bay and Betty's Bay, multiple fires necessitated evacuations and
1385 destroyed properties. The Hangklip area between Pringle Bay and Betty's Bay was particularly
1386 affected with the fires destroying properties in the Sea Farm private nature reserve. On
1387 January 29, a "code red" status was declared, indicating a serious threat to residential areas,
1388 and evacuations were advised for communities including Silversands and Seafarms (*Crisis24*,
1389 2024; *AfricaNews*, 2024). A wildfire swept from Simonstown to Scarborough in Cape Town,
1390 necessitating large-scale evacuation (Hough, *IOL News*, 2023). This fire was challenging due
1391 to its rapid spread fueled by strong south-easterly winds and high temperatures. The
1392 firefighting efforts were supported by multiple helicopters and ground teams (*South African
1393 Broadcasting Corporation*, 2023a). The most extensive damage was reported from the
1394 Kluitjieskraal fire near Wolseley, where over 220 km² were burned, and more than 40
1395 structures were destroyed. This fire also prompted evacuations and remained uncontained for
1396 several days due to its size and complex terrain that hindered ground access (*Crisis24*, 2024).
1397 . Despite these extreme wildfires, the plantation forestry industry was not affected, with
1398 relatively low losses due to fire.

1399

1400 3.1.3.2 Asia

1401



1402 The 2023-24 fire season in Asia was generally not an extreme one, with much of central Asia
1403 experiencing low BA. Siberia, which has seen several record-breaking fire seasons since 2020
1404 resulting in globally significant fire emissions (Zheng et al., 2021), also experienced a
1405 somewhat typical year for BA and fire C emissions. Likewise most provinces of China and
1406 states of India experience a fairly typical fire season.

1407
1408 Nonetheless, there were regional examples of high fire activity in the 2023-24 fire season. The
1409 Dornod Aimag province of eastern Mongolia, near the borders with Russia and China,
1410 experienced several extreme fires during April 2023 that are also visible as anomalies in the
1411 global fire observations (**Figure 2, Figure 4**). Over 15% of the area of Dornod Aimag burned
1412 in 2023-24 in contrast to the 23-year average of below 5%. The province includes the
1413 Mongolian part of the Daurian steppe, notable for being one of the last remaining undisturbed
1414 steppes in the world (UNESCO World Heritage Centre, 2017). Unusually dry and warm
1415 conditions in eastern Mongolia during spring led to severe wildfires. A notable wildfire spread
1416 into Dornod from neighbouring Sukhbaatar province, fanned by windy, dry conditions (*Borneo
1417 Bulletin*, 2023). The National Emergency Management Agency mobilised over 250 individuals,
1418 including firefighters and local residents, and helicopters were deployed to manage the fast-
1419 spreading fires (*Borneo Bulletin*, 2023). The effects of these wildfires on herder and nomadic
1420 populations compounded the losses of 2 million livestock over the harsh winter in Mongolia,
1421 and the Mongolian Red Cross has provided aid to 4,800 herder households (International
1422 Federation of Red Cross and Red Crescent Societies, 2023).

1423
1424 Although BA extent and fire counts were overall below the 2001-2023 average along the
1425 southern border regions of Russia during 2023-24 (**Figure 2, Figure 4**), a number of disruptive
1426 wildfires fanned by strong winds broke out during April and May and affected regions bordering
1427 Kazakhstan, such as in the Tyumenskaya, Omskaya, and Amurskaya Oblasts where an
1428 emergency was declared, and Mongolia, such as in Irkutsk and Krasny Yar where at least one
1429 fatality was recorded (*Le Monde*, 2023). As well as detecting anomalies in fire size and rate of
1430 spread in these areas, the Global Fire Atlas also identified regionally large and fast-moving
1431 wildfires in the Russia-China border zone of Manchuria (**Figure 4**), however these were not
1432 widely reported on by media outlets or local authorities.

1433
1434 Lao People's Democratic Republic (PDR) experienced a notable fire season in 2023-24,
1435 marked by record-setting BA at national level since 2001 in the MODIS BA data (**Figure 2;**
1436 **Figure S6**). The fires were widespread, affecting various provinces from the south to the north,
1437 including Attapu, Khammouan, Louangphabang, Xaignabouli, and Bokeo. In Attapeu, BA in
1438 2023-24 was over twice the average of prior fire seasons since 2001. The fires in 2023-24
1439 were generally small in scale but anomalously numerous, consistent with the widespread use
1440 of slash-and-burn agricultural fires in these regions that have been problematic for regional air
1441 quality in this region during recent years (Meadley, *Laotian Times*, 2024). The uptick in fire
1442 counts in 2023-24 has been attributed in part to economic factors such as the high price of
1443 cassava and demand for greater corn supplies to supply animal feed, which act as incentives
1444 for farmers to clear forests for additional planting (Bhandari, *Radio Free Asia*, 2024). On top
1445 of economic factors, an enabling driver was an extreme heatwave that extended eastward
1446 from South Asia to Southeast Asia in April 2023 (Zachariah et al., 2023). The persistent smoke
1447 from these fires worsened air quality significantly in southeast Asia, where efforts to manage
1448 transboundary haze have been challenging during regional droughts, despite a new
1449 transboundary agreement being signed in 2023 (Antara News, 2023). Differences in fire
1450 management between Thailand and Lao PDR were evident during the 2023 event, with
1451 authorities intensifying patrols and seeking to control forest fires and agricultural burning for
1452 improved air quality in Thailand (Meadley, *Laotian Times*, 2024). Conversely, deforestation
1453 remains a critical issue in Lao PDR, with the Laotian government facing challenges in gaining
1454 local community support for the prevention of agricultural expansion and logging.

1455



1456 Earth Observations data showed high-ranking BA anomalies and fires with large size and rate
1457 of growth during 2023-24 in several regions of Pakistan, Iran, Iraq, and parts of the Levant
1458 region (**Figure 4**), consistent with reports of extreme drought-driven wildfires in some of these
1459 regions (*Reuters*, 2023b).

1461 **3.1.3.3 Europe**

1462
1463 Overall, fires burned 8,400 km² in Europe from March 2023 to February 2024 according to the
1464 European Forest Fire Information System (EFFIS, 2024), of which 64.5% were from July to
1465 September and 18.1% were in March and April. Large fires (>5 km²) amounted to 53.4% of
1466 the total BA, and those particularly large (>100 km², n=5) accounted for 17.7% of the total
1467 burned area. More than half (52.6%) of the BA corresponded to transitional woodland, with
1468 forests, shrublands and grasslands, and agriculture respectively amounting to 19.1%, 13.2%,
1469 and 14.4%. At least 44 people died as a direct result of wildfires (Copernicus Climate Change
1470 Service, 2024; Centre for Research on the Epidemiology of Disasters, 2024).

1471
1472 Most countries in the Mediterranean Basin experienced mild to typical fire seasons in general,
1473 with variable timing but affecting mostly non-forest (open) vegetation types (EFFIS, 2024). In
1474 the Balkans, fire activity varied among countries, but was mostly very low by historical patterns
1475 such as in Croatia, however, a major exception was Greece described in more detail below
1476 (**Figure 2**, **Figure 4**, **Figure 5**). The other exceptions were North Macedonia, with a typical
1477 fire year and Bulgaria, the worst year in a decade, with fire activity extending into October in
1478 both countries; and Bosnia and Herzegovina, Serbia and Montenegro, where collectively ~270
1479 km² burned in January-February 2024.

1480
1481 Greece's 2023 fire season was reviewed at length by Xanthopoulos et al. (2024). It was the
1482 second worst on record regarding total area burned (1,727 km²), despite the recent efforts to
1483 strengthen the firefighting mechanism of the country with more aerial resources and new
1484 personnel, after another challenging fire season in 2021. The situation was kept under control
1485 until mid-July, but in the period July 13-27, maximum temperature in many parts of the country
1486 exceeded the average for the 2010-2019 period by as much as 10°C, according to the records
1487 of the National Observatory of Athens. This resulted in multiple fire starts pushing the limits of
1488 firefighting, which relies heavily on the aerial resources. The fires starting 18th of July on the
1489 tourist island of Rhodes grew rapidly on the second day, finally burning 207 km² and stopping
1490 at the sea. About 20,000 tourists had to be evacuated from hotels along the coast. While the
1491 fire on Rhodes was still burning, three forest fires started on 3rd of July started near the city
1492 of Aigio, in North Peloponnese, on the island of Corfu and near the town of Karystos in the
1493 south of Evia island. On July 25th a Canadair CL-215 crashed near the village of Platanistos
1494 while fighting this last fire. Then, on July 26th, the tail of a cold front that passed over Greece,
1495 with the characteristic wind direction change that accompanies it, created further challenges,
1496 as a number of fire starts in central Greece and Thessaly spread fast, burning mostly in light
1497 fuels, challenged firefighters and threatened inhabited areas. One of the fires entered an Air
1498 Force base on the 27th, causing a powerful explosion of ammunition that resulted in damages
1499 to the town of Nea Aghialos 5 km away. By the end of July, the BA across the country had
1500 reached 550 km².

1501
1502 The next wave of multiple challenging fires in Greece began on 19th August. A lightning-
1503 caused fire that started before dawn NE of Alexandroupolis in the prefecture of Evros received
1504 limited attention at first and was destined to become the largest fire in recent European history.
1505 The fact that firefighting resources were focussed on evacuation of the villages in the path of
1506 the fire, rather than fire suppression may have contributed to its eventual size. On the 21st of
1507 August, a second fire started to the north of the first one, near the village of Dadia. Fanned by
1508 a strong NE wind, it spread quickly and within a few hours it reached the rear of the first one.
1509 On that day fire behaviour both in terms of spread and intensity was extreme (Athanasίου,
1510 2024). Nineteen immigrants who had illegally entered the country and were trekking through



1511 the forest, were trapped by the flames and were found dead on the 22nd of August. Another
1512 group was saved by the firefighters at the last moment. The authorities emphasised safety
1513 and evacuated the hospital in the outskirts of Alexandroupolis.

1514
1515 On Aug. 22, while the Evros fire was the focus of attention, a fire originating at more than one
1516 point near the village of Phylli, south of mount Parnis in Attica, at the outskirts of Athens started
1517 growing against the strong NE wind. Once more, many settlements were evacuated and
1518 firefighting attention focused on protecting homes, as the fire moved slowly up the mountain
1519 slopes finally burning 62 km² in three days. The Evros fire kept growing at various rates for
1520 the next 15 days, finally reaching 938 km² and becoming the largest on record in recent history
1521 in Europe. The simultaneous spread of the Evros fire, the fire in Attica and a number of smaller
1522 fires, is likely to have increased the growth rate statistics (km day⁻¹) for fires in the region
1523 (**Figure 4** and **Figure 5**).

1524
1525 The BA of the Evros fire included 258 km² of deciduous oak forest and 218 km² of oak forest
1526 mixed with other species (Konstantinos Kaoukis, personal communication). The usually most
1527 challenging forest types regarding fire behaviour, contributed less to burned area: 128 km²
1528 forest and 152 km² of evergreen shrubs. The fire was mostly brought into control only when it
1529 reached agricultural areas and barren lands. The final size of the Evros fire may not be solely
1530 attributed to adverse meteorological conditions. One aggregating factor may have been the
1531 recent shift in directing firefighting personnel more strongly from suppression towards
1532 evacuation, another the emphasis on aerial firefighting resources (Xanthopoulos et al., 2024).
1533 The latter was not effective once the extreme fire behaviour commenced (21st to 23rd of
1534 August). Deep forest litter layers further hampered fire suppression in some areas, although
1535 a group of local forest workers working with handtools, were credited by the local forest service
1536 officers with control of a large part of the fire perimeter to the north, saving an estimated 100
1537 ha of forest (Athanasiou, 2024).

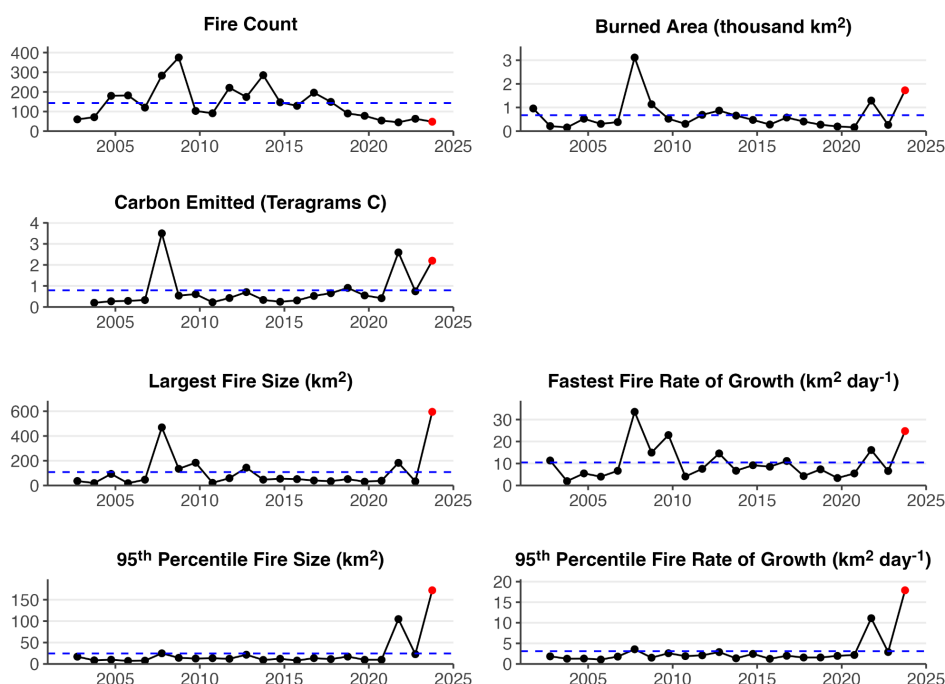
1538
1539 Italy was the second most affected country after Greece, with continuous fire activity from July
1540 to October. More than 1,000 km² burned in the country, of which 69% were in Sicily (including
1541 17 fires >10 km²), although the largest fire (31 km²) occurred in the nearby region of Calabria
1542 (Istituto Superiore per la Protezione e la Ricerca Ambientale, 2023). A defining characteristic
1543 of these large fires was the importance (42% overall) of agricultural land in the BA composition.
1544 The outskirts of Palermo and the Madonie Natural Regional Park were impacted by multiple
1545 wildfires in late September, causing one fatality and affecting wildland-urban interfaces, farms,
1546 and tourism.

1547
1548 Fire activity was insignificant in France, except for benign mountain burning (175 km²) in
1549 March-April and then in January-February, mostly in the western Pyrenees. Like in France,
1550 the north of Spain (Asturias-Cantabria) experienced unusual Spring burning activity,
1551 amounting to 423 km² during late March and early April (Educación Forestal, 2023a). In
1552 particular, the Foyedo wildfire (27th March 2023) was the largest on record for Asturias,
1553 burning 101 km² across variable vegetation but with the predominance of conifer plantations,
1554 mostly *Pinus pinaster*. It was a wind- and spot-driven fire but its soil and overstorey burn
1555 severity were respectively low and mostly moderate, as slower-drying fuels were not available
1556 to burn (Cátedra Cambio Climático de la Universidad de Oviedo, 2023).

1557
1558 Only two other notable large wildfires occurred in 2023 in continental Spain, and again were
1559 unusual in that they happened in spring rather than summer. The Villanueva de Viver wildfire
1560 (23rd March 2023, Castellón and Teruel) burned around 50 km² and was driven by abnormal
1561 seasonally dry conditions, combined with a shift in wind direction. It mostly burned naturally-
1562 regenerated continuous pine forest of *Pinus halepensis*. Canopy fire severity was
1563 heterogeneous, with 39% of the wildfire area being classified as high to very high severity
1564 (Mediterranean Center for Environmental Studies, 2023). The cost of fire suppression was
1565 2M€ and 1,800 people were evacuated (*Las Provincias*, 2023).



1566
1567 At over 100 km², the Pinofranqueado wildfire (17th May 2023, Cáceres) was the largest fire in
1568 the Iberian Peninsula in 2023 (Copernicus Emergency Management Service, 2023b). The BA
1569 was 90% forest, mostly pine (*Pinus pinaster*; Juntaex.es, 2023). It was a wind-driven fire and
1570 the Canadian FWI indexes indicate all fine fuel was available to burn and extreme fire
1571 behaviour (FWI>50). The fire significantly impacted the nesting of protected bird species and
1572 rainfall shortly after the wildfire caused important runoff, erosion, and disruption of water
1573 supply to the local population (Armero, Hoy, 2023).
1574
1575 The two other significant fires in Spain happened in the Canary Islands, the Puntagorda
1576 wildfire (14th July 2023, La Palma, 32 km²) and the Arafo-Candelaria wildfire (15th August
1577 2023, Tenerife, 123 km²; Copernicus Emergency Management Service, 2023c). The latter
1578 spread for 9 days and 94% of its area was forest under conservation status, mostly of Canary
1579 pine (*Pinus canariensis*). While drought was advanced, atmospheric conditions were not
1580 particularly severe. The fire was topographically driven and highly heterogeneous in severity,
1581 but low to moderate severity prevailed (Educación Forestal, 2023b). Nonetheless, 26,000
1582 people were evacuated, 364 farms and 246 buildings (none residential) were affected, smoke
1583 impacts were substantial and damage was estimated at 80.4M€.
1584
1585 Like in Spain, winter shrubland burning was relevant in continental Portugal (~50 km² in
1586 February) but subsequent significant wildfire activity was restricted to two fires. The Sarzedas
1587 (66 km² ha) and Baiona (75 km²) wildfires started on the 5th of August under extreme fire
1588 weather (FWI>50), and burned mostly (~70%) forest, respectively of pine (*P. pinaster*) and
1589 eucalypt (*Eucalyptus globulus*) stands (Direção Nacional de Gestão do Programa de Fogos
1590 Rurais, 2023). Prevailing burn severity was moderate and damage to infrastructure and
1591 emergency restoration amounted to 6.4 M€ cost for the Sarzedas fire and a forest value loss
1592 of 1.4 M€ (Instituto da Conservação da Natureza e das Florestas, 2023). The major run of the
1593 Baiona wildfire was on August 7, corresponding to 73% of the total BA, when it threatened
1594 wildland-urban interfaces and damaged several buildings; one camping park and 20 small
1595 villages were evacuated (*Economia Online*, 2023). Moderate to high burn severity classes
1596 were dominant and costs were estimated at 2.7 M€ (tourism) and 7 M€ (houses), plus 1.4 M€
1597 in forest values loss and 2.9 M€ for emergency stabilisation (*Rádio e Televisão de Portugal*,
1598 2023; SIC Notícias, 2023). Finally, on 12th October, and under anomalously extreme fire
1599 weather for the time of the year, the Ponta do Pargo wildfire burned 48 km² in Madeira island,
1600 with an estimated agriculture-related cost of 3 M€ (*Rádio e Televisão de Portugal*, 2023).
1601
1602 The year was also mild in other European countries where burned areas can be extensive,
1603 namely Romania, Hungary, and Poland, which collectively summed only ~210 km² burned.
1604 EFFIS recorded 2461 km² burned in Ukraine, the largest fire attaining 42 km², but these figures
1605 are far from those registered in recent years. In northern Europe, a notable fire occurred in
1606 Scotland near Cannich, during the spring, the primary fire season in the humid Atlantic climate
1607 of the UK (Belcher et al., 2021). It started on 19th of April and burned ~33 km² of mainly
1608 moorland making it one of the largest fires in the UK in recent history (Sabljak, *The Herald*,
1609 2023; personal communication Niall MacLennan, Scottish Fire and Rescue Service).
1610
1611



1612

1613

Figure 5: Summary of the 2023-2024 fire season in Greece. Time series of annual fire count, BA, C emissions, PM_{2.5} emissions, 95th percentile fire size, fastest daily rate of growth, and 95th percentile fire daily rate of growth. Black dots show annual values prior to the latest fire season, red dots the values during the latest fire season, and blue dashed lines the average values across all fire seasons.

1616

1617

1618

1619

3.1.3.4 North America

1620

1621

Wildfire across North America in 2023-2024 was characterised by record fire activity across Canada, lower than normal BA in the most flammable regions of the western US, above average fire activity across Mexico, and several extreme events that resulted in disastrous impacts to human communities. North America contributed the majority of the Northern Hemisphere area burned for the year, and two-thirds of the global C emissions from wildfire (Friedlingstein et al., 2023; Kolden et al., 2024). Canada burned over 150,000 km² in 2023, over twice the previous record and over seven times the annual average (Jain et al. 2024). The US burned 10,900 km² in 2023, well below the long-term annual average (National Interagency Fire Center [NIFC], 2024a). Mexico has a relatively short historical record of wildfires, but March 2023-February 2024 saw the highest area burned in the last decade (10,000 km²) due to strong ongoing drought conditions (Comisión Nacional Forestal, 2024).

1626

1627

1628

1629

1630

1631

1632

1633

The fire season began earlier than normal in Canada, driven by early snowmelt across much of the country and persistent drought conditions in the west. Abnormally high temperatures and lack of rainfall also saw forested regions of eastern Canada, including Quebec, transition rapidly to drought conditions at the end of May. British Columbia province recorded its first wildfire evacuation in mid-April, and in late May, over 16,000 people were evacuated from Halifax, the capital city of Nova Scotia, which saw its largest ever wildfire in 2023 (Jain et al. 2024). In June, two lightning outbreaks in Quebec initiated several hundred new fires in what would eventually become a record BA year for the province (4,300 km²) (Boulanger et al.,

1637

1638

1639

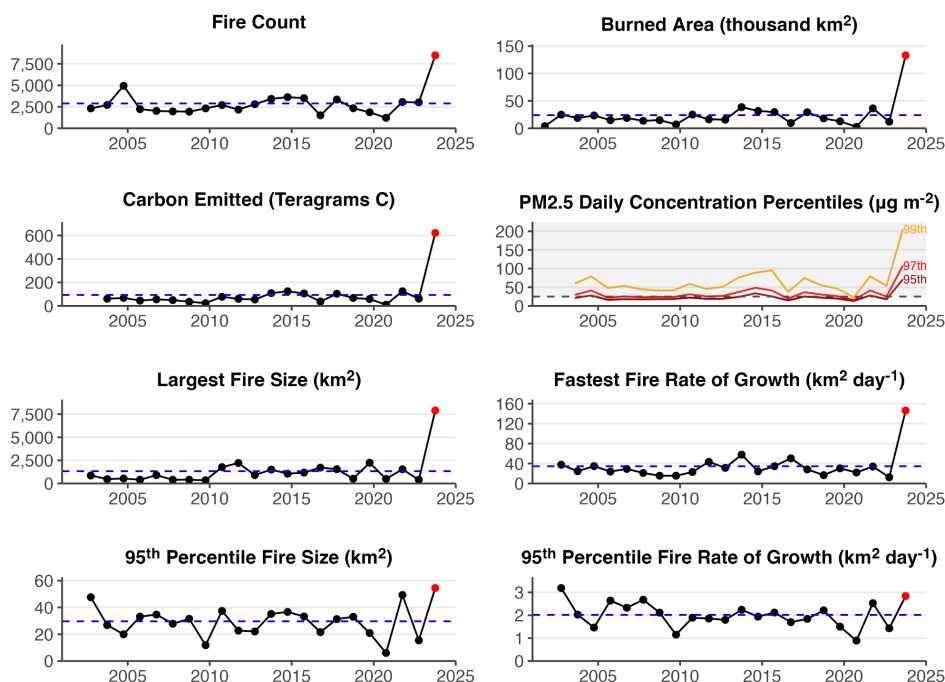
1640



1641 2024). While the majority of the Quebec fires were in remote regions, the smoke they
1642 generated blanketed several major cities in eastern North America, including New York which
1643 experienced its worst air quality in half a century as the observed daily mean PM_{2.5}
1644 concentration rose to 148.3 µg m⁻³, over 4x the recommended daily limit (Wang et al. 2023).
1645 In total over 50 million people were exposed to high levels of PM_{2.5} for several days (Yu et
1646 al. 2024). This situation was further exacerbated in New York City by several wildfires in the
1647 nearby New Jersey pine barrens, a fire-prone dry pine forest that sees large fires during
1648 periods of drought.
1649
1650 The year started with low fire activity across the USA. In the high plains of the central US, an
1651 outbreak of large wildfires occurred coincident with dry conditions and strong winds in March-
1652 April 2023. One wind-driven wildfire started by power lines in Oklahoma destroyed several
1653 dozen homes (Oklahoma Department of Emergency Management, 2023). Outside of the high
1654 plains, dry conditions also elevated fire activity across the Southern, Eastern, and New
1655 England regions of the USA. Mexico saw slightly above average fire activity during spring,
1656 which is the peak period of the fire season as debris burning and field clearing activities provide
1657 ignitions for predominantly shrubland and grassland wildfires.
1658
1659 As summer arrived in Canada, the western and boreal provinces and territories saw extreme
1660 and widespread fire activity, even as Quebec continued to burn. By the end of the year, record
1661 area had burned in British Columbia (2,300 km²), Alberta (2,700 km²), and the Northwest
1662 Territories (3,500 km²) accompanied evacuations of 232,000 people in numerous rural villages
1663 and large cities such as Yellowknife, NT and Kelowna/West Kelowna, BC, where a wildfire
1664 jumped the 2 km-wide Okanagan Lake (Jain et al., 2024; *CBC News*, 2023). The extreme
1665 behaviour of these fires not only shrouded large swaths of North America in smoke, but also
1666 generated an unprecedented 140 pyrocumulonimbus clouds (Jain et al. 2024). Eight
1667 firefighters were killed during summer 2023 in Canada (Jain et al. 2024), but miraculously no
1668 civilians died directly in the fires. Canada was at the highest National Preparedness Level 5
1669 for an unprecedented 120 continuous days starting on May 11, indicative of the significant
1670 resource sharing required by fire management; in all, over 5500 international personnel from
1671 12 countries and the EU were deployed to Canada during the 2023 fire season (Canadian
1672 Interagency Forest Fire Centre, 2023).
1673
1674 In the US, a relatively low activity fire season became deadly in August owing to unusual
1675 weather conditions facilitating extreme fire behaviour in multiple areas around the country. On
1676 8th August, a pressure gradient-induced katabatic wind event fanned several small wildfires in
1677 Hawai'i, and 101 civilians died as the town of Lahaina on the island of Maui was consumed in
1678 the worst wildfire disaster in the US in a century (Pyne, 2017). Over 2,000 homes were
1679 destroyed and over 10,000 people were displaced as a result. Extreme heat and flash drought
1680 produced fire behaviour that killed five additional civilians in the US states of Washington (2
1681 fatalities), Louisiana (2 fatalities) and California (C. Kolden, unpublished data). These extreme
1682 events stood in contrast to overall low fire activity and were notable for where they occurred.
1683 Washington does not typically see many extreme, wind-driven wildfires, and Louisiana is one
1684 of the wettest states in the US. By the end of August, the US BA was only 40 percent of normal
1685 and the lowest since at least 2000 (NIFC, 2023; National Oceanic and Atmospheric
1686 Administration [NOAA], 2023).
1687
1688 As North America transitioned to fall and then winter, Canada continued to burn nearly a month
1689 longer than normal, with the last large fires not controlled until late October. On 22nd
1690 September, remarkably late in the fire season, Canada saw its largest ever one-day total for
1691 BA at approximately 4,400 km² (Jain et al., 2024). While many of the Canadian fires were fully
1692 extinguished by winter, others simply smouldered into the deep peat layers, aided by a
1693 warmer-than-normal winter with a reduced snowpack. At the end of February 2024,
1694 spaceborne thermal sensors detected several dozen fires in northern Alberta and British



1695 Columbia that were overwintering fires, likely sustained by peat smouldering (Shingler, *CBC*
 1696 *News*, 2024; Scholten et al., 2021).
 1697

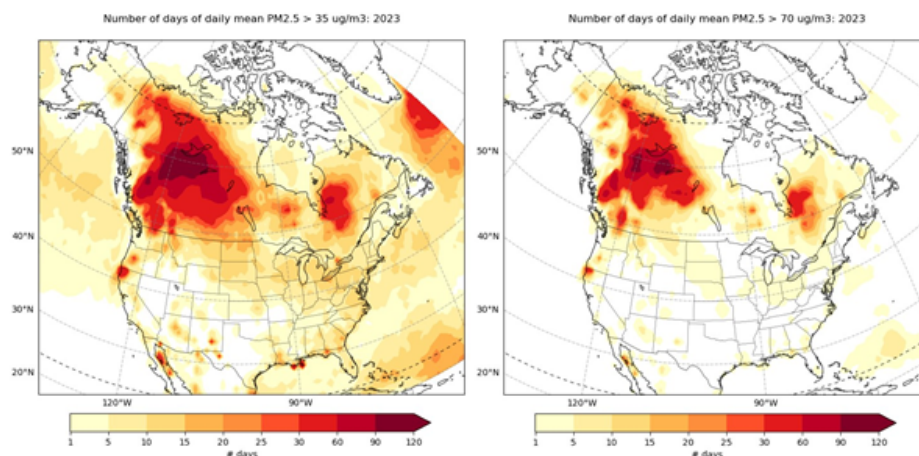


1698
 1699 **Figure 6:** Summary of the 2023-2024 fire season in Canada. Time series of annual fire count,
 1700 BA, C emissions, PM2.5 daily concentration percentiles (95th, 97th, and 99th), 95th percentile
 1701 fire size, fastest daily rate of growth, and 95th percentile fire daily rate of growth. Black dots
 1702 show annual values prior to the latest fire season, red dots the values during the latest fire
 1703 season, and blue dashed lines the average values across all fire seasons. The PM2.5 daily
 1704 concentration percentiles are based on area-weighted daily mean PM2.5 concentrations
 1705 across Canada (see Methods). The 95th, 97th, and 99th percentiles correspond to PM2.5
 1706 concentrations that are breached on 18, 10, and 3 days of the year, respectively. Grey shading
 1707 represents concentrations that exceed the reference levels for 24-hour mean PM2.5
 1708 concentration in Canada, statistically derived on the basis of several key epidemiological
 1709 studies (Canadian Environmental Protection Act Federal-Provincial Working Group on Air
 1710 Quality, 1998).
 1711
 1712

1713 US fire agencies recorded just over 10,900 km² burned in 2023, just over half of the 20-year
 1714 mean of 29,000 km² (NIFC, 2024a). Notably, over half of the BA was associated with higher
 1715 fire activity in the central plains grasslands and the southeastern US, while below normal fire
 1716 activity characterised California and the western US throughout 2023 as the region exited a
 1717 multi-year drought. However, the number of fires recorded was only slightly smaller than
 1718 average. This quiet pattern broke in February 2024, however, when drought conditions from
 1719 the high plains region of the US down into north central Mexico coupled with strong winds to
 1720 produce massive, fast moving wildfires across multiple states on both sides of the US-Mexico
 1721 border. The US state of Texas recorded its largest ever single fire at over 4,000 km²
 1722 (Smokehouse Creek fire) in late February and early March that destroyed 130 homes across
 1723 the high plains region of the central US (NIFC, 2024b). Two civilians were killed by the flames



1724 in the relatively rural area dominated by ranching, over 10,000 head of cattle died, and
1725 damages are estimated to be at least \$4.6 million (NOAA, 2024).
1726
1727



1728
1729 **Figure 7:** Impact of Canadian wildfires visible in air quality metrics for North America. Panels
1730 show the number of days in 2023 with mean PM_{2.5} concentration over a threshold of (**left**
1731 **panel**) 35 µg m⁻³ and (**right panel**) 70 µg m⁻³. Both the National Ambient Air Quality Standards
1732 (NAAQS) in the USA and the Canadian Ambient Air Quality Standards (CAAQS) have
1733 exposure targets of 35 µg/m³ on average within a single day.

1734

1735 The impact of North American fires on air quality is significant with half of the PM_{2.5} in America
1736 suggested to originate from fires (O'Dell et al. 2019). An exceptional fire season, such as seen
1737 in Canada in 2023, therefore poses an elevated level of health risk. Canada's wildfires
1738 produced levels of PM_{2.5} across the Country that were well in excess of the last 20 years
1739 (**Figure 6**). Additionally, long-range transport of pollution from Canada affected the Pacific
1740 Northwest, northern Midwest, and many eastern states (**Figure 7**). According to the National
1741 Ambient Air Quality Standards (NAAQS) in the USA, the threshold for PM_{2.5} exposure is not
1742 to exceed 35 µg/m³ on average within a single day. CAMS analysis suggests that people living
1743 within over half of US states experienced up to 2 weeks of exposure at or above this level. In
1744 Canada, the safe limit for PM_{2.5} exposure, as defined by the Canadian Ambient Air Quality
1745 Standards (CAAQS), is also 35 µg/m³ over a 24-hour period. However, the situation was worse
1746 in Canada due to closer proximity to fires, with many territories along the border experiencing
1747 up to a month of degraded air quality that exceeded national recommended exposure limits,
1748 British Columbia possibly facing twice the number of days at up to 2 months, and the Northern
1749 Territories potentially with 3 to 4 months of exposure.

1750 The scale of the impact becomes particularly evident when comparing the number of days at
1751 double the exceedance level (70 µg/m³) due to short-range versus long-range transport of
1752 pollutants. In Canada, where the pollution sources were more localised, the number of days
1753 above this higher level remains substantial, ranging from a week along the border to months
1754 still at the fire epicentres. In contrast, the USA, affected primarily by long-range transport from
1755 Canada, experienced approximately half the number of such high-pollution days. It is also
1756 important to consider the context of interannual variability in fire occurrence. Last year the
1757 USA experienced its lowest number of fires in 2 decades (**Figure 4**), so most of the pollution
1758 impacts came from Canada. Consequently, if the USA had also experienced a high fire year,
1759 the air quality would have worsened in many states.



1760 **3.1.3.5 Oceania**

1761

1762 As is commonly the case, there was a marked latitudinal difference in wildfire patterns in
1763 Oceania in 2023-24. Fire activity was above average in the savannahs, grasslands and
1764 shrublands of tropical, subtropical and arid northern Australia. In contrast, fire activity in the
1765 southern states of Australia was generally below average, and well below the levels seen
1766 during the high impacting 'Black Summer' fires of 2019-20. In New Zealand and the Pacific
1767 Islands, fire activity was relatively low compared to the preceding two decades.

1768

1769 Given the vast scale of savannah fires, 2023-24 ranked among the top five years in BA for
1770 Australia as a whole since 2001 (Fisher, 2024; **Figure 2**). Fire in tropical and arid areas is
1771 tightly linked to rainfall in the preceding season (Alvarado et al., 2020). The above average
1772 fire seasons in the Northern Territory and northern Western Australia were driven to a large
1773 extent by elevated fuel growth associated with the La Nina conditions of the previous three
1774 years. These fires represented the vast majority of areas burned across the country in 2023-
1775 24 (**Figure S7**).

1776

1777 In the monsoonal north, savannah fires follow a strong seasonal pattern, with regular summer
1778 rain predictably followed by fire in the dry winter and spring months. In arid regions further
1779 south, fire remains tightly coupled to rain, but the seasonality is less pronounced. Anomalous
1780 large fires began as early as May and June in Western Australia and the Northern Territory
1781 respectively, continuing to as late as January.

1782

1783 The year was also marked by a series of early season, high impact fires in populated areas of
1784 southwestern Western Australia, southeast Queensland, NSW, Victoria and Tasmania. Hot,
1785 dry, windy conditions, and extended dry periods, are a major driver of forest, woodland and
1786 shrubland fires of the subtropical and temperate south of Australia (Collins et al., 2022). In
1787 addition to 2023 being the eighth-warmest year on record, the three months from August to
1788 October were the driest in over 100 years of records (Bureau of Meteorology).

1789

1790 From October to January a string of fire events led to loss of life, property and a range of other
1791 human and environmental impacts throughout the country's southeast and southwest. In some
1792 cases, significant fire activity was observed in areas impacted by the 2019-20 fire season.
1793 Despite these impacts, average rain in southern and eastern parts of Australia tempered fire
1794 activity for the austral summer. In Queensland and NSW, large fires in remote areas pushed
1795 the total BA in line with the long term mean, but this figure was well below average in Victoria,
1796 the Australian Capital Territory and Tasmania.

1797

1798 In the southwest of Australia, a volunteer firefighter was killed while responding to a fire near
1799 Esperance. The Kings Park fire in October occurred in a popular tourist area containing
1800 vulnerable flora and threatened Perth Children's Hospital. Perth was again affected by fires in
1801 December, with several injured and five homes lost. A further two homes were lost in the
1802 region in mid-January from fires that burned 60 km². A similar sized fire burned through rugged
1803 terrain in the Gammon Ranges 600 km north of Adelaide, threatening highly significant cultural
1804 and ecological values.

1805

1806 A large number of significant fires affected the eastern States of Australia in October. The
1807 Tara and Mount Isa fires in Queensland burned well over 400 km² combined, destroying 65
1808 homes and claiming the lives of two people. International and interstate support were deployed
1809 from New Zealand and Victoria to respond to the fires. Further south in New South Wales,
1810 significant fires included the Coolagolite Rd fire in Bega (over 70 km², 2 houses destroyed),
1811 the Willi Willi Rd fire in Kempsey (over 290 km², 8 houses destroyed, one person killed)
1812 and large fires around Tenterfield (approximately 300 km², four homes destroyed). In
1813 November the Hudson Fire burned 228 km², destroyed 4 properties and led to the death of a
1814 volunteer fire fighter, who was killed by a falling tree while fighting the fire. In December the



1815 Duck Creek Pilliga Forest fire burned 1,385 km² and initiated 3 documented fire-generated
1816 thunderstorms, with smoke impacts extending 500 km away and reaching Sydney.
1817

1818 In neighbouring Victoria the fire season was bookended by high impact events in October and
1819 then in February and March. Fires in Gippsland during October totalled 120 km² and exhibited
1820 some overnight fire runs that were regarded as unusual (Mills et al., 2022). An extended dry
1821 period saw fires impacting towns in central and western parts of the state in late February and
1822 early March. Over 40 homes were lost and five firefighters were injured fighting two fires that
1823 originated in the Grampians National Park and burned 60 km². Interactions with the
1824 atmosphere and topography were suggested to explain extreme behaviour that was reported.
1825 This fire was followed by another near Ballarat affecting grass, forest and a pine plantation.
1826 Despite several extreme fire weather days and evacuation advice, a significant suppression
1827 effort aided by interstate deployments minimised impacts. The fire burned over 200 km².
1828

1829 In the island state of Tasmania the fire season began early with the Coles Bay Bushfire burning
1830 27 km² of both private land and national park in September and then fires on Flinders Island
1831 in October. Other impactful fires that occurred during the season include the Dolphin Sands
1832 fire on the east coast of Tasmania that destroyed two homes and burned 2.5 km² and the
1833 multiple fires in the Brady lake area (Tasmania's central highlands) in February that destroyed
1834 two homes and burned up to 100 km² and a fire in the Waterhouse Conservation areas that
1835 required campers to evacuate.
1836

1837 New Zealand experienced a normal fire season after three well below average seasons prior
1838 under La Nina conditions. The fire season began early with a relatively large fire in September
1839 on the western side of Lake Pukaki in the central South Island in wilding pines. This fire totalled
1840 29 km² and this was the third major wildfire event in recent years in this area at an earlier than
1841 normal stage of the fire season, following the 2020 Pukaki (Aug.) and Ohau (Oct.) fires. New
1842 Zealand then experienced a spate of fires around Canterbury, on the South Island between
1843 late Jan. and mid Feb. 2024 with several houses burned and farmlands affected.
1844

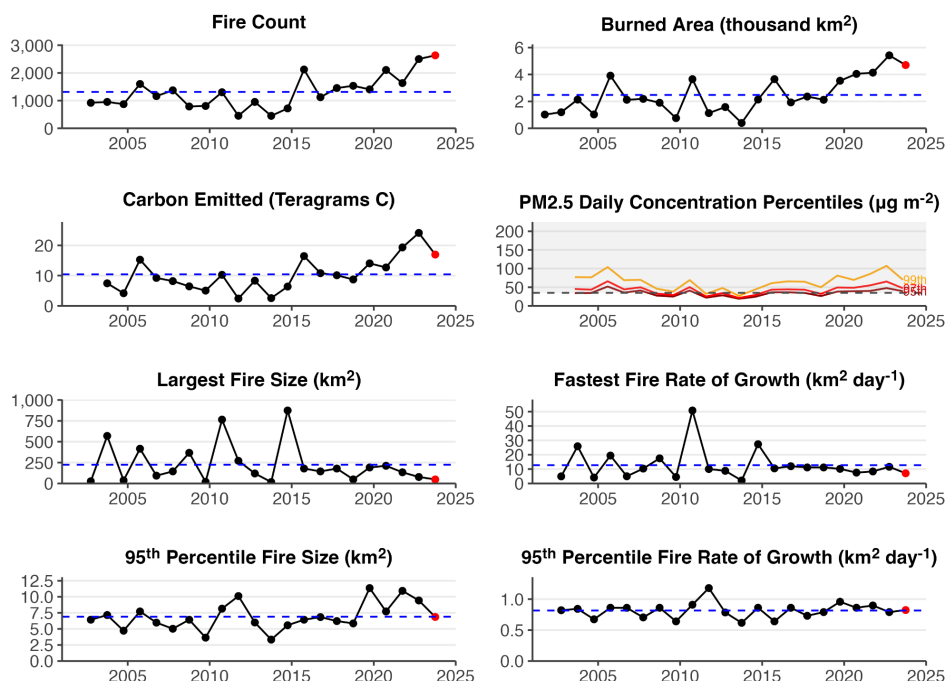
1845 **3.1.3.6 South America**

1846

1847 The 2023-24 fire season in South America was characterised by a moderately below average
1848 fire activity but with positive wildfire anomalies in specific regions, which were exacerbated by
1849 extended periods of drought and heatwave across the continent (Clarke et al., 2024; **Figure**
1850 **2, Figure 3, Figure 4**). In the Brazilian State of Amazonas, which features the largest extent
1851 of preserved old growth forests in Amazonia, June and October 2023 saw the highest fire
1852 counts since records began in 1998 (National Institute for Space Research, 2024; see also
1853 **Figure 8**). This continues a recent trend towards record-setting months for fire in Amazonas
1854 state, with new maxima being set in 7 months of the year since 2019 (National Institute for
1855 Space Research, 2024). Recent changes in deforestation and land use patterns are
1856 contributing to elevated fire ignitions in the state, amplified by climatic extremes in 2023 by a
1857 historic drought and heatwave driven by El Niño (Espinoza et al., 2024, Clarke et al., 2024).
1858 Due to emissions of wildfire smoke, many areas of Amazonas experienced poor air quality
1859 from September to December 2023, including in the state capital, Manaus, where over 2
1860 million people were exposed to the second-worst air quality in the world in October (Ministério
1861 Público Federal, 2023). The event was so severe that, in November 2023, the Federal Public
1862 Ministry opened a Civil Action case against the State of Amazonas, demanding evidence that
1863 the State was investing in fire prevention and combat in line with the Plan for the Prevention
1864 and Control of Deforestation and Fires (Estado do Amazonas, 2020). This procedure
1865 evaluates whether Amazonas authorities are accountable for environmental damage causing
1866 severe air pollution, reflecting the Public Ministry's growing involvement at both federal and
1867 state levels in monitoring environmental degradation and seeking to make authority figures
1868 accountable (Ministério Público Federal, 2023).
1869



1870



1871

1872

1873

1874

1875

1876

1877

1878

1879

Figure 8: Summary of the 2023-2024 fire season in the Brazilian state of Amazonas. Time series of annual fire count, BA, C emissions, PM2.5 emissions, 95th percentile fire size, fastest daily rate of growth, and 95th percentile fire daily rate of growth. Black dots show annual values prior to the latest fire season, red dots the values during the latest fire season, and blue dashed lines the average values across all fire seasons.

1880

1881

1882

1883

1884

1885

1886

1887

1888

1889

1890

1891

1892

1893

1894

1895

1896

1897

1898

National fire monitoring systems in Brazil indicate that some areas of Amazonia experienced anomalies in BA at the sub-state level. For example, BA in the municipality of Santarém in the State of Pará rose from an average of 70 km² in 2019 to 2022 to over 1,000 km² in 2023, and has already exceeded 250 km² in 2024 (MapBiomias Brasil, 2024). Similarly, in neighbouring Belterra municipality, BA extent was more than 3 times greater during the year 2023 than in 2019-2022 (MapBiomias Brasil, 2024). In Floresta Nacional do Tapajós, one of the most studied forest sites in the Amazon which spans Satarém and Belterra, forest fires accounted for more than 60% of the burned areas (MapBiomias Brasil, 2024). 4 thousand people live in 24 communities of traditional and Indigenous populations in the region and depend on protected forest resources for their cultural heritage, food security, economy and livelihood in Floresta Nacional do Tapajós and Reserva Extrativista Tapajós-Arapiuns (Instituto Chico Mendes de Conservação da Biodiversidade, 2019). Fires in 2023 compounded the challenges faced by these communities, who were already isolated by low river levels resulting from the drought that severely reduced their mobility and fishing, impacting on food security and enhancing socio-economic vulnerabilities.

In Chile, the 2023-24 fire season was marked by a significant escalation in both the number and size of wildfires, especially in the central and southern regions (**Figure 4**). Chile experienced its second-highest BA in the past 20 years (>4,000 km²; Jones et al., 2024). The peaks in BA at national scale were accompanied by peaks in the 95th percentile of fire size



1899 and daily rate of growth in highly-populated regions such as Valparaíso (**Figure 2, Figure 4**),
1900 indicating unusually large and fast-moving fires. These fires drew international attention due to
1901 their deadly impacts on society. In February 2024, severe wildfires struck the Valparaíso
1902 region in Chile, particularly affecting Viña del Mar and other surrounding areas (NASA Earth
1903 Observatory, 2024). These fires, fueled by a prolonged heatwave, resulted in the deaths of at
1904 least 131 people and destroyed thousands of homes, leaving at least 1,600 people homeless
1905 (UN Resident Coordinator in Chile, 2024; *Al Jazeera*, 2024; *El Disconcierto*, 2024). The
1906 emergency impacted the Lago Peñuelas National Reserve where more than 60 km² of forest
1907 were affected (Oberholtz, *Fox Weather*, 2024). The National System for Disaster Prevention,
1908 Mitigation and Attention (SENAPRED) issued a red alert and ordered the evacuation of over
1909 18 nearby towns (Oberholtz, *Fox Weather*, 2024). The February 2024 wildfires in Valparaíso
1910 followed other major disruptive wildfires in February 2023, which affected nearby regions of
1911 central Chile including Maule, Nuble, Bio bio, La Araucanía and Los Rios.

1912
1913 Several countries with land in the west of Amazonia experienced anomalies in BA and fire
1914 behaviour during the 2023-24 fire season, which correlated with specific regional climatic and
1915 environmental conditions. Bolivia, Peru, Ecuador and Colombia did not experience particularly
1916 extreme levels of BA at national scale, possibly influenced by above-average rainfall over
1917 three consecutive years of La Niña between 2020 and 2022 (iMMAP Inc., 2023). However,
1918 Peru's Loreto region, which neighbours the Brazilian state of Amazonas, faced its highest BA
1919 on record in the 2023-2024 fire season signalling the wider impacts of drought conditions in
1920 western Amazonia (**Figure 2**). The timing of peak anomalies in BA also coincided with those
1921 in Amazonas, around September-October 2023 (**Figure S2**). The northern Bolivian
1922 departments of La Paz and Beni experienced similarly-timed anomalies in BA. Remote parts
1923 of the Colombian Amazon also saw a significant uptick in BA since November 2023 which
1924 peaked in January 2024 (Mongabay, 2024). As a result of months of record-high temperatures
1925 and drought conditions since the beginning of El Niño, the region recorded higher C emissions,
1926 reflecting the severity of the burning at the end of the studied fire season. While the direct
1927 impacts on society throughout these regions was not as pointed as in the case of fires in Chile,
1928 the events are likely to have contributed to reductions in regional air quality and also impacted
1929 forest ecosystems and raised C emissions from fires in South America. At the end of January
1930 there was a wildfire in the mountains surrounding Bogota that affected the air quality that
1931 affected thousands of citizens of the capital of Colombia (France-Presse, *VOA News*, 2024).

1932
1933 In 2023-2024, Venezuela experienced its highest level of fire activity on record, particularly in
1934 January and February 2024 (ALER, 2024; *Tiempo*, 2024; **Figure 4, Figure S2, Figure S8**),
1935 notably affecting the states of Anzoátegui, Cojedes, Guárico, and Monagas, areas which
1936 dominant land cover primarily consists of savannas and extensive grasslands. This surge in
1937 fires during the dry season was intensified by unusually warm and dry conditions in the
1938 preceding months. These conditions, likely a result of global warming and changes in
1939 circulation and rainfall patterns associated with El Niño, making the landscapes more
1940 vulnerable to fires.

1941 1942 **3.1.4 Context of Recent Extremes**

1943
1944 The anomalies of 2023-24 occur against a backdrop of trends in BA this century that point
1945 towards shifts in fire regime. **Figure 9** shows significant trends in BA and forest BA across the
1946 fire seasons in the period March 2001-February 2024 derived from MODIS BA data (see
1947 Methods). While many world regions are experiencing declines in total BA, increases in forest
1948 BA are far more prevalent than declines at the scale of continental biomes, countries, and
1949 administrative regions.

1950
1951 Northern hemisphere extratropical biomes in North America and Asia show a clear signal
1952 towards increased forest BA since 2001, which are also visible on national and provincial
1953 scales in Canada, the US and Russia and on provincial scales in various states of western



1954 and eastern Canada, the western US, and Siberia. These trends occasionally propagate to
1955 trends in total BA, for example in western and northern Canada and in the Sakha Republic
1956 (eastern Siberia). The large 2023-24 anomalies in BA in Canada align with the doubling of
1957 forest BA in Canada across fire seasons since 2001 (a significant trend, $p < 0.05$) and a 23%
1958 increase in total BA in Canada (marginally significant at $p < 0.1$). Three Canadian provinces
1959 showed significant increases in both total and forest BA this century: British Columbia (+35-
1960 42%); Northwest Territories (+55-68%), and; Yukon (+60-135%). No Canadian provinces
1961 experienced a significant decline in forest BA or total BA. More widely, there was a 58%
1962 increase in forest BA in the North American boreal forest biome since 2001, and a 134%
1963 increase across the pan-boreal forest biome of North America and Eurasia. The succession
1964 of events affecting boreal forests in Canada in 2023, Siberia in 2020, and both North America
1965 and Asia during 2021 appear to be part of a continued trend towards rising fire extent in the
1966 high latitudes this century.

1967
1968 Elsewhere in the southern hemisphere extratropics, significant rises in forest BA are seen in
1969 Chile since 2001 (+87%), including in the central regions of Araucanía, Bio bío, Maule, Ñuble,
1970 and Valparaíso ranging from 35 to 109%. Extreme fires in Valparaíso during 2023-24 and in
1971 Araucanía, Biobío and Ñuble in the 2022-23 fire season Maule, Ñuble, Bio bío, Araucanía
1972 (**Section 3.1.3.6**) are also consistent with a longer-term rise BA in central Chile (**Figure 9**).
1973 Increases in BA are not generally significant in fire-prone parts of the southern hemisphere
1974 extratropics, such as Africa or Australia.

1975
1976 In the tropics, trends in total and forest BA show a variety of patterns. While total BA has
1977 reduced across much of the savannah-occupied regions of South America, Africa and northern
1978 Australia, trends in forest BA (>30% tree cover) are far more varied (**Figure 9**). Hence, fires
1979 in woody tropical vegetation show a less consistent global trend. In addition, exceptions to the
1980 general decline in total BA across the tropics are seen in the Brazilian state of Amazonas, the
1981 Congo basin, and across much of India (**Figure 9**). The trend in Amazonas, among the most
1982 pristine parts of Amazonia, contrasts with other states of Brazil such as Mato Grosso and
1983 Pará, where declines in deforestation rates and deforestation-related fires have fallen since
1984 their peak during the early 2000s (Silva Junior, 2020). The anomalous fire activity and C
1985 emissions in Amazonas state during the 2023-24 fire season (but not other states of Brazil)
1986 thus appear to be consistent with the emerging pattern of increased fire in the region.
1987 Meanwhile, the 2023-24 anomalies in BA and other fire properties in the Bolivian, Peruvian,
1988 Colombian and Venezuelan parts of Amazonia (**Section 3.1.3.6**) typically occurred against a
1989 backdrop of reduced BA or no significant trend in recent decades (**Figure 9**).

1990
1991
1992
1993



1994
 1995
 1996
 1997
 1998

1999
 2000

2001
 2002

2003
 2004
 2005

2006
 2007

2008

2009

2010

2011

2012

2013

2014

2015

2016

2017

2018

2019

2020

2021

2022

2023

2024

2025

2026

2027

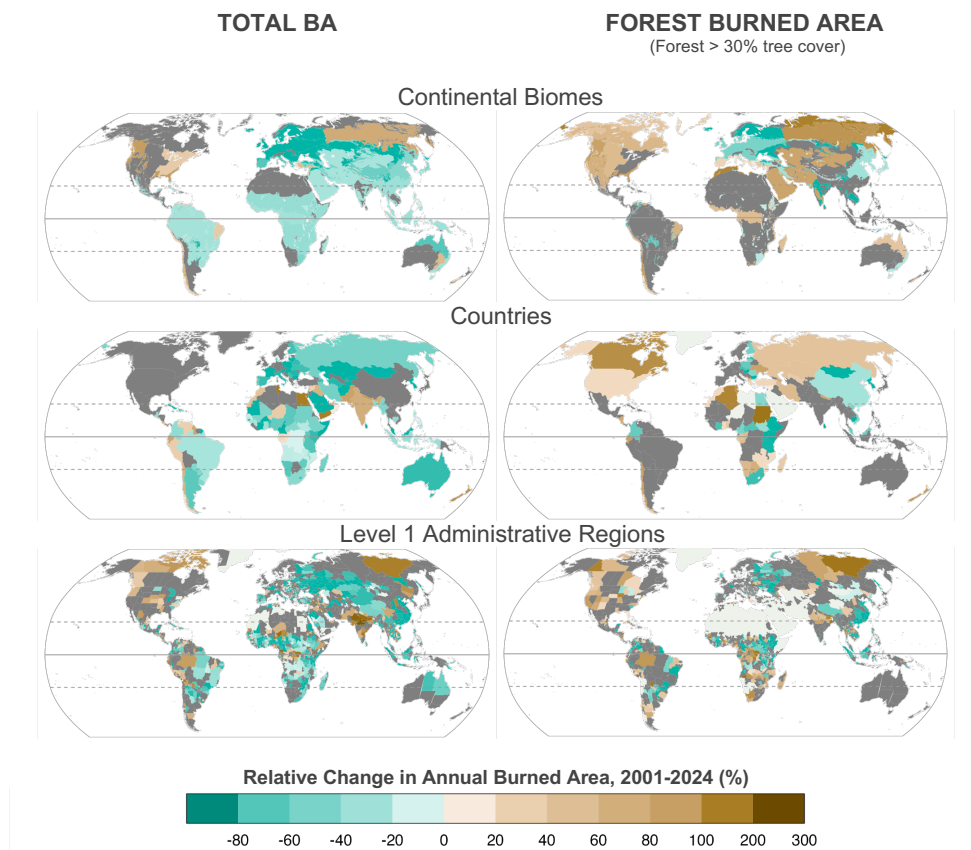


Figure 9: Relative changes (%) in (left panels) total annual BA and (right panels) forest BA across March-February fire seasons during 2001-2024 for three regional layers: (top panels) continental biomes; (middle panels) countries, and; (bottom panels) level 1 administrative regions (e.g. states or provinces). Forest BA considers only areas with tree cover over 30% at the native (500 m) resolution of the BA observations. Relative changes are calculated as the trend in BA across fire seasons March 2001-February 2022 through March 2023-February 2024 multiplied by the number of years in the time series and divided by the mean annual BA during the period. Trends in BA are derived using the Theil-Sen slope estimator. Only significant trends in BA are shown (dark grey fill signifies no significant trend).

3.2 Focal Events of this Report

3.2.1.1 Canada

In this year's report, the extreme wildfire season in Canada is selected as one of our focal events. It emerges as a major event of global relevance for the following reasons:

- **Record-Breaking Burned Area:** The North American boreal forests, particularly in Canada, experienced an unprecedented fire season. The BA reached six times the average since 2001.



- 2028
 - 2029
 - 2030
 - 2031
 - 2032
 - 2033
 - 2034
 - 2035
 - 2036
 - 2037
 - 2038
 - 2039
 - 2040
 - 2041
 - 2042
 - 2043
 - 2044
 - 2045
 - 2046
 - 2047
 - 2048
 - 2049
 - 2050
 - 2051
 - 2052
 - 2053
 - 2054
 - 2055
 - 2056
 - 2057
 - 2058
 - 2059
 - 2060
 - 2061
 - 2062
 - 2063
 - 2064
 - 2065
 - 2066
 - 2067
 - 2068
 - 2069
 - 2070
 - 2071
 - 2072
 - 2073
 - 2074
 - 2075
 - 2076
 - 2077
 - 2078
 - 2079
 - 2080
 - 2081
 - 2082
- **High C Emissions:** Fire C emissions in Canada were over nine times the average since 2003, contributing significantly to global C emission totals for the year.
 - **Early and Persistent Fires:** Positive BA anomalies were visible from April 2023 (**Figure S9**) and persisted through to October, with some regions experiencing fires until January 2024. The fire season lasted nearly a month longer than normal, with the largest one-day BA total ever recorded in Canada occurring on 22nd September 2023.
 - **Regional Anomalies:** Peak fire anomalies were observed in Eastern Canada in June 2023 and later in Western Canada (August-September), indicating widespread and prolonged fire activity across the country.
 - **Record Fire Size and Spread:** New records for individual fire size and rate of spread were set, with many provinces experiencing high-ranking anomalies in fire count and daily growth rates.
 - **Extensive Impact Across Provinces:** The highest BA or fire C emissions on record were observed in Northwest Territories, British Columbia, Alberta, and Quebec, with other provinces like Yukon, New Brunswick, and Ontario also experiencing significant fire activity.
 - **Air Quality Impact:** Smoke from these fires led to severe air quality issues, affecting major cities in North America, including New York, which experienced its worst air quality in half a century.
 - **Firefighting Challenges:** Canada was at its highest National Preparedness Level for an unprecedented 120 continuous days, indicating the significant resource sharing and international assistance required to manage the fires.
 - **Human and Economic Toll:** Over 232,000 people were evacuated across various regions, and despite the extreme fire activity, no civilian deaths were directly attributed to the fires, showcasing the effective, albeit strained, emergency response efforts.
 - **Global Significance:** The extreme fire season in Canada was a major contributor to the overall above-average global fire C emissions in 2023-24, highlighting its global environmental impact.

To assess the causes of specific regional BA anomalies, four anomalous BA regions/month combinations were chosen across Canada: Western Taiga Shield and Taiga Boreal Plains for May and June (includes Alberta and British Columbia Boreal plains, and the Mountain Cordillera); and Eastern Taiga Shield in Quebec for June and July. **Figure 10** maps the magnitude of anomalies in these regions and months. Though note the size and long period this protracted event means that even these regions/month to not capture all the anomalous BA over Canada in 2023 (**Figure S9**).

3.2.1.2 Greece

In this year's report, the extreme wildfire season in Greece is selected as one of our focal events. It emerges as a major event of global relevance for the following reasons:

- **Second-Highest BA on Record:** Greece experienced its second worst fire season in terms of total area burned, with 1,727 km² affected, despite recent efforts to strengthen firefighting mechanisms. The 2023 fire season was notably more severe than typical years, with the total BA significantly exceeding the country's historical averages and recent challenging fire seasons.
- **Multiple Large Fires:** From mid-July to late August, Greece faced numerous large fires that overwhelmed firefighting capabilities. Key fires included those on the island of Rhodes, which burned 207 km², and the massive Evros fire, which reached 938 km².
- **Evros Fire Disaster:** The Evros fire became the largest on record in recent European history, significantly impacting both forested and agricultural areas. It also led to the tragic deaths of 19 immigrants who were trapped by the flames.
- **Urban and Infrastructural Impact:** Fires near populated areas necessitated large-scale evacuations, including 20,000 tourists on Rhodes and multiple settlements



2083 around Mount Parnis in Attica. The Evros fire also caused a powerful explosion at an
2084 Air Force base, resulting in damage to the town of Nea Aghialos.
2085 ● **Significant Evacuations:** Numerous evacuations took place, highlighting the severity
2086 of the situation. These included evacuations in Alexandroupolis and its surrounding
2087 villages due to the Evros fire.
2088 ● **Economic and Environmental Damage:** The fires caused extensive damage to
2089 properties, infrastructure, and natural reserves, with significant impacts on biodiversity
2090 and local economies.
2091 ● **Firefighting Challenges:** The simultaneous spread of multiple fires stretched
2092 firefighting resources to their limits, with a notable focus on evacuations rather than
2093 fire suppression in some instances.
2094
2095 Abnormally high burned areas were reported around Alexandroupolis in August and extended
2096 further west across the administrative region of Macedonia and Thrace. Anomalies were also
2097 present in central Greece and around Athens in July and August (**Figure S10**). **Figure 10**
2098 maps the magnitude of the anomalies for August.
2099

2100 **3.2.1.3 Western Amazonia**

2101 Our final focal event of 2023-24 is a box drawn in western Amazonia with bounding
2102 coordinates 2.25° N, -56.00° E, -9.75° S, -77.75° W. It includes Amazonas (Brazil), Loreto
2103 (Peru), and La Paz and Beni (Bolivia) where peak fire anomalies occurred simultaneously and
2104 coincided with a historic drought and heatwave. It emerges as a major event of global
2105 relevance for the following reasons:

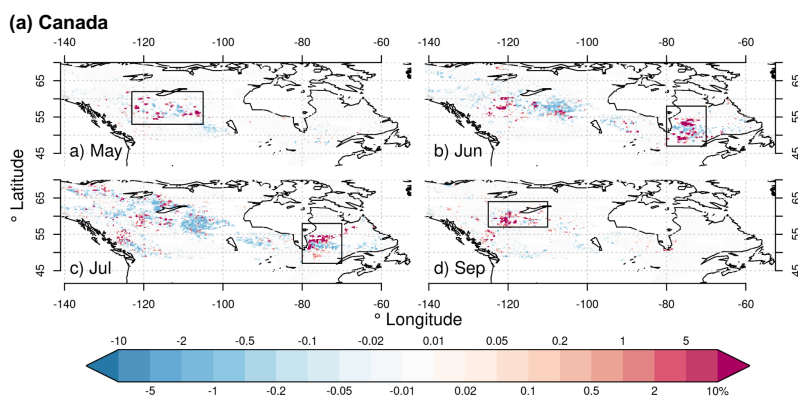
- 2106 ● **Record-Setting Fire Activity:** The 2023 fire season in Western Amazonia saw
2107 unprecedented fire counts, with new records set across Amazonas state in Brazil,
2108 Loreto department in Peru, and La Paz and Beni departments in Bolivia.
- 2109 ● **Severe Air Quality Degradation:** Smoke from widespread fires led to significantly
2110 degraded air quality across the region, impacting millions of people and posing serious
2111 public health risks.
- 2112 ● **Broad Socio-Economic and Health Impacts:** The fires caused extensive socio-
2113 economic disruptions, including health issues from poor air quality, legal actions for
2114 inadequate fire prevention, and impacts on livelihoods, particularly for Indigenous and
2115 traditional communities.
- 2116 ● **Widespread Environmental Degradation:** The fires contributed to significant C
2117 emissions and environmental degradation, affecting forest ecosystems and increasing
2118 the region's vulnerability to future climatic extremes. Western Amazonia has global
2119 significance due to its critical role in C storage and biodiversity and relatively low levels
2120 of disturbance.
- 2121 ● **Impact on Indigenous and Traditional Communities:** Fires in key areas disrupted
2122 the lives of Indigenous and traditional populations, exacerbating their vulnerabilities
2123 due to isolation and reduced access to resources.

2124 Abnormally high burned areas were reported in Western Amazonia during September and
2125 October. **Figure 10** maps the magnitude of these anomalies. Some anomalous BA starting in
2126 August and extending to November (**Figure S11**).

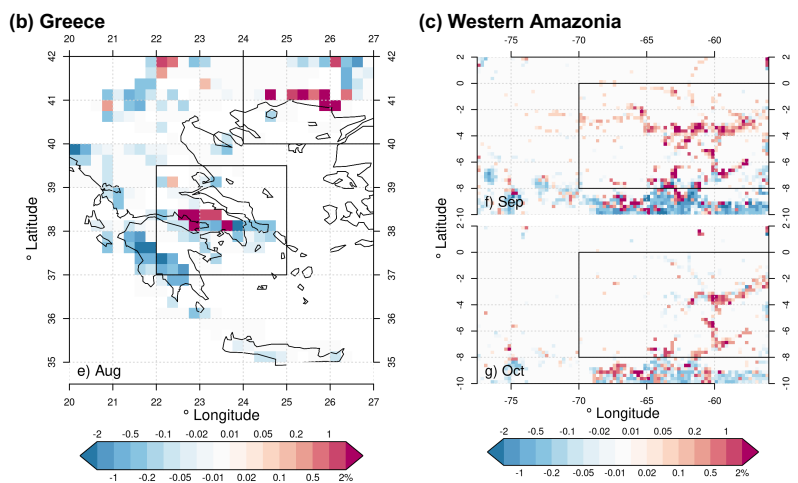
2127
2128
2129



2130



2131
2132
2133



2134
2135

Figure 10: Spatially explicit anomalies in BA fraction (%) during key months for focal events in (a) Canada, (b) Greece and (c) Western Amazonia. Plotted data are the absolute change from the climatological mean BA fraction for the month (%), based on MODIS MCD64A1 aggregated to 0.25°. Red indicates higher BA in that month of 2023 vs the 2002-2022 climatological average for that month. Boxes indicate focus events for our analyses in this report. The top panels show anomalies in Canada for various months, the lower-left panel shows anomalies in Greece for August, and the lower-right panels show anomalies in Western Amazonia during September and August.

2144
2145

3.3 Diagnosing Drivers and Assessing Predictability

2146

2147

2148

3.3.1 Highlights

2149

In Canada, fire weather conditions were the primary drivers of the extent of most fire activity. However, instances of intense burning events, particularly in mid-July, early August, and late September were missed by the driver attribution analysis, resulting in 'others'. This, highlighted potential inadequacies in predicting certain ignition sources or accurately representing fire propagation across vast landscapes in current forecasting systems.

2154
2155



2156 **The exceptional nature of the event in Alexandroupolis, Greece, could not have been**
2157 **predicted using fire weather forecasts.** While there were discernible indications in the Fire
2158 Weather Index (FWI) records that the days around the event were more extreme than most
2159 days in the fire season, similar conditions were also observed in the last 10 days of July without
2160 resulting in the same catastrophic impacts. This underscores the importance of expanding
2161 early warning beyond fire weather, considering fuel availability and ignition variability, to
2162 enhance reliability in fire risk assessment.

2163
2164 **The extreme fire season in South America was driven by prolonged drought conditions**
2165 **linked to the strong El Niño.** Many fires developed, triggered by lightning ignitions early in
2166 the season amidst high FWI values. Other than weather conditions that acted as persistent
2167 controls for fire activity, several intense active fire periods were not predicted in late August
2168 and throughout September likely due to the result of unrepresented ignition sources.

2169
2170 **Extreme burned areas were driven by anomalies in multiple controls, with weather, fuel**
2171 **abundance, and moisture being the most relevant factors.** The synchrony of all three
2172 factors resulted in the most severe BA anomalies in the three highlighted events. This
2173 underscores that no single factor can explain the most severe fires. Instead, multiple
2174 contributing controls must often coincide for the most extreme events to occur.

2175
2176 **Fuel load is a critical modulator for burned extent.** Higher and/or drier fuel loads combined
2177 with high fire weather conditions determined the unprecedented extent of burning in Canada
2178 and Western Amazonia. Conversely, the boundaries of extreme fires in Canada and Greece
2179 often corresponded to areas with lower fuel loads, demonstrating that discontinuity in fuel
2180 availability influenced fire behaviour and may have created firebreaks.

2181

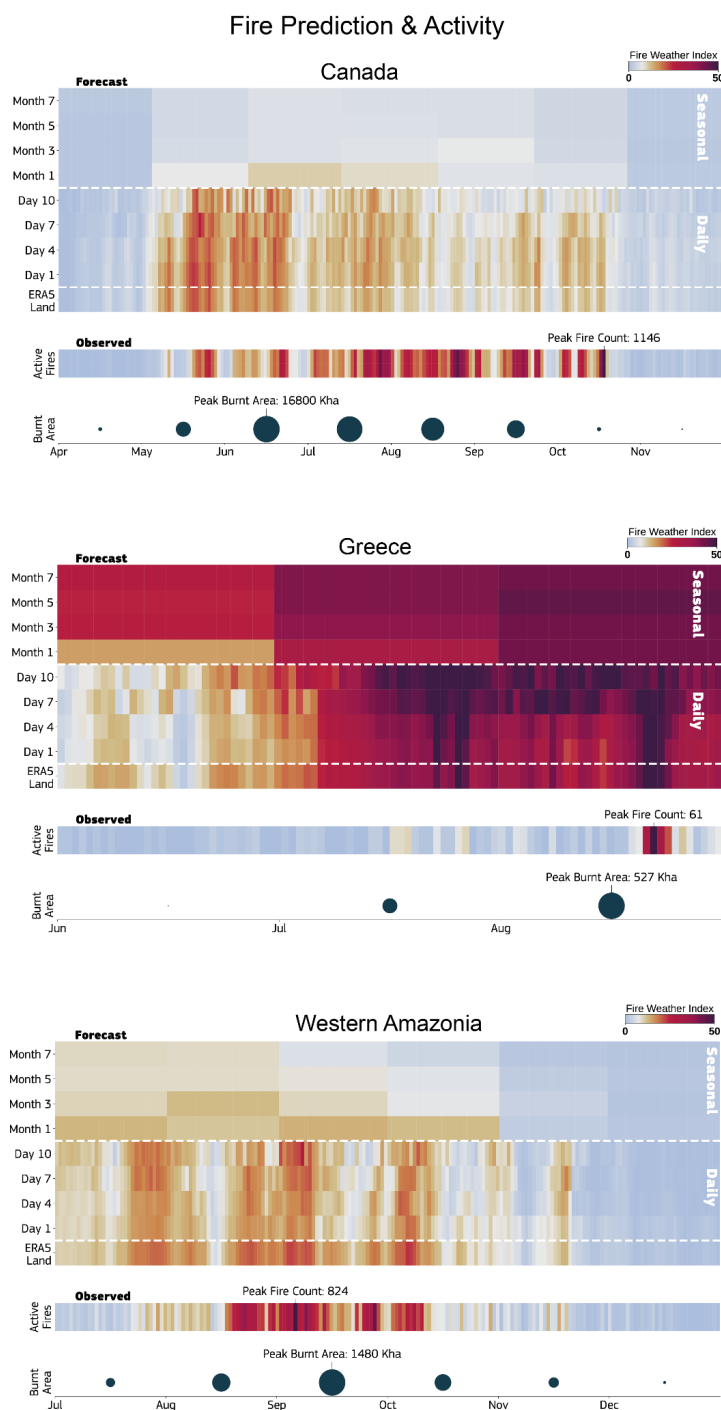
2182 **3.3.2 Predictability of Focal Events using Fire Weather Forecasts**

2183

2184 **3.3.2.1 Canada**

2185

2186 The early establishment of fire weather conditions as well as the late cessation of the fire
2187 season are well captured in the FWI reanalysis in Canada (**Figure 11**). The FWI also captures
2188 the intermittent pattern of fire danger and its correlation to actual fire activity. However, at the
2189 seasonal time scale, the signal is weakened, and there were no prior indications that the
2190 upcoming season would have been as extreme as it was with respect to fire activity (**Figure**
2191 **11**). For most part of 2023 Canada was in drought. The analysis of the other subindices of the
2192 FWI system, notably the drought code shows more persistent patterns in fire weather with
2193 longer predictability lead times (not-shown). The weather-limited nature of the Canadian fire
2194 season means that the FWI modelling framework serves as an essential indicator of
2195 anomalous conditions, acting as a prerequisite for the intensity and spread of fires. It provides
2196 valuable insights into the sequence and extent of extreme fire weather days during such
2197 events.



2198
2199
2200
2201

Figure 11: Chicklet plots displaying seamless FWI predictions over time from various forecasting systems of the ECMWF (see Methods). The x-axis corresponds to specific dates throughout the year, while the y-axis denotes either observations or the time leading up to the



2202 date when a forecast was generated. The vertical colour coherence allows for quick
2203 identification of the time windows of predictability associated to the observed fire activity both
2204 provided in terms of number of detected active in a day fires and total burned areas in a month
2205 (circles).

2206
2207

2208 **3.3.2.2 Greece**

2209

2210 The establishment of fire-prone conditions in the Mediterranean, particularly in Greece, is part
2211 of the region's seasonal weather cycle (**Figure 11**). In 2023, this pattern persisted, and
2212 extreme landscape flammability could be forecasted well in advance. In arid and semi-arid
2213 regions fire occurrence is driven not solely by weather but also by fuel availability and its
2214 intermittent short-term drying. In these regions the FWI often reaches extreme levels for much
2215 of the summer. However, fires do not always occur even when the FWI is extreme, as ignition
2216 and early suppression play a crucial role. The anomalous event in Alexandroupolis, highlights
2217 the limitations of relying solely on fire weather indices in these areas. There were no
2218 discernible indications in the FWI records that the particular day was more extreme than the
2219 day before or the one afterward, emphasising the need for a more holistic approach to fire risk
2220 assessment in regions where fuel is a limiting factor or live fuel moisture plays a crucial role
2221 in the extent of the burnings (Di Giuseppe, 2023).

2222

2223 **3.3.2.3 Western Amazonia**

2224

2225 The correlation between FWI and fire activity in the South America region at the shorter lead
2226 times is generally poor, primarily due to the strong dependency on either lightning or human
2227 ignitions (Kelley et al., 2021). In 2023, this pattern persisted (**Figure 11**), with the onset of fire
2228 weather following the seasonal pattern well ahead of the time where fires were triggered.
2229 Seasonal predictions indicated high fire danger during the summer period probably driven by
2230 El Niño conditions.

2231

2232 **3.3.3 Identifying Key Drivers of Focal Events**

2233

2234 Weather, fuel moisture, fuel abundance, and ignitions are the four primary controls identified
2235 as influencing the occurrence and intensity of the focal fire events. Anomalies in individual
2236 drivers of these controls, such as temperature or soil moisture, are calculated by comparing
2237 regional daily 2023 averages with the average for 2003-2022.

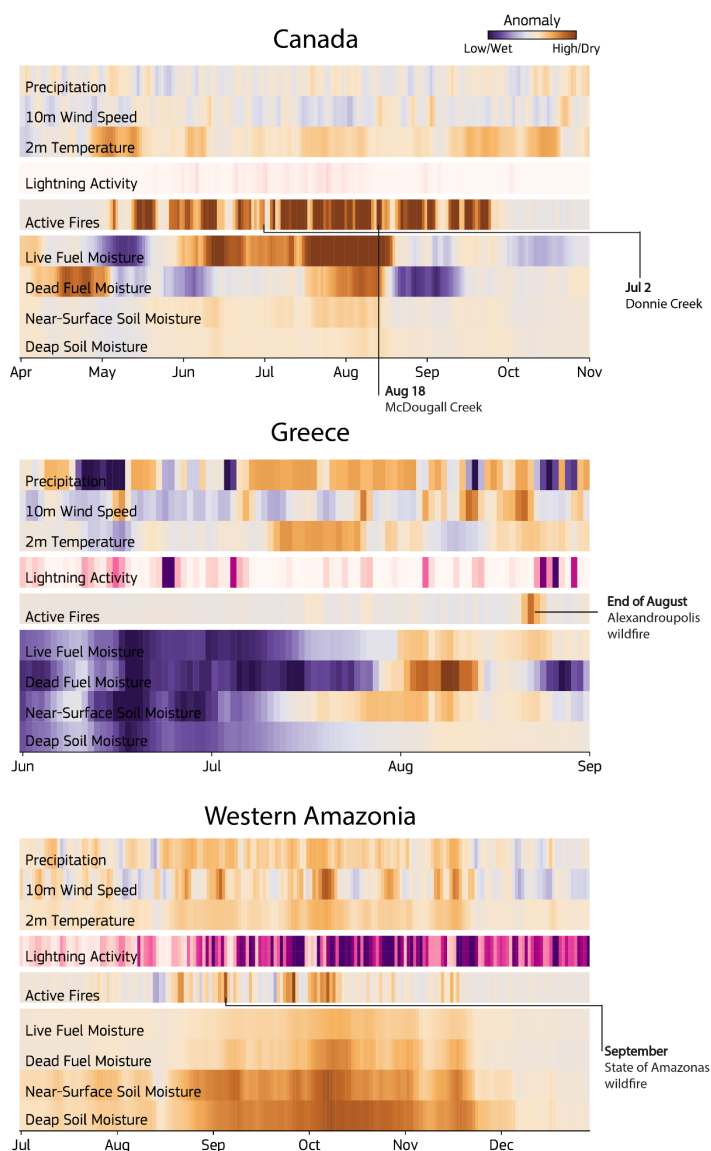
2238

2239 Analysing the time series of a few key drivers helps contextualise the conditions under which
2240 the examined events took place (see **Figure 12**). However, it is by leveraging the infrastructure
2241 provided by PoF and ConFire models that we can perform a statistical causality attribution of
2242 the four controls for the observed fire occurrence (see **Figure 13**). By design, the PoF and
2243 ConFire models provide control attribution even if a fire event is not recorded. In such cases,
2244 a low probability across all controls indicates an accurate prediction. However, even in
2245 instances where no fire event is recorded, the models enable us to gain insight into the
2246 complex interactions among weather conditions, fuel characteristics, ignition sources, and
2247 other environmental factors. For example, a high probability of fire not associated with any AF
2248 could indicate successful suppression or fire-prevention policies implemented at a local level.
2249 Moreover, as our driver selection may not fully account for human influence, it is important to
2250 note that the category of "other" also encompasses unaccounted-for variables, as well as a
2251 measure of observed active fires and partially burned areas that were not forecasted by the
2252 models. Therefore, this analysis not only enhances our ability to understand the main controls
2253 on fire activity, but it also helps identify missing pieces of information needed to fully
2254 comprehend the events. It is important to note there is not a one-to-one correspondence



2255 between observed fire activity and the attribution analysis, as the analysis is based on model
2256 predictions alone.
2257
2258

Fire drivers 2023



2259
2260 **Figure 12:** Anomaly driver stripes for the three focal events. The drivers are selected to
2261 contextualise the conditions under which the examined events took place. All values are
2262 expressed as anomalies compared to the 2003-2021 climatology with the exception of lightning
2263 activity which is expressed as absolute flash density.
2264
2265



2266 **3.3.4 Drivers of Active Fire Extremes**

2267

2268 **3.3.4.1 Canada**

2269 Persistent fire-favourable weather conditions played a crucial role in controlling the extent of
2270 active fires in Canada during the summer of 2023. Dry weather contributed to extensive drying
2271 of both live and dead vegetation, further exacerbating fire risk (**Figure 12, 13**). Most of the
2272 explainability of the Canada event comes from anomalous weather conditions. Increased
2273 lightning activity often coincides with or precede significant fire periods, indicating lightning as
2274 a key source of ignitions in the region, in agreement with the attribution of 59% of wildfires and
2275 93% of total BA to lightning ignition sources in Canada during 2023 (Jain et al., 2024). Adverse
2276 weather conditions in mid-May in western Canada were identified as influential factors in
2277 shaping fire events. However, multiple instances of intense burning events, notably in mid-
2278 July, early August, and late September, fall into the 'Other' category, heavily contributing to
2279 the total number of events for which there is no attribution among the controls. The fact that
2280 clusters of events were not predicted, suggests potential inadequacies in accounting for some
2281 ignition sources or accurately representing fire propagation across vast, densely vegetated
2282 landscapes.

2283

2284 **3.3.4.2 Greece**

2285

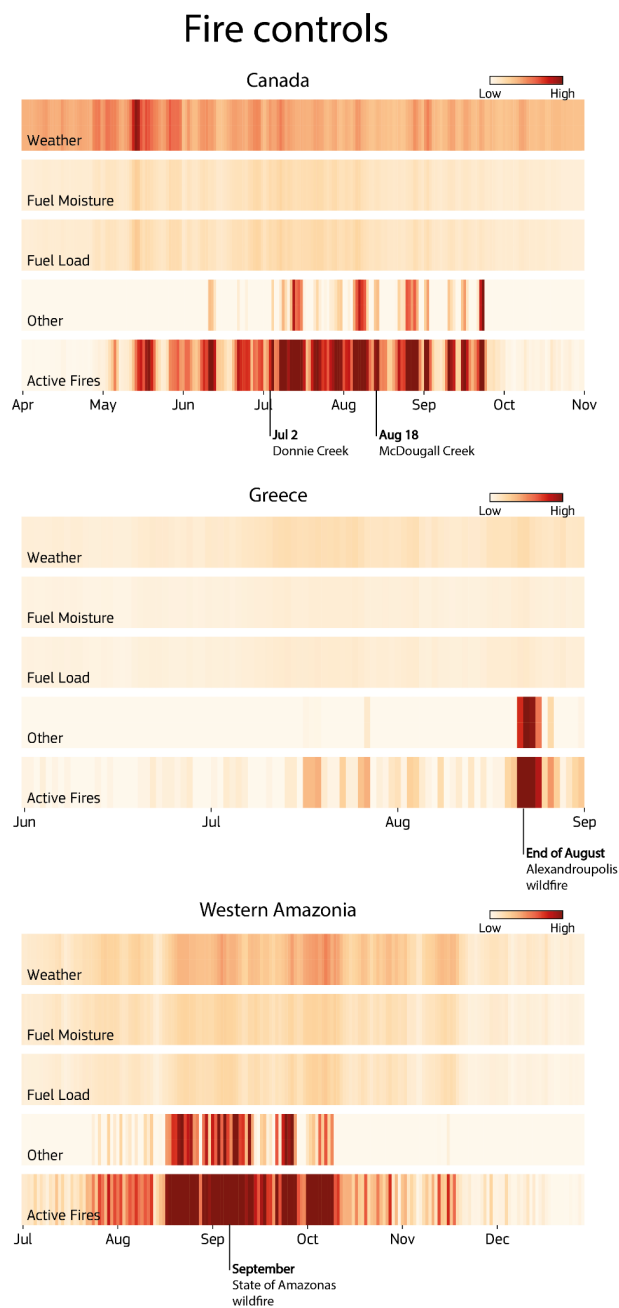
2286 The driver anomalies (**Figure 12**) and control attribution (**Figure 13**) do not suggest an
2287 abnormally fire-prone year in Greece, failing to justify the extent and severity of the
2288 Alexandroupolis fire. An anomalously wet spring may have led to increased foliage and
2289 subsequently quick drying of plant material. A sustained dry period in late July and August
2290 further dried out new foliage, creating favourable conditions for fire activity, as indicated by the
2291 anomalously dry live and dead fuel moisture content in August. Despite these conditions, the
2292 unexpected extent and severity of the Alexandroupolis fire were not predicted, highlighting the
2293 intrinsic difficulties in forecasting isolated extreme events even when most predictors are
2294 included. Additionally, the high wind speeds at the time partially contributed to the extensive
2295 BA during the fire.

2296

2297 **3.3.4.3 Western Amazonia**

2298

2299 Prolonged drought conditions, stemming from anomalously low rainfall and high temperatures,
2300 created favourable conditions for an active fire season in Western Amazonia (**Figure 12,**
2301 **Figure 13**). These conditions had a significant impact on the typically wet ecosystem, affecting
2302 soil moisture as well as live and dead fuel moisture. Despite weather conditions serving as a
2303 persistent control for fire activity, several intense active fire periods in late August and
2304 throughout September were not predicted, possibly due to unrepresented ignition sources.
2305 Additionally, fire activity from September onwards was intensified by intense lightning activity,
2306 characteristic of the region, which substantially contributed to ignitions.



2307
2308
2309
2310
2311
2312
2313
2314

Figure 13: Contributions of different fire controls to daily active fire anomalies in our focal events. All values are scaled to the observed daily fire anomaly such that the sum of the 4 daily control values matches the total observed anomaly.



2315 **3.3.5 Drivers of Regional Burned Area Extremes**

2316

2317 **3.3.5.1 Canada**

2318

2319

2320

2321

2322

2323

2324

2325

2326

2327

2328

2329

2330

2331

2332

2333

2334

2335

2336

2337

2338

2339

2340

2341

2342

2343

2344

2345

2346

2347

2348

2349

2350

2351

2352

2353

2354

2355

2356

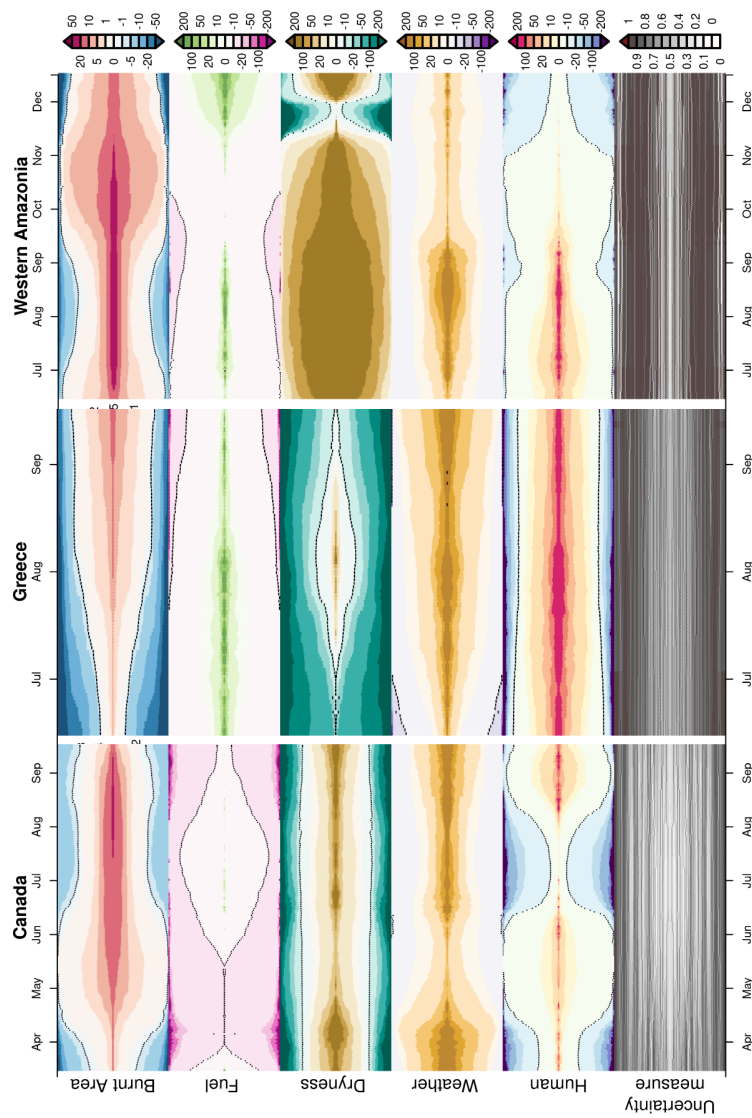
2357

2358

ConFire detected a significant anomaly in BA starting in late April, as seen in the observations (**Figure S9**) with very high confidence between May (99.2% likelihood) and June 2023 (>99.9% likelihood; **Figure 14**). While less confident in a positive anomaly in September and August (71% likelihood), ConFire detects the possibility of much higher burning in August and September, corresponding with the increase in burning in the Western Shield (**Figure S9**). **Figure 14** shows the controls that contribute to these anomalies. Our analysis indicates a >99.9% likelihood that elevated fire weather conditions persisting throughout the 2023 fire season, led to a notable increase in burning, explaining between 4.6-45% (based on 10 to 90th percentile confidence range) of the BA anomaly in May and 1-110% in June. If fire weather did explain more than 100% of the BA anomaly, then other controls must have acted to suppress BA. However, the anomalous weather conditions subsided later in the fire season. Drier fuel conditions could have contributed significantly to the increase in BA (up to 65% of Mays burnt area anomaly and 45% of Junes), though with low confidence (60.5% in May and 61.3% in June), and wetter fuels exerting a suppressive effect on fire spread was also possible, suggesting their potential role in mitigating fire severity. A small but confident suppressive effect (100% likelihood in May, 64.8% likelihood in June) from fuel load was observed, reducing relative increases in BA between 1.7-7.1% in May. Direct human-induced landscape changes exhibited a small impact on the extent of burned areas (likelihood of 97.4% in May), explaining between 1.2-22% of Mays increased burning and 0.6-24% of Junes. The analysis revealed relatively low noise levels in the results (“uncertainty measure” in **Figure 14**), indicating a robust signal despite uncertainties associated with the controls. This is shows that the higher burnt area anomalies have the most confident signal. This robustness is partly attributed to the large spatial coverage of Canada’s grid cells, enhancing the signal-to-noise ratio.

3.3.5.2 Greece

The analysis reveals an anomalously high BA, particularly from mid-August onwards, though with a lower confidence level compared to the Canadian case (69.9% likelihood; **Figure 14**). **Figure 14** shows the controls that contribute to these anomalies. Our findings demonstrate with very high confidence the presence of anomalously high fire weather conditions during the 2023 fire season in Greece (98.3% in July, and >99.9% in August and September). In August, these conditions explained between 4.3-140% of the increased BA, escalating to 5.6-170% by September. Assessing the impact of fuel moisture on BA, our analysis shows a wide range of possibilities, with confidence ranging from a 21% increase to 180% decrease in relative BA extent, which would have offset some of the increases from fire weather. This uncertainty underscores the complexity of the interactions between fuel moisture and fire behaviour in Greece. Similar to the findings in Canada, direct human-induced landscape changes exerted minimal influence on the extent of burned areas in Greece during the analysed period. While the analysis indicates a slightly higher than normal fuel load



2359
 2360
 2361 **Figure 14:** Influence of Fuel Load, Fuel Dryness, Fire Weather, and Human Controls on BA Anomalies in 2023. **(Top row)** The colour indicates
 2362 the modelled BA anomalies as relative increases/decreased in BA extent (% relative to the climatology). **(Rows 2-4)** The % of the anomaly
 2363 explained by each control. At each timestep, the gradient of colours along the y-axis represent the range of modelled outcomes: high diversity in
 2364 the colours indicates high uncertainty, whereas a consistent colour (e.g., red for positive BA anomalies) indicates greater confidence in the
 2365 projected direction and magnitude of change. Dotted black line indicated threshold between positive and negative anomaly. **(Bottom row)**
 2366 Uncertainty measure representing potential variations around our simulated BA anomaly as a result of factors not considered by the modelling
 framework, as a fraction of land area. Lower numbers (lighter colours) indicate higher confidence in the BA anomaly in the top row.



2367 **3.3.5.3 Western Amazonia**

2368
2369 Our analysis indicates a reasonably high confidence that the considered drivers contributed
2370 to anomalous high burning during September (73.8% likelihood), October (94.9% likelihood)
2371 and November (96.1% likelihood; **Figure 14**). **Figure 14** shows the controls that contribute to
2372 these anomalies. The primary driver of the observed BA anomaly appears to be dry fuel
2373 conditions, with a very high likelihood (99.7%) of drier-than-normal conditions persisting
2374 through November. This led to a substantial increase in BA, explaining at least 57% of the
2375 increase in BA. While fire weather conditions were also elevated (likelihood >99.9%), their
2376 impact on BA was comparatively lower, resulting in at least 2% increase in BA during October
2377 and November, though with a small probability of contributing much more. Direct human
2378 influence was identified as a contributing factor, with a high likelihood (92.9% in September,
2379 94.5% in October) of increasing burned area. However, the magnitude of this influence was
2380 approximately one-tenth of that attributed to fuel dryness. The influence of fuel load on BA
2381 was found to be small and statistically insignificant, with likely influences ranging from a small
2382 suppressive effect to explaining a maximum of the increased BA in September, to virtually no
2383 influence in October, suggesting that fuel dynamics played a minor role in driving the observed
2384 fire activity. The analysis reveals a higher confidence in the simulations indicating positive
2385 anomalies, indicating a robust signal in the attribution of drivers to observed BA anomalies.
2386

2387 **3.3.6 Spatial Variation in Drivers of Burned Area Extremes**

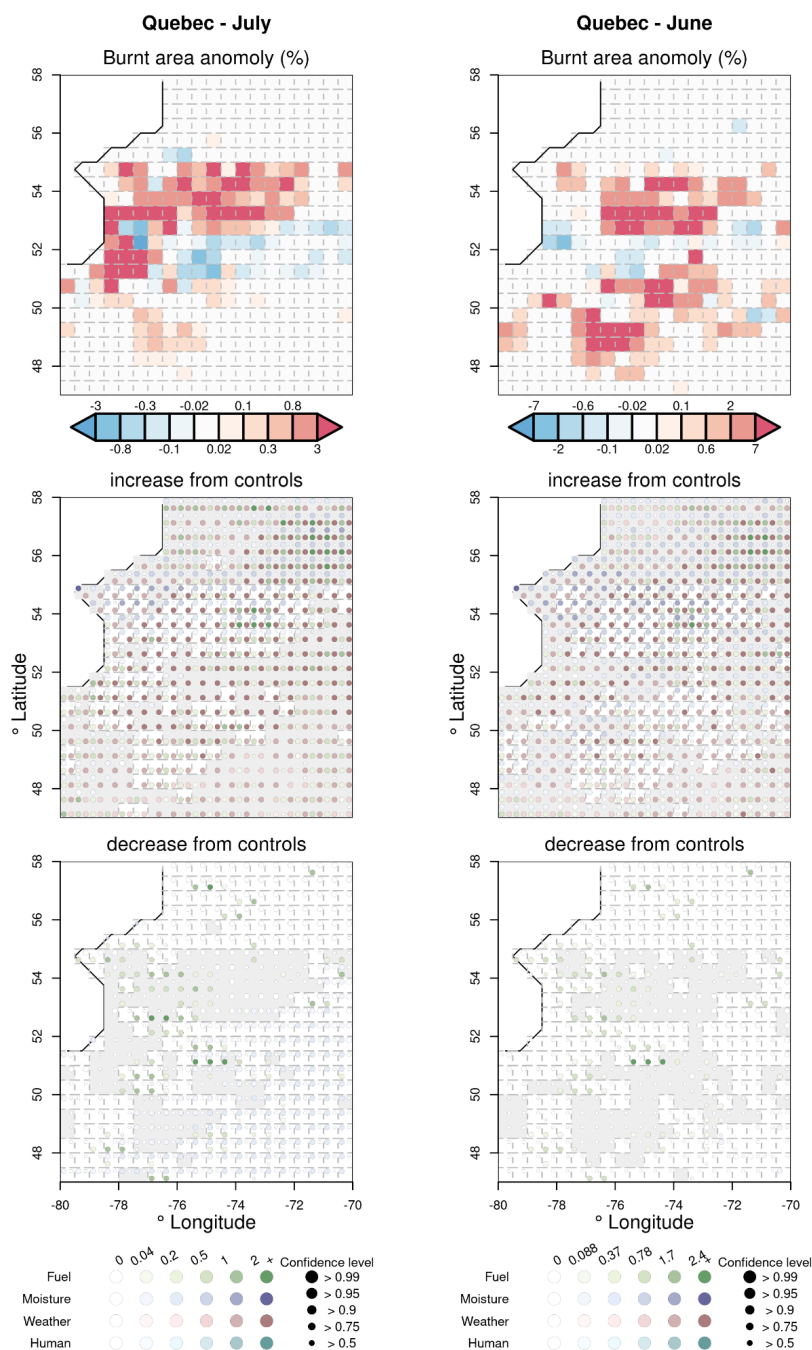
2388

2389 **3.3.6.1 Canada**

2390

2391 In Canada, most BA anomalies were linked to widespread high fire weather, with 95% of the
2392 country being influenced by higher-than-normal fire weather (**Figure S12**). There was a
2393 tendency for fuels to dry out, although this was not as widespread. Fuel load anomalies were
2394 more scattered, but areas of low fuel anomaly did correspond to some boundaries in fire
2395 extremes (**Figure 15, S12**). Increased human influence may have had some influence at
2396 suppressing fires, but this is not significant, and in some places, the model indicates a small
2397 possibility of increased fire from human activity. In the Eastern Shield, fire extremes in some
2398 areas were driven by high fire weather and dry fuel, compounded with more vegetation cover
2399 and hence higher-than-normal fuel load in some places (**Figure 15**). However, the borders of
2400 extreme fires corresponded to a suppressive effect from decreased fuel load. In the Western
2401 Shield, dry fuel and high fire weather drove fire incidents, with high fire weather dominating in
2402 some areas. Increased suppression may have had some influence at suppressing fires, but
2403 this is not significant, and in some places, the model indicates a small possibility of increased
2404 fire from human activity.
2405

2406 In June, there were high anomalous burned areas in Quebec's Eastern Shield, which were
2407 divided into two major fire components with a slightly reduced BA in between (**Figure 15**).
2408 Both components were associated with high fire weather, but in areas where high fire weather
2409 occurred without the contribution of other controls, it tended not to cause high levels of burning.
2410 The highest burned areas were mainly found in the northern component and were associated
2411 with anomalously low levels of moisture and high fire weather. Some cells with the very highest
2412 BA also showed anomalously high fuel load (**Figure 15**). In a region further north, around 56-
2413 57 degrees north and 72-80 degrees west, there was high fuel load, dry conditions, and high
2414 fire weather, but fire in the area was found to be highly fuel limited and largely insensitive to
2415 even large changes in controls (Kelley et al. 2019). The southern component of high burning
2416 corresponded with high fire weather and either fire fuel or high fuel load. Additionally, any
2417 boundaries between higher and normal/lower levels of BA also saw lower than average fuel
2418 loads, which may have inhibited fire spread (**Figure 15**).



2419
 2420
 2421
 2422
 2423

Figure 15: Anomalies in controls during months and regions of high BA in Quebec. The top left map of each region shows BA anomalies at 0.5 degrees for that month in 2023 versus the 2014-2023 monthly average. The left of the other two maps looks at anomalies in controls that would cause higher BA, with areas not greyed out representing regions with greater than



2424 monthly average BA in 2023. The right map shows drivers that would have led to lower than
2425 normal levels of burning, with areas not greyed out showing lower or non-change from monthly
2426 average BA in 2023. Each grid cell has four points: green points show anomalies in fuel load,
2427 purple in fuel moisture, red in fire weather, and cyan in humans. This way, we can see if
2428 controls acted in unison to cause extreme levels of burning or prevent extreme fires from
2429 extending further. The shade of the point shows the most likely expected level of anomaly in
2430 that control, while the size shows how confident we are in the direction of the anomaly.

2431
2432

2433 In May, the Western Shield and Taiga/Boreal plains experienced higher-than-normal fire
2434 weather across the region (**Figure S13**). The increased burned areas in the west were due to
2435 extreme low fuel moisture and high fire weather, as well as higher fuel loads. In contrast, areas
2436 to the south experienced high fire weather without the extreme burned areas. Additionally,
2437 anomalies in fuel loads and burning levels became more evident in September, with some
2438 areas displaying lower-than-average fuel and burning (**Figure S13**). These anomalies
2439 persisted, with regions still experiencing high fire weather and variations in fuel moisture
2440 levels. Furthermore, the eastern areas with higher fire weather also showed higher fuel loads,
2441 while drier fuel moisture was observed in less extreme regions to the east. Additionally,
2442 specific locations saw higher fire weather and above-average fuel moisture, while areas just
2443 north of the extreme fires experienced wetter-than-normal fuel moisture (**Figure S13**).

2444

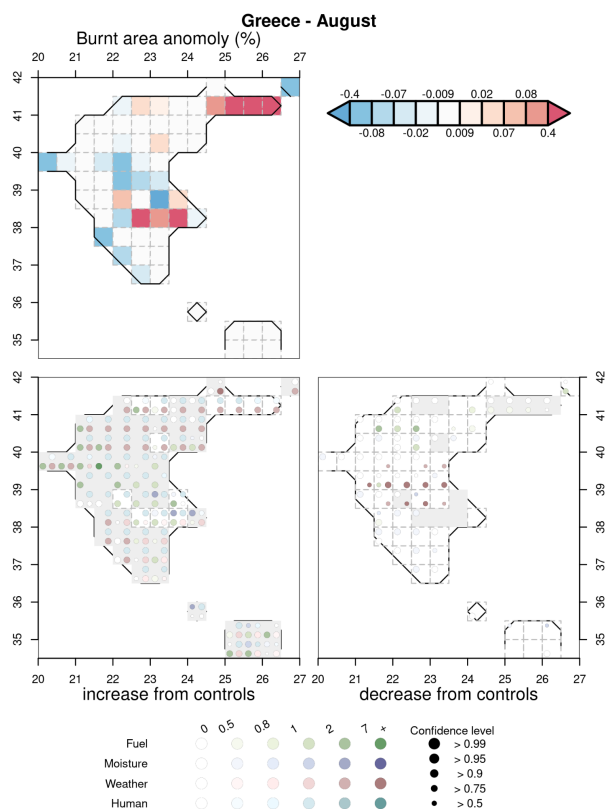
2445 3.3.6.2 Greece

2446

2447 Interestingly, most of Greece showed a tendency towards less suppression from people
2448 (**Figure S12**). However, the dominant driver over most (73%) of Greece was high fire weather,
2449 with some areas in central Greece showing notably low fire weather. These areas do not
2450 correspond to a fire anomaly, though higher fuel loads were detected. Except for central
2451 Greece, other areas of lower than average BA correspond to lower than average fuel loads
2452 (**Figure 16**). There was no significant anomaly in fuel moisture across Greece, though the
2453 northeastern fire extreme does correspond to a joint increase in fire weather and decrease in
2454 fuel moisture. Extremes in Eastern Coastal Greece correspond to anomalies in fuel load, fuel
2455 dryness, and heightened fire weather (**Figure 16**).

2456

2457 In August, Northern Greece experienced high fire weather and low fuel moisture, particularly
2458 around the Alexandroupolis fires and Macedonia and Thrace (**Figure 16**). The region
2459 extended further east, experiencing extreme fires that reached into Central Macedonia. Unlike
2460 Canada, the framework in North Greece did not show the same level of detail in the boundaries
2461 around extreme levels of burning. However, the transition to less burning in the South of West
2462 Macedonia did correspond to reduced fuel load. Areas around Athens and Central Greece
2463 that saw unusually high levels of burning also experienced decreased fuel moisture and
2464 increased fuel load (**Figure 16**). In contrast, areas in Southern Thessaly and Central Greece
2465 that did not experience high burned areas saw lower than normal fire weather. In the
2466 Peloponnese region, there was either high fire weather or reduced fuel moisture, but these
2467 conditions rarely occurred together, which might explain the lack of increased BA throughout
2468 the region. (**Figure 16**)



2469

2470 **Figure 16:** Same as Figure 15 but for Greece.

2471

2472 3.3.6.3 Western Amazonia

2473

2474 High fire weather anomalies were almost universal across our Western Amazonia region
 2475 (**Figure S12**). However, anomalies in other controls varied widely across the region, which
 2476 appears to modulate the occurrence of areas with higher than average burning (**Figure S12**,
 2477 **S14**). In September, the regions of high burning in the Western Amazon all exhibited higher
 2478 than average fire weather, with the highest BA anomalies associated with the highest fire
 2479 weathers. The areas with the highest BA anomalies along the Amazon River were located
 2480 around Manaus and also showed lower than average fuel moisture and higher than average
 2481 fuel load. The very highest pixels exhibited the anomaly in increased fuel loads. In the southern
 2482 and central part of the region (65 to 62 west/7/8 south), near Porto Velho, BA anomalies were
 2483 associated with extremely high fire weather and higher fuel loads. The areas of highest burning
 2484 also showed an increase in human-driven burning. Further east (59 west, 7 south), the highest
 2485 fire weather and decreased fuel moisture occurred alongside higher burning. Areas of higher
 2486 BA in the north (63 west, 0 north) were associated with extreme fire weather, though offset by
 2487 lower than normal fuel loads. This may explain why they were not as extreme as the fires
 2488 around Manaus, though the area is not generally considered fuel-limited (Kelley et al. 2019),
 2489 and fuel had little overall impact across the region **Figure 14**).

2490



2491

2492 **3.4 Attribution to Global Change**

2493

2494 **3.4.1 Highlights**

2495

2496 **In Canada, anthropogenic forcing increased the chance of high fire weather in 2023,**
2497 **total climate forcing has led to higher present-day BA and socio-economic factors have**
2498 **likely decreased burning.** Human influence at least doubled the probability of experiencing
2499 high fire weather in June 2023. It is virtually certain that total climate forcing increased recent
2500 high BA in the region by up to 38%, but it is less certain that socioeconomic factors decreased
2501 high burning. All forcings combined have led to an overall reduction in today's average BA
2502 across Canada.

2503

2504 **In Greece, anthropogenic forcing increased the chance of high fire weather in 2023.**
2505 **total climate forcing has likely led to higher present-day BA and socio-economic factors**
2506 **have likely decreased burning.** Human influence increased the probability of experiencing
2507 high fire weather in August 2023 by 1.9-4.1 times. It is likely that total climate forcing increased
2508 recent high BA in the region by up to 30%, but socio-economic factors could have led to an
2509 increase or decrease. Climate change has increased today's average BA in the Mediterranean
2510 region, but this has been mainly offset by socio-economic factors.

2511

2512 **In western Amazonia, anthropogenic forcing has greatly increased the chance of high**
2513 **fire weather in 2023. It is virtually certain that total climate forcing has led to higher BA,**
2514 **and very likely that socio-economic factors also contributed.** Human influence increased
2515 the probability of experiencing high fire weather by 20.0-28.5 times. It is virtually certain that
2516 total climate forcing increased recent high BA in the region by up to 47%, and very likely that
2517 socio-economic factors exacerbated the increase. Climate change has increased today's
2518 average BA in the Northwest region, and all forcings have led to an overall increase in burning.

2519

2520 **3.4.2 Change in Likelihood of High Fire Weather due to Anthropogenic Forcing**

2521

2522 **3.4.2.1 Canada**

2523

2524 The fire weather conditions we saw in Canada during June 2023 were 2.9-3.6 times more
2525 likely due to anthropogenic forcing. Here we assess the 95th percentile of FWI over the country
2526 during the month of peak anomaly in BA (June) in the ALL and NAT HadGEM3 simulations.
2527 More of the ALL distribution lies above the observed 95th percentile of FWI from ERA5
2528 compared to the NAT distribution (**Figure 17**), and we therefore conclude that the probability
2529 of experiencing the high fire weather observed during June 2023 is more likely in a climate
2530 forced with anthropogenic emissions.

2531

2532 **3.4.2.2 Greece**

2533

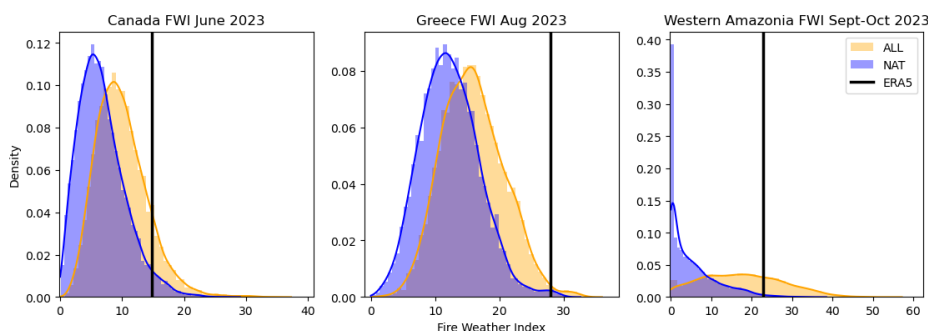
2534 The high fire weather conditions experienced during the peak anomaly in BA in August 2023
2535 were 1.9-4.1 times more likely due to anthropogenic forcing (**Figure 17**). In this case the 95th
2536 percentile of FWI is outside of the distribution so we instead assess the 90th percentile of FWI
2537 over the country. This is likely a result of our linear inference of 2023 for the bias correction
2538 based on the 1960-2013 period, where in fact 2023 was so anomalous that it doesn't fit this
2539 trend. The 2023 event threshold here also lies at the very high end of simulated fire weather,
2540 meaning it was very unusual in the model simulations. The result range here is also larger
2541 than for Canada, meaning there is less certainty about how much human influence has
2542 increased the probability, although it does highlight at least a 50% increase in likelihood of
2543 high fire weather.



2544
2545
2546
2547
2548
2549
2550
2551
2552

3.4.2.3 Western Amazonia

High fire weather in western Amazonia during Sept-Oct 2023 was 20.0-28.5 times more likely due to anthropogenic forcing (**Figure 17**). In this region there is a large shift in the ALL forcing distribution compared to the NAT only forcing for the 95th percentile of FWI, and the high risk ratio shows a strong anthropogenic signal in driving the meteorological conditions that led to high fires over this period.



2553
2554
2555
2556
2557
2558
2559

Figure 17: 95th percentile of FWI for June 2023 over (left) Canada, (middle) Greece and (right) western Amazonia, in the HadGEM3 ensemble of ALL (anthropogenic plus natural forcing, orange) and NAT (natural-only forcing, blue) bias-corrected simulations, and ERA5 reanalysis (black line).

2560
2561
2562

3.4.3 Change in Likelihood of High Burned Area in 2023 due to Total Climate Forcing and Socioeconomic factors

2563
2564

3.4.3.1 Canada

2565
2566
2567
2568
2569
2570
2571
2572
2573
2574
2575
2576
2577
2578
2579
2580
2581
2582

We show that total climate forcing was virtually certain (99.9% likelihood) to have led to more burning in events such as those observed in Canada in June 2023 (**Figure 18**). In the cells of Canada that burn most regularly (95th percentile burned area), our attribution results indicate that total climate forcing increased the extent of area burned in Canada by between 0.7 - 6.22% during the month of June in the period 2003-2019. This estimate is almost certainly conservative, as we are testing the influence of climate change on the likelihood of equivalent levels of burning in years preceding 2023, and these years have experienced less warming. Additionally in **Figure 14**, considering the anomalies of 2023, we show between 1-30% additional increase in BA extent caused by anomalous weather conditions during this heatwave on top of the 2003-2019 period. The impact of socio-economic factors is less certain, with only a 54.77% likelihood of decreasing burning, affecting BA by between -10.12 and 3.03% during 2003-2019.

Overall, we estimate that BA in Canada in June 2023 was 0.8-38.0% greater due to total climate forcing in the 2003-2019 period combined with this year's anomaly in the climatic variables. As a caveat, we note that this is not a formal attribution of the 2023 anomaly because no counterfactual exists for the year, but rather an attribution of the change in BA in 2003-2019 with the additional influence of climate factors on BA in 2023 superimposed.



2583 **3.4.3.2 Greece**

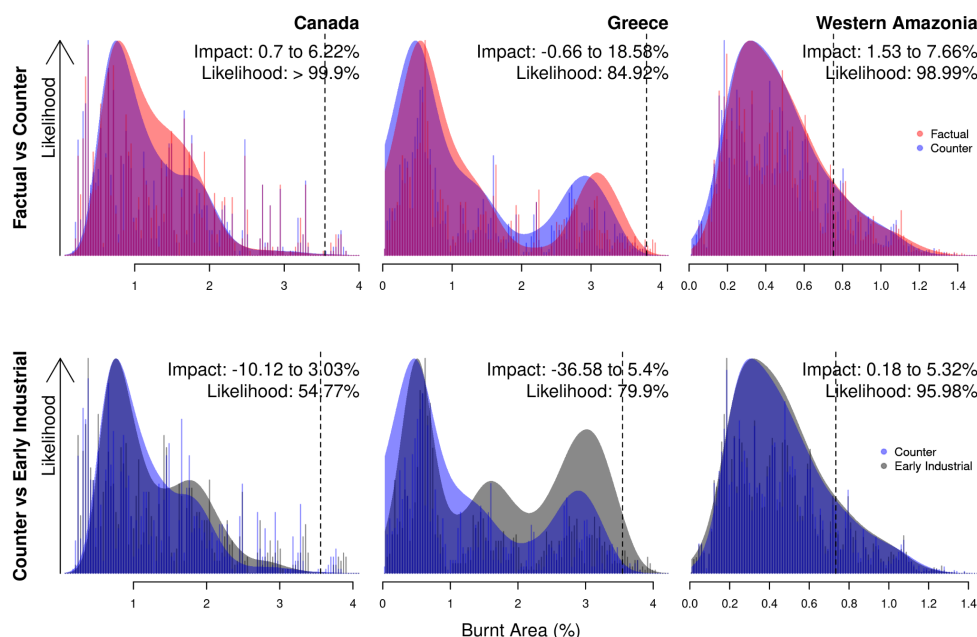
2584
2585 We show total climate forcing caused a change in high BA in Greece of between -0.66 and
2586 18.58% in the period 2003-2019, with a likelihood of an increase of 84.92% (**Figure 18**). In
2587 this case we use the 90th percentile (gridcell with the 10% highest burned areas) to represent
2588 high BA over the region for the month of August, over 2003-2019. Again this increase is likely
2589 a conservative figure given the additional warming since 2019, and estimating the additional
2590 burning that might have been experienced during the anomalous conditions of 2023, we find
2591 an additional change of -9.3-11%. Socioeconomic factors likely (79.9%) caused a decrease in
2592 burning, though could have caused an increase, affecting BA extent by -36.58 to 5.4%.

2593
2594 Overall we estimate that BA in Greece in August 2023 was influenced by -15.2-29.6% due to
2595 total climate forcing in the 2003-2019 period combined with this year's anomaly in the climatic
2596 variables. As per the results for Canada, we note that this is not a formal attribution of the
2597 2023 anomaly, but an attribution of the change in BA in 2003-2019 with the additional influence
2598 of climate factors on BA in 2023 superimposed. In the case of Greece, uncertainties around
2599 whether total climate forcing and socioeconomic factors caused an increase or decrease in
2600 BA are higher, and the smaller region size makes detecting a strong signal of change more
2601 challenging.

2602
2603 **3.4.3.3 Western Amazonia**

2604
2605 Over the period 2003-2019, total climate forcing was virtually certain to have caused an
2606 increase in burned areas like the one experienced in western Amazonia in September and
2607 Oct 2023 (99% likelihood), with a likely range of increase in extent of 1.53-7.66% (**Figure 18**).
2608 Here we assess the change in BA due to total climate forcing in the cells that burn most
2609 regularly (95th percentile) of our defined region of western Amazonia over Sept and Oct 2003-
2610 2019. Extending our analysis to the 2023 anomaly, we estimate that additional burning could
2611 have been up to 0.8-36.2% on top of the 2003-2019 levels. Despite finding little influence of
2612 humans specifically in 2023 compared to the previous 10 years in (**Figure 14**), since early-
2613 industrial, we show socioeconomic factors have had a large influence on the occurrence of
2614 extreme levels of burning. Events similar to 2023 were very likely exacerbated by
2615 socioeconomic conditions (95.98% likelihood) increasing BA by 0.18-5.32%.

2616
2617 Overall we estimate that BA in western Amazonia in September-October 2023 was increased
2618 by 2.3-46.7% due to total climate forcing in the 2003-2019 period combined with this year's
2619 anomaly in the climatic variables. Though again, we note that we determine this by convoluting
2620 the change in BA in 2003-2019 with the additional influence of climate factors on BA in 2023
2621 superimposed, and therefore it is not a formal attribution statement of the 2023 anomaly.



2622
 2623
 2624
 2625
 2626
 2627
 2628
 2629
 2630

Figure 18: Likelihood of high BA from ConFire ISIMIP3a. Panels show **(top row)** the likelihood (probability) of an extreme event such as experienced in the month of peak burning in 2023 with (red) and without (blue) total climate forcing, and **(bottom row)** likelihood of the same extreme event with (blue) and without (grey) socioeconomic forcing for **(left)** Canada, **(middle)** Greece (Centre) and **(right)** Western Amazonia. Likelihood shown on each plot, and impact refers to the increase in BA due to the forcing.

2631
 2632
 2633

3.4.4 Change in Burned Area Anomaly due to Total Climate Forcing, Socioeconomic Factors, and All Forcing

2634
 2635

3.4.4.1 Canada

2636
 2637
 2638
 2639
 2640
 2641
 2642
 2643
 2644
 2645

As reported in Burton, Lampe et al. (2023), we also show how median BA for months of interest has changed overall in the region today due to total climate forcing (**Figure 19**), socioeconomic forcing (**Figure S15**), and all forcings (**Figure S16**). Using AR6 regions that best match our focus areas, we show that BA has increased by 1.9% [0.1, 3.6] in North West North America (NWN) due to total climate forcing, but reduced by -0.2% [-1.7, 1.3] in North East North America (NEN) (**Figure 19**). In these regions, socioeconomic forcing has dampened the effects of climate change, by reducing BA by -9.5% [-13.6, -6.3] in NWN, and -8.5% [-12.5, -5.7] in NEN (see Supplement). All forcings combined have led to an overall reduction in BA of -8.3% [-12.5, -4.9] in NWN and -8.7% [-12.8, -5.8] in NEN (**Figure S16**).

2646
 2647

3.4.4.2 Greece

2648
 2649
 2650
 2651
 2652

Burton, Lampe et al. (2023) find a larger increase in median BA for months of interest due to total climate forcing in the Mediterranean region (MED), with an increase of 14.5% [11.5, 18.1] today compared to the counterfactual (**Figure 19**). This is particularly the case for the high burned areas, where the increase is larger compared to the lower end of the distribution. However, socioeconomic factors have largely offset this by reducing BA by -10.2% [-13.6, -



2653 6.6]. However all forcings combined have led to an overall regional increase in BA of 0.5% [-
2654 3.5, 5.5] (see **Figure S16**).

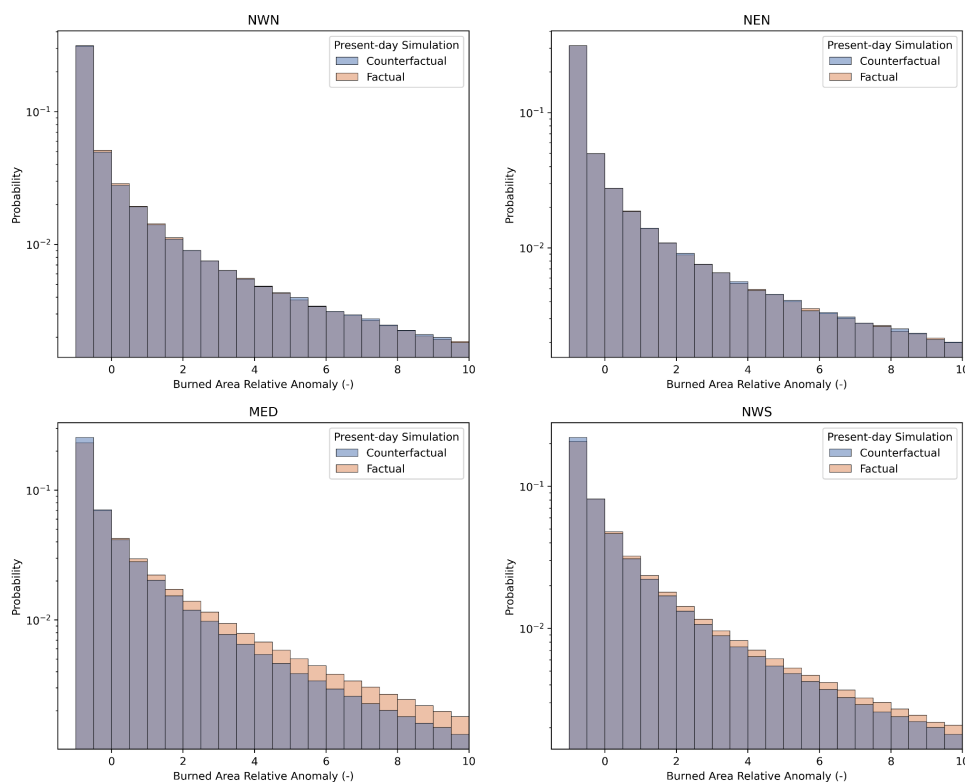
2655

2656 3.4.4.3 *Western Amazonia*

2657

2658 As per Burton, Lampe et al. (2023), total climate forcing has increased median BA for months
2659 of interest by 11.5% [5.4, 18.4] in Northwest South America (NWS) today compared to the
2660 counterfactual (**Figure 19**). Again, this increase is mostly impacting the BA at the higher end
2661 of the distribution. This is mostly offset by socioeconomic factors (-9.0% [-18.9, 1.2]), although
2662 all forcings combined have still led to an overall increase in BA of 1.5% [-6.9, 10.5] in the
2663 region (see Supplement).

2664



2665

2666

2667 **Figure 19:** Change in median BA due to total climate forcing from FireMIP. Present day BA
2668 (2003-2019) for factual (historical forcing, orange) and counterfactual (detrended climate,
2669 for AR6 regions. Panels show (**top left**) North West North America (NWN), (**top right**)
2670 North East North America NEN, (**bottom left**) Mediterranean (MED), and (**bottom right**) North
2671 West South America (NWS). Probability is shown on a log scale.

2672

2673



2674 3.5 Seasonal and Decadal Outlook

2675

2676 3.5.1 Highlights

2677

2678

2679

2680

2681

2682

2683

2684

2685

2686

2687

2688

2689

2690

2691

2692

2693

2694

2695

2696

2697

2698

2699

2700

2701

2702

2703

2704

2705

2706

2707

2708

2709

2710

2711

2712

2713

2714

2715

2716

2717

2718

2719

2720

2721

2722

2723

2724

2725

2726

2727

- **Predictions see the Indian Ocean Dipole persisting in its positive phase well into 2024.** The 2023–2024 El Niño event emerged as the fourth-most powerful on record. As 2024 comes to an end most simulations forecast a transition to ENSO-neutral conditions. Positive IOD phases are associated with elevated BA Amazonia, Indonesia, and parts of Australia though these tend to depend on interactions with ENSO.
- **Seasonal predictions of fire weather through August 2024 highlight moderate positive anomalies in Western Canada, South America (including southern Amazonia)** but no clear signal for extreme anomalies is present in the forecast. These forecasts have limited skills beyond month 1-2 (e.g., **Section 3.3.2**).
- **Effective strong mitigation efforts could limit increases in future fire extremes.** Canada in particular is very likely to see substantial increases in BA under high emissions scenarios (SSP370, SSP585) compared to high mitigation (SSP126), driven by dry conditions and climate and CO₂ driven increase in fuel load. However the lack of significant difference between middle-of-the-road (some mitigation e.g. SSP370) and no mitigation (SSP585) scenarios in this region highlights the need to constrain uncertainties in subsequent studies. In Western Amazonia, while SSP585 predicts significant increases in fire likelihood by 2100, the SSP126 scenario suggests that proactive climate strategies could maintain conditions that largely remain unchanged, underscoring the importance of mitigation actions for this region.
- **However, even with mitigation, we will still see an increase of extremes in Canada.** This necessitates robust adaptation strategies to manage and prepare for the expected rise in extreme fire events as global mean temperature continues to rise towards 1.5C above PI, ensuring that communities and ecosystems are better equipped to handle future challenges.
- **There is still a lot of uncertainty regarding how extreme fire events will change with current efforts to reduce emissions.** Our projections show a high level of uncertainty in all regions for the expected increase in extreme events under moderate mitigation efforts (SSP370 scenario) and without any mitigation (SSP585 scenario). The wide range of projections means that we cannot determine if current mitigation efforts are effective, and more research is needed to reduce uncertainties in future projections. However, even in the best-case scenarios, both SSP370 and SSP585 show significant increases in the frequency of extreme events in Canada and Western Amazonia. While all regions show, with confidence, that strong mitigation (SSP126) will reduce the occurrence of extreme events, there is still a large plausible set of future increases in extremes. Combined with the lack of understanding in future land use and direct human influence on fire, this makes it hard to inform adaptation efforts.
- **Greece’s smaller domain size means that Global Climate Models (GCMs) introduce biases and uncertainties making future projections of extremes difficult.** This highlights the need to improve model projections of future climate or incorporate other information, observations or model/statistical approaches to constrain uncertainties on small scales.

2721 3.5.2 Seasonal Outlook for 2024

2722
2723 The 2023–2024 El Niño event emerged as the fourth-most powerful on record, unleashing
2724 widespread droughts, as well as floods and other anomalous conditions worldwide. Officially
2725 declared by the World Meteorological Organization (WMO) on July 4, 2023, its meteorological
2726 impacts have unfolded between November 2023 and April 2024 (Joshi, 2023). Climate
2727 scientists have found that the 2023–24 El Niño event, compounded by the climate change

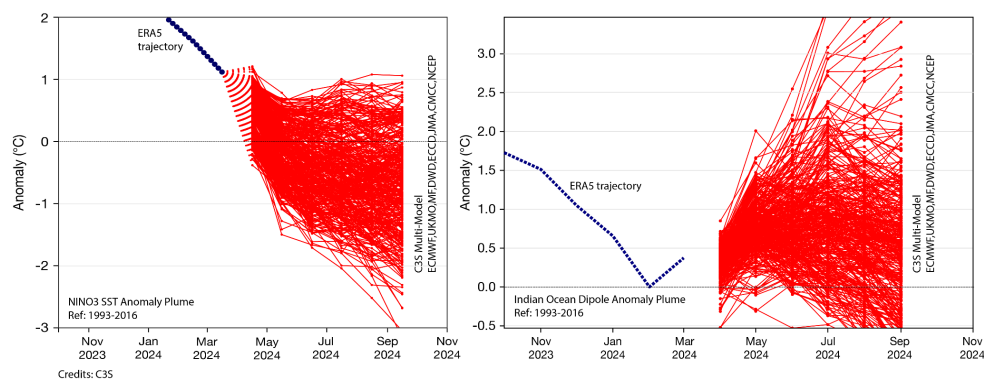


2728 crisis, has elevated global temperatures beyond the records set during the 2016 El Niño event.
2729 This has caused a 1.5°C increase in global temperature compared to pre-industrial times for
2730 most of the year and established new temperature records in 2024 (McCulloch et al., 2024).

2731
2732 As of mid-April 2024, El Niño conditions persist in the central-eastern equatorial Pacific, with
2733 important oceanic and atmospheric indicators aligning with an ongoing El Niño event that is
2734 gradually diminishing (**Figure 20**). Most simulation prediction plumes forecast a transition of
2735 the El Niño event to ENSO-neutral in Apr-Jun, 2024, which then persists during the boreal
2736 summer. The Indian Ocean Dipole (IOD) index is currently positive with the most recent value
2737 of +0.95 °C and forecasts indicate that it will remain in a positive state for the next season.
2738 Connections are established between a positive IOD phase and fire risk in Indonesia and parts
2739 of Australia, though outcomes generally depend on interactions with the ENSO phase (Pan et
2740 al., 2018; Ren et al., 2024; Abram et al., 2021). Similarly, the positive phase of the IOD is
2741 linked with heightened fire risk in South America, particularly in the Amazon basin, where it
2742 can interact with other climate teleconnections to exacerbate droughts and increase wildfire
2743 risk (Cardil et al., 2023; Dong et al., 2021).

2744
2745 **Figure 21** shows the predicted probabilities of the monthly average FWI exceeding moderate
2746 (75th percentile) or high (95th percentile) thresholds of the monthly climatology. As the
2747 strength of a positive ENSO diminishes, most areas in Southeast Asia and South America are
2748 predicted to experience a decrease in the likelihood of anomalous conditions over the next
2749 three months. Parts of Western Canada are predicted to reach moderate anomalous
2750 conditions once again in early summer, and this combined with overwintering fires could
2751 promote a second consecutive high fire season as has already been reported in the media
2752 (*BBC News*, 2024, *New York Times*, 2024). Predictions also suggest that the moderate FWI
2753 threshold will be exceeded in southeast, central, and western Brazil with the high threshold
2754 exceeded in southern and western parts. In parts of Africa, moderate FWI anomalies may be
2755 experienced throughout June-August.

2756
2757
2758

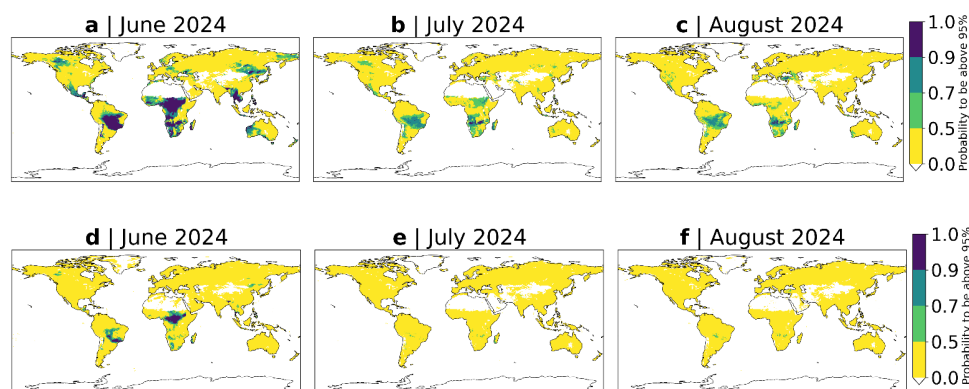


2759
2760 **Figure 20:** Anomaly plume for the ENSO and IOD as forecasted by the multimodal C3S
2761 ensemble system for April 2024. Ongoing positive ENSO event is gradually diminishing while
2762 Indian Ocean dipole is likely to remain in a positive state until September 2024 (Copernicus
2763 Climate Change Service, 2024b).

2764
2765
2766



2767



2768

2769

Figure 21: Probability for the monthly average FWI exceeding the **(top row)** 75th percentile threshold (anomalous conditions) and **(bottom row)** 95th percentile threshold (extremely anomalous conditions) of the monthly climatological distributions. The probability is calculated using the 51 ensemble member realisation from ECMWF's long-range forecasting system, SEAS5 FWI, and comparing them with the 1991-2016 climatology (Copernicus Emergency Management Service, 2019).

2770

2771

2772

2773

2774

2775

2776

3.5.3 Future Changes in Likelihood of Extreme Fire Events

2777

2778

3.5.3.1 Canada

2779

2780

2781

2782

2783

2784

2785

2786

2787

2788

2789

2790

2791

2792

2793

2794

2795

2796

2797

2798

2799

2800

2801

2802

2803

The probability of Canada experiencing a fire event similar to June 2023 (measured in terms of BA in the cells with the highest 5% burned areas) is estimated to be 0.14% under the climate conditions of 2010-2020 (**Table 7; Figure 22**). This corresponds to a return time of approximately once every 700 years. Even though the GCMs were bias-corrected to 1979-2014 values as part of the ISIMIP3b protocol, internal variability and trends were maintained. This difference can lead to discrepancies between models due to the non-linear response of fire to small changes in climate variables and simulated vegetation between ISIMIP3a and ISIMIP3b, which substantially altered the results over our baseline periods. When using bias-corrected GCM model output instead of reanalysis data, the likelihood ranges from 0.08% to 0.31%, indicating a slight bias of the probability of the event introduced by using GCM historical simulations. We describe future changes as significant if the range across GCM projects does not overlap with this range.

Over the next 10 years, the likelihood of a similar fire event occurring increases significantly to between 0.14% and 0.48%, with no significant difference across scenarios. This suggests that a 2023 fire event could be up to three times more likely by the 2030s than in the last decade. By the middle of the century, the likelihood of a 2023 fire event recurrence increases to 0.31% - 0.9% - two to almost four times as likely as today (**Table 7; Figure 22**). The different SSP scenarios diverge significantly by 2070. Under SSP126, the likelihood of a 2023 fire event recurring stabilises and remains largely unchanged until 2100, with a range of 3.07% to 3.5%. This means the recurrence of a 2023-like event would be around 2.8% to 8.3% in the last decade. Integrating between today and 2100, under SSP126, the probability of at least one event similar to or worse than the 2023 event occurring again is estimated to be between 16% and 25%.



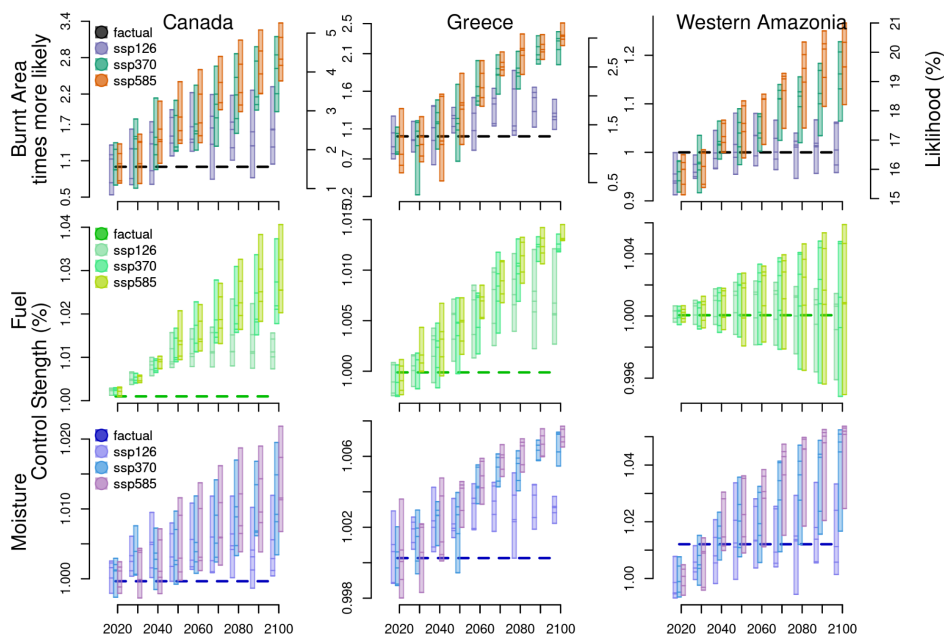
Table 7: Summary of the likelihood of extreme events today using reanalysis ‘factual’ and today and into the future using bias-corrected GCMs for our three focal regions. ‘2023’ events focuses on the BA extreme identified in **Section 3.4.3**. 1-in-100 for Western Amazonia additionally looks at the likelihood of a 1-in-100 event under present day climate conditions, following the definition of extreme in (UNEP, 2024). We also determine how much more frequent the events will be at two different time horizons based on each models likelihood in the future projections over likelihood during 2010–2020. * indicates non-significant result.

| Region | Event | SSP | Represents | | Likelihood (%/year) | | | | | | How much more frequent | | | | | | | |
|------------------|------------------|---------|--------------------|-----------|---------------------|-----------|-----------|-----------|-----------|-------|------------------------|-------|-------|-----|-----|--|--|--|
| | | | 2010-2020 | 2040-2050 | 2090-2100 | 2040-2050 | 2090-2100 | 2040-2050 | 2090-2100 | min | max | min | max | min | max | | | |
| Canada | 2023 (~1-in-700) | Factual | observed | 0.14 | | | | | | | | | | | | | | |
| | | SSP126 | strong mitigation | 0.08 | 0.27 | 0.31 | 0.6 | 0.28 | 0.83 | 2.22 | 3.88 | 3.07 | 3.5 | | | | | |
| | | SSP370 | middle of the road | 0.13 | 0.31 | 0.36 | 0.69 | 0.93 | 1.91 | 2.23 | 2.77 | 6.16 | 7.15 | | | | | |
| | | SSP585 | no mitigation | 0.12 | 0.29 | 0.46 | 0.9 | 1.15 | 2.2 | 3.1 | 3.82 | 7.59 | 9.58 | | | | | |
| Greece | 2023 (~1-in-80) | Factual | observed | 1.3 | | | | | | | | | | | | | | |
| | | SSP126 | strong mitigation | 0.91 | 1.65 | 1.36* | 1.8* | 1.42* | 1.94* | 1.09* | 1.49* | 1.18* | 1.56* | | | | | |
| | | SSP370 | middle of the road | 0.99 | 1.46 | 0.87* | 2.2* | 2.54 | 3.11 | 0.88* | 1.51* | 2.13 | 2.57 | | | | | |
| | | SSP585 | no mitigation | 0.67 | 1.78 | 1.16* | 2.39* | 2.87 | 3.26 | 1.34* | 1.73* | 1.83 | 4.28 | | | | | |
| Western Amazonia | 2023 (~1-in-6) | Factual | observed | 16.58 | | | | | | | | | | | | | | |
| | | SSP126 | strong mitigation | 15.13 | 16.57 | 15.83* | 17.92* | 15.89* | 17.61* | 1.05* | 1.08* | 1.05* | 1.06* | | | | | |
| | | SSP370 | middle of the road | 15.22 | 16.29 | 16.16* | 18.07* | 17.65 | 20.36 | 1.06* | 1.11* | 1.16 | 1.25 | | | | | |
| | | SSP585 | no mitigation | 15.13 | 16.5 | 16.39* | 18.34* | 18.21 | 21 | 1.08* | 1.11* | 1.2 | 1.27 | | | | | |
| | | Factual | observed | 1.0 | | | | | | | | | | | | | | |
| | | SSP126 | strong mitigation | 0.82 | 1.53 | 1.28* | 2.16* | 1.23* | 2.01* | 1.41* | 1.46* | 1.31* | 1.5* | | | | | |
| 1-in-100 | | SSP370 | middle of the road | 0.81 | 1.46 | 1.29* | 2.23* | 1.97 | 3.14 | 1.53* | 1.59* | 2.15 | 2.43 | | | | | |
| | | SSP585 | no mitigation | 0.8 | 1.49 | 1.43* | 2.36* | 2.32 | 3.34 | 1.58* | 1.79* | 2.24 | 2.9 | | | | | |



2810 Mitigation efforts under SSP370 have some impact, lowering the likelihood to 0.93% to 1.91%
 2811 by 2100 compared to 1.15% to 2.2% in SSP585 (no mitigation; **Table 7; Figure 22**). The
 2812 probability of an event like 2023 occurring at least once by 2100 is estimated to be between
 2813 30% and 52% under SSP370 and between 35% and 56% under SSP585. Someone born in
 2814 Canada in the current decade, with a life expectancy of 83 years (United Nations Population
 2815 Division, 2022), has a 43-66% probability of seeing a similar event in their lifetimes under
 2816 SSP585, compared with only an 11% likelihood of someone who was 83 years old in the
 2817 2010s. Someone born in Canada today would also have a 18-45% probability of seeing an
 2818 event of similar magnitude *twice* under SSP585. This reduces substantially to 20-31% for one
 2819 occurrence and 4-10% for two occurrences under SSP126.

2820
 2821 The divergence between shared socioeconomic pathways (SSPs; **Table 7; Figure 22**) is
 2822 primarily driven by variations in the increase in fuel load, although an increase in fuel dryness
 2823 is a major driver of increased burning across SSPs, particularly in SSP585. The worst-case
 2824 scenario within SSP585 sees a substantial increase in both and changes in both controls are
 2825 needed to explain divergence between SSPs.
 2826



2827
 2828 **Figure 22:** Future projections from ConFire of the likelihood of BA extremes and their
 2829 corresponding fuel and moisture controls. Each set of bars shows changes in each decade,
 2830 with each bar representing a different SSP scenario and the spread of bars indicating the
 2831 variation across GCMs. The BA data indicates (**right axis**) the likelihood of the defined event
 2832 occurring in any given year for future decades and (**left axis**) the frequency of occurrence for
 2833 relative to reanalysis-driven simulations (factual ISIMIP3a – dashed line) of the years 2010-
 2834 2020. The fuel and moisture rows illustrate the change in the maximum burning allowed by
 2835 that control relative to reanalysis-driven simulations for the years 2010-2020.

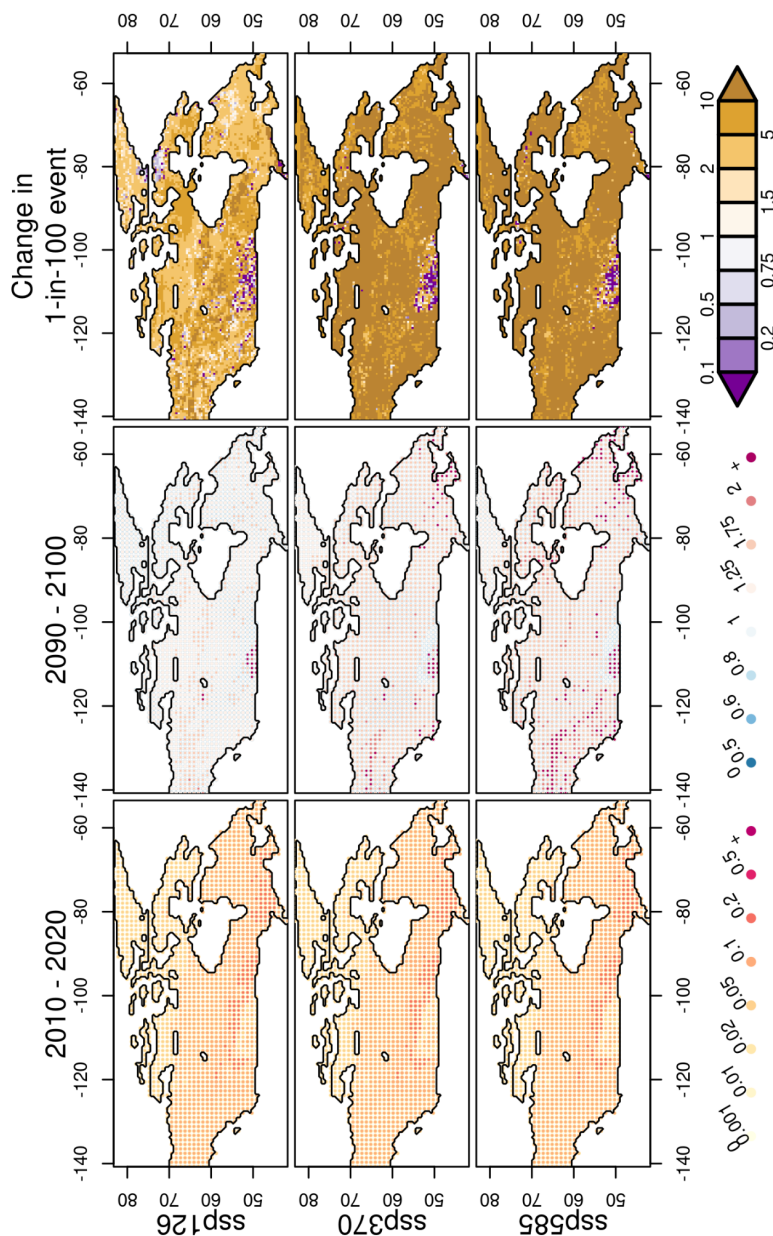


Figure 23: Projected changes in June-August BA over Canada by 2090-2100 under three SSP scenarios, with BA simulated by ConFire. **(Left)** Average June-August BA fraction (%) for 2010-2020. **(Middle)** Relative change in June-August BA extent projected for 2090-2100 values. **(Right)** Increased (or decreased) frequency in 2090-2100 of a 1-in-100 year event defined for the period 2010-2020 values. In the left column, the size of the dot in each grid cell indicates the likelihood (larger = higher likelihood) of a BA fraction (or being greater than the threshold indicated by the coloured dot (see legend at the base)). Likewise, the size of the dot varies with likelihood that the BA fraction exceeds the threshold indicated by the coloured dot (see legend at the base). For example, a large pale orange dot in the left column indicates a high likelihood of the BA fraction exceeding 0.05%, whereas a small dark red dot indicates a small (but non-zero) likelihood of the BA fraction exceeding 0.5%.

2836
 2837
 2838
 2839
 2840
 2841
 2842
 2843

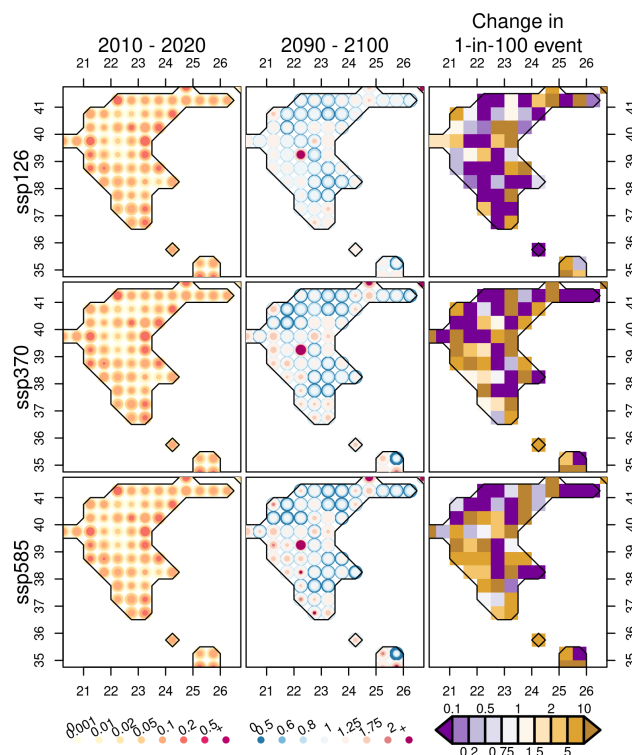


2844 While some areas of Canada see increases in BA and fire extremes (spatially measured as
2845 the proportional change in probability of a 2010-2020 1-in-100 annual event, as per UNEP
2846 (2024) almost everywhere (**Figure 23**), increases in BA are likely to be particularly strong in
2847 the critical regions of agriculture in Southern Alberta and Saskatchewan, starting from 2030
2848 (**Figure S17**) and becoming particularly strong by 2090s (**Figure 23**). However, some regions
2849 just to the North of this region may see a decrease in future extremes. While Yukon and
2850 Northwest Territories will see an increase in BA and fire extremes from 2040 (**Figure S18**),
2851 the increase in extremes remains similar to the rest of Canada, at around a doubling in
2852 occurrence. By the end of the century, however, SSP370 and SSP585 diverged from the high
2853 mitigation SSP126, and both scenarios see a much larger increase in burned areas and some
2854 areas with extreme occurrences becoming 5 times more common. SSP585 sees these
2855 increase in fire risk extending down through British Columbia.
2856

2857 **3.5.3.2 Greece**

2858
2859 Using the ISIMIP3b GCMs for Greece introduced a strong bias when using the 95% of burned
2860 areas. We therefore used the 90% percentile (i.e BA in the 10% cells that see the most BA)
2861 to measure areas showing extreme burning. Here, using GCMs instead of reanalysis changed
2862 the likelihood of Greece's August 2023 event from 1.3% to 0.67-1.78% for 2010-2020 (**Table**
2863 **7**; **Figure 22**). While there is an indication of increased likelihood of extensive BA by the middle
2864 of the century, the projected range of changes in future extremes remains smaller than the
2865 introduced historical bias and is, therefore, insignificant. For SSP126, this small but
2866 insignificant increase remains until 2100, though at times, SSP126 shows the possibility of a
2867 substantial increase – up to 2.3 times more likely than today. This shows that Greece may still
2868 see large increases in the occurrence of extreme BAs even under strong mitigation, though
2869 uncertainties are too large to state this confidently. This may be due to Greece's smaller region
2870 and the need for a larger sample of points to overcome the inherent noise in simulating BA
2871 extremes. Our uncertainty quantification was necessary to determine these significant/non-
2872 significant results. SSP350 and SSP585 show significant increases by 2070, and significantly
2873 diverge from SSP126 by 2080. There is no significant difference between the scenarios by
2874 2100, which indicate a likelihood of seeing an annual recurrence of 2023's event of between
2875 2-54-3.26% by 2100 – a 1.83-to-4.28-fold increase today and an average return time of every
2876 39-31 years. While fuel loads show a larger increase than fuel moisture in future projections,
2877 the regions are less sensitive to fuel (Kelley et al. 2019; **Figure 14**), and differential increases
2878 in fuel dryness dominate the variations between SSPs by 2100.
2879

2880 While it is hard to ascertain a clearer climate signal on area extremes across Greece, there
2881 are some spatial patterns in likelihood of extreme occurrence with Greece (**Figure 24**). The
2882 middle of Greece may see a decrease in extremes in the future as early as the 2030s and
2883 2040s (**Figure S20, S21**), with Central Greece and Macedonia seeing that large decreases
2884 by 2090 (**Figure 24**), though some areas of Central Greece, West Greece and Peloponnese
2885 seeing a potential rise in extremes. Changes in BA are less pronounced and future projections
2886 suggest either decreases or increases in summer burning is possible.
2887



2888
 2889
 2890
 2891

Figure 24: Same as **Figure 23**, but for Greece and months July-September.

2892
 2893

3.5.3.3 Western Amazonia

2894
 2895
 2896
 2897
 2898
 2899
 2900
 2901
 2902

The analysis of the South American region suggests a 16.58% chance of experiencing high burned areas (measured in terms of BA in the cells with the highest 5% burned areas) in Sep/Oct 2023, based on data from 2010-2020 using ISIMIP3a (**Table 7**; **Figure 22**). Replacing this with ISIMIP3b introduces a small bias, with a likelihood of 15.13-16.57%. These events, while higher than average, are not as extreme as those in Canada and Greece, with a likely return time of 6 years in ISIMIP3a and 6-7 years in ISIMIP3b. However, this may hide the spatial variations and shift in locations of extremes, particularly along the deforestation front, as highlighted in **Figure S14**.

2903
 2904
 2905
 2906
 2907
 2908
 2909
 2910
 2911

There are only small increases in projected future extremes, noting that we do not consider land use change, which can be a major driver of BA in some regions (Lapola et al., 2023; Kelley et al., 2021; Silveira et al., 2020). Under the SSP585 scenario, there is a notable and significant increase in future burning, estimated to be 1.2-1.27 times more likely than current levels by 2100. This increase is primarily attributed to drier fuel moisture, in line with the trend suggested by the FWI analysis in **Section 3.4.2**. There is potential for mitigation, particularly under the SSP126 scenario, which converges with the other two SSPs. This suggests that the levels of extreme fire activity may largely remain unchanged by 2100.

2912
 2913
 2914

While fuel load could potentially have a significant impact, it remains uncertain whether it would lead to an increase or decrease in burning. **Section 3.3** emphasises the positive influence of land use on the 2023 burning levels in some locations. However, despite the likely



2915 substantial impact inferred from results in these sections, future land use projections were not
2916 available at the time of writing and should be prioritised for next year's report.

2917
2918 The likelihood of the occurrence of the 2023 event increases substantially in the centre of the
2919 region by the 2030s (**Figure S21**) and is almost universal across the region by 2024 (**Figure**
2920 **S22**), though small pockets around Manaus and roads in the south may see either not much
2921 change or the chance of a decrease. Perhaps more important for the region's fire-sensitive
2922 forests is the projected increase in BA in SSP370 and SSP585 across forests in the north of
2923 the region could have a significant impact on local vital ecosystems within the next few
2924 decades (**Figure S23**).

2925
2926 When testing more extreme levels of burning of a 1% likelihood in ISIMIP3a, there is a
2927 noticeable divergence compared to present conditions and between different SSP scenarios
2928 in future projections (**Table 7**). Introducing a minimal bias using ISIMIP3b changes the
2929 likelihood to between 0.8-1.53. Across all scenarios, there is an increase in extreme events
2930 throughout the 21st century, although the significance is only reached in the last couple of
2931 decades in SSP370 and SSP585. Without mitigation, there is a likelihood of 2.32-3.34 of a 1-
2932 in-100 event by 2100, representing an increase of 2.24-2.9 times. However, stringent
2933 mitigation measures show a decrease in extremes, with a 1-in-100 event only increasing to
2934 1.31-1.5. This suggests that strong mitigation measures may offset the risk of extreme burned
2935 areas in the region in the future.

2936

2937 **4 Discussion and Conclusions**

2938

2939 **4.1 Summary of the State of Wildfires in 2023-24**

2940

2941 **Objective 1: Regionally identify extreme individual wildfires or extreme wildfire seasons** 2942 **of the past 12 months, and place them in context of recent trends**

2943

2944 In this report, we used a combination of data from global Earth Observation products and data-
2945 driven models (Jones et al., 2024; Giglio et al., 2018; van der Werf et al. 2017; Kaiser et al.
2946 2012), regional products (e.g. EFFIS), and insights from regional experts to identify key events
2947 of the period March 2023-February 2024. Highlighted results are provided in **Section 3.1.1**
2948 and summarised here. The 2023-24 fire season saw 3.9 million km² burned globally, slightly
2949 below the previous average, yet carbon emissions were 16% above average due to severe
2950 fires in Canada's boreal forests and despite low fire activity in African savannahs. In North
2951 America, Canada experienced record-breaking fires, with extensive damage and significant
2952 evacuations, while there were also localised yet severe incidents in the US (notably in Lahaina,
2953 Hawai'i, where 100 people lost their lives). South America saw below-average fire activity
2954 overall, but with an anomalous high fire season in Western Amazonia in 2023 and northern
2955 parts of the continent so far in 2024. Severe impacts of individual fires were also seen, notably
2956 in Paraíso, Chile, where 131 people lost their lives. Europe had generally low fire activity,
2957 except for significant incidents in Greece which included the largest fire on record in the EU.
2958 Oceania saw above-average fire activity focussed on Western and Northern parts of Australia.
2959 Asia experienced low fire activity overall, but with some significant regional impacts in
2960 Southeast Asia and parts of Russia. Africa's fire extent was low, although notable fire-related
2961 emergencies occurred in Northern and Southern Africa.

2962

2963 **Objective 2: Shortlist a selective number of focal events (extreme individual wildfires** 2964 **of extreme wildfire seasons) with notable impacts on society or the environment.**

2965

2966 While identifying events to become foci of the report is not trivial due to the diversity of impacts
2967 that wildfires present, we selected a pragmatic set of three events for further analysis. In



2968 **Canada**, the 2023-24 fire season was marked by an unprecedented burned area, high carbon
2969 emissions, and a prolonged fire season with severe air quality impacts and significant human
2970 and economic tolls. **Greece** experienced its second-worst fire season on record, with
2971 extensive damage, large-scale evacuations, and significant urban and infrastructural impacts,
2972 particularly from the massive Evros fire. **Western Amazonia** faced unprecedented fire counts,
2973 severe air quality degradation, and broad socio-economic and environmental impacts,
2974 highlighting the critical global significance of the region's fire activity.

2975
2976 **Objective 3: Diagnose the contributions of fuel dryness, fuel load, ignitions and**
2977 **suppression to the occurrence of each focal event.**

2978
2979 Using Bayesian inference and data-driven methods, we attributed observed fire activity and
2980 resulting burned areas to four controls: weather, fuel abundance and status, and others. The
2981 "others" category includes human influences, ignition sources like lightning, and residuals of
2982 all missing predictions. For BA, we can still include long-term variations in "other" human
2983 drivers to test anomalies in direct human influences on fire. We found that fire weather
2984 conditions alone do not entirely drive the occurrence of significant fire events in 2023-24. Even
2985 in Canada, where fires are primarily weather-driven, the most intense burning events in mid-
2986 July, early August, and late September were not predicted, highlighting potential shortcomings
2987 in forecasting specific ignition sources and accurately depicting fire spread across extensive
2988 landscapes. By incorporating variables beyond fire weather, however, we successfully
2989 attributed drivers of much of the fire activity and BA with reanalysis meteorology and remote
2990 sensed land data. The event in Greece could not be uniquely attributed to one source; instead,
2991 all elements, including human influence, strongly contributed to the prediction. Availability of
2992 input data, related to the complexity of fire at the urban interface, limited the ability of the
2993 modelling frameworks to accurately diagnose contributions to the Alexandroupolis fire. Future
2994 developments aim to further expand on the variables related to manmade ignition sources and
2995 suppression efforts (e.g. urbanisation). A similar situation occurred in the Amazonian domain,
2996 where a combination of extended drought, human-induced practices, and weather explained
2997 fire activity. Additionally, changing patterns of human activity and fuel loads explained fire
2998 anomaly edges. It was found that the most severe burning could not be explained by one
2999 single control and often multiple factors were concomitant. Across all three regions, the extent
3000 of fire anomalies and the boundaries between extreme and non-extreme burned areas were
3001 often influenced by lack of anomalous control or by lower-than-average fuel anomalies.

3002
3003 **Objective 4: Assess the capacity of operational predictive systems to forecast each**
3004 **focal event.**

3005
3006 Employing fire weather indices, we have analysed current capability to pre-alert for the
3007 extreme events highlighted in this report in line with fire agency practices. Fire agencies
3008 typically use local fuel condition data to interpret FWI values, which reduces intervention on
3009 high FWI values when fuel conditions aren't hazardous. The analysis mostly concentrated on
3010 the ability of metrics such as the FWI to indicate anomalous conditions rather than their
3011 reliability in prediction. In Canada, conditions were well predicted, and FWI could even capture
3012 the timing of the release break. However, this metric is less successful in the Amazon domain,
3013 where weather is not the primary driver of fire activity. Of particular concern is our current poor
3014 capacity to pre-alert for extreme fires such as the one in Alexandroupolis, Greece. Despite
3015 indications of extreme conditions in FWI records surrounding the event, similar circumstances
3016 in late July did not yield catastrophic impacts. Comparable findings in South America further
3017 emphasise that despite weather conditions serving as persistent controls, several intense fire
3018 periods in late August and September went unpredicted, likely due to unrepresented ignition
3019 sources. This highlights the necessity of broadening early warning systems beyond fire
3020 weather, taking into account fuel availability, fuel types, and ignition variability, to enhance the
3021 reliability of fire risk assessment. The primary goal and philosophy of fire danger rating is to



3022 indicate potential fire behaviour in presence of ignitions, and so our results are consistent with
3023 and emphasise the caveats of FWI.

3024

3025 **Objective 5: Attribute each focal event to anthropogenic factors including climate**
3026 **change and land use.**

3027 Using three methods of fire attribution, we find that the probability of high fire weather has
3028 been increased in all of the focal regions due to anthropogenic forcing, extreme fires have
3029 increased due to climate change, but average BA has been largely offset by socioeconomic
3030 factors. The highest increase in FWI has been in western Amazonia, where the probability of
3031 high fire weather has increased by 20.0-28.5 times due to human influence. In Canada we
3032 find that the probability of high FWI at least doubled as a result of anthropogenic forcing, in
3033 line with findings from the World Weather Attribution (Barnes et al., 2023). In both Canada and
3034 western Amazonia it is virtually certain that climate change has increased the extreme BA
3035 experienced in the region (by up to an estimated 38% and 47% respectively), such as the
3036 events witnessed in 2023. The influence of socioeconomic factors on extreme burning is less
3037 certain for each region, except for western Amazonia where it is very likely that they
3038 exacerbated the fires. When considering how median BA has changed in the present day
3039 period, results show that climate change has led to an increase in most of the AR6 regions
3040 related to our case study areas. However in all three areas, socioeconomic factors have
3041 reduced BA, dampening the effects of climate change that would otherwise have been
3042 experienced. When the impact of all forcings is assessed, we find there is a net increase in
3043 mean BA in Northwest South America and the Mediterranean, but an overall reduction in mean
3044 BA in North West and East North America, signalling that socioeconomic factors outweigh the
3045 increase from climate change in these areas.

3046 **Objective 6: Provide an outlook on the probability of extreme events in the coming fire**
3047 **season**

3048 With the weakening of a positive ENSO, it is anticipated that most regions in Southeast Asia
3049 and South America will witness a decrease in the likelihood of anomalous conditions persisting
3050 over the next three months. However, the ongoing Indian Ocean Dipole (IOD) is expected to
3051 elevate landscape flammability across South America and West Africa. We provide the
3052 expected anomaly in the next 3 months for the FWI, highlighting the likelihood of moderate
3053 anomalous conditions in western Canada in early summer. Given the severity of the previous
3054 fire season and the possibility of overwintering fires, this could once again lead to an early
3055 start of the Canadian fire season. At extended lead times (greater than 2 months), forecast
3056 skills are limited, and the model is likely to represent climatological values, so no discernible
3057 signal about moderate or anomalous conditions is identified (Di Giuseppe et al., 2024).

3058 **Objective 7: Project future changes in the probability of each focal event under future**
3059 **climate scenarios.**

3060 We projected future changes in the annual likelihood of each focal event under different
3061 climate scenarios. In Canada, we project significant increases in the likelihood of burned areas
3062 over the coming decades, driven by dry conditions and a climate- and CO₂-driven increase in
3063 fuel load. Climate-change mitigation efforts, particularly low emissions scenarios such as
3064 SSP126, offer potential to limit future fire extremes. Similarly, projections for Western
3065 Amazonia indicate a notable increase in future burning, primarily attributed to drier fuel trends.
3066 Using a more extreme baseline than the observed event - a 1-in-100 year event under recent
3067 climate, shows that likelihood of extremes increases with the magnitude of the extreme.
3068 Effective mitigation actions are crucial in keeping existing conditions largely unchanged,
3069 emphasising the importance of limiting temperature rise to well below 2.0°C. However, even
3070 with mitigation efforts, an increase in extremes is expected in Canada as global temperatures
3071 continue to rise towards 1.5°C, necessitating robust adaptation strategies to manage and



3072 prepare for the rise in extreme fire events. Meanwhile, Greece's smaller domain size makes
3073 confident projections difficult, given remaining biases and uncertainties in future projections,
3074 highlighting the necessity of improving model projections or incorporating additional
3075 information to constrain uncertainties on smaller scales.

3076 4.2 Frontiers in Observing and Modelling Extreme Fire Occurrence

3077
3078 As part of this inaugural edition of the State of Wildfires report, we review current capabilities
3079 in the observation and modelling of extreme fire. This section will not be revised annually but
3080 will be revisited on longer intervals at times that are appropriate given progress in the
3081 observational and modelling fields. The review serves to define the current challenges that
3082 studies such as our face and identify pathways to overcoming those challenges harnessing
3083 new capabilities and technologies.
3084

3085 4.2.1 Defining of Extreme Fire Events

3086
3087 While the study of impactful fires or unusual fire seasons is critical for understanding changes
3088 in the exposure and vulnerability of people and the environment to fire, a number of challenges
3089 hinder our ability to arrive at a clear and universally-accepted definition of "extreme" event.
3090

3091 Key challenges to the data-oriented identification of extreme events include:

- 3092
3093 • **Lack of Consensus on Quantitative Criteria:** There is considerable variability in the
3094 measurable criteria used to define "extreme fire" across different studies, such as fire
3095 size and area affected. Additionally, there is no well-defined statistical threshold
3096 established for what constitutes an outlier event, which is crucial for consistent data
3097 analysis and classification.
- 3098 • **Geographic Variability:** Definitions of what constitutes an extreme fire vary
3099 significantly by region, complicating the establishment of a universally accepted
3100 definition. The size threshold can range from >100 hectares to >100,000 hectares
3101 depending on geographic location, influenced by local fire regimes.
- 3102 • **Evolving Definitions:** Over time, the definition of extreme fire has evolved and
3103 expanded, leading to ambiguity. This evolution means the term now encompasses a
3104 wider range of fire types and behaviours. Climate change is imposing an increasing
3105 trend in fire severity in many regions, suggesting that definitions should have the
3106 flexibility to evolve.
- 3107 • **Context Dependence:** Definitions of extreme fire are often context-dependent,
3108 varying with ecosystem types and fire histories. The baseline for defining what is
3109 considered extreme is not standardised, such as whether it should be based on fire
3110 return intervals or on the quantified damage to ecosystems and societies.
3111

3112 Key challenges to the knowledge-oriented identification of extreme events include:

- 3113
3114 • **Lack of Consensus on Qualitative Criteria:** There is significant variability in how
3115 criteria such as fire behaviour, resistance to control, and ecosystem and socio-
3116 economic impacts are interpreted and integrated into definitions of "extreme fire." This
3117 variability reflects differing expert opinions and knowledge bases. The challenges here
3118 principally relate to the subjective nature of what constitutes significant impact, whether
3119 ecological, economic, or societal, further complicating the establishment of a clear and
3120 universally accepted definition.
- 3121 • **Terminological Overlap and Redundancy:** The term "extreme fire" overlaps with
3122 other fire-related terms such as "catastrophic fire" and "megafire", which may also lack
3123 clear definitions or be used interchangeably, leading to confusion.



- 3124 • ***Influence of Language and Culture:*** The interpretation and usage of the term can
3125 differ across languages and cultures, influencing how extreme fires are defined and
3126 reported in the global scientific community.
- 3127 • ***Societal Influence on Scientific Terminology:*** Scientific terminology often evolves
3128 in response to its usage in broader societal contexts, such as media or public
3129 discourse. As the societal challenges arising from wildfires ultimately motivate
3130 scientific inquiry, the language used in scientific communication must be adaptable
3131 and responsive to ensure it remains relevant and accessible to non-scientific
3132 audiences.
- 3133 • ***Scientific Rigour and Clarity:*** There is a need for a definition that is clear, consistent,
3134 and scientifically rigorous to allow for standardised and repeatable measurements
3135 across studies. Existing definitions often fail to meet these criteria comprehensively.
3136

3137 Defining the term 'extreme fire' and how to address it requires a significant and inclusive effort
3138 across the fire science community. We actively avoid a strict definition of 'extreme fire' here
3139 due to the risk that the wider fire science community rejects our proposed solution, prompting
3140 confusion. Instead, we adopt a broad definition of 'extreme fire' as discussed in **Section 2.1.2**.
3141 Both of the challenges above can be addressed by developing standardised criteria and
3142 protocols for defining extreme fires (Chu et al., 2023). This task has been approached with
3143 respect to the term "megafire" although it remains to be seen if that intervention will be effective
3144 (Linley et al., 2022). Doing so requires a transdisciplinary approach, including input from the
3145 science community, fire practitioners, legislators, and impacted communities at a minimum
3146 (Shuman et al., 2022).
3147

3148 **4.2.2 Observing Extreme Fire Events**

3149
3150 Global-scale data for characterising extreme fire events are primarily sourced from satellite
3151 observations, notably active fire detections, BA maps, and tracking of smoke plumes.
3152 However, to accurately define how extreme a fire event is, it is crucial to contextualise present-
3153 day observations within historical data. Unfortunately, the historical records of satellite-derived
3154 active fire and BA products are relatively short. The longest coherent observations on a global
3155 scale are derived from the MODIS instruments onboard the Aqua and Terra satellites,
3156 launched in 1999 and 2002 respectively. Various global BA products, such as MCD64 product
3157 family (Giglio et al., 2018) and FireCCI51 (Lizundia-Loiola et al., 2020), as well as active fire
3158 data like the MCD14 product family (Giglio et al., 2016), have been generated based on
3159 imagery acquired by MODIS. Although these time-series now span over two decades, they
3160 are still relatively short when compared to the decadal to centennial fire return intervals observed
3161 in many ecosystems.
3162

3163 Pre-MODIS satellite data, like that from the AVHRR program, exists and provides a continuous
3164 imagery archive from 1982 onwards. Although efforts are ongoing to generate a coherent BA
3165 product from AVHRR data (Otón et al., 2021), there are limits to the global applicability of
3166 these products. For example, unresolved challenges stemming from coherence issues
3167 between imagery from different AVHRR sensors result in artefacts and spurious trends in
3168 various regions worldwide (Giglio and Roy, 2022), although this has been debated by other
3169 authors (Pullabhotla et al., 2023). Other pre-MODIS data available are the Along-Track
3170 Scanning Radiometer (ATSR) and Visible and Infrared Scanner (VIRS) active fire data (Giglio
3171 et al., 2013; Arino et al., 1999), but with important limitations concerning detection sensitivity,
3172 missing data and only allow for the expansion of existing time-series by 3 years (start in 1997).
3173

3174 Efforts are ongoing to extend the MODIS time-series by incorporating active fire data from
3175 ATSR and VIRS with BA data (e.g. Chen et al. 2023). However, due to the different
3176 characteristics of these data, creating a coherent, multi-satellite time-series of active fire data
3177 and/or BA is not straightforward. Concerns also arise with the impending decommissioning of



3178 MODIS-Terra, raising doubts about the continuity of existing long-term fire records. However,
3179 operational satellite sensors such as VIIRS onboard NOAA's series of satellites and SLSTR
3180 onboard the Sentinel-3 satellites offer promising capabilities for medium-resolution BA
3181 mapping (e.g. Román et al., 2024; Lizundia-Loiola et al., 2022). Urgent attention should be
3182 directed towards developing methodologies to integrate these new datasets into a coherent,
3183 long-term BA dataset. Furthermore, advancements in medium-resolution satellite data
3184 availability and revisit times, particularly from Landsat and Sentinel-2, now enable global BA
3185 mapping at spatial resolutions as fine as 20-30m (e.g., Roteta et al., 2021; Chuvieco et al.,
3186 2022), suggesting a potential future direction for coherent long-term global BA monitoring.
3187

3188 While BA is a key variable to characterise extreme fire occurrence, multiple other aspects of
3189 extreme fires can be characterised using satellite data. BA products can be used to cluster
3190 burned pixels in burned patches to obtain the number and size of individual fires (Archibald
3191 and Roy, 2009). Furthermore, the daily fire rate-of -spread, length of the active fire line and
3192 spread direction can be extracted from the daily fire expansion (Andela et al., 2019). These
3193 algorithms, such as the Global Fire Atlas used in this study, give global scale, coherent
3194 estimates of patterns and trends in fire number, fire size and rate of spread. However, these
3195 algorithms are sensitive to the temporal accuracy of the per-pixel burned date detection, the
3196 spatial resolution of the BA product, and any errors within each product. Recent advances
3197 focusing on clustering VIIRS thermal anomalies and extracting fire rate of spread, fire
3198 expansion and length of the active fire line show promising results (Andela et al., 2022,
3199 Hantson et al., 2022, Chen et al., 2022) but have so far not been developed globally. Future
3200 development towards a global product should allow for a more detailed characterization of fire
3201 characteristics in near real-time, well-suited for detection and quantification of fire extremes.
3202

3203 Active fire detections also record the amount of radiation emitted by the fire at the moment of
3204 satellite overpass (Fire Radiative Power, FRP), within the pixel detected by the satellite. While
3205 this information is related to the intensity of the fire, the usage of FRP has been difficult as a
3206 low-intensity fire burning a large extent of the pixel can have a higher FRP than a high-intensity
3207 fire burning a small fraction of a pixel. These complications have limited a more standardised
3208 and operational usage of FRP for quantifying fire extremes. Advances in active fire detection
3209 from higher resolution sensors may allow for a more comprehensive estimate of fire intensity
3210 when combined with FRP estimates from coarse resolution sensors (Schroeder et al., 2014,
3211 2016).
3212

3213 **4.2.3 Predicting Extreme Fire Events**

3214
3215 Since the 1970s, fire predictions have relied on empirical fire behaviour models tailored to
3216 specific ecosystems (Bradshaw et al., 1983; Noble et al., 1980; Stocks et al., 1980; van
3217 Wagner, 1987), becoming pivotal tools for fire management agencies (San-Miguel-Ayanz et
3218 al., 2013). The ease of implementation and the availability of weather data have contributed
3219 significantly to their widespread adoption. However, despite their utility, several studies have
3220 highlighted the limited effectiveness of the FWI and similar metrics in fuel-limited ecosystems,
3221 where fires are driven by the short-term superficial drying of intermittently available biomass
3222 (Yebra et al., 2013). The absence of consideration for actual fuel availability presents a
3223 constraint to the meaningful application of the FWI in savanna-type ecosystems. Beyond
3224 weather conditions, the remaining prerequisites for fire activity—namely, fuel and ignitions—
3225 are intricately linked to vegetation state, lightning activity, and human behaviours. Improving
3226 fire forecasts beyond solely considering fire weather could be achievable by accurately
3227 describing these components. This has been widely recognised in the global vegetation-fire
3228 community for several decades (Hantson et al., 2016), and consequently great advances have
3229 been made to address this through the development of fire-enabled DGVMs, as used in this
3230 report. However, explicit representation of these processes introduces biases and instabilities
3231 that, when used in isolation, limits their utility for assessing climate and human drivers of BA
3232 extremes (Hantson et al., 2020; Burton, Lampe et al., 2023).



3233

3234 The availability of remote observations for fuel, either independently (Yebara et al., 2018) or
3235 supported by modelling frameworks (McNorton and Di Giuseppe, 2024), has demonstrated
3236 potential in aiding the development of new fire models and indices that partially incorporate
3237 fuel considerations into their formulation (Di Giuseppe, 2023, Hantson et al., 2016). However,
3238 it is the emergence of the data-driven revolution that holds the promise of significantly
3239 enhancing our predictive capabilities for extreme fires (McNorton et al., 2024), and has driven
3240 the development of the semi-empirical tools used in this report. Not only can these tools
3241 enhance predictive capability for extreme fires, they also present an opportunity to disentangle
3242 the drivers of the prediction, giving us the capability to address or at least understand the
3243 causes of the event, as demonstrated by the POF and ConFire frameworks used here. The
3244 coupling of FireMIP models with observational data (Burton, Lampe et al., 2023 and used
3245 here), also showcases the potential to bridge the advanced modelling capabilities of FireMIP
3246 with application-specific approaches such as ConFire and POF.

3247

3248 Despite these technological advancements, widespread adoption is unlikely to occur
3249 suddenly, as there typically exists a delay between the creation of new indices, their
3250 operationalization, and global acceptance by those responsible for fire prevention and control.

3251

3252 Another emerging element is the recent availability of fire danger predictive systems at the
3253 seasonal and subseasonal timescales (Di Giuseppe et al., 2024). Currently, there is limited
3254 evidence on how these longer-range tools could contribute to prevention planning and
3255 adaptation strategies. While they exhibit minimal skill beyond two months, they may offer
3256 valuable pre-seasonal warnings under specific conditions established during important
3257 atmospheric modes of variability. Certainly, this aspect will need to be further investigated in
3258 the following issues of this report.

3259

3260 **4.2.4 Attributing Extreme Fires to Global Change**

3261

3262 The prediction and management of extreme fire events have become increasingly complex
3263 due to the multifaceted impacts of global change. Climate change exacerbates fire risks
3264 through rising temperatures, altered precipitation patterns, and more frequent and severe
3265 droughts, as shown in Canada and NW Amazon in this report. These climatic shifts affect
3266 vegetation productivity, with elevated CO₂ levels potentially increasing biomass and thereby
3267 providing more fuel for fires. Nutrient deposition and other environmental changes influence
3268 ecosystem responses, further altering fire potential. Land use changes and management
3269 practices also significantly influence fire dynamics. For example, human activities such as
3270 deforestation, urban expansion, and agricultural practices can both mitigate and exacerbate
3271 fire risks, with socioeconomic factors shown to have a strong influence on overall extreme fire
3272 likelihood in NW Amazon, and potentially contributing to increases in BA in 2023 in some
3273 areas of Greece. Effective land management strategies, including prescribed burns and forest
3274 thinning, are crucial for reducing fuel loads and minimising fire impacts. While climate driven
3275 estimates of extreme behaviour are plentiful, few modelling frameworks take into account most
3276 of these dynamic factors and their interactions (Rabin et al., 2017).

3277

3278 We have used model-data fusion techniques that account for these factors in this report, and
3279 have been able to attribute some of their influences in certain places. This report utilises semi-
3280 empirical models that blend empirical data with process-based understanding to better predict
3281 fire behaviour. Quantifying uncertainty in these models is essential, especially when dealing
3282 with extremes. By generating probability distributions, researchers can better understand the
3283 likelihood of various fire scenarios, informing more effective management and policy
3284 decisions.

3285

3286 Thanks to the uncertainty quantification techniques, we have been able to ascertain where we
3287 are confident in our attributions. However, uncertainties still remain, many from not considering



3288 the complex interactions and feedback onto fire, some from fire itself as it consumes fuel, and
3289 affects from weather. Coupled vegetation-fire models explicitly represent many of these
3290 feedbacks. However, current FireMIP models struggle to accurately simulate extreme fire
3291 events (Hantson et al., 2020). One key factor hampering improvements in model development
3292 is our limited understanding of factors driving fire extinguishers in a natural setting. While much
3293 process based knowledge exists on the factors influencing fire start and fire spread, only
3294 limited knowledge exists on the myriad of factors that can stop a fire, from changes in fuel
3295 moisture, structure and heterogeneity to landscape fragmentation and fire fighting, and how
3296 these interact (e.g. Finney et al., 2012). Without a strong theoretical understanding of these
3297 factors, process based modelling of extremes at a global scale might be limited in the near
3298 future. For the 2023 focal events, we have shown that low fuel loads and variations in human
3299 modification of the landscape can limit fuel spread (**Figure 15, Figure 16, Figure S13, Figure**
3300 **S14**). However, we only look at a handful of events and further examples are required at larger
3301 scales to inform improvement of process-based rates of spread in fire models.

3302
3303 To move forward, we need to combine these concepts in attribution techniques and quantifying
3304 uncertainty with coupled vegetation fire models, such as in FireMIP. Early attempts of this are
3305 promising – ConFire (used in **Section 3.3, Section 3.4** and **Section 3.5**) borrows many of the
3306 FireMIP-style model concepts, though it still lacks many feedbacks from fire itself. We have
3307 also used the latest FireMIP models coupled to an uncertainty framework for broad-scale,
3308 uncertainty-based attribution (obtained from Burton, Lampe et al., 2024). But they struggle at
3309 reproducing the tails of distributions where extreme events are found. Another way to develop
3310 these techniques is to move towards an integrated system that would inform both attribution
3311 and future projections in a seamless way. We make some progress in this direction here using
3312 tools such as ConFire, by using the information gained from fire drivers to build future
3313 projections, however there is more work to do to link statistical approaches for today's fires to
3314 future projections.

3315
3316 The human role in driving fire and extremes is hard to represent. Despite the often reported
3317 influences people have on both increasing extreme burning or causing the observed decline
3318 in global BA, the role of humans in the landscape remains hard to capture and on the whole,
3319 remains one of the most uncertain aspects of this report. Agent-based modelling (ABM) is
3320 trying to address this by simulating the behaviours and interactions of individual human entities
3321 (e.g., deforestation, crop residue burning, suppression, etc.) within a given environment (Ford
3322 et al., 2021). This approach provides a dynamic representation of how different factors
3323 contribute to fire risk and links well with subsequent sections of the report. These approaches
3324 could be a major contributor to subsequent issues of this report. However, the integration of
3325 these advanced modelling techniques into operational use faces challenges, as there is often
3326 a delay between the development of new approaches and their widespread adoption by fire
3327 management agencies. This underscores the need for continuous improvement and adoption
3328 of innovative modelling approaches to address the growing threat of extreme fire events
3329 effectively.

3330
3331 In addition to fire weather index (FWI) and BA projections, it is crucial to go beyond these
3332 metrics to consider wider impacts such as intensity, and emissions. Understanding the
3333 intensity of fires helps in assessing their destructive potential and the severity of their
3334 ecological and societal impacts. Emissions from fires, including C dioxide and other
3335 greenhouse gases, contribute to climate change and air quality issues. Finally, evaluating the
3336 broader impacts of fires, such as on biodiversity, human health, and economic stability, is
3337 essential for developing comprehensive adaptation and mitigation strategies. Quantifying and
3338 understanding the uncertainty in these projections is crucial for developing adaptive strategies
3339 that can effectively respond to the evolving fire risks posed by global change.

3341 **4.2.5 Modelling Future Projections of Fire Extremes**

3342



3343 Projections of extreme fire events under future climate scenarios indicate a significant increase
3344 in their frequency and intensity. Semi-empirical models used in this report project that extreme
3345 BA events, currently rare, are likely to become more common by the end of the century. These
3346 projections highlight the urgent need for robust fire management strategies and policies to
3347 mitigate the impacts of these increasingly severe fire events on ecosystems, communities,
3348 and global C dynamics. Quantifying and understanding the uncertainty in these projections is
3349 crucial for developing adaptive strategies that can effectively respond to the evolving fire risks
3350 posed by global change. In our ConFire uncertainty quantification framework, we have been
3351 able to make some confident inferences about the potential state of wildfires in the coming
3352 decades. However, we have also identified that there is a significant amount of crucial
3353 information that is currently beyond our reach due to the uncertainties involved. Our ability to
3354 forecast for the upcoming season, as well as for the next 2-3 decades, requires further
3355 refinement as we are observing mixed and uncertain responses. Beyond that, we still show
3356 similar uncertainties in responses of Canada and Western Amazonia under different scenarios
3357 as highlighted by UNEP (2022), which uses the previous generation of climate models – shows
3358 a large overlap in the potential range of changes in the occurrence of fire extremes between
3359 SSP370 and SSP585. This does not imply that mitigation efforts for one scenario will be
3360 ineffective compared to another, but rather indicates a lack of understanding regarding the
3361 response of extremes to these scenarios. By narrowing down the uncertainty ranges, we can
3362 better target adaptation efforts and evaluate the effectiveness of mitigation strategies. The
3363 reduced likelihood of extreme event recurrence in our high mitigation, however, does show
3364 that we can start separating out how mitigation efforts might affect fire extremism, though not
3365 in the level of detail needed for policy.
3366

3367 There are three main ways we may be able to constrain uncertainties in the coming reports.
3368 The first is development of the underlying GCMs that project future change in the drivers of
3369 BA. For individual models, this is a slow process and, beyond informing CMIP model
3370 development, is outside what the State of Wildfires can contribute to. However, bringing in
3371 more models, including having another model to incorporate any remaining biases in
3372 simulated fire from the correct models into our uncertainty projection, will help us constrain
3373 uncertainties more (Kelley et al., 2023) The second is obtaining more information and
3374 understanding of how fire drivers relate to fire extreme's as outlined in the previous section.
3375

3376 Better ways of describing the statistical relationship between observed and modelled climate,
3377 land surface and fire today is a third approach. Investigating the dynamical climatic drivers of
3378 extreme fire conditions in different regions can help to physically disentangle and potentially
3379 constrain sources of uncertainty in future climate projections, for example by constructing
3380 physical storylines (Shepherd et al., 2018; Mindlin et al., 2023). These storylines of plausible
3381 future change, or other similar approaches to quantify and explain uncertainty in projections,
3382 provide critical information for communities to develop robust adaptation strategies (Lemos et
3383 al., 2012) and prepare for future losses and damage caused by evolving fire risks posed by
3384 global change. Next to understanding future uncertainty, further insights into these dynamical
3385 drivers can support the development of improved physics-informed bias adjustment of climate
3386 models (Maraun et al. 2017). Currently available methods to bias adjust climate models for
3387 their use in fire models, such as the ISIMIP3BASD method, have been shown to modify the
3388 climate change trend, particularly in extreme threshold indices (Casanueva et al 2020, Spuler
3389 et al 2024) or increase spread in climate model projections (Lafferty and Sriver, 2023). Bias
3390 adjustment methods should therefore be evaluated carefully and leave scope for future
3391 method development that physically links present-day biases to future uncertainty.
3392

3393 **4.3 Frontiers in Studying Extreme Fire Impacts**

3394



3395 As above, this section will not be revised annually but will be revisited on longer intervals at
3396 times consistent with progress in the fields of extreme fire impact assessment. This section
3397 identifies current challenges and emerging opportunities for overcoming them.

3398

3399 **4.3.1 Direct Exposure of People and the Built Environment**

3400

3401 The wildland urban interface (WUI) has been the focus of much of the direct exposure of
3402 populations to fire (i.e., populations residing within the footprint of a fire). While extreme fires
3403 can become urban conflagrations – including the Lahaina fire in August 2023 – there has been
3404 a focus on reducing fire losses in WUI through fire prevention, fuel reduction, and other
3405 mitigation efforts (Calkin et al., 2023). The dual roles of increased population living in the WUI
3406 in some areas (Radeloff et al., 2018) and increased fire potential has contributed to
3407 accelerated community impacts (Higuera et al., 2023). Recent studies in the US have shown
3408 a doubling in the direct population exposure to large fires during 2000-2019 (Modaresi Rad et
3409 al., 2023), yet with a majority of the increase attributable to fires encroaching on the WUI rather
3410 than recent increases in human settlement in such landscapes. They showed similar increases
3411 in wildfires intersecting roads and energy infrastructure, thereby causing additional
3412 complexities to transportation and energy reliability. In the US, most of the structures lost in
3413 fires occurred in grasslands and shrublands, rather than forested environments, underscoring
3414 the importance of looking beyond traditional forest-centric fire risk assessments. Recently
3415 developed efforts to map the WUI at global scales (Schug et al., 2023) present opportunities
3416 for identifying areas most vulnerable to direct fire impacts, and characterise trends in fire
3417 exposure more broadly (Chen et al., 2024; Tang et al., 2024).

3418

3419 Moreover, efforts are needed to better understand characteristics of fires that result in direct
3420 exposure of people, loss of structures, and loss of life. For example, Abatzoglou et al. (2023)
3421 showed that fires coincident with strong downslope winds in the western US were responsible
3422 for a majority of structure loss and fatalities during 1999-2020 despite accounting for only 12%
3423 of all fires and burned areas. Downslope wind driven fires defy typical terrain-driven fire
3424 behaviour by pushing fire downhill from wildlands and into communities in the WUI – often
3425 overwhelming both fire suppression efforts and fuel treatments. During the 2023 fire year,
3426 many of the large loss fires in Hawaii, Greece, and Chile were driven by such conditions
3427 (Synolakis and Karagiannis, 2024). Focused efforts to diagnose characteristics accompanying
3428 other extreme fires, including meteorological conditions such as dry cold frontal passage (Van
3429 Wagtendonk, 2006) and pyrocumulonimbus (Lareau et al., 2018), as well as pre-existing
3430 vegetation conditions such as extensive tree mortality (Stephens et al., 2022), can lead to
3431 additional insight on fires most likely to result in impacts. Highlighting geographic areas prone
3432 to such conditions and how they may change into the future can help prioritise mitigation
3433 efforts.

3434

3435 One of the current gaps inhibiting the characterisation of extreme fires and understanding
3436 drivers of fire impacts on humans, such as fatalities, evacuations, structure loss, secondary
3437 morbidity from toxic smoke, economic losses, and impacts to food, water, energy, and
3438 transportation systems, is the lack of comprehensive data at national-to-global scales
3439 quantifying such outcomes. For example, wildfire morbidity data are collected in only a few
3440 countries due to the relatively infrequent occurrence of wildfires that incur fatalities and
3441 the lack of clear responsibility for cataloguing such information, particularly for civilians (Haynes
3442 et al. 2019). Estimates of smoke-induced morbidities rely on identifying spikes in hospital visits
3443 above a baseline and then extrapolating, nearly always associated with a specific event
3444 (Johnston et al. 2021). The US state of California pioneered a systematic cataloguing of
3445 structure losses to wildfire beginning in 2013 (California Department of Forestry and Fire
3446 Protection, 2024). However, this initiative required a commitment of fiscal and personnel
3447 resources from the state wildfire agency and has not been adopted elsewhere in the US,
3448 despite the programme's success in yielding substantial additional insights about wildfire
3449 structure loss mechanisms (Kolden and Henson, 2019; Syphard and Keeley, 2019). Canada



3450 now catalogues wildfire evacuations, but there is considerable complexity in characterising
3451 initiation responsibility, duration, and number of people impacted (Beverly and Bothell, 2011).
3452 Global insurance companies document insured losses as one mechanism of economic
3453 impacts from wildfires, but such records are neither representative of the broader losses due
3454 to high rates of uninsured or under-insured property ownership (Hazra and Gallagher, 2022)
3455 nor are they publicly available from private companies, leaving researchers to attempt
3456 imperfect estimations from websites that model property prices (e.g., Conlisk et al., 2024).
3457

3458 While the global disaster database EM-DAT and others like it have attempted to rectify this
3459 gap in recent years, such data often overgeneralize both the spatial extent and the impacts of
3460 wildfire disasters (e.g., reporting all of the fires across a country for an entire summer as a
3461 single event) because they rely on news reporting that varies widely in accuracy, rather than
3462 official record-keeping. Expanding and improving quantification of wildfire impacts on humans
3463 is critical to overcoming the BA fallacy that fire size is a proxy for impact and aids in developing
3464 models that can point to the most effective mitigation solutions (Kolden, 2020). This is
3465 challenging for many metrics, but remote-sensing based documenting of structure loss and
3466 fire incursion into the WUI is now possible with the availability of high-resolution sensor arrays
3467 (Frazier and Hemingway, 2021), and the widespread distribution of air quality monitoring
3468 sensors should enable an increase in more interdisciplinary research on relationships between
3469 wildfire smoke events and medical morbidity outcomes (Liang et al., 2021).
3470

3471 **4.3.2 Air Quality and Health Impacts**

3472
3473 Exposure to outdoor pollution is recognized as a major global risk to human health (Murray et
3474 al., 2020). The abundance of fine-sized particles with a diameter less than 2.5 μm (PM_{2.5}) are
3475 of particular concern due to their ability to cause a range of cardiovascular diseases. A growing
3476 concern is the contribution of fire smoke to air quality, not only due to increasingly large and
3477 severe fire events across the globe degrading air quality (**Figure 7**) but also because fire has
3478 been suggested to be more toxic per unit of PM exposure than other pollution sources
3479 (Aguilera et al., 2021). The World Health Organization (WHO) sets global Air Quality Guidelines
3480 on the threshold for PM_{2.5} exposure. Thresholds are continually revised and in September 2021
3481 they reduced guidelines for an annual mean exposure limit for PM 2.5 from 10 $\mu\text{g}/\text{m}^3$ to 5 $\mu\text{g}/\text{m}^3$.
3482 Given that 95% of the world's population is estimated to be exposed to annual mean PM_{2.5}
3483 concentrations of at least 10 $\mu\text{g}/\text{m}^3$ (Shaddick et al., 2018), additional pollution exposure due to
3484 increasing or severe wildfire pollution events creates an elevated health risk that also goes beyond
3485 both current and past guideline limits.
3486

3487 Here we discuss three of the major challenges in quantifying the impact of extreme fire
3488 pollution on human health. The first is accurately measuring the amount of pollution that a
3489 wide variety of communities are exposed to and then attributing the contribution of a wildfire
3490 event, that could be 100s or 1000s of km away, to the measured concentration. The second
3491 is that PM_{2.5} is not the only pollutant of concern, the EPA regulates six pollutants of concern
3492 for American citizens and a wildfire produces them all. The third is accurately linking exposure
3493 to a wide range of pollutants to their associated short-term and long-term health impacts.
3494

3495 Tools to assess air quality primarily consist of ground-based measurements and modelling.
3496 Ground based observations provide an accurate measurement of pollution at their location.
3497 However, measurement locations are spatially sparse. Ongoing efforts to increase spatial
3498 coverage include deployment of small relatively affordable particulate matter sensors, such as
3499 the PurpleAir network, by a wide range of communities (not just scientists), and efforts to relate
3500 surface PM concentrations to measured aerosol optical depth from satellites (Li et al., 2021).
3501 One additional constraint of observations is that they cannot differentiate pollution sources,
3502 but modelling can. Dispersion modelling uses emission estimates, reanalysis meteorology,
3503 and topography to provide estimates of ambient pollutant concentrations at varying
3504 spatiotemporal scales.



3505

3506 A challenge for models currently lies in the large uncertainty in fire emissions (Reddington et
3507 al., 2016; Carter et al., 2020; Pan et al., 2020). Emission data will therefore require calibration
3508 against observations and adjusting before the contribution of fire to pollution can be quantified.
3509 Improved emission datasets will increase confidence in these assessments. Given the
3510 complexity of smoke composition, other pollutants, such as gases and metals, are also present
3511 and have deleterious health implications. Increased study of the chemical composition of fire
3512 smoke plumes is therefore needed alongside monitoring of short and long range transport of
3513 these pollutants.

3514

3515 Environmental and personal factors both influence cardiovascular health, making it
3516 challenging to isolate the effects of fire smoke. Impacts may also not be immediate; some
3517 effects can be acute, such as exacerbation of asthma, while others emerge over a longer
3518 period, like the development of cardiovascular disease, and are thus much more difficult to
3519 directly connect to a specific extreme fire event. Conducting epidemiological studies that link
3520 fire smoke exposure to specific health outcomes requires comprehensive data collection and
3521 follow-up. These studies are resource-intensive, time consuming, and subject to potential
3522 limitations in data. In the shorter-term development of effective response planning that
3523 includes coordinated efforts between public health officials, environmental agencies, and
3524 emergency services could help in mitigating some of the health impacts of fire smoke.

3525

3526 **4.3.3 Impacts on Indigenous and Traditional Communities**

3527

3528 Indigenous peoples and local communities (IP&LC) are disproportionately exposed to extreme
3529 fire impacts because of their proximity to the land and resources from which their cultures,
3530 livelihoods and often food and medicines derive. Once landscapes are degraded through fire
3531 the access and abundance of various resources can be shifted. At the same time these
3532 communities are often less supported by the state due to access and their political and
3533 economic marginalisation linked to systemic socioeconomic disadvantages. These
3534 communities suffer not only post-fire impacts, but can be disincentivized from particular land
3535 and resource use activities because of the increasing threat of forthcoming wildfires. Whilst
3536 the multiple important values (e.g. instrumental, intrinsic and relational) associated with
3537 landscapes by IP&LCs are threatened by fire, there is a lack of systematic pre- and post-fire
3538 assessment of these impacts (van Leeuwen and Miller-Sabbioni, 2023).

3539

3540 Historically fire governance has added an additional burden to IP&LC, often prohibiting cultural
3541 fire use and management to the detriment of local knowledge and values, and in some cases
3542 also increasing the propensity of wildfire in tropical systems as well as savannahs (Carmenta
3543 et al., 2019; Daeli et al., 2021; Croker et al., 2023). In some contexts there is a shift towards
3544 correcting these issues and renewed interest in and support for cultural burning and
3545 Indigenous approaches to land management. For example, integrated fire management is
3546 gaining traction globally and sits at the heart of a number of interventions and international
3547 policy efforts (e.g. Fire Hub, 2023). The premise of IFM is to maximise the 'good' fire and
3548 minimise the occurrence of wildfire often through an approach of connecting knowledges (i.e.
3549 expert and place-based or Indigenous). Whilst nations sit at different stages of development
3550 in respect to IFM, and many IP&LC feel there is a long way to go, the growing interest is
3551 promising (Bilbao et al., 2019; Luque et al., 2020; Rodríguez-Trejo et al., 2022). Research is
3552 needed to better understand the effectiveness of IFM and what mechanisms and processes
3553 work best for rebalancing the influence of various forms of knowledge on fire management.
3554 For instance in North America where fire use is considered a form of medicine to the land, and
3555 anointed to particular patches of the landscape for care (Palmer, 2021). These approaches
3556 are perceived as potentially more just as they allow for the many meanings and uses of fire to
3557 exist and persist. For example, In Australia, the term 'Country' is used to convey the cultural
3558 and spiritual connection of Aboriginal peoples to the land and water in specific regions. This



3559 link profoundly colours Indigenous peoples' experience of extreme fire events such as the
3560 Black Summer fires of 2019-20 (Nolan et al., 2021b).

3561

3562 **4.3.4 Economic Impacts**

3563

3564 Extreme wildfires cause economic disturbance worldwide, with the nature of their impacts
3565 varying across regions due to distinct economic structures, environmental conditions, and
3566 mitigation and response strategies. These economic impacts arise through a myriad of
3567 channels including property and infrastructure loss, business downtimes, supply chain
3568 disruptions, decreased tourism revenues, health costs, reduced economic productivity, and
3569 damages to ecosystem services. While tangible costs (e.g., insured losses such as property
3570 or infrastructure) are relatively straightforward to measure, intangible costs (e.g., lives lost,
3571 shortened lifespans and impaired performance/productivity due to smoke exposure, damage
3572 to species and habitats) are more challenging to quantify owing to issues of data availability
3573 and their occurrence over varying temporal and spatial (geopolitical) scales. Consequently,
3574 assessing the true economic costs of an extreme wildfire event or season is inherently
3575 challenging. Furthermore, while wildfires are predominantly destructive, certain economic
3576 sectors may experience positive effects such as those arising from reconstruction and
3577 rehabilitation in the aftermath, or even from the fire suppression efforts during the event
3578 (Nielsen-Pincus et al., 2014, Meier et al., 2023a).

3579

3580 Building upon these challenges, existing work on quantifying the economic impacts of wildfires
3581 has largely focussed on developed economies in Europe (World Bank, 2023), the US, and
3582 Australia. For example, modelling extreme wildfires in Mediterranean Europe, Meier et al.
3583 (2023b) estimate that economic losses caused by a single 1-in-10 year extreme wildfire event
3584 amount to €162–439 million in Portugal, €81–219 million in Spain, €41–290 million in Greece,
3585 and €18–78 million in Italy. The unprecedented 2018 and 2020 wildfire seasons in California
3586 are estimated to have resulted in approximately \$150 billion (including indirect costs beyond
3587 the immediate burn zone) and \$19 billion in economic damages, respectively (Wang et al.,
3588 2021; Safford et al. 2022). Similarly, Australia's 2019-2020 fire season has been documented
3589 as the country's costliest natural disaster, with economic damages, measured as a decrease
3590 in GDP, estimated at \$10 billion (Wittwer and Waschik, 2021).

3591

3592 While proxies of economic data can be publicly accessible from satellite data shortly after
3593 events, this is often not the case for more traditional economic indicators such as sectoral
3594 GDP (or alternative wealth measures), employment, hospitalisations, fire prevention and
3595 suppression spending, house prices, or tourism revenues. These data are often not publicly
3596 available, not harmonised across larger geographic areas, or unable to capture medium and
3597 long-term effects. Consequently, the full economic costs of such events may only become
3598 apparent years, or even decades, after they occur.

3599

3600 In addition to these data challenges, the econometric analysis of wildfires is arguably more
3601 challenging than for other natural hazards such as earthquakes or hurricanes, because wildfire
3602 occurrence is largely shaped by human activity through land-use choices, fire prevention and
3603 suppression policies, and socioeconomic factors. While earthquakes can be seen as non-
3604 human induced and therefore it is easier to find a counterfactual for a causal analysis, wildfire
3605 occurrence correlates with many economic outcome variables of interest. Despite these
3606 drawbacks, carefully constructed counterfactual analyses or other econometric approaches,
3607 such as instrumental variables, can provide reliable causal estimates of different aspects of
3608 economic impact estimations of extreme wildfires. These methods hold significant promise for
3609 future research, offering the potential to better understand and mitigate the economic
3610 consequences of wildfires through more accurate and comprehensive analyses, while also
3611 helping to target suppression policies and allocate resources effectively.

3612



3613 **4.3.5 Loss of Biodiversity, Ecosystem Function and Carbon Storage**

3614
3615 The reshaping of fire regimes and ecosystem functioning by climate change and altered
3616 ignition and suppression patterns has a range of consequences for biodiversity, ecosystem
3617 function, and ecosystem services such as C storage. Mechanisms such as reduced seed
3618 quantity or quality, resprouting exhaustion, organic soil burning, and misalignment of key
3619 reproductive processes with optimal conditions under intensified fire regimes can hamper
3620 post-fire regeneration (Burell et al., 2022; Nolan et al., 2021a; Johnstone et al., 2016),
3621 interaction with other disturbance mechanisms (e.g. drought and insect infestation) can further
3622 compound these effects. For example, in boreal forests, rising fire activity has reduced the
3623 prevalence of fire-adapted species like black spruce, with more frequent and severe fires
3624 hindering their regeneration and favouring deciduous species such as birch and aspen, thus
3625 altering forest structure and C dynamics (Baltzer et al., 2021). In Western North America, the
3626 growing frequency of high-severity fires coupled with warmer and drier post-fire conditions has
3627 been linked with poor forest recovery and transition to non-forest vegetation types such as
3628 shrublands or grasslands, impacting ecosystem services like habitat provision, water
3629 regulation, and C storage (Coop et al., 2020). Likewise, in transitional systems where tropical
3630 savannas and tropical forests can exist under the same climatic conditions depending on fire
3631 history, increased frequency can favour savannah establishment and reduced frequency can
3632 promote forest establishment (Staver et al., 2011).

3633
3634 There are a range of significant challenges to observing and modelling the impacts of shifting
3635 fire regimes on ecosystems and C storage. Fire regimes vary widely, leading to
3636 inconsistencies in historical data and complicating model development. Short-term
3637 observations often miss long-term trends, especially in areas with episodic recruitment (Nolan
3638 et al., 2021a; Coop et al., 2020). Ecosystem responses are complex, with species-specific
3639 reactions influenced by fire-adaptive traits and genetic variability (Grau-Andrés et al., 2024).
3640 Fire regimes also respond to multiple disturbances that can be difficult to disentangle, such as
3641 climate change and extreme events alongside land use change or fire suppression (Nolan et
3642 al., 2021a; Coop et al., 2020).

3643
3644 To overcome these challenges, researchers are leveraging new technologies. Advanced
3645 remote sensing, including satellite imagery and drones, provides detailed data on fire extent
3646 and severity, enabling real-time and long-term monitoring of outcomes (Burell et al., 2022;
3647 Baltzer et al., 2021). Improved modelling techniques, such as process-based simulation
3648 models and the integration of big data with machine learning, enhance predictive capabilities
3649 (Coop et al., 2020; Nolan et al., 2021a). Enhanced field data collection through long-term
3650 monitoring networks and citizen science initiatives also contributes to comprehensive datasets
3651 (Baltzer et al., 2021; Coop et al., 2020). Other opportunities include advances in genomic tools
3652 for understanding species-specific fire adaptations, climate-adaptive management
3653 frameworks incorporating real-time data and predictive models, and the use of AI and machine
3654 learning for better fire impact predictions (Nolan et al., 2021a; Coop et al., 2020; Grau-Andrés
3655 et al., 2024).

3656
3657 A good example of emerging opportunities stemming from the assemblage of large datasets
3658 and application of AI is the comprehensive meta-analysis by Grau-Andrés et al. (2024). By
3659 analysing data from published studies, the meta-analysis detected systematic tendencies for
3660 intensified fire regimes to reduce plant abundance, diversity, and overall health globally, with
3661 stronger effects from increased fire severity than frequency. Forests, particularly conifer and
3662 mixed forests, are more negatively impacted than open-canopy ecosystems. Woody plants
3663 are more susceptible than herbs to frequent fires due to their slower growth and recovery
3664 rates. These impacts are more severe in ecosystems with arid and cold climates, where plant
3665 recovery is further hindered by limited water and lower temperatures. Additionally, step-
3666 changes from surface to crown fires in forests can significantly reduce plant abundance,
3667 diversity, and health.



3668

3669

4.3.6 Nature-based Solutions and Net Zero

3670

3671

Terrestrial ecosystems remove about 30% of annual anthropogenic C emissions through enhanced growth and ecosystem recovery, but this is partly offset by land use change that increases annual C emissions by about 12% (Friedlingstein et al., 2023). Emissions removal or avoidance through nature-based solutions has therefore emerged as a key component of regional, national and corporate net zero strategies (Seddon et al., 2020). Forestry projects, focused on planting, restoration, or conservation of forests, are one sector of nature based solutions that are at particular risk of fire, which can result in inaccurate C accounting and reversal risks. Spatial clustering of C projects in specific geographic areas may compound risk from climate variability or change, like the impacts of El Niño. In C markets, projects often account for reversal risks by contributing a proportion of their credits to a buffer pool. Nevertheless, such allocations may not be adequate in regions exposed to increasing wildfire extremes (Badgley et al., 2022; Anderegg et al., 2024).

3683

3684

Despite these challenges, C markets also provide opportunities to unlock the resources required to improve management of fire prone ecosystems, like savannas (Russel-Smith et al., 2015) and temperate forests (Nikolakis et al., 2022) with benefits for ecosystems, climate, and local communities. For these markets to be effective and scale, they require accurate and transparent monitoring systems, enabling science based fire management, accurate accounting of C losses from fire, and assessment of reversal risk from fire. Novel satellite based monitoring systems can provide early warning and response to wildfire activity and improved estimates of ecosystem C stocks. Nevertheless, field based studies remain critical for understanding both immediate and long-term impacts of fire on forest ecosystems (Silva et al., 2020) and novel models forecasting evolving fire risk at decadal time scales are required to improve management strategies and making credible C claims.

3695

3696

4.3.7 Water Quality and other Aquatic Impacts

3697

Fire impacts freshwater ecosystems mainly through (i) the loss of vegetation and litter cover and (ii) the enhanced input of soil, sediment and residual ash. The former leads to a reduction in rainfall interception and evapotranspiration from plants, and thus a greater proportion of rainfall reaching streams, lakes and reservoirs (Smith et al., 2011). This increased runoff from burned hillslopes can lead to accelerated erosion, debris flows and localised flooding (Shakesby and Doerr, 2006).

3703

3704

Wildfire ash is typically enriched in nutrients and contaminants (e.g. metals, polycyclic aromatic hydrocarbons) compared to vegetation and soil (Bodi et al., 2014; Sánchez-García et al., 2023) and together with soil and organic debris can directly and indirectly affect water quality. These include enhanced turbidity, temperature, nutrient and toxin content, and decreased dissolved oxygen. Associated effects can be increased mortality in freshwater ecosystems, algal blooms, as well as water quality impacts for water supply catchments (Smith et al., 2011). For example, increased organic matter in water can be costly for water treatment plants to remove. The 2016 Horse River Fire affecting Fort McMurray, Canada, caused \$9 M in additional water treatment expenditures (Pomeroy et al., 2019). The magnitude of such impacts will depend on the type of ecosystem burned (including the presence of any legacy contamination), the size and severity of the fire, the rate of vegetation recovery and critically also the intensity and patterns of rainfall events following the fire (Shakesby and Doerr, 2006; Nunes et al., 2018). The direct hydrological impacts of fire are relatively well understood, and models have been developed to support catchment managers in assessing risks to water supply (Nunes et al., 2018; Neris et al., 2021), however, given the wide range of potential post-fire rainfall events, large uncertainties remain in predicting actual outcomes.

3718



3719 Fire emissions to the atmosphere also contain compounds that can be either nutrient-enriching
3720 or toxic in aquatic ecosystems at high concentrations (Hamilton et al. 2022; Perron et al.,
3721 2022). While the impact of 2023 fire events on marine ecosystems has not yet been
3722 extensively evaluated in the literature, past extreme fire events were linked to disturbance of
3723 the open ocean productivity, sometimes thousands of kilometres down the fire plume pathway.
3724 In the Northern Hemisphere large fires across Siberian forests and peatlands during the
3725 summer of 2014 were suggested to contribute significant reactive nitrogen inputs to the
3726 surface Arctic ocean, helping boost and sustain an unusually large phytoplankton bloom
3727 (Ardyna et al., 2022). A similar increase in East Siberian Sea productivity (by over 200%) was
3728 attributed to direct nutrient (nitrogen) deposition and black carbon-induced fast-ice melting
3729 from increased fires on the Eurasian continent in 2019-2020 (Seok et al., 2024). Coastal
3730 community shifts were observed in the Santa Barbara Channel (California, USA) during the
3731 2017 record-breaking Thomas fires (Kramer et al., 2020; Ladd et al., 2023). In the Southern
3732 Hemisphere, the unprecedented Black Summer fires which occurred in southeastern Australia
3733 in 2019/2020 fueled a continent-sized phytoplankton bloom in the iron-depleted southern
3734 Pacific Ocean (Tang et al., 2021). The C uptaken and sequestered to ocean depths by this
3735 bloom was reported to have offset the C emitted by the fire itself (Tang et al., 2021), although
3736 this enhanced oceanic C uptake is likely to be temporary as changes in oceanic productivity
3737 and C sequestration efficiency, as a function of wildfire nutrient inputs, fluctuates each fire
3738 season (Hamilton et al., 2022; Wang et al., 2022).
3739

3740 **4.4 Roadmap for Advancing the State of Wildfires Report**

3741
3742 The fire science community is currently navigating several research frontiers to support better
3743 societal and environmental outcomes related to wildfire. By addressing these frontiers, the
3744 field aims to provide new observations and tools that enhance preparedness, response,
3745 mitigation, and adaptation strategies. The field is advancing its ability to observe individual
3746 fires, assess conditions leading to extreme fires, and predict their occurrence on timescales
3747 ranging from hours to decades. Additionally, there is increasing focus on monitoring and
3748 modelling the diverse impacts of extreme fires on society, the environment, and the economy.
3749

3750 The State of Wildfires report presents key opportunities to harness new advances and
3751 highlight key priorities. Here, we outline the roadmap for the State of Wildfires report in
3752 facilitating improvements in the observation, prediction, and modelling of extreme fires and
3753 their impacts.
3754

3755 **4.4.1 Observability**

3756
3757 **The State of Wildfires report will advocate for and utilise new harmonised fire**
3758 **observation products.**
3759

3760 Consistent, long-term records of fire extent and properties are fundamental for studying
3761 extremes, which cannot be characterised without reference to historical ranges. On a global
3762 scale, the MODIS instrument has provided valuable data on BA and active fires, underpinning
3763 key advances in tracking daily fire progression and fire emissions models. Over two decades,
3764 MODIS data has enabled the detection of trends and patterns in fire activity and properties.
3765 However, the consistency of these records is now at risk as the Terra satellite, which houses
3766 one of the two MODIS sensors, nears decommissioning.
3767

3768 While fire observations from other moderate-resolution datasets (such as VIIRS) and high-
3769 resolution datasets (e.g. Landsat and Sentinel sensors) are increasingly available, there is an
3770 urgent need to harmonise these records with MODIS data to ensure consistent observation
3771 across datasets. The State of Wildfires report further underscores the critical strategic need
3772 for a continuous and harmonised dataset of fire observations beyond the MODIS era. To



3773 support future iterations of the report, we will advocate for the provision of harmonised
3774 products within the Earth Observations communities.

3775

3776 **The State of Wildfires Report will facilitate a community effort on a protocol for defining**
3777 **extreme fire events or fire seasons.**

3778

3779 This report emphasises important issues in the identification of fire extremes, consistent with
3780 those raised elsewhere in similar contexts such as the definition of the term ‘megafire’ (Linley
3781 et al., 2022). In future years, regional experts would benefit from a protocol or guidelines that
3782 can be used for categorising extreme fire events. To support future iterations of the State of
3783 Wildfires report, we will coordinate workshops with broader sections of the fire science
3784 community with the aim to produce guidance for future years. Central to this task is the
3785 inclusion of communities from broad geographies so that any output respects fire impacts that
3786 are considered to be regionally significant.

3787

3788 **The State of Wildfires Report will stimulate progress on combining multiple fire**
3789 **observation streams to better identify and characterise extreme fire.**

3790

3791 This report highlights the need to advance our capacity to observe fires that are impactful in
3792 diverse ways at large scales. In particular, there is a growing need to move ‘beyond burned
3793 area’ and towards a wider set of intensity, severity and behaviour metrics that often relate
3794 more strongly to impacts on society and the environment than BA. The integration of individual
3795 fire data from the Global Fire Atlas in this iteration of the State of Wildfires Report is one
3796 example of including wider fire parameters such as size and rate of growth, which are
3797 expected to correlate more strongly. Applications of the dataset could be explored further; for
3798 example, with the Global Fire Atlas it would be feasible to assess the occurrence of days with
3799 a large number of synchronous large fires which are known to present among the greatest
3800 challenges to fire management and suppression attempts (e.g. Abatzoglou et al., 2021).
3801 Impactful fires might also be better identified if their intersection with exposure layers, such as
3802 population centres (e.g. Modaresi Rad et al., 2023), is considered in such assessments.
3803 Similarly, combining datasets that describe individual fire behaviour with observations of fire
3804 radiative power and estimates of biomass combustion from data-driven models might further
3805 inform the identification of intense or severe fires that are often tied to the greatest
3806 consequences for ecosystems and society (e.g. Nolan et al., 2021a). The State of Wildfires
3807 report must stimulate progress on moving ‘beyond burned area’ and combining diverse
3808 observational capacities to better identify and characterise extreme fire events, and we intend
3809 to expand our use of such insights in future iterations.

3810

3811 **4.4.2 Predictability**

3812

3813 **The State of Wildfire will advocate for the use of extended range forecast to identify**
3814 **early onset of fire weather conditions**

3815 Currently, global systems for monitoring fire danger primarily rely on short to medium-range
3816 weather forecasts, typically up to 10 days. However, evidence suggests that anomalous
3817 conditions conducive to fire weather can be confidently predicted up to one month in advance
3818 using state-of-the-art seasonal forecasting systems. In certain regions, this prediction window
3819 can extend to two months. Generally, beyond this period, forecasts do not outperform
3820 climatology.

3821 However, an extended predictability window of up to 6-7 months is possible when anomalous
3822 fire weather results from large-scale phenomena such as the El Niño-Southern Oscillation
3823 (ENSO) and the Indian Ocean Dipole (IOD), which have teleconnections affecting regions like
3824 Indonesia and Australia.



3825 The State of Wildfires report further emphasises the benefits of extending the forecast range
3826 to the subseasonal to seasonal timescale. This extension provides an outlook for the
3827 establishment of anomalous fire weather conditions, offering valuable advance warning and
3828 preparation time.

3829 **The State of Wildfire will stimulate progress on the use of AI and informatics methods**
3830 **to aid the forecast of fire activity globally.**

3831 Despite the increasing importance of fire management, prediction systems still rely on
3832 methodologies developed (and ongoing) since the 1960s, utilising empirical models of
3833 landscape flammability tailored to specific biomes. The Fire Weather Index (FWI), widely
3834 employed by fire management agencies due to its ease of implementation, has limited skills
3835 in fuel-limited ecosystems like savannahs. Tropical savannahs globally account for over two-
3836 thirds of mean annual BA (Jones et al., 2024). Additionally, while FWI metrics express the
3837 potential for various aspects of fire behaviour if ignited, they do not consider human or natural
3838 sources of ignition, making their correlation with fire activity limited in many parts of the planet.

3839 Recently, there has been a notable surge in the potential of data-driven applications.
3840 Employing machine learning techniques to accurately predict fire occurrence globally at high
3841 resolution, up to ten days in advance, could become a reality. Data-driven methods could
3842 attribute a probability of fire occurrence with increasing precision, learning from available data
3843 where and when human behaviour will trigger an ignition. A notable advantage of these
3844 techniques is the facility to ingest novel input data, such as road density, without needing to
3845 directly explore the complex physical relationships that govern the occurrence of fires.

3846 While not technically AI, ConFire uses Bayesian statistics within an informatics framework to
3847 combine a data-driven approach with process-based modelling, advancing our understanding
3848 of uncertainty around fire drivers and future projections. Current ongoing developments in
3849 ConFire, aimed at a more flexible modelling structure, could be utilised in future reports and
3850 would further reduce uncertainty, providing higher accuracy in predicting fire event drivers. For
3851 example, the controls in ConFire are currently assumed to be linearly related to burned area,
3852 and this is in the process of being updated to more accurate relationship curves that are
3853 informed and optimised by the model, based on observed data (Barbosa 2024). Another
3854 development in progress is updating the framework to enable one probability distribution to be
3855 applied to both the mean or the tails of the distribution of burned area, instead of having to
3856 select between them as is currently the case.

3857 A priority for these developments is obtaining more data, including near real time
3858 counterfactual data, improved fuel information, and more detailed data on human/fire
3859 interactions, especially over deforestation areas such as Amazonia (See Evaluation section
3860 in the Supplement).

3861 More generally, we also need to find better ways to represent extremes in the data, which
3862 includes an improved understanding of what classes as an extreme. A data-driven approach
3863 could be used to inform this; for example, machine-learning could be applied to large
3864 observation datasets to find any clustering of 'normal' fires, and pick out unusual fires as
3865 extremes. This would still need to be used in combination with expert solicitation though, to
3866 understand where fires have had extreme impacts on the ground that may not show up in the
3867 data.

3868 The State of Wildfires report underscores the benefits of exploring the emergence of these
3869 new technologies to understand their potential and assess prediction skills.



3870 4.4.3 Attribution

3871 Fire attribution techniques are still relatively new compared with more established approaches
3872 for extremes such as heatwaves. Part of the challenge in attributing fire is that it is a complex
3873 hazard comprising multiple compound risks across both meteorological and human drivers,
3874 as shown in this report. A wide variety of techniques therefore exist across the attribution
3875 literature to represent fire, from fire weather indices, drought indices, and fire weather proxies
3876 such as vapour pressure deficit or individual driving variables (temperature, precipitation,
3877 relative humidity), to BA from fire models or data-driven techniques. We have applied 3
3878 different approaches here to give a robust answer to the questions of how anthropogenic
3879 forcing and climate change are driving changes in the fires we experience today. We address
3880 changes in both fire weather and burned area. Further work could use other fire weather
3881 indices, multiple CMIP Global Climate Models, or ensembles from other climate models as
3882 another approach.

3883 Using the ISIMIP impacts attribution framework enables us to tackle the questions of how BA
3884 has changed in response to total climate forcing, socioeconomic factors, and all forcing across
3885 multiple fire models for the first time. There is the opportunity to extend this to more fire models,
3886 other reanalysis driving datasets, and ideally to extend this up to the period covered in this
3887 report. Currently the driving data and simulations go up to 2019 for example, and we can only
3888 estimate the additional changes in BA due to climate change covering 2019 to 2023 through
3889 extrapolation. However our analysis suggests that this could make an important difference in
3890 the results, for example ConFire results for Canada show a 0.7-6.22% increase in BA over
3891 2000-2019, whereas if the analysis is extended to include the 2023 anomaly this increases to
3892 0.7-38.0%. Achieving near-real-time data and analysis has been one of the driving ambitions
3893 of this report, and can help us better address policy-relevant impact questions more quickly
3894 after an event has happened. This is becoming increasingly possible, with operational
3895 attribution tools coming online, and initiatives such as the World Weather Attribution tackling
3896 extreme events quickly after their occurrence. However only one of these studies has included
3897 fire so far, and a challenge for the community is therefore to be able to address these extreme
3898 fires from an attribution perspective quickly and more frequently.

3900 4.4.4 Future Projections

3901
3902 In the coming few years, more data will become available through projects such as FireMIP
3903 and ISIMIP3b, which will provide multi-fire model projections of future BA for the first time.
3904 Using fire-enabled DGVMs enables us to more accurately model the interactions of fire and
3905 vegetation, as well as some representations of human processes of ignition and suppression.
3906 On a slightly longer time horizon, CMIP7 will also provide more Earth System Models with
3907 integrated fire feedbacks, and the community should take advantage of these modelling
3908 advances to reassess our current understanding of how fire will change in response to climate
3909 change over the next century. Currently only one model is used for future projections in this
3910 report, and in future years a more robust approach would be to include more models, as we
3911 have done in other sections of this report.

3912
3913 However, addressing the current limitations in wildfire modelling is crucial for this
3914 development. Models like FireMIP and ensemble approaches provide valuable insights into
3915 BA and feedbacks within the carbon cycle. To improve the utility and relevance of these
3916 models for policy and impact assessment, immediate goals include enhancing the predictions
3917 of fire beyond burned area, to consider intensity, spread and combustion rates for example.
3918 The models also provide information on emissions from fires, which could be explored in future
3919 reports using a similar weighted-multi-model ensemble to inform air quality impacts. However
3920 their performance in predicting extreme fire events is currently limited, which is where other
3921 tools such as ConFire and POF are useful to fill this gap. Addressing the critical feedback
3922 mechanisms and uncertainties in models like ConFire and POF is essential for a more



3923 accurate representation of fire impacts, and immediate goals for development of these
3924 methods includes integrating more comprehensive fuel data to improve predictions of burned
3925 area, expanding the uncertainty schemes to include intensity, fire spread and emissions, and
3926 better constraining uncertainties between SSP scenarios through improved representation of
3927 BA drivers and their trends.

3928
3929 Over the next couple of years, the focus should be on the rapid integration of near-real-time
3930 (NRT) data and leveraging advancements in remote sensing and machine learning. These
3931 innovations will enhance the accuracy and timeliness of fire models for future projections. By
3932 focusing on these targeted actions over the next few years, we can significantly advance the
3933 state of wildfire modelling, making it more accurate, reliable, and relevant for policy and impact
3934 assessment.

3935 3936 **4.5 Competing Interests Statement**

3937
3938 SV is a member of the editorial board of Earth System Science Data. The authors declare no
3939 further conflict of interest.

3940 3941 **4.6 Acknowledgements**

3942
3943 The authors thank the following for their contributions to the identification and description of
3944 key events in the 2023-24 fire season: Robert Ang'ila (Karatina University, Kenya); Miltiadis
3945 Athanasiou (Institute of Mediterranean Forest Ecosystems, Greece); Davide Ascoli (University
3946 of Turin); Chris Collins (Tasmania Fire Service, Australia); Abigail Coker (Imperial College,
3947 London); Helen De Klerk (Stellenbosch University); Kebonyethata Dintwe (University of
3948 Botswana); David Field (NSW Rural Fire Service, Australia); Ronald Heath (Forestry South
3949 Africa); Konstantinos Kaoukis (Institute of Mediterranean Forest Ecosystems, Greece); Agnes
3950 Kristina (Department of Fire and Emergency Services, Australia); Niall MacLennan (Scottish
3951 Fire and Rescue Service); John Mendelsohn (Okavango Research Institute); Grant Pearce
3952 (Fire and Emergency NZ, New Zealand); Galia Selaya (Ecosconsult, Bolivia); Russell
3953 Stephens Peacock (QLD Fire and Emergency Services, Australia); Simeon Telfer (SA Country
3954 Fire Service, Australia); Emmanuela Zevgoli (Agricultural University of Athens, Greece);
3955 Hellenic Agricultural Organization "DIMITRA"; The Chico Mendes Institute for Biodiversity
3956 Conservation (ICMBio, Brazil, Santarém Office). The authors thank Andrew Ciavarella (Met
3957 Office) for guidance on using the HadGEM3-A data for the fire weather index. The authors
3958 thank Anna Bradley (UK Met Office) for JULES-ES-ISIMIP data processing and submission to
3959 ISIMIP repository. The authors thank the working groups "FLARE: Fire science Learning
3960 AcROSS the Earth System" and "TerraFIRMA: Dummies Guide to using Fire Models" for
3961 contributing to defining the report scope and establishing contributor links.

3962 3963 **4.7 Author Contributions**

3964
3965 **Conceptualization:** Jones, M. W., Kelley, D. I., Burton, C. A., Di Giuseppe, F.
3966 **Project Administration:** Jones, M. W., Kelley, D. I., Burton, C. A., Di Giuseppe, F.
3967 **Data Curation:** Jones, M. W., Kelley, D. I., Burton, C. A., Di Giuseppe, F., Barbosa, M. L. F.,
3968 Brambleby, E., Lampe, S., Mataveli, G., McNorton, J., Spuler, F., Wessel, J., Parrington, M.
3969 **Formal Analysis:** Jones, M. W., Kelley, D. I., Burton, C. A., Di Giuseppe, F., Brambleby, E.,
3970 Lampe, S., Mataveli, G., McNorton, J., Spuler, F., Wessel, J., Parrington, M.
3971 Jones, M. W., Kelley, D. I., Burton, C. A., Di Giuseppe, F., Barbosa, M. L. F., Brambleby, E.,
3972 Hartley, A., Lampe, S., McNorton, J., Spuler, F., Wessel, J., Parrington, M., Hamilton, D. S.
3973 **Resources/Software:** Andela, N., Giglio, L., Parrington, M., van der Werf, G. R., Barbosa, M.
3974 L. F., Brambleby, E., Hartley, A., Lampe, S., McNorton, J., Spuler, F., Wessel, J., Burke, E.,
3975 San-Miguel-Ayanz, J., Qu, Y.



3976 **Visualisation:** Jones, M. W., Kelley, D. I., Burton, C. A., Di Giuseppe, F., Mataveli, G.,
3977 McNorton, J., Qu, Y., Lombardi, A.
3978 **Writing – Original Draft Preparation:** Jones, M. W., Kelley, D. I., Burton, C. A., Di Giuseppe,
3979 F., McNorton, J., Anderson, L., Archibald, S., Armenteras, D., Clarke, H., Doerr, S.,
3980 Fernandes, P., Harris, S., Jain, P., Kolden, C., Ribeiro, N., Saharjo, B., Shuman, J., Tanpipat,
3981 V., Xanthopoulos, G., Carmenta, R., Hamilton, D. S., Hantson, S., Meier, S., Perron, M. M. G.,
3982 Parrington, M., Hartley, A., J., Spuler, F., Wessel
3983 **Writing – Review & Editing:** All authors.
3984

4.8 Data Availability

3985
3986
3987 BA data from NASA's MODIS BA product (MCD64A1) are extended from Giglio et al. (2018)
3988 and are available at Giglio et al. (2021, <https://lpdaac.usgs.gov/products/mcd64a1v061/>,
3989 last access: 2 June 2024). GFED4.1s fire C emissions data are extended from van der Werf and
3990 are available at <https://globalfiredata.org/> (last access: 2 June 2024). GFAS fire C emissions
3991 data are extended from Kaiser et al. (2012) and are available at
3992 [https://confluence.ecmwf.int/display/CKB/CAMS+global+biomass+burning+emissions+base
3993 d+on+fire+radiative+power+%28GFAS%29%3A+data+documentation](https://confluence.ecmwf.int/display/CKB/CAMS+global+biomass+burning+emissions+base+d+on+fire+radiative+power+%28GFAS%29%3A+data+documentation) (last access: 2 June
3994 2024). Global Fire Atlas are extended from Andela et al. (2019) and are available at Andela
3995 and Jones (2024, <https://doi.org/10.5281/zenodo.11400062>,
3996 last access: 2 June 2024). Regional summaries of the MODIS BA, GFED4.1s, GFAS, and the Global Fire Atlas are
3997 presented here are available at Jones et al. (2024, <https://doi.org/10.5281/zenodo.11400540>,
3998 last access: 2 June 2024). Studies utilising our regional summaries should cite both the current
3999 article and the primary reference for the variable(s) of interest: Giglio et al. (2018) for BA; van
4000 der Werf et al. (2017) for GFED4.1s fire C emissions; Kaiser et al. (2012) for GFAS fire C
4001 emissions; Andela et al. (2019) for the Global Fire Atlas.
4002

4003 Driving data, re-gridded BA target data for ConFire and ConFire outputs are available at Kelley
4004 et al. (2024, <https://doi.org/10.5281/zenodo.11420743>, last access: 2 June 2024). Historical
4005 (1960-2013) HadGEM3-A are available through the Centre for Environmental Data Analysis
4006 (CEDA) archive of the NERC's Environmental Data Service (EDS) at
4007 <http://catalogue.ceda.ac.uk/uuid/99b29b4bfeae470599fb96243e90cde3> (last access, last
4008 access: 2 June 2024). FireMIP / ISIMIP driving and output data is available from the Inter-
4009 Sectoral Impact Model Intercomparison Project (ISIMIP) repository at <https://data.ISIMIP.org/>
4010 (last access: 2 June 2024).
4011

4.9 Code Availability

4012
4013
4014 ConFire attribution framework code (Kelley et al., 2021; Barbosa, 2024), was incorporated into
4015 the FLAME repository (https://github.com/douglask3/Bayesian_fire_models/tree/ConFire) and
4016 will be archived with a doi upon publication. Configuration settings for **Section 3.3** are in
4017 `namelists/nrt.ini`, while **Section 3.4** and **Section 3.5** are in `namelists/ISIMIP.ini`. Scripts for
4018 reproducing plots can be found in State of Wildfire GitHub repo (currently available at
4019 https://github.com/douglask3/State_of_Wildfires_report, with an archived doi available upon
4020 final publication).
4021

4022 The code used to produce the FWI attribution results is available in State of Wildfire GitHub
4023 repo (currently available at https://github.com/douglask3/State_of_Wildfires_report, with an
4024 archived doi available upon final publication). FWI code can be accessed via the ECMWF
4025 GitHub (<https://github.com/ecmwf-projects/geff>). Met Office implementation of the FWI is
4026 based on this code, and can be accessed at
4027 <https://github.com/MetOffice/impactstoolbox/tree/main> with registration. All details of the data
4028 and code used for the FireMIP attribution results is documented in Burton, Lampe et al. (2023).
4029



4030 The current version of *ibicus*, used for JULES-ES bias correction, is available from PyPI
4031 (<https://pypi.org/project/ibicus/>, last access: 2 June 2024) under the Apache License version
4032 2.0, and is described in detail in <https://ibicus.readthedocs.io/en/latest/> (last access: 2 June
4033 2024). The source code is available via GitHub (<https://github.com/ecmwf-projects/ibicus>, last
4034 access: 2 June 2024). *Ibicus* is also archived on Zenodo by Spuler and Wessel (2023;
4035 <https://doi.org/10.5281/zenodo.8101898>, last access: 2 June). Model code and evaluation for
4036 bias-correction of JULES-ES model output can be found at the State of Wildfire GitHub repo
4037 (currently available at <https://github.com/jakobwes/State-of-Wildfires---Bias-Adjustment>, with
4038 an archived doi available upon final publication).
4039

4.10 Financial support

4040
4041
4042 MWJ was funded by the UK Natural Environment Research Council (NERC) (NE/V01417X/1).
4043 DIK was supported by NERC as part of the LTSM2 TerraFIRMA project and NC-International
4044 programme (NE/X006247/1) delivering National Capability. CAB was funded by the Met Office
4045 Climate Science for Service Partnership (CSSP) Brazil project which is supported by the
4046 Department for Science, Innovation & Technology (DSIT), and by the Met Office Hadley
4047 Centre Climate Programme funded by DSIT. PMF acknowledges support by National Funds
4048 by FCT - Portuguese Foundation for Science and Technology (project UIDB/04033/2020,
4049 <https://doi.org/10.54499/UIDB/04033/2020>). FDG and JMC are both funded by a service
4050 contract (n 942604) issued by the Joint Research Center on behalf of the European
4051 Commission. LOA acknowledges support by the São Paulo Research Foundation
4052 (FAPESP)(projects: 2021/07660-2 and 2020/16457-3) and by the National Council for
4053 Scientific and Technological Development (CNPq), productivity scholarship (process:
4054 314473/2020-3). GM acknowledges support by FAPESP (grants 2019/25701-8, 2020/15230-
4055 5 and 2023/03206-0). SL was supported by a PhD Fundamental Research Grant by Fonds
4056 Wetenschappelijk Onderzoek - Vlaanderen (11M7723N). SM gratefully acknowledges the
4057 support of the Dragon Capital Chair on Biodiversity Economics. ECh is being supported by
4058 the European Space Agency's Climate Change Initiative (ESA CCI) programme (FireCCI:
4059 Contract No. 4000126706/19/I-NB). CAK acknowledges support from USDA NIFA (award
4060 2022-67019-36435). YQ was supported by the China Scholarship Council (CSC) under grant
4061 number 201906040220. MMGP was supported by a Marie Skłodowska-Curie Actions 2021
4062 Postdoctoral Fellow funding number 101064063. HC was funded by the Westpac Scholars
4063 Trust via a Westpac Research Fellowship. SHD acknowledges support from NERC (grant
4064 NE/X005143/1) and the FirEUrisk project, which has received funding from the European
4065 Union's Horizon 2020 research and innovation programme under grant agreement No
4066 101003890. EB was supported by the NERC ARIES Doctoral Training Partnership (grant
4067 number NE/S007334/1). JKS acknowledges support from the National Aeronautics and Space
4068 Administration (NASA) FireSense Project. NA was supported by the Sense4Fire project as
4069 part of ESA's C Cycle Cluster (ESA contract number: 4000134840/21/I-NB). MLFB was
4070 supported by the Coordination for the Improvement of Higher Education Personnel (CAPES),
4071 Finance Code 001. The contribution of SV was funded by the European Research Council
4072 through a Consolidator grant under the European Union's Horizon 2020 research and
4073 innovation program (grant agreement No. 101000987). RC is grateful to the Tyndall Centre
4074 for Climate Change Research for financial support.
4075

5 References

- 4076
4077
4078 Abatzoglou, J. T., Williams, A. P., Boschetti, L., Zubkova, M., and Kolden, C. A.: Global patterns of interannual climate–fire
4079 relationships, *Glob Change Biol*, 24, 5164–5175, <https://doi.org/10.1111/gcb.14405>, 2018.
- 4080
4081 Abatzoglou, J. T., Williams, A. P., and Barbero, R.: Global Emergence of Anthropogenic Climate Change in Fire Weather Indices,
Geophys. Res. Lett., 46, 326–336, <https://doi.org/10.1029/2018GL080959>, 2019.



- 4082 Abatzoglou, J. T., Juang, C. S., Williams, A. P., Kolden, C. A., and Westerling, A. L.: Increasing Synchronous Fire Danger in
4083 Forests of the Western United States, *Geophysical Research Letters*, 48, e2020GL091377,
4084 <https://doi.org/10.1029/2020GL091377>, 2021.
- 4085 Abatzoglou, J. T., Kolden, C. A., Williams, A. P., Sadegh, M., Balch, J. K., and Hall, A.: Downslope Wind-Driven Fires in the
4086 Western United States, *Earth's Future*, 11, e2022EF003471, <https://doi.org/10.1029/2022EF003471>, 2023.
- 4087 Abram, N. J., Henley, B. J., Sen Gupta, A., Lippmann, T. J. R., Clarke, H., Dowdy, A. J., Sharples, J. J., Nolan, R. H., Zhang, T.,
4088 Wooster, M. J., Wurtzel, J. B., Meissner, K. J., Pitman, A. J., Ukkola, A. M., Murphy, B. P., Tapper, N. J., and Boer, M. M.:
4089 Connections of climate change and variability to large and extreme forest fires in southeast Australia, *Commun Earth Environ*, 2,
4090 8, <https://doi.org/10.1038/s43247-020-00065-8>, 2021.
- 4091 Adzhar, R., Kelley, D. I., Dong, N., George, C., Torello Raventos, M., Veenendaal, E., Feldpausch, T. R., Phillips, O. L., Lewis,
4092 S. L., Sonké, B., Taedoumg, H., Schwantes Marimon, B., Domingues, T., Arroyo, L., Djagbletey, G., Saiz, G., and Gerard, F.:
4093 MODIS Vegetation Continuous Fields tree cover needs calibrating in tropical savannas, *Biogeosciences*, 19, 1377–1394,
4094 <https://doi.org/10.5194/bg-19-1377-2022>, 2022.
- 4095 AfricaNews: Wildfires force evacuations of South African coastal towns, available at:
4096 <https://www.africanews.com/2024/01/31/wildfires-force-evacuations-of-south-african-coastal-towns/>, last access: 2 June 2024,
4097 Africanews, 31st January, 2024.
- 4098 Aguilera, R., Corringham, T., Gershunov, A., and Benmarhnia, T.: Wildfire smoke impacts respiratory health more than fine
4099 particles from other sources: observational evidence from Southern California, *Nat Commun*, 12, 1493,
4100 <https://doi.org/10.1038/s41467-021-21708-0>, 2021.
- 4101 Agustí-Panareda, A., Diamantakis, M., Massart, S., Chevallier, F., Muñoz-Sabater, J., Barré, J., Curcoll, R., Engelen, R.,
4102 Langerock, B., Law, R. M., Loh, Z., Morguí, J. A., Parrington, M., Peuch, V.-H., Ramonet, M., Roehl, C., Vermeulen, A. T.,
4103 Warneke, T., and Wunch, D.: Modelling CO₂ weather – why horizontal resolution matters, *Atmospheric Chemistry and Physics*,
4104 19, 7347–7376, <https://doi.org/10.5194/acp-19-7347-2019>, 2019.
- 4105 Al Jazeera: 2023a From Algeria to Syria, heatwaves scorch Middle East, North Africa, available at:
4106 <https://www.aljazeera.com/news/2023/7/19/from-algeria-to-syria-heatwaves-scorch-middle-east-north-africa>, last access: 2 June
4107 2024, Al Jazeera, 19th July, 2023a.
- 4108 Al Jazeera: 2023b Wildfires in Algeria kill dozens, force hundreds to flee homes, available at:
4109 <https://www.aljazeera.com/news/2023/7/24/deadly-algeria-wildfires-amid-extreme-heat-high-winds>, last access: 2 June 2024, Al
4110 Jazeera, 24th July, 2023b.
- 4111 Al Jazeera: More than 60 people killed as forest fires rage in Chile, available at: [https://www.aljazeera.com/news/2024/2/3/chile-](https://www.aljazeera.com/news/2024/2/3/chile-declares-state-of-emergency-over-raging-forest-fires)
4112 [declares-state-of-emergency-over-raging-forest-fires](https://www.aljazeera.com/news/2024/2/3/chile-declares-state-of-emergency-over-raging-forest-fires), last access: 2 June 2024, Al Jazeera, 4th February, 2024.
- 4113 ALER: Alarmantes cifras de incendios forestales se registran en Venezuela durante el primer trimestre de 2024 – ALER, available
4114 at: [https://aler.org/nota_informativa/alarmantes-cifras-de-incendios-forestales-se-registran-en-venezuela-durante-el-primer-](https://aler.org/nota_informativa/alarmantes-cifras-de-incendios-forestales-se-registran-en-venezuela-durante-el-primer-trimestre-de-2024/)
4115 [trimestre-de-2024/](https://aler.org/nota_informativa/alarmantes-cifras-de-incendios-forestales-se-registran-en-venezuela-durante-el-primer-trimestre-de-2024/), last access: 2 June 2024, 2024.
- 4116 Alvarado, S. T., Andela, N., Silva, T. S. F., and Archibald, S.: Thresholds of fire response to moisture and fuel load differ between
4117 tropical savannas and grasslands across continents, *Global Ecol Biogeogr*, 29, 331–344, <https://doi.org/10.1111/geb.13034>,
4118 2020.
- 4119 Andela, N. and Jones, M. W.: Update of: The Global Fire Atlas of individual fire size, duration, speed and direction,
4120 <https://doi.org/10.5281/zenodo.11400062>, 2024.
- 4121 Andela, N., Morton, D. C., Giglio, L., Chen, Y., van der Werf, G. R., Kasibhatla, P. S., DeFries, R. S., Collatz, G. J., Hantson, S.,
4122 Kloster, S., Bachelet, D., Forrest, M., Lasslop, G., Li, F., Mangeon, S., Melton, J. R., Yue, C., and Randerson, J. T.: A human-
4123 driven decline in global burned area, *Science*, 356, 1356–1362, <https://doi.org/10.1126/science.aal4108>, 2017.
- 4124 Andela, N., Morton, D. C., Giglio, L., Paugam, R., Chen, Y., and Hantson, S.: The Global Fire Atlas of individual fire size, duration,
4125 speed and direction, 24, 2019.



- 4126 Andela, N., Morton, D. C., Schroeder, W., Chen, Y., Brando, P. M., and Randerson, J. T.: Tracking and classifying Amazon fire
4127 events in near real time, *Science Advances*, 8, eabd2713, <https://doi.org/10.1126/sciadv.abd2713>, 2022.
- 4128 Anderegg, W. R. L., Trugman, A. T., Vargas, G., Wu, C., and Yang, L.: Current forest carbon offset buffer pools do not adequately
4129 insure against disturbance-driven carbon losses, <https://doi.org/10.1101/2024.03.28.587000>, 31 March 2024.
- 4130 Antara News: ASEAN inaugurates ACC THPC to combat haze pollution, available at:
4131 <https://en.antaranews.com/news/292902/asean-inaugurates-acc-thpc-to-combat-haze-pollution>, last access: 2 June 2024,
4132 Antara News, 2023.
- 4133 Aragão, L. E. O. C., Anderson, L. O., Fonseca, M. G., Rosan, T. M., Vedovato, L. B., Wagner, F. H., Silva, C. V. J., Silva Junior,
4134 C. H. L., Arai, E., Aguiar, A. P., Barlow, J., Berenguer, E., Deeter, M. N., Domingues, L. G., Gatti, L., Gloor, M., Malhi, Y., Marengo,
4135 J. A., Miller, J. B., Phillips, O. L., and Saatchi, S.: 21st Century drought-related fires counteract the decline of Amazon
4136 deforestation carbon emissions, *Nat Commun*, 9, 536, <https://doi.org/10.1038/s41467-017-02771-y>, 2018.
- 4137 ArcGIS Hub: World Continents, available at: <https://hub.arcgis.com/maps/CESJ::world-continents>, last access: 2 June 2024,
4138 2024.
- 4139 Archibald, S. and Roy, D. P.: Identifying individual fires from satellite-derived burned area data, in: 2009 IEEE International
4140 Geoscience and Remote Sensing Symposium, 2009 IEEE International Geoscience and Remote Sensing Symposium, III-160-
4141 III-163, <https://doi.org/10.1109/IGARSS.2009.5417974>, 2009.
- 4142 Archibald, S., Roy, D. P., van WILGEN, B. W., and Scholes, R. J.: What limits fire? An examination of drivers of burnt area in
4143 Southern Africa, *Global Change Biology*, 15, 613–630, <https://doi.org/10.1111/j.1365-2486.2008.01754.x>, 2009.
- 4144 Ardyna, M., Hamilton, D. S., Harmel, T., Lacour, L., Bernstein, D. N., Laliberté, J., Horvat, C., Laxenaire, R., Mills, M. M., van
4145 Dijken, G., Polyakov, I., Claustre, H., Mahowald, N., and Arrigo, K. R.: Wildfire aerosol deposition likely amplified a summertime
4146 Arctic phytoplankton bloom, *Commun Earth Environ*, 3, 1–8, <https://doi.org/10.1038/s43247-022-00511-9>, 2022.
- 4147 Arino, O., Rosaz, J.-M., and Goloub, P.: The ATSR World Fire Atlas A synergy with 'Polder' aerosol products, *Earth Observation*
4148 *Quarterly*, 64, 30, 1999.
- 4149 Armero, A. J.: El fuego en Las Hurdes y Sierra de Gata deja a Pinofranqueado sin agua potable, available at:
4150 <https://www.hoy.es/extremadura/fuego-hurdes-sierra-gata-deja-pinofranqueado-agua-20230624190605-nt.html>, last access: 2
4151 June 2024, Hoy, 2023.
- 4152 Artés, T., Oom, D., de Rigo, D., Durrant, T. H., Maianti, P., Libertà, G., and San-Miguel-Ayanz, J.: A global wildfire dataset for the
4153 analysis of fire regimes and fire behaviour, *Sci Data*, 6, 296, <https://doi.org/10.1038/s41597-019-0312-2>, 2019.
- 4154 Athanasiou, M.: Preliminary findings on the behaviour and spread of the wildfire of August 2023 in Evros, Greece (in Greek with
4155 English abstract). Project "Learning from the Evros wildfire: Firefighting effectiveness evaluation and proposals". WWF Greece,
4156 Athens, 76 p., WWF Greece, Athens, 2024.
- 4157 Atlas of Namibia: Atlas of Namibia Chapter 8: Conservation, available at: <https://atlasofnamibia.online/chapter-8/conservation>,
4158 last access: 2 June 2024, 2021.
- 4159 Austen, I.: As 'Zombie Fires' Smolder, Canada Braces for Another Season of Flames, available at:
4160 <https://www.nytimes.com/2024/03/04/canada-zombie-fires-wildfire.html>, last access: 2 June 2024, New York Times, 4th March,
4161 2024.
- 4162 B. Ankhtuya: Bush fire in Dornod spreads to Russia - News.MN, available at: <https://news.mn/en/791879/>, last access: 2 June
4163 2024, News.MN, 2020.
- 4164 Badgley, G., Chay, F., Chegwidan, O. S., Hamman, J. J., Freeman, J., and Cullenward, D.: California's forest carbon offsets
4165 buffer pool is severely undercapitalized, *Front. For. Glob. Change*, 5, <https://doi.org/10.3389/ffgc.2022.930426>, 2022.
- 4166 Baltzer, J. L., Day, N. J., Walker, X. J., Greene, D., Mack, M. C., Alexander, H. D., Arseneault, D., Barnes, J., Bergeron, Y.,
4167 Boucher, Y., Bourgeau-Chavez, L., Brown, C. D., Carrière, S., Howard, B. K., Gauthier, S., Parisien, M.-A., Reid, K. A., Rogers,



- 4168 B. M., Roland, C., Sirois, L., Stehn, S., Thompson, D. K., Turetsky, M. R., Veraverbeke, S., Whitman, E., Yang, J., and Johnstone,
4169 J. F.: Increasing fire and the decline of fire adapted black spruce in the boreal forest, *Proceedings of the National Academy of*
4170 *Sciences*, 118, e2024872118, <https://doi.org/10.1073/pnas.2024872118>, 2021.
- 4171 Barbosa, M. L. F.: *Tracing the Ashes: Uncovering Burned Area Patterns and Drivers Over the Brazilian Biomes* (PhD Thesis
4172 supervised by Liana Anderson), Instituto Nacional de Pesquisas Espaciais, São José dos Campos, 2024.
- 4173 Barlow, J., Parry, L., Gardner, T. A., Ferreira, J., Aragão, L. E. O. C., Carmenta, R., Berenguer, E., Vieira, I. C. G., Souza, C.,
4174 and Cochrane, M. A.: The critical importance of considering fire in REDD+ programs, *Biological Conservation*, 154, 1–8,
4175 <https://doi.org/10.1016/j.biocon.2012.03.034>, 2012.
- 4176 Barlow, J., França, F., Gardner, T. A., Hicks, C. C., Lennox, G. D., Berenguer, E., Castello, L., Economo, E. P., Ferreira, J.,
4177 Guénard, B., Gontijo Leal, C., Isaac, V., Lees, A. C., Parr, C. L., Wilson, S. K., Young, P. J., and Graham, N. A. J.: The future of
4178 hyperdiverse tropical ecosystems, *Nature*, 559, 517–526, <https://doi.org/10.1038/s41586-018-0301-1>, 2018.
- 4179 Barlow, J., Berenguer, E., Carmenta, R., and França, F.: Clarifying Amazonia's burning crisis, *Glob Change Biol*, 26, 319–321,
4180 <https://doi.org/10.1111/gcb.14872>, 2020.
- 4181 Barnes, C., Boulanger, Y., Keeping, T., Gachon, P., Gillett, N., Boucher, J., Roberge, F., Kew, S., Haas, O., Heinrich, D.,
4182 Vahlberg, M., Singh, R., Elbe, M., Sivanu, S., Arrighi, J., Van Aalst, M., Otto, F., Zachariah, M., Krikken, F., Wang, X., Erni, S.,
4183 Pietropalo, E., Avis, A., Bisailon, A., and Kimutai, J.: Climate change more than doubled the likelihood of extreme fire weather
4184 conditions in Eastern Canada, available at: <http://spiral.imperial.ac.uk/handle/10044/1/105981>, last access: 2 June 2024,
4185 <https://doi.org/10.25561/105981>, 2023.
- 4186 BBC News: Why is Canada having so many wildfires this season?, available at: [https://www.bbc.com/news/world-us-canada-](https://www.bbc.com/news/world-us-canada-69011493)
4187 [69011493](https://www.bbc.com/news/world-us-canada-69011493), last access: 2 June 2024, BBC News, 15th May, 2024.
- 4188 Bedia, J., Herrera, S., Gutiérrez, J. M., Benali, A., Brands, S., Mota, B., and Moreno, J. M.: Global patterns in the sensitivity of
4189 burned area to fire-weather: Implications for climate change, *Agricultural and Forest Meteorology*, 214–215, 369–379,
4190 <https://doi.org/10.1016/j.agrformet.2015.09.002>, 2015.
- 4191 Bedia, J., Golding, N., Casanueva, A., Iturbide, M., Buontempo, C., and Gutiérrez, J. M.: Seasonal predictions of Fire Weather
4192 Index: Paving the way for their operational applicability in Mediterranean Europe, *Climate Services*, 9, 101–110,
4193 <https://doi.org/10.1016/j.cliser.2017.04.001>, 2018.
- 4194 Belcher, C. M., Brown, I., Clay, G. D., Doerr, S. H., Elliott, A., Gazzard, R., Kettridge, N., Morison, J., Perry, M., Santin, C., and
4195 Smith, T. E. L.: UK Wildfires and their Climate Challenges, Expert Led Report Prepared for the Third UK Climate Change Risk
4196 Assessment (CCRA3), available at: [https://www.ukclimaterisk.org/wp-content/uploads/2021/06/UK-Wildfires-and-their-Climat-](https://www.ukclimaterisk.org/wp-content/uploads/2021/06/UK-Wildfires-and-their-Climat-Challenges.pdf)
4197 [Challenges.pdf](https://www.ukclimaterisk.org/wp-content/uploads/2021/06/UK-Wildfires-and-their-Climat-Challenges.pdf), last access: 2 June 2024, University of Exeter Global Systems Institute, Exeter, 2021.
- 4198 Betts, R. A., Belcher, S. E., Hermanson, L., Klein Tank, A., Lowe, J. A., Jones, C. D., Morice, C. P., Rayner, N. A., Scaife, A. A.,
4199 and Stott, P. A.: Approaching 1.5 °C: how will we know we've reached this crucial warming mark?, *Nature*, 624, 33–35,
4200 <https://doi.org/10.1038/d41586-023-03775-z>, 2023.
- 4201 Beverly, J. L. and Bothwell, P.: Wildfire evacuations in Canada 1980–2007, *Nat Hazards*, 59, 571–596,
4202 <https://doi.org/10.1007/s11069-011-9777-9>, 2011.
- 4203 Bhandari, S. R.: Culprits behind dense smog in northern Thailand, Laos: corn and wildfires, available at:
4204 <https://www.rfa.org/english/news/environment/smog-04172023135125.html>, last access: 2 June 2024, Radio Free Asia, 2023.
- 4205 Bilbao, B., Mistry, J., Millán, A., and Berardi, A.: Sharing Multiple Perspectives on Burning: Towards a Participatory and
4206 Intercultural Fire Management Policy in Venezuela, Brazil, and Guyana, *Fire*, 2, 39, <https://doi.org/10.3390/fire2030039>, 2019.
- 4207 Bistinas, I., Harrison, S. P., Prentice, I. C., and Pereira, J. M. C.: Causal relationships versus emergent patterns in the global
4208 controls of fire frequency, *Biogeosciences*, 11, 5087–5101, <https://doi.org/10.5194/bg-11-5087-2014>, 2014.



- 4209 Bodí, M. B., Martin, D. A., Balfour, V. N., Santín, C., Doerr, S. H., Pereira, P., Cerdà, A., and Mataix-Solera, J.: Wildland fire ash:
4210 Production, composition and eco-hydro-geomorphic effects, *Earth-Science Reviews*, 130, 103–127,
4211 <https://doi.org/10.1016/j.earscirev.2013.12.007>, 2014.
- 4212 Borneo Bulletin: Mongolia battles wildfire in eastern region, available at: [https://borneobulletin.com.bn/mongolia-battles-wildfire-](https://borneobulletin.com.bn/mongolia-battles-wildfire-in-eastern-region/)
4213 [in-eastern-region/](https://borneobulletin.com.bn/mongolia-battles-wildfire-in-eastern-region/), last access: 2 June 2024, Mongolia battles wildfire in eastern region, 2023.
- 4214 Boschetti, L. and Roy, D. P.: Defining a fire year for reporting and analysis of global interannual fire variability, *Journal of*
4215 *Geophysical Research: Biogeosciences*, 113, <https://doi.org/10.1029/2008JG000686>, 2008.
- 4216 Boucher, O., Servonnat, J., Albright, A. L., Aumont, O., Balkanski, Y., Bastrikov, V., Bekki, S., Bonnet, R., Bony, S., Bopp, L.,
4217 Braconnot, P., Brockmann, P., Cadule, P., Caubel, A., Cheruy, F., Codron, F., Cozic, A., Cugnet, D., D'Andrea, F., Davini, P., de
4218 Lavergne, C., Denvil, S., Deshayes, J., Devilliers, M., Ducharne, A., Dufresne, J.-L., Dupont, E., Éthé, C., Fairhead, L., Falletti,
4219 L., Flavoni, S., Foujols, M.-A., Gardoll, S., Gastineau, G., Ghattas, J., Grandpeix, J.-Y., Guenet, B., Guez, E., Lionel, Guilyardi,
4220 E., Guimberteau, M., Hauglustaine, D., Hourdin, F., Idelkadi, A., Joussaume, S., Kageyama, M., Khodri, M., Krinner, G., Lebas,
4221 N., Levavasseur, G., Lévy, C., Li, L., Lott, F., Lurton, T., Luyssaert, S., Madec, G., Madeleine, J.-B., Maignan, F., Marchand, M.,
4222 Marti, O., Mellul, L., Meurdesoif, Y., Mignot, J., Musat, I., Ottlé, C., Peylin, P., Planton, Y., Polcher, J., Rio, C., Rochetin, N.,
4223 Rousset, C., Sepulchre, P., Sima, A., Swingedouw, D., Thiéblemont, R., Traore, A. K., Vancoppenolle, M., Vial, J., Vialard, J.,
4224 Viovy, N., and Vuichard, N.: Presentation and Evaluation of the IPSL-CM6A-LR Climate Model, *Journal of Advances in Modeling*
4225 *Earth Systems*, 12, e2019MS002010, <https://doi.org/10.1029/2019MS002010>, 2020.
- 4226 Boulanger, Y., Arseneault, D., Bélisle, A. C., Bergeron, Y., Boucher, J., Boucher, Y., Danneyrolles, V., Erni, S., Gachon, P.,
4227 Girardin, M. P., Grant, E., Grondin, P., Jetté, J.-P., Labadie, G., Leblond, M., Leduc, A., Puigdevall, J. P., St-Laurent, M.-H.,
4228 Tremblay, J. A., and Waldron, K.: The 2023 wildfire season in Québec: an overview of extreme conditions, impacts, lessons
4229 learned and considerations for the future, <https://doi.org/10.1101/2024.02.20.581257>, 22 February 2024.
- 4230 Boussetta, S., Balsamo, G., Arduini, G., Dutra, E., McNorton, J., Choulga, M., Agustí-Panareda, A., Beljaars, A., Wedi, N., Munõz-
4231 Sabater, J., de Rosnay, P., Sandu, I., Hadade, I., Carver, G., Mazzetti, C., Prudhomme, C., Yamazaki, D., and Zsoter, E.: ECLand:
4232 The ECMWF Land Surface Modelling System, *Atmosphere*, 12, 723, <https://doi.org/10.3390/atmos12060723>, 2021.
- 4233 Bradshaw, L. S., Deeming, J. E., Burgan, R. E., and compilers.Cohen, J. D.: The 1978 National Fire-Danger Rating System:
4234 technical documentation, General Technical Report INT-169. Ogden, UT: U.S. Department of Agriculture, Forest Service,
4235 Intermountain Forest and Range Experiment Station. 44 p., 169, <https://doi.org/10.2737/INT-GTR-169>, 1984a.
- 4236 Bradshaw, L. S., Deeming, J., Burgan, R., and Cohen, J.: The 1978 National Fire-Danger Rating System: Technical
4237 Documentation, U.S. Department of Agriculture, Forest Service, Intermountain Forest and Range Experiment Station, 52 pp.,
4238 1984b.
- 4239 Bureau of Meteorology: Annual Australian Climate Statement 2023, scheme=AGLSTERMS.AglsAgent;
4240 corporateName=Australian Government - Bureau of Meteorology, 2024.
- 4241 Burrell, A. L., Sun, Q., Baxter, R., Kukavskaya, E. A., Zhila, S., Shestakova, T., Rogers, B. M., Kaduk, J., and Barrett, K.: Climate
4242 change, fire return intervals and the growing risk of permanent forest loss in boreal Eurasia, *Science of The Total Environment*,
4243 831, 154885, <https://doi.org/10.1016/j.scitotenv.2022.154885>, 2022.
- 4244 Burton, C., Lampe, S., Kelley, D., Thiery, W., Hantson, S., Christidis, N., Gudmundsson, L., Forrest, M., Burke, E., Chang, J.,
4245 Huang, H., Ito, A., Kou-Giesbrecht, S., Lasslop, G., Li, W., Nieradzki, L., Li, F., Chen, Y., Randerson, J., Reyer, C., and Mengel,
4246 M.: Global burned area increasingly explained by climate change, <https://doi.org/10.21203/rs.3.rs-3168150/v1>, 20 July 2023.
- 4247 Cai, W., Cowan, T., and Raupach, M.: Positive Indian Ocean Dipole events precondition southeast Australia bushfires,
4248 *Geophysical Research Letters*, 36, <https://doi.org/10.1029/2009GL039902>, 2009.
- 4249 California Department of Forestry and Fire Protection: CAL FIRE Damage Inspection (DINS) Data, available at:
4250 <https://www.arcgis.com/sharing/rest/content/items/994d3dc4569640caadb3198d5a3da1>, last access: 2 June 2024, 2024.



- 4251 Calkin, D. E., Barrett, K., Cohen, J. D., Finney, M. A., Pyne, S. J., and Quarles, S. L.: Wildland-urban fire disasters aren't actually
4252 a wildfire problem, Proceedings of the National Academy of Sciences, 120, e2315797120,
4253 <https://doi.org/10.1073/pnas.2315797120>, 2023.
- 4254 Canadell, J. G., Meyer, C. P. (Mick), Cook, G. D., Dowdy, A., Briggs, P. R., Knauer, J., Pepler, A., and Haverd, V.: Multi-decadal
4255 increase of forest burned area in Australia is linked to climate change, Nat Commun, 12, 6921, <https://doi.org/10.1038/s41467-021-27225-4>, 2021.
- 4257 Canadian Environmental Protection Act Federal-Provincial Working Group on Air Quality: National ambient air quality objectives
4258 for particulate matter. Part 1, Science assessment document : executive summary / a report by the Canadian Environmental
4259 Protection Act (CEPA)/Federal-Provincial Advisory Committee (FPAC) Working Group on Air Quality Objectives and
4260 Guidelines.25p., Health Canada, Environmental Health Directorate, Ottawa, Ontario, 25 pp., 1998.
- 4261 Canadian Interagency Forest Fire Centre: CIFFC Canada Report 2023 Fire Season, available at:
4262 https://ciffc.ca/sites/default/files/2024-03/CIFFC_2023CanadaReport_FINAL.pdf, last access: 2 June 2024, Canadian
4263 Interagency Forest Fire Centre, Canada, 2023.
- 4264 Cardil, A., Rodrigues, M., Tapia, M., Barbero, R., Ramirez, J., Stooft, C. R., Silva, C. A., Mohan, M., and de-Miguel, S.: Climate
4265 teleconnections modulate global burned area, Nat Commun, 14, 427, <https://doi.org/10.1038/s41467-023-36052-8>, 2023.
- 4266 Carmenta, R., Coudel, E., and Steward, A. M.: Forbidden fire: Does criminalising fire hinder conservation efforts in swidden
4267 landscapes of the Brazilian Amazon?, Geographical Journal, 185, 23–37, <https://doi.org/10.1111/geoi.12255>, 2019.
- 4268 Carmenta, R., Cammelli, F., Dressler, W., Verbicaro, C., and Zaehring, J. G.: Between a rock and a hard place: The burdens
4269 of uncontrolled fire for smallholders across the tropics, World Development, 145, 105521,
4270 <https://doi.org/10.1016/j.worlddev.2021.105521>, 2021.
- 4271 Carter, T. S., Heald, C. L., Jimenez, J. L., Campuzano-Jost, P., Kondo, Y., Moteki, N., Schwarz, J. P., Wiedinmyer, C., Darmenov,
4272 A. S., Da Silva, A. M., and Kaiser, J. W.: How emissions uncertainty influences the distribution and radiative impacts of smoke
4273 from fires in North America, Atmos. Chem. Phys., 20, 2073–2097, <https://doi.org/10.5194/acp-20-2073-2020>, 2020.
- 4274 Carvalho, A., Flannigan, M. D., Logan, K., Miranda, A. I., and Borrego, C.: Fire activity in Portugal and its relationship to weather
4275 and the Canadian Fire Weather Index System, Int. J. Wildland Fire, 17, 328–338, <https://doi.org/10.1071/WF07014>, 2008.
- 4276 Casanueva, A., Herrera, S., Iturbide, M., Lange, S., Jury, M., Dosio, A., Maraun, D., and Gutiérrez, J. M.: Testing bias adjustment
4277 methods for regional climate change applications under observational uncertainty and resolution mismatch, Atmospheric Science
4278 Letters, 21, e978, <https://doi.org/10.1002/asl.978>, 2020.
- 4279 Cátedra Cambio Climático de la Universidad de Oviedo: Evaluación de los Impactos Medioambientales Producidos por el
4280 Incendio de Foyedo (Asturias) Ocurrido en Primavera de 2023, available at: <https://cucc-uo.es/evaluacion-de-los-impactos-medioambientales-producidos-por-el-incendio-de-foyedo-asturias-ocurrido-en-primavera-de-2023/>, last access: 2 June 2024,
4281 2023.
- 4283 CBC News: Kelowna declares state of emergency after wildfire jumps Okanagan Lake, prompting more evacuations, available
4284 at: <https://www.cbc.ca/news/canada/british-columbia/what-you-need-to-know-about-bc-wildfires-aug-17-2023-1.6938796>, last
4285 access: 2 June 2024, CBC News, 17th August, 2023.
- 4286 Cecil, D. J., Buechler, D. E., and Blakeslee, R. J.: Gridded lightning climatology from TRMM-LIS and OTD: Dataset description,
4287 Atmospheric Research, 135–136, 404–414, <https://doi.org/10.1016/j.atmosres.2012.06.028>, 2014.
- 4288 Centre for Research on the Epidemiology of Disasters: EM-DAT International Disaster Database, available at:
4289 <https://public.emdat.be/>, last access: 2 June 2024, 2024.
- 4290 Chen, B., Wu, S., Jin, Y., Song, Y., Wu, C., Venevsky, S., Xu, B., Webster, C., and Gong, P.: Wildfire risk for global wildland-
4291 urban interface areas, Nat Sustain, 7, 474–484, <https://doi.org/10.1038/s41893-024-01291-0>, 2024.



- 4292 Chen, T. and Guestrin, C.: XGBoost: A Scalable Tree Boosting System, in: Proceedings of the 22nd ACM SIGKDD International
4293 Conference on Knowledge Discovery and Data Mining, New York, NY, USA, 785–794, <https://doi.org/10.1145/2939672.2939785>,
4294 2016.
- 4295 Chen, Y., Morton, D. C., Andela, N., van der Werf, G. R., Giglio, L., and Randerson, J. T.: A pan-tropical cascade of fire driven
4296 by El Niño/Southern Oscillation, *Nature Clim Change*, 7, 906–911, <https://doi.org/10.1038/s41558-017-0014-8>, 2017.
- 4297 Chen, Y., Hantson, S., Andela, N., Coffield, S. R., Graff, C. A., Morton, D. C., Ott, L. E., Fofoula-Georgiou, E., Smyth, P.,
4298 Goulden, M. L., and Randerson, J. T.: California wildfire spread derived using VIIRS satellite observations and an object-based
4299 tracking system, *Sci Data*, 9, 249, <https://doi.org/10.1038/s41597-022-01343-0>, 2022.
- 4300 Chen, Y., Hall, J., van Wees, D., Andela, N., Hantson, S., Giglio, L., van der Werf, G. R., Morton, D. C., and Randerson, J. T.:
4301 Multi-decadal trends and variability in burned area from the fifth version of the Global Fire Emissions Database (GFED5), *Earth
4302 System Science Data*, 15, 5227–5259, <https://doi.org/10.5194/essd-15-5227-2023>, 2023.
- 4303 Christidis, N., Stott, P. A., Scaife, A. A., Arribas, A., Jones, G. S., Copsey, D., Knight, J. R., and Tennant, W. J.: A New HadGEM3-
4304 A-Based System for Attribution of Weather- and Climate-Related Extreme Events, *Journal of Climate*, 26, 2756–2783,
4305 <https://doi.org/10.1175/JCLI-D-12-00169.1>, 2013.
- 4306 Chu, L., Grafton, R. Q., and Nelson, H.: Accounting for forest fire risks: global insights for climate change mitigation, *Mitig Adapt
4307 Strateg Glob Change*, 28, 48, <https://doi.org/10.1007/s11027-023-10087-0>, 2023.
- 4308 Chuvieco, E., Mouillot, F., van der Werf, G. R., San Miguel, J., Tanase, M., Koutsias, N., García, M., Yebra, M., Padilla, M., Gitas,
4309 I., Heil, A., Hawbaker, T. J., and Giglio, L.: Historical background and current developments for mapping burned area from satellite
4310 Earth observation, *Remote Sensing of Environment*, 225, 45–64, <https://doi.org/10.1016/j.rse.2019.02.013>, 2019.
- 4311 Chuvieco, E., Roteta, E., Sali, M., Stroppiana, D., Boettcher, M., Kirches, G., Storm, T., Khairoun, A., Pettinari, M. L., Franquesa,
4312 M., and Albergel, C.: Building a small fire database for Sub-Saharan Africa from Sentinel-2 high-resolution images, *Science of
4313 The Total Environment*, 845, 157139, <https://doi.org/10.1016/j.scitotenv.2022.157139>, 2022.
- 4314 Chuvieco, E., Yebra, M., Martino, S., Thonicke, K., Gómez-Giménez, M., San-Miguel, J., Oom, D., Velea, R., Mouillot, F., Molina,
4315 J. R., Miranda, A. I., Lopes, D., Salis, M., Bugaric, M., Sofiev, M., Kadantsev, E., Gitas, I. Z., Stavrakoudis, D., Eftychidis, G., Bar-
4316 Massada, A., Neidermeier, A., Pampanoni, V., Pettinari, M. L., Arrogante-Funes, F., Ochoa, C., Moreira, B., and Viegas, D.:
4317 Towards an Integrated Approach to Wildfire Risk Assessment: When, Where, What and How May the Landscapes Burn, *Fire*, 6,
4318 215, <https://doi.org/10.3390/fire6050215>, 2023.
- 4319 Ciais, P., Bastos, A., Chevallier, F., Lauerwald, R., Poulter, B., Canadell, J. G., Hugelius, G., Jackson, R. B., Jain, A., Jones, M.,
4320 Kondo, M., Lujikx, I. T., Patra, P. K., Peters, W., Pongratz, J., Petrescu, A. M. R., Piao, S., Qiu, C., Von Randow, C., Regnier, P.,
4321 Saunio, M., Scholes, R., Shvidenko, A., Tian, H., Yang, H., Wang, X., and Zheng, B.: Definitions and methods to estimate
4322 regional land carbon fluxes for the second phase of the REgional Carbon Cycle Assessment and Processes Project (RECCAP-
4323 2), *Geoscientific Model Development*, 15, 1289–1316, <https://doi.org/10.5194/gmd-15-1289-2022>, 2022.
- 4324 Ciavarella, A., Christidis, N., Andrews, M., Groenendijk, M., Rostron, J., Elkington, M., Burke, C., Lott, F. C., and Stott, P. A.:
4325 Upgrade of the HadGEM3-A based attribution system to high resolution and a new validation framework for probabilistic event
4326 attribution, *Weather and Climate Extremes*, 20, 9–32, <https://doi.org/10.1016/j.wace.2018.03.003>, 2018.
- 4327 Citizen Digital: Wildfires ravage over 40,000 acres of Aberdare forest, available at: <https://www.citizen.digital/news/wildfires-ravage-over-40000-acres-of-aberdare-forest-n314597>, last access: 2 June 2024, Citizen Digital, 2023.
- 4329 Clarke, B., Barnes, C., Rodrigues, R., Zachariah, M., Stewart, S., Raju, E., Baumgart, N., Heinrich, D., Libonati, R., Santos, D.,
4330 Albuquerque, R., Alves, L., Pinto, I., Otto, F., Kimutai, J., Philip, S., Kew, S., Bazo, J., and Wynter, A.: Climate change, not El
4331 Niño, main driver of extreme drought in highly vulnerable Amazon River Basin, Imperial College London,
4332 <https://doi.org/10.25561/108761>, 2024.
- 4333 Collins, L., Clarke, H., Clarke, M. F., McColl Gausden, S. C., Nolan, R. H., Penman, T., and Bradstock, R.: Warmer and drier
4334 conditions have increased the potential for large and severe fire seasons across south-eastern Australia, *Global Ecology and
4335 Biogeography*, 31, 1933–1948, <https://doi.org/10.1111/geb.13514>, 2022.



- 4336 Comisión Nacional Forestal: CONAFOR Reporte semanal de incendios 2024, available at:
4337 <https://www.gob.mx/conafor/documentos/reporte-semanal-de-incendios>, last access: 2 June 2024, 2024.
- 4338 Conlisk, E., Butsic, V., Syphard, A. D., Evans, S., and Jennings, M.: Evidence of increasing wildfire damage with decreasing
4339 property price in Southern California fires, *PLoS ONE*, 19, e0300346, <https://doi.org/10.1371/journal.pone.0300346>, 2024.
- 4340 Coop, J. D., Parks, S. A., Stevens-Rumann, C. S., Crausbay, S. D., Higuera, P. E., Hurteau, M. D., Tepley, A., Whitman, E.,
4341 Assal, T., Collins, B. M., Davis, K. T., Dobrowski, S., Falk, D. A., Fornwalt, P. J., Fulé, P. Z., Harvey, B. J., Kane, V. R., Littlefield,
4342 C. E., Margolis, E. Q., North, M., Parisien, M.-A., Prichard, S., and Rodman, K. C.: Wildfire-Driven Forest Conversion in Western
4343 North American Landscapes, *BioScience*, 70, 659–673, <https://doi.org/10.1093/biosci/biaa061>, 2020.
- 4344 Copernicus Climate Change Service: The European heatwave of July 2023 in a longer-term context, available at:
4345 <https://climate.copernicus.eu/european-heatwave-july-2023-longer-term-context>, last access: 2 June 2024, 2023.
- 4346 Copernicus Climate Change Service (C3S): ERA5 hourly data on single levels from 1940 to present,
4347 <https://doi.org/10.24381/CDS.ADBB2D47>, 2018.
- 4348 Copernicus Climate Change Service (C3S): 2023a European State of the Climate 2023, available at:
4349 <https://climate.copernicus.eu/esotc/2023>, last access: 2 June 2024, 2024a.
- 4350 Copernicus Climate Change Service (C3S): C3S Seasonal Charts, available at:
4351 https://climate.copernicus.eu/charts/packages/c3s_seasonal/, last access: 2 June 2024, 2024b.
- 4352 Copernicus Emergency Management Service: Copernicus EMS Fire danger indices historical data from the Copernicus
4353 Emergency Management Service, <https://doi.org/10.24381/CDS.0E89C522>, 2019.
- 4354 Copernicus Emergency Management Service: 2023a Copernicus EMS Rapid Mapping Activation Viewer: EMSR715 - Wildfire in
4355 Valparaiso region, Chile, available at: <https://rapidmapping.emergency.copernicus.eu/EMSR715/download>, last access: 2 June
4356 2024, 2023a.
- 4357 Copernicus Emergency Management Service: 2023b Copernicus EMS Rapid Mapping Activation Viewer: EMSR667 - Wildfire in
4358 Caceres, Spain, available at: <https://rapidmapping.emergency.copernicus.eu/EMSR667>, last access: 2 June 2024, 2023b.
- 4359 Copernicus Emergency Management Service: 2023c Copernicus EMS Situational Reporting: EMSR685 - Fire in Tenerife, Spain,
4360 available at: <https://storymaps.arcgis.com/stories/0f6c7842e2aa412db35d4f14ecc292ec>, last access: 2 June 2024, ArcGIS
4361 StoryMaps, 2023c.
- 4362 Crisis24: South Africa: Emergency crews continue to respond to wildfires across parts of Western Cape as of Jan. 30 /update 1,
4363 available at: [https://crisis24.garda.com/alerts/2024/01/south-africa-emergency-crews-continue-to-respond-to-wildfires-across-](https://crisis24.garda.com/alerts/2024/01/south-africa-emergency-crews-continue-to-respond-to-wildfires-across-parts-of-western-cape-as-of-jan-30-update-1)
4364 [parts-of-western-cape-as-of-jan-30-update-1](https://crisis24.garda.com/alerts/2024/01/south-africa-emergency-crews-continue-to-respond-to-wildfires-across-parts-of-western-cape-as-of-jan-30-update-1), last access: 2 June 2024, South Africa: Emergency crews continue to respond to
4365 wildfires across parts of Western Cape as of Jan. 30 /update 1 | Crisis24, 2024.
- 4366 Croker, A. R., Woods, J., and Kountouris, Y.: Community-Based Fire Management in East and Southern African Savanna-
4367 Protected Areas: A Review of the Published Evidence, *Earth's Future*, 11, e2023EF003552,
4368 <https://doi.org/10.1029/2023EF003552>, 2023.
- 4369 Cunningham, C. X., Williamson, G. J., Nolan, R. H., Teckentrup, L., Boer, M. M., and Bowman, D. M. J. S.: Pyrogeography in
4370 flux: Reorganization of Australian fire regimes in a hotter world, *Global Change Biology*, 30, e17130,
4371 <https://doi.org/10.1111/gcb.17130>, 2024.
- 4372 Cunningham, D., Cunningham, P., and Fagan, M. E.: Evaluating Forest Cover and Fragmentation in Costa Rica with a Corrected
4373 Global Tree Cover Map, *Remote Sensing*, 12, 3226, <https://doi.org/10.3390/rs12193226>, 2020.
- 4374 Daeli, W., Carmenta, R., Monroe, M. C., and Adams, A. E.: Where Policy and Culture Collide: Perceptions and Responses of
4375 Swidden Farmers to the Burn Ban in West Kalimantan, Indonesia, *Hum Ecol*, 49, 159–170, [https://doi.org/10.1007/s10745-021-](https://doi.org/10.1007/s10745-021-00227-y)
4376 [00227-y](https://doi.org/10.1007/s10745-021-00227-y), 2021.



- 4377 Deeming, J. E., Burgan, R. E., and Cohen, J. D.: The National Fire-Danger Rating System - 1978, Gen. Tech. Rep. INT-GTR-39.
4378 Ogden, UT: U.S. Department of Agriculture, Forest Service, Intermountain Forest and Range Experiment Station. 63 p., 39, 1977.
- 4379 Di Giuseppe, F.: Accounting for fuel in fire danger forecasts: the fire occurrence probability index (FOPI), *Environ. Res. Lett.*, 18,
4380 064029, <https://doi.org/10.1088/1748-9326/acd2ee>, 2023.
- 4381 Di Giuseppe, F., Vitolo, C., Krzeminski, B., Barnard, C., Maciel, P., and San-Miguel, J.: Fire Weather Index: the skill provided by
4382 the European Centre for Medium-Range Weather Forecasts ensemble prediction system, *Natural Hazards and Earth System
4383 Sciences*, 20, 2365–2378, <https://doi.org/10.5194/nhess-20-2365-2020>, 2020.
- 4384 Di Giuseppe, F., Benedetti, A., Coughlan, R., Vitolo, C., and Vuckovic, M.: A Global Bottom-Up Approach to Estimate Fuel
4385 Consumed by Fires Using Above Ground Biomass Observations, *Geophysical Research Letters*, 48, e2021GL095452,
4386 <https://doi.org/10.1029/2021GL095452>, 2021.
- 4387 Di Giuseppe, F., Vitolo, C., Barnard, C., Libertá, G., Maciel, P., San-Miguel-Ayanz, J., Villaume, S., and Wetterhall, F.: Global
4388 seasonal prediction of fire danger, *Sci Data*, 11, 128, <https://doi.org/10.1038/s41597-024-02948-3>, 2024.
- 4389 DiMiceli, C., Carroll, M., Sohlberg, R., Kim, D.-H., Kelly, M., and Townshend, J.: MOD44B MODIS/Terra Vegetation Continuous
4390 Fields Yearly L3 Global 250m SIN Grid V006, https://doi.org/10.5067/MODIS/MOD44B_006, 2015.
- 4391 DiMiceli, C., Carroll, M., Sohlberg, R., Huang, C., Hansen, M., and Townshend, J.: Annual Global Automated MODIS Vegetation
4392 Continuous Fields (MOD44B) at 250 m Spatial Resolution for Data Years Beginning Day 65, 2000-2010, Collection 5 Percent
4393 Tree Cover, University of Maryland, 2017.
- 4394 DiMiceli, C., Sohlberg, R., and Townshend, J.: MODIS/Terra Vegetation Continuous Fields Yearly L3 Global 250m SIN Grid
4395 V061, https://doi.org/10.5067/MODIS/MOD44B_061, 2022.
- 4396 Direção Nacional de Gestão do Programa de Fogos Rurais: 8.º Relatório Provisório de Incêndios Rurais – 2023 - 1 de Janeiro a
4397 15 de Outubro, available at: <https://www.icnf.pt/api/file/doc/058d65a2c60898dc>, last access: 2 June 2024, 2023.
- 4398 Dong, X., Li, F., Lin, Z., Harrison, S. P., Chen, Y., and Kug, J.-S.: Climate influence on the 2019 fires in Amazonia, *Science of
4399 The Total Environment*, 794, 148718, <https://doi.org/10.1016/j.scitotenv.2021.148718>, 2021.
- 4400 Dowdy, A. J.: Seamless climate change projections and seasonal predictions for bushfires in Australia, *JSHES*, 70, 120–138,
4401 <https://doi.org/10.1071/ES20001>, 2020.
- 4402 Economia Online: Violento incêndio em Odemira agita turismo e economia local, available at:
4403 <https://eco.sapo.pt/2023/08/08/violento-incendio-em-odemira-agita-turismo-e-economia-local/>, last access: 2 June 2024, ECO,
4404 2023.
- 4405 Educación Forestal: Grandes Incendios Forestales en España durante 2023: Incendio de Villanueva de Viver, Iniciado el
4406 23/03/2023, available at: https://edu.forestry.es/p/grandes-incendios-forestales-en-espana_23.html#01, last access: 2 June
4407 2024, 2023.
- 4408 Educación Forestal: Grandes Incendios Forestales en España durante 2023: Incendios en Asturias-Cantabria, Iniciado el
4409 28/03/2023, available at: https://edu.forestry.es/p/grandes-incendios-forestales-en-espana_23.html#03, last access: 2 June
4410 2024, 2024.
- 4411 El Desconcierto: Saldo de incendios forestales: 131 muertos, 7.000 viviendas destruidas y 5.000 damnificados, available at:
4412 [https://www.eldesconcierto.cl/nacional/2024/02/11/saldo-de-incendios-forestales-131-muertos-7-000-viviendas-destruidas-y-5-
4413 000-damnificados.html](https://www.eldesconcierto.cl/nacional/2024/02/11/saldo-de-incendios-forestales-131-muertos-7-000-viviendas-destruidas-y-5-000-damnificados.html), last access: 2 June 2024, El Desconcierto / Periodismo digital independiente, 2024.
- 4414 Erraji, A.: 182 Wildfires Reported Across Morocco in 2023, available at:
4415 <https://www.morocoworldnews.com/2023/07/356405/182-wildfires-reported-nationwide-in-2023>, last access: 2 June 2024,
4416 Morocco World News, 2023.



- 4417 Espinoza, J.-C., Jimenez, J. C., Marengo, J. A., Schongart, J., Ronchail, J., Lavado-Casimiro, W., and Ribeiro, J. V. M.: The new
4418 record of drought and warmth in the Amazon in 2023 related to regional and global climatic features, *Sci Rep*, 14, 8107,
4419 <https://doi.org/10.1038/s41598-024-58782-5>, 2024.
- 4420 Estado do Amazonas: Plano Estadual de Prevenção e Controle do Desmatamento e Queimadas do Estado do Amazonas
4421 PPCDQ-AM 2020-2022, 2020.
- 4422 EU Eurostat: Countries - GISCO - Eurostat, available at: [https://ec.europa.eu/eurostat/web/gisco/geodata/reference-](https://ec.europa.eu/eurostat/web/gisco/geodata/reference-data/administrative-units-statistical-units/countries)
4423 [data/administrative-units-statistical-units/countries](https://ec.europa.eu/eurostat/web/gisco/geodata/reference-data/administrative-units-statistical-units/countries), last access: 2 June 2024, 2020.
- 4424 euronews: Wildfires tear through Algeria and Tunisia as temperatures near 50C, available at:
4425 [https://www.euronews.com/green/2023/07/25/north-africa-heatwave-wildfires-kill-dozens-and-force-over-1500-people-to-](https://www.euronews.com/green/2023/07/25/north-africa-heatwave-wildfires-kill-dozens-and-force-over-1500-people-to-evacuate)
4426 [evacuate](https://www.euronews.com/green/2023/07/25/north-africa-heatwave-wildfires-kill-dozens-and-force-over-1500-people-to-evacuate), last access: 2 June 2024, euronews, 2023.
- 4427 European Centre for Medium-Range Weather Forecasts: CAMS global biomass burning emissions based on fire radiative power
4428 (GFAS): data documentation, available at:
4429 [https://confluence.ecmwf.int/display/CKB/CAMS+global+biomass+burning+emissions+based+on+fire+radiative+power+%28GF](https://confluence.ecmwf.int/display/CKB/CAMS+global+biomass+burning+emissions+based+on+fire+radiative+power+%28GFAS%29%3A+data+documentation)
4430 [AS%29%3A+data+documentation](https://confluence.ecmwf.int/display/CKB/CAMS+global+biomass+burning+emissions+based+on+fire+radiative+power+%28GFAS%29%3A+data+documentation), last access: 2 June 2024, CAMS global biomass burning emissions based on fire radiative
4431 power (GFAS): data documentation, 2024.
- 4432 European Commission EU Science Hub: Wildfires in the Mediterranean: EFFIS data reveal extent this summer, available at:
4433 [https://joint-research-centre.ec.europa.eu/jrc-news-and-updates/wildfires-mediterranean-effis-data-reveal-extent-summer-2023-](https://joint-research-centre.ec.europa.eu/jrc-news-and-updates/wildfires-mediterranean-effis-data-reveal-extent-summer-2023-09-08_en)
4434 [09-08_en](https://joint-research-centre.ec.europa.eu/jrc-news-and-updates/wildfires-mediterranean-effis-data-reveal-extent-summer-2023-09-08_en), last access: 2 June 2024, 2023.
- 4435 European Commission Joint Research Centre: Forest fires in Europe, Middle East and North Africa 2022., Publications Office,
4436 LU, 2023.
- 4437 European Forest Fire Information System: EFFIS - Statistics Portal, available at: [https://forest-](https://forest-fire.emergency.copernicus.eu/apps/effis.statistics/)
4438 [fire.emergency.copernicus.eu/apps/effis.statistics/](https://forest-fire.emergency.copernicus.eu/apps/effis.statistics/), last access: 2 June 2024, Copernicus Forest Fire, 2024.
- 4439 Feng, M., Sexton, J. O., Huang, C., Anand, A., Channan, S., Song, X.-P., Song, D.-X., Kim, D.-H., Noojipady, P., and Townshend,
4440 J. R.: Earth science data records of global forest cover and change: Assessment of accuracy in 1990, 2000, and 2005 epochs,
4441 *Remote Sensing of Environment*, 184, 73–85, <https://doi.org/10.1016/j.rse.2016.06.012>, 2016.
- 4442 Fernandes, P. M. and Botelho, H. S.: A review of prescribed burning effectiveness in fire hazard reduction, *Int. J. Wildland Fire*,
4443 12, 117–128, <https://doi.org/10.1071/wf02042>, 2003.
- 4444 Ferreira Barbosa, M. L., Haddad, I., da Silva Nascimento, A. L., Máximo da Silva, G., Moura da Veiga, R., Hoffmann, T. B.,
4445 Rosane de Souza, A., Dalagnol, R., Susin Streher, A., Souza Pereira, F. R., Oliveira e Cruz de Aragão, L. E., and Oighenstein
4446 Anderson, L.: Compound impact of land use and extreme climate on the 2020 fire record of the Brazilian Pantanal, *Global Ecology*
4447 *and Biogeography*, 31, 1960–1975, <https://doi.org/10.1111/qeb.13563>, 2022.
- 4448 Field, R. D., van der Werf, G. R., Fanin, T., Fetzer, E. J., Fuller, R., Jethva, H., Levy, R., Livesey, N. J., Luo, M., Torres, O., and
4449 Worden, H. M.: Indonesian fire activity and smoke pollution in 2015 show persistent nonlinear sensitivity to El Niño-induced
4450 drought, *Proceedings of the National Academy of Sciences*, 113, 9204–9209, <https://doi.org/10.1073/pnas.1524888113>, 2016.
- 4451 Finney, D. L., Doherty, R. M., Wild, O., Stevenson, D. S., MacKenzie, I. A., and Blyth, A. M.: A projected decrease in lightning
4452 under climate change, *Nature Clim Change*, 8, 210–213, <https://doi.org/10.1038/s41558-018-0072-6>, 2018.
- 4453 Finney, M. A., Cohen, J. D., McAllister, S. S., and Jolly, W. M.: On the need for a theory of wildland fire spread, *Int. J. Wildland*
4454 *Fire*, 22, 25–36, <https://doi.org/10.1071/WF11117>, 2012.
- 4455 Fire Hub - The Global Fire Management Hub: 1st Technical Workshop – Summary Report, available at:
4456 <https://openknowledge.fao.org/server/api/core/bitstreams/491e9112-8106-4b02-97f1-0a27f3e1f6d6/content>, last access: 2 June
4457 2024, FAO Headquarters, 2023.



- 4458 Fire Safety Research Institute, Kerber, S., and Alkonis, D.: Lahaina Fire Comprehensive Timeline Report, available at:
4459 <https://fsri.org/research-update/lahaina-fire-comprehensive-timeline-report-released-attorney-general-hawaii>, last access: 2
4460 June 2024, UL Research Institutes, <https://doi.org/10.54206/102376/VQKQ5427>, 2024.
- 4461 Fisher, R.: Vastly bigger than the Black Summer: 84 million hectares of northern Australia burned in 2023, available at:
4462 [http://theconversation.com/vastly-bigger-than-the-black-summer-84-million-hectares-of-northern-australia-burned-in-2023-](http://theconversation.com/vastly-bigger-than-the-black-summer-84-million-hectares-of-northern-australia-burned-in-2023-227996)
4463 227996, last access: 2 June 2024, The Conversation, 2024.
- 4464 Food and Agriculture Organization of the United Nations: Global Fire Management Hub, available at: [https://www.fao.org/forestry-](https://www.fao.org/forestry-fao/firemanagement/101248/en/)
4465 [fao/firemanagement/101248/en/](https://www.fao.org/forestry-fao/firemanagement/101248/en/), last access: 2 June 2024, Global Fire Management Hub, 2024.
- 4466 Ford, A. E. S., Harrison, S. P., Kountouris, Y., Millington, J. D. A., Mistry, J., Perkins, O., Rabin, S. S., Rein, G., Schreckenberger,
4467 K., Smith, C., Smith, T. E. L., and Yadav, K.: Modelling Human-Fire Interactions: Combining Alternative Perspectives and
4468 Approaches, *Frontiers in Environmental Science*, 9, 418, <https://doi.org/10.3389/fenvs.2021.649835>, 2021.
- 4469 Forster, P. M., Smith, C. J., Walsh, T., Lamb, W. F., Lamboll, R., Hauser, M., Ribes, A., Rosen, D., Gillett, N., Palmer, M. D.,
4470 Rogelj, J., Von Schuckmann, K., Seneviratne, S. I., Trewin, B., Zhang, X., Allen, M., Andrew, R., Birt, A., Borger, A., Boyer, T.,
4471 Broersma, J. A., Cheng, L., Dentener, F., Friedlingstein, P., Gutiérrez, J. M., Gütschow, J., Hall, B., Ishii, M., Jenkins, S., Lan, X.,
4472 Lee, J.-Y., Morice, C., Kadow, C., Kennedy, J., Killick, R., Minx, J. C., Naik, V., Peters, G. P., Pirani, A., Pongratz, J., Schleussner,
4473 C.-F., Szopa, S., Thorne, P., Rohde, R., Rojas Corradi, M., Schumacher, D., Vose, R., Zickfeld, K., Masson-Delmotte, V., and
4474 Zhai, P.: Indicators of Global Climate Change 2022: annual update of large-scale indicators of the state of the climate system
4475 and human influence, *Earth Syst. Sci. Data*, 15, 2295–2327, <https://doi.org/10.5194/essd-15-2295-2023>, 2023.
- 4476 France-Presse, A.: Colombia Declares Emergency Over Forest Fires, available at: [https://www.voanews.com/a/colombia-](https://www.voanews.com/a/colombia-declares-emergency-over-forest-fires/7456551.html)
4477 [declares-emergency-over-forest-fires/7456551.html](https://www.voanews.com/a/colombia-declares-emergency-over-forest-fires/7456551.html), last access: 2 June 2024, Voice of America, 2024.
- 4478 Frazier, A. E. and Hemingway, B. L.: A Technical Review of Planet Smallsat Data: Practical Considerations for Processing and
4479 Using PlanetScope Imagery, *Remote Sensing*, 13, 3930, <https://doi.org/10.3390/rs13193930>, 2021.
- 4480 Friedlingstein, P., O'Sullivan, M., Jones, M. W., Andrew, R. M., Bakker, D. C. E., Hauck, J., Landschützer, P., Le Quééré, C.,
4481 Lujikx, I. T., Peters, G. P., Peters, W., Pongratz, J., Schwingshackl, C., Sitch, S., Canadell, J. G., Ciais, P., Jackson, R. B., Alin,
4482 S. R., Anthoni, P., Barbero, L., Bates, N. R., Becker, M., Bellouin, N., Decharme, B., Bopp, L., Brasika, I. B. M., Cadule, P.,
4483 Chamberlain, M. A., Chandra, N., Chau, T.-T., Chevallier, F., Chini, L. P., Cronin, M., Dou, X., Enyo, K., Evans, W., Falk, S.,
4484 Feely, R. A., Feng, L., Ford, D. J., Gasser, T., Ghattas, J., Gkritzalis, T., Grassi, G., Gregor, L., Gruber, N., Gürses, Ö., Harris, I.,
4485 Hefner, M., Heinke, J., Houghton, R. A., Hurtt, G. C., Iida, Y., Ilyina, T., Jacobson, A. R., Jain, A., Jarníková, T., Jersild, A., Jiang,
4486 F., Jin, Z., Joos, F., Kato, E., Keeling, R. F., Kennedy, D., Klein Goldewijk, K., Knauer, J., Korsbakken, J. I., Körtzinger, A., Lan,
4487 X., Lefèvre, N., Li, H., Liu, J., Liu, Z., Ma, L., Marland, G., Mayot, N., McGuire, P. C., McKinley, G. A., Meyer, G., Morgan, E. J.,
4488 Munro, D. R., Nakaoka, S.-I., Niwa, Y., O'Brien, K. M., Olsen, A., Omar, A. M., Ono, T., Paulsen, M., Pierrot, D., Pocock, K.,
4489 Poulter, B., Powis, C. M., Rehder, G., Resplandy, L., Robertson, E., Rödenbeck, C., Rosan, T. M., Schwinger, J., Séférian, R.,
4490 et al.: Global Carbon Budget 2023, *Earth System Science Data*, 15, 5301–5369, <https://doi.org/10.5194/essd-15-5301-2023>,
4491 2023.
- 4492 Frieler, K., Volkholz, J., Lange, S., Schewe, J., Mengel, M., del Rocio Rivas López, M., Otto, C., Reyer, C. P. O., Karger, D. N.,
4493 Malle, J. T., Treu, S., Menz, C., Blanchard, J. L., Harrison, C. S., Petrik, C. M., Eddy, T. D., Ortega-Cisneros, K., Novaglio, C.,
4494 Rousseau, Y., Watson, R. A., Stock, C., Liu, X., Heneghan, R., Tittensor, D., Maury, O., Büchner, M., Vogt, T., Wang, T., Sun,
4495 F., Sauer, I. J., Koch, J., Vanderkelen, I., Jägermeyr, J., Müller, C., Rabin, S., Klar, J., Vega del Valle, I. D., Lasslop, G., Chadburn,
4496 S., Burke, E., Gallego-Sala, A., Smith, N., Chang, J., Hantson, S., Burton, C., Gädeke, A., Li, F., Gosling, S. N., Müller Schmied,
4497 H., Hattermann, F., Wang, J., Yao, F., Hickler, T., Marcé, R., Pierson, D., Thiery, W., Mercado-Bettín, D., Ladwig, R., Ayala-
4498 Zamora, A. I., Forrest, M., and Bechtold, M.: Scenario setup and forcing data for impact model evaluation and impact attribution
4499 within the third round of the Inter-Sectoral Impact Model Intercomparison Project (ISIMIP3a), *Geoscientific Model Development*,
4500 17, 1–51, <https://doi.org/10.5194/gmd-17-1-2024>, 2024.
- 4501 Fuller, D. O. and Murphy, K.: The ENSO-Fire Dynamic in Insular Southeast Asia, *Climatic Change*, 74, 435–455,
4502 <https://doi.org/10.1007/s10584-006-0432-5>, 2006.
- 4503 Garnett, S. T., Burgess, N. D., Fa, J. E., Fernández-Llamazares, Á., Molnár, Z., Robinson, C. J., Watson, J. E. M., Zander, K. K.,
4504 Austin, B., Brondizio, E. S., Collier, N. F., Duncan, T., Ellis, E., Geyle, H., Jackson, M. V., Jonas, H., Malmer, P., McGowan, B.,



- 4505 Sivongxay, A., and Leiper, I.: A spatial overview of the global importance of Indigenous lands for conservation, *Nat Sustain*, 1,
4506 369–374, <https://doi.org/10.1038/s41893-018-0100-6>, 2018.
- 4507 Gauldie, R.: Coming to the rescEU: European firefighting, available at: <https://www.airmedandrescue.com/latest/long-read/coming-resceu-european-firefighting>, last access: 2 June 2024, *AirMed&Rescue*, 2024.
- 4509 Gelman, A., Carlin, J. B., Stern, H. S., Dunson, D. B., Vehtari, A., and Rubin, D. B.: *Bayesian Data Analysis*, 0 ed., Chapman and
4510 Hall/CRC, <https://doi.org/10.1201/b16018>, 2013.
- 4511 Giglio, L. and Roy, D. P.: Assessment of satellite orbit-drift artifacts in the long-term AVHRR FireCCILT11 global burned area
4512 data set, *Science of Remote Sensing*, 5, 100044, <https://doi.org/10.1016/j.srs.2022.100044>, 2022.
- 4513 Giglio, L., Randerson, J. T., and van der Werf, G. R.: Analysis of daily, monthly, and annual burned area using the fourth-
4514 generation global fire emissions database (GFED4), *Journal of Geophysical Research: Biogeosciences*, 118, 317–328,
4515 <https://doi.org/10.1002/jgrg.20042>, 2013.
- 4516 Giglio, L., Schroeder, W., and Justice, C. O.: The collection 6 MODIS active fire detection algorithm and fire products, *Remote
4517 Sensing of Environment*, 178, 31–41, <https://doi.org/10.1016/j.rse.2016.02.054>, 2016.
- 4518 Giglio, L., Boschetti, L., Roy, D. P., Humber, M. L., and Justice, C. O.: The Collection 6 MODIS burned area mapping algorithm
4519 and product, *Remote Sensing of Environment*, 217, 72–85, <https://doi.org/10.1016/j.rse.2018.08.005>, 2018.
- 4520 Giglio, L., Justice, C., Boschetti, L., and Roy, D.: MODIS/Terra+Aqua Burned Area Monthly L3 Global 500m SIN Grid V061,
4521 <https://doi.org/10.5067/MODIS/MCD64A1.061>, 2021.
- 4522 Grau-Andrés, R., Moreira, B., and Pausas, J. G.: Global plant responses to intensified fire regimes, *Global Ecology and
4523 Biogeography*, n/a, e13858, <https://doi.org/10.1111/geb.13858>, 2024.
- 4524 Haas, O., Prentice, I. C., and Harrison, S. P.: Global environmental controls on wildfire burnt area, size, and intensity, *Environ.
4525 Res. Lett.*, 17, 065004, <https://doi.org/10.1088/1748-9326/ac6a69>, 2022.
- 4526 Hamilton, D. S., Perron, M. M. G., Bond, T. C., Bowie, A. R., Buchholz, R. R., Guieu, C., Ito, A., Maenhaut, W., Myriokefalitakis,
4527 S., Olgun, N., Rathod, S. D., Schepanski, K., Tagliabue, A., Wagner, R., and Mahowald, N. M.: Earth, Wind, Fire, and Pollution:
4528 Aerosol Nutrient Sources and Impacts on Ocean Biogeochemistry, *Annual Review of Marine Science*, 14, 303–330,
4529 <https://doi.org/10.1146/annurev-marine-031921-013612>, 2022.
- 4530 Hantson, S., Padilla, M., Corti, D., and Chuvieco, E.: Strengths and weaknesses of MODIS hotspots to characterize global fire
4531 occurrence, *Remote Sensing of Environment*, 131, 152–159, <https://doi.org/10.1016/j.rse.2012.12.004>, 2013.
- 4532 Hantson, S., Arneth, A., Harrison, S. P., Kelley, D. I., Prentice, I. C., Rabin, S. S., Archibald, S., Mouillot, F., Arnold, S. R., Artaxo,
4533 P., Bachelet, D., Ciais, P., Forrest, M., Friedlingstein, P., Hickler, T., Kaplan, J. O., Kloster, S., Knorr, W., Lasslop, G., Li, F.,
4534 Mangeon, S., Melton, J. R., Meyn, A., Sitch, S., Spessa, A., van der Werf, G. R., Voulgarakis, A., and Yue, C.: The status and
4535 challenge of global fire modelling, *Biogeosciences*, 13, 3359–3375, <https://doi.org/10.5194/bg-13-3359-2016>, 2016.
- 4536 Hantson, S., Kelley, D. I., Arneth, A., Harrison, S. P., Archibald, S., Bachelet, D., Forrest, M., Hickler, T., Lasslop, G., Li, F.,
4537 Mangeon, S., Melton, J. R., Nieradzik, L., Rabin, S. S., Prentice, I. C., Sheehan, T., Sitch, S., Teckentrup, L., Voulgarakis, A.,
4538 and Yue, C.: Quantitative assessment of fire and vegetation properties in simulations with fire-enabled vegetation models from
4539 the Fire Model Intercomparison Project, *Geoscientific Model Development*, 13, 3299–3318, <https://doi.org/10.5194/gmd-13-3299-2020>,
4540 2020.
- 4541 Hantson, S., Andela, N., Goulden, M. L., and Randerson, J. T.: Human-ignited fires result in more extreme fire behavior and
4542 ecosystem impacts, *Nat Commun*, 13, 2717, <https://doi.org/10.1038/s41467-022-30030-2>, 2022.
- 4543 Harris, S. and Lucas, C.: Understanding the variability of Australian fire weather between 1973 and 2017, *PLOS ONE*, 14,
4544 e0222328, <https://doi.org/10.1371/journal.pone.0222328>, 2019.



- 4545 Haynes, K., Short, K., Xanthopoulos, G., Viegas, D., Ribeiro, L. M., and Bianchi, R.: Wildfires and WUI Fire Fatalities, in:
4546 Encyclopedia of Wildfires and Wildland-Urban Interface (WUI) Fires, edited by: Manzello, S. L., Springer International Publishing,
4547 Cham, 1–16, https://doi.org/10.1007/978-3-319-51727-8_92-1, 2019.
- 4548 Hazra, D. and Gallagher, P.: Role of insurance in wildfire risk mitigation, *Economic Modelling*, 108, 105768,
4549 <https://doi.org/10.1016/j.econmod.2022.105768>, 2022.
- 4550 Hegerl, G. C., Hoegh-Guldberg, O., Casassa, G., Hoerling, M., Kovats, S., Parmesan, C., Pierce, D., and Stott, P.: IPCC WGI
4551 Expert Meeting on Detection and Attribution Related to Anthropogenic Climate Change: Good Practice Guidance Paper on
4552 Detection and Attribution Related to Anthropogenic Climate Change, available at: [https://archive.ipcc.ch/pdf/supporting-](https://archive.ipcc.ch/pdf/supporting-material/ipcc_good_practice_guidance_paper_anthropogenic.pdf)
4553 [material/ipcc_good_practice_guidance_paper_anthropogenic.pdf](https://archive.ipcc.ch/pdf/supporting-material/ipcc_good_practice_guidance_paper_anthropogenic.pdf), last access: 2 June 2024, edited by: Stocker, T., Field, C.,
4554 Dahe, Q., Barros, V., Plattner, G.-K., Tignor, M., Midgley, P., and Ebi, K., Geneva, 2009.
- 4555 Held, I. M., Guo, H., Adcroft, A., Dunne, J. P., Horowitz, L. W., Krasting, J., Shevliakova, E., Winton, M., Zhao, M., Bushuk, M.,
4556 Wittenberg, A. T., Wyman, B., Xiang, B., Zhang, R., Anderson, W., Balaji, V., Donner, L., Dunne, K., Durachta, J., Gauthier, P.
4557 P. G., Ginoux, P., Golaz, J.-C., Griffies, S. M., Hallberg, R., Harris, L., Harrison, M., Hurlin, W., John, J., Lin, P., Lin, S.-J.,
4558 Malyshev, S., Menzel, R., Milly, P. C. D., Ming, Y., Naik, V., Paynter, D., Paulot, F., Ramaswamy, V., Reichl, B., Robinson, T.,
4559 Rosati, A., Seman, C., Silvers, L. G., Underwood, S., and Zadeh, N.: Structure and Performance of GFDL's CM4.0 Climate Model,
4560 *Journal of Advances in Modeling Earth Systems*, 11, 3691–3727, <https://doi.org/10.1029/2019MS001829>, 2019.
- 4561 Higuera, P. E. and Abatzoglou, J. T.: Record-setting climate enabled the extraordinary 2020 fire season in the western United
4562 States, *Glob. Change Biol.*, 27, 1–2, <https://doi.org/10.1111/gcb.15388>, 2021.
- 4563 Higuera, P. E., Cook, M. C., Balch, J. K., Stavros, E. N., Mahood, A. L., and St. Denis, L. A.: Shifting social-ecological fire regimes
4564 explain increasing structure loss from Western wildfires, *PNAS Nexus*, 2, pgad005, <https://doi.org/10.1093/pnasnexus/pgad005>,
4565 2023.
- 4566 Hollis, J. J., Matthews, S., Fox-Hughes, P., Grootemaat, S., Heemstra, S., Kenny, B. J., and Sauvage, S.: Introduction to the
4567 Australian Fire Danger Rating System†, *Int. J. Wildland Fire*, 33, NULL-NULL, <https://doi.org/10.1071/WF23140>, 2024.
- 4568 Hough, A.: The battle for Scarborough, available at: [https://www.iol.co.za/capetimes/news/the-battle-for-scarborough-f9d4ce5c-](https://www.iol.co.za/capetimes/news/the-battle-for-scarborough-f9d4ce5c-223e-4fd9-97e3-ce23c58b12b9)
4569 [223e-4fd9-97e3-ce23c58b12b9](https://www.iol.co.za/capetimes/news/the-battle-for-scarborough-f9d4ce5c-223e-4fd9-97e3-ce23c58b12b9), last access: 2 June 2024, IOL News, 2023.
- 4570 iMMAP Inc.: La Niña phenomenon in Colombia – Dashboard - iMMAP Inc., available at: [https://immap.org/product/la-nina-](https://immap.org/product/la-nina-phenomenon-in-colombia-dashboard/)
4571 [phenomenon-in-colombia-dashboard/](https://immap.org/product/la-nina-phenomenon-in-colombia-dashboard/), last access: 2 June 2024, 2023.
- 4572 Inness, A., Ades, M., Agustí-Panareda, A., Barré, J., Benedictow, A., Blechschmidt, A.-M., Dominguez, J. J., Engelen, R., Eskes,
4573 H., Flemming, J., Huijnen, V., Jones, L., Kipling, Z., Massart, S., Parrington, M., Peuch, V.-H., Razinger, M., Remy, S., Schulz,
4574 M., and Suttie, M.: The CAMS reanalysis of atmospheric composition, *Atmospheric Chemistry and Physics*, 19, 3515–3556,
4575 <https://doi.org/10.5194/acp-19-3515-2019>, 2019.
- 4576 Instituto Chico Mendes de Conservação da Biodiversidade: Plano de Manejo Floresta Nacional do Tapajós, available at:
4577 [https://www.gov.br/icmbio/pt-br/assuntos/biodiversidade/unidade-de-conservacao/unidades-de-biomas/amazonia/lista-de-](https://www.gov.br/icmbio/pt-br/assuntos/biodiversidade/unidade-de-conservacao/unidades-de-biomas/amazonia/lista-de-ucs/flona-do-tapajos/arquivos/plano_de_manejo_flona_do_tapajos_2019_vol2.pdf)
4578 [ucs/flona-do-tapajos/arquivos/plano_de_manejo_flona_do_tapajos_2019_vol2.pdf](https://www.gov.br/icmbio/pt-br/assuntos/biodiversidade/unidade-de-conservacao/unidades-de-biomas/amazonia/lista-de-ucs/flona-do-tapajos/arquivos/plano_de_manejo_flona_do_tapajos_2019_vol2.pdf), last access: 2 June 2024, 2019.
- 4579 Instituto da Conservação da Natureza e das Florestas: IR de Carrascal (Sarzedas) Castelo Branco - Proença-a-Nova Relatório
4580 de Estabilização de Emergência Pós-Incêndio, available at: <https://www.icnf.pt/api/file/doc/058d65a2c60898dc>, last access: 2
4581 June 2024, 2023.
- 4582 Intergovernmental Panel on Climate Change (IPCC): IPCC WGI Sixth Assessment Report Interactive Atlas, available at:
4583 <https://interactive-atlas.ipcc.ch/atlas>, last access: 2 June 2024, 2021.
- 4584 Intergovernmental Panel on Climate Change (IPCC) (Ed.): 2023a Changing State of the Climate System, in: *Climate Change*
4585 *2021 – The Physical Science Basis: Working Group I Contribution to the Sixth Assessment Report of the Intergovernmental Panel*
4586 *on Climate Change*, Cambridge University Press, Cambridge, 287–422, <https://doi.org/10.1017/9781009157896.004>, 2023a.
- 4587 Intergovernmental Panel on Climate Change (IPCC) (Ed.): 2023b Key Risks across Sectors and Regions, in: *Climate Change*
4588 *2022 – Impacts, Adaptation and Vulnerability: Working Group II Contribution to the Sixth Assessment Report of the*



- 4589 Intergovernmental Panel on Climate Change, Cambridge University Press, Cambridge, 2411–2538,
4590 <https://doi.org/10.1017/9781009325844.025>, 2023b.
- 4591 Intergovernmental Panel on Climate Change (IPCC) (Ed.): 2023c Point of Departure and Key Concepts, in: Climate Change 2022
4592 – Impacts, Adaptation and Vulnerability: Working Group II Contribution to the Sixth Assessment Report of the Intergovernmental
4593 Panel on Climate Change, Cambridge University Press, Cambridge, 121–196, <https://doi.org/10.1017/9781009325844.003>,
4594 2023c.
- 4595 International Federation of Red Cross and Red Crescent Societies: Mongolia: IFRC network mid-year report, January - June
4596 2023 (14 December 2023) - Mongolia, available at: [https://reliefweb.int/report/mongolia/mongolia-ifrc-network-mid-year-report-](https://reliefweb.int/report/mongolia/mongolia-ifrc-network-mid-year-report-january-june-2023-14-december-2023)
4597 [january-june-2023-14-december-2023](https://reliefweb.int/report/mongolia/mongolia-ifrc-network-mid-year-report-january-june-2023-14-december-2023), last access: 2 June 2024, 2023.
- 4598 Istituto Superiore per la Protezione e la Ricerca Ambientale (ISPRA): Gli incendi boschivi in Italia: stagione degli incendi 2023,
4599 Roma, 2023.
- 4600 Jain, P., Barber, Q. E., Taylor, S., Whitman, E., Castellanos Acuna, D., Boulanger, Y., Chavardès, R. D., Chen, J., Englefield, P.,
4601 Flannigan, M., Girardin, M. P., Hanes, C. C., Little, J., Morrison, K., Skakun, R. S., Thompson, D. K., Wang, X., and Parisien, M.-
4602 A.: Canada Under Fire – Drivers and Impacts of the Record-Breaking 2023 Wildfire Season,
4603 <https://doi.org/10.22541/essoar.170914412.27504349/v1>.
- 4604 Johnson, S. J., Stockdale, T. N., Ferranti, L., Balmaseda, M. A., Molteni, F., Magnusson, L., Tietsche, S., Decremmer, D.,
4605 Weisheimer, A., Balsamo, G., Keeley, S. P. E., Mogensen, K., Zuo, H., and Monge-Sanz, B. M.: SEAS5: the new ECMWF
4606 seasonal forecast system, *Geoscientific Model Development*, 12, 1087–1117, <https://doi.org/10.5194/gmd-12-1087-2019>, 2019.
- 4607 Johnston, F. H., Henderson, S. B., Chen, Y., Randerson, J. T., Marlier, M., DeFries, R. S., Kinney, P., Bowman, D. M. J. S., and
4608 Brauer, M.: Estimated Global Mortality Attributable to Smoke from Landscape Fires, *Environmental Health Perspectives*, 120,
4609 695–701, <https://doi.org/10.1289/ehp.1104422>, 2012.
- 4610 Johnston, F. H., Borchers-Arriagada, N., Morgan, G. G., Jalaludin, B., Palmer, A. J., Williamson, G. J., and Bowman, D. M. J. S.:
4611 Unprecedented health costs of smoke-related PM2.5 from the 2019–20 Australian megafires, *Nat Sustain*, 4, 42–47,
4612 <https://doi.org/10.1038/s41893-020-00610-5>, 2021.
- 4613 Jones, M. W., Abatzoglou, J. T., Veraverbeke, S., Andela, N., Lasslop, G., Forkel, M., Smith, A. J. P., Burton, C., Betts, R. A.,
4614 van der Werf, G. R., Sitch, S., Canadell, J. G., Santin, C., Kolden, C., Doerr, S. H., and Le Quéré, C.: Global and Regional Trends
4615 and Drivers of Fire Under Climate Change, *Reviews of Geophysics*, 60, e2020RG000726,
4616 <https://doi.org/10.1029/2020RG000726>, 2022.
- 4617 Jones, M. W., Brambleby, E., Andela, N., van der Werf, G. R., Parrington, M., and Giglio, L.: State of Wildfires 2023-24: Anomalies
4618 in Burned Area, Fire Emissions, and Individual Fire Characteristics by Continent, Biome, Country, and Administrative Region,
4619 <https://doi.org/10.5281/zenodo.11400540>, 2024.
- 4620 Joshi, M.: El Niño could push global warming past 1.5°C – but what is it and how does it affect the weather in Europe?, available
4621 at: [http://theconversation.com/el-nino-could-push-global-warming-past-1-5-but-what-is-it-and-how-does-it-affect-the-weather-in-](http://theconversation.com/el-nino-could-push-global-warming-past-1-5-but-what-is-it-and-how-does-it-affect-the-weather-in-europe-208412)
4622 [europe-208412](http://theconversation.com/el-nino-could-push-global-warming-past-1-5-but-what-is-it-and-how-does-it-affect-the-weather-in-europe-208412), last access: 2 June 2024, *The Conversation*, 2023.
- 4623 Juntaex.es: El incendio de Pinofranqueado y Gata ha afectado a 10.863 hectáreas según las primeras estimaciones, available
4624 at: <https://www.juntaex.es/w/superficie-incendio-hurdes-gata>, last access: 2 June 2024, *Juntaex.es*, 2023.
- 4625 Kaiser, J. W., Heil, A., Andreae, M. O., Benedetti, A., Chubarova, N., Jones, L., Morcrette, J.-J., Razinger, M., Schultz, M. G.,
4626 Suttie, M., and van der Werf, G. R.: Biomass burning emissions estimated with a global fire assimilation system based on
4627 observed fire radiative power, *Biogeosciences*, 9, 527–554, <https://doi.org/10.5194/bg-9-527-2012>, 2012.
- 4628 Keeley, J. E.: Fire intensity, fire severity and burn severity: a brief review and suggested usage, *Int. J. Wildland Fire*, 18, 116–
4629 126, <https://doi.org/10.1071/WF07049>, 2009.
- 4630 Kelley, D., Gerard, F., Dong, N., Burton, C., Argles, A., Li, G., Whitley, R., Marthews, T., Roberston, E., Weedon, G., Lasslop, G.,
4631 Ellis, R., Bistinas, I., and Veendendaal, E.: Observational constraints of fire, environmental and anthropogenic on pantropical tree
4632 cover, <https://doi.org/10.21203/rs.3.rs-3413013/v1>, 16 October 2023.



- 4633 Kelley, D. I., Harrison, S. P., and Prentice, I. C.: Improved simulation of fire–vegetation interactions in the Land surface Processes
4634 and eXchanges dynamic global vegetation model (LPX-Mv1), *Geoscientific Model Development*, 7, 2411–2433,
4635 <https://doi.org/10.5194/gmd-7-2411-2014>, 2014.
- 4636 Kelley, D. I., Bistinas, I., Whitley, R., Burton, C., Marthews, T. R., and Dong, N.: How contemporary bioclimatic and human
4637 controls change global fire regimes, *Nat. Clim. Chang.*, 9, 690–696, <https://doi.org/10.1038/s41558-019-0540-7>, 2019.
- 4638 Kelley, D. I., Burton, C., Huntingford, C., Brown, M. A. J., Whitley, R., and Dong, N.: Technical note: Low meteorological influence
4639 found in 2019 Amazonia fires, *Biogeosciences*, 18, 787–804, <https://doi.org/10.5194/bg-18-787-2021>, 2021.
- 4640 Kelley, D. I., Ferreira Barbosa, M. L., Burke, E., Burton, C. A., Bradley, A., Jones, M. W., Spuler, F., Wessel, J., McNorton, J., and
4641 Di Giuseppe, F.: State of Wildfires 2023-24: ConFire data, <https://doi.org/10.5281/zenodo.11420743>, 2024.
- 4642 Klein Goldewijk, K., Beusen, A., Van Drecht, G., and De Vos, M.: The HYDE 3.1 spatially explicit database of human-induced
4643 global land-use change over the past 12,000 years: HYDE 3.1 Holocene land use, *Global Ecology and Biogeography*, 20, 73–
4644 86, <https://doi.org/10.1111/j.1466-8238.2010.00587.x>, 2011.
- 4645 Kolden, C.: Wildfires: count lives and homes, not hectares burnt, *Nature*, 586, 9–9, <https://doi.org/10.1038/d41586-020-02740-4>,
4646 2020.
- 4647 Kolden, C. A. and Henson, C.: A Socio-Ecological Approach to Mitigating Wildfire Vulnerability in the Wildland Urban Interface:
4648 A Case Study from the 2017 Thomas Fire, *Fire*, 2, 9, <https://doi.org/10.3390/fire2010009>, 2019.
- 4649 Kolden, C. A., Abatzoglou, J. T., Jones, M. W., and Jain, P.: Wildfires in 2023, *Nat Rev Earth Environ*, 5, 238–240,
4650 <https://doi.org/10.1038/s43017-024-00544-y>, 2024.
- 4651 Kramer, S. J., Bisson, K. M., and Fischer, A. D.: Observations of Phytoplankton Community Composition in the Santa Barbara
4652 Channel During the Thomas Fire, *Journal of Geophysical Research: Oceans*, 125, e2020JC016851,
4653 <https://doi.org/10.1029/2020JC016851>, 2020.
- 4654 Ladd, T. M., Cattlett, D., Maniscalco, M. A., Kim, S. M., Kelly, R. L., John, S. G., Carlson, C. A., and Iglesias-Rodríguez, M. D.:
4655 Food for all? Wildfire ash fuels growth of diverse eukaryotic plankton, *Proceedings of the Royal Society B: Biological Sciences*,
4656 290, 20231817, <https://doi.org/10.1098/rspb.2023.1817>, 2023.
- 4657 Lafferty, D. C. and Sriver, R. L.: Downscaling and bias-correction contribute considerable uncertainty to local climate projections
4658 in CMIP6, *npj Clim Atmos Sci*, 6, 1–13, <https://doi.org/10.1038/s41612-023-00486-0>, 2023.
- 4659 Lange, S.: Trend-preserving bias adjustment and statistical downscaling with ISIMIP3BASD (v1.0), *Geoscientific Model
4660 Development*, 12, 3055–3070, <https://doi.org/10.5194/gmd-12-3055-2019>, 2019.
- 4661 Lapola, D. M., Pinho, P., Barlow, J., Aragão, L. E. O. C., Berenguer, E., Carmenta, R., Liddy, H. M., Seixas, H., Silva, C. V. J.,
4662 Silva-Junior, C. H. L., Alencar, A. A. C., Anderson, L. O., Armenteras, D., Brovkin, V., Calders, K., Chambers, J., Chini, L., Costa,
4663 M. H., Faria, B. L., Fearnside, P. M., Ferreira, J., Gatti, L., Gutierrez-Velez, V. H., Han, Z., Hibbard, K., Koven, C., Lawrence, P.,
4664 Pongratz, J., Portela, B. T. T., Rounsevell, M., Ruane, A. C., Schaldach, R., da Silva, S. S., von Randow, C., and Walker, W. S.:
4665 The drivers and impacts of Amazon forest degradation, *Science*, 379, eabp8622, <https://doi.org/10.1126/science.abp8622>, 2023.
- 4666 Lareau, N. P., Nauslar, N. J., and Abatzoglou, J. T.: The Carr Fire Vortex: A Case of Pyrotornadogenesis?, *Geophysical Research
4667 Letters*, 45, <https://doi.org/10.1029/2018GL080667>, 2018.
- 4668 Las Provincias: Las terribles cifras del incendio de Villanueva de Viver, available at:
4669 <https://www.lasprovincias.es/sucesos/terribles-cifras-incendio-villanueva-viver-20230602133033-nt.html>, last access: 2 June
4670 2024, Las Provincias, 2023.
- 4671 Laurent, P., Mouillot, F., Yue, C., Ciais, P., Moreno, M. V., and Nogueira, J. M. P.: FRY, a global database of fire patch functional
4672 traits derived from space-borne burned area products, *Sci Data*, 5, 180132, <https://doi.org/10.1038/sdata.2018.132>, 2018.



- 4673 Le Monde: Russia: Forest fires break out in Siberia amid heatwave, available at:
4674 https://www.lemonde.fr/en/russia/article/2023/05/08/russia-forest-fires-break-out-in-siberia-amid-heatwave_6025902_140.html,
4675 last access: 2 June 2024, Le Monde.fr, 8th May, 2023.
- 4676 van Leeuwen, S. and Miller-Sabbioni, C.: Australia's Megafires: Biodiversity Impacts and Lessons from 2019-2020, in: Australia's
4677 Megafires: Biodiversity Impacts and Lessons from 2019-20, Rumpff, L.; Legge, S. M.; van Leeuwen, S.; Wintle, B. A.; Woinarski,
4678 J. C. Z., 2023.
- 4679 Lemos, M. C., Kirchoff, C. J., and Ramprasad, V.: Narrowing the climate information usability gap, *Nature Clim Change*, 2, 789–
4680 794, <https://doi.org/10.1038/nclimate1614>, 2012.
- 4681 Li, S., Sparrow, S. N., Otto, F. E. L., Rifai, S. W., Oliveras, I., Krikken, F., Anderson, L. O., Malhi, Y., and Wallom, D.:
4682 Anthropogenic climate change contribution to wildfire-prone weather conditions in the Cerrado and Arc of deforestation, *Environ.*
4683 *Res. Lett.*, 16, 094051, <https://doi.org/10.1088/1748-9326/ac1e3a>, 2021a.
- 4684 Li, Y., Sulla-Menashe, D., Motesharrei, S., Song, X.-P., Kalnay, E., Ying, Q., Li, S., and Ma, Z.: Inconsistent estimates of forest
4685 cover change in China between 2000 and 2013 from multiple datasets: differences in parameters, spatial resolution, and
4686 definitions, *Sci Rep*, 7, 8748, <https://doi.org/10.1038/s41598-017-07732-5>, 2017.
- 4687 Li, Y., Yuan, S., Fan, S., Song, Y., Wang, Z., Yu, Z., Yu, Q., and Liu, Y.: Satellite Remote Sensing for Estimating PM2.5 and Its
4688 Components, *Curr Pollution Rep*, 7, 72–87, <https://doi.org/10.1007/s40726-020-00170-4>, 2021b.
- 4689 Liang, Y., Sengupta, D., Campmier, M. J., Lunderberg, D. M., Apte, J. S., and Goldstein, A. H.: Wildfire smoke impacts on indoor
4690 air quality assessed using crowdsourced data in California, *Proc. Natl. Acad. Sci. U.S.A.*, 118, e2106478118,
4691 <https://doi.org/10.1073/pnas.2106478118>, 2021.
- 4692 Linley, G. D., Jolly, C. J., Doherty, T. S., Geary, W. L., Armenteras, D., Belcher, C. M., Bliege Bird, R., Duane, A., Fletcher, M.-
4693 S., Giorgis, M. A., Haslem, A., Jones, G. M., Kelly, L. T., Lee, C. K. F., Nolan, R. H., Parr, C. L., Pausas, J. G., Price, J. N., Regos,
4694 A., Ritchie, E. G., Ruffault, J., Williamson, G. J., Wu, Q., and Nimmo, D. G.: What do you mean, 'megafire'?, *Global Ecology and*
4695 *Biogeography*, 31, 1906–1922, <https://doi.org/10.1111/geb.13499>, 2022.
- 4696 Lizundia-Loiola, J., Otón, G., Ramo, R., and Chuvieco, E.: A spatio-temporal active-fire clustering approach for global burned
4697 area mapping at 250 m from MODIS data, *Remote Sensing of Environment*, 236, 111493,
4698 <https://doi.org/10.1016/j.rse.2019.111493>, 2020.
- 4699 Lizundia-Loiola, J., Franquesa, M., Khairoun, A., and Chuvieco, E.: Global burned area mapping from Sentinel-3 Synergy and
4700 VIIRS active fires, *Remote Sensing of Environment*, 282, 113298, <https://doi.org/10.1016/j.rse.2022.113298>, 2022.
- 4701 Lundberg, S. M. and Lee, S.-I.: A unified approach to interpreting model predictions, in: *Proceedings of the 31st International*
4702 *Conference on Neural Information Processing Systems*, Red Hook, NY, USA, 4768–4777, 2017.
- 4703 Luque, M. A. M., Leon, E., Ardila, J. G. B., Gutiérrez, G., Bilbao, B., Rivera-Lombardi, R., and Milán, A.: Community Forest
4704 Brigades and their implementation as part of a new vision in the integrated fire management in the Bolivarian Republic of
4705 Venezuela, *Biodiversidade Brasileira*, 10, 49–49, <https://doi.org/10.37002/biodiversidadebrasileira.v10i1.1624>, 2020.
- 4706 Majasalmi, T. and Rautiainen, M.: Representation of tree cover in global land cover products: Finland as a case study area,
4707 *Environ Monit Assess*, 193, 121, <https://doi.org/10.1007/s10661-021-08898-2>, 2021.
- 4708 MapBiomass Brasil: Plataforma - Monitor do Fogo, available at: <https://plataforma.brasil.mapbiomas.org/monitor-do-fogo>, last
4709 access: 2 June 2024, 2024.
- 4710 Maraun, D., Shepherd, T. G., Widmann, M., Zappa, G., Walton, D., Gutiérrez, J. M., Hagemann, S., Richter, I., Soares, P. M. M.,
4711 Hall, A., and Mearns, L. O.: Towards process-informed bias correction of climate change simulations, *Nature Clim Change*, 7,
4712 764–773, <https://doi.org/10.1038/nclimate3418>, 2017.
- 4713 Mariani, M., Fletcher, M.-S., Holz, A., and Nyman, P.: ENSO controls interannual fire activity in southeast Australia, *Geophysical*
4714 *Research Letters*, 43, 10,891–10,900, <https://doi.org/10.1002/2016GL070572>, 2016.



- 4715 Mataveli, G., Jones, M. W., Carmenta, R., Sanchez, A., Dutra, D. J., Chaves, M., de Oliveira, G., Anderson, L. O., and Aragão,
4716 L. E. O. C.: Deforestation falls but rise of wildfires continues degrading Brazilian Amazon forests, *Global Change Biology*, 30,
4717 e17202, <https://doi.org/10.1111/gcb.17202>, 2024.
- 4718 Mathison, C., Burke, E., Hartley, A. J., Kelley, D. I., Burton, C., Robertson, E., Gedney, N., Williams, K., Wiltshire, A., Ellis, R. J.,
4719 Sellar, A. A., and Jones, C. D.: Description and evaluation of the JULES-ES set-up for ISIMIP2b, *Geoscientific Model*
4720 *Development*, 16, 4249–4264, <https://doi.org/10.5194/gmd-16-4249-2023>, 2023.
- 4721 Matthews, S.: A comparison of fire danger rating systems for use in forests, *Australian Meteorological and Oceanographic*
4722 *Journal*, 58, 41–48, <https://doi.org/10.22499/2.5801.005>, 2009.
- 4723 Mauritsen, T., Bader, J., Becker, T., Behrens, J., Bittner, M., Brokopf, R., Brovkin, V., Claussen, M., Crueger, T., Esch, M., Fast,
4724 I., Fiedler, S., Fläschner, D., Gayler, V., Giorgetta, M., Goll, D. S., Haak, H., Hagemann, S., Hedemann, C., Hohenegger, C.,
4725 Ilyina, T., Jahns, T., Jimenez-de-la-Cuesta, D., Jungclaus, J., Kleinen, T., Kloster, S., Kracher, D., Kinne, S., Kleberg, D., Lasslop,
4726 G., Kornblueh, L., Marotzke, J., Matei, D., Meraner, K., Mikolajewicz, U., Modali, K., Möbis, B., Müller, W. A., Nabel, J. E. M. S.,
4727 Nam, C. C. W., Notz, D., Nyawira, S.-S., Paulsen, H., Peters, K., Pincus, R., Pohlmann, H., Pongratz, J., Popp, M., Raddatz, T.
4728 J., Rast, S., Redler, R., Reick, C. H., Rohrschneider, T., Schemann, V., Schmidt, H., Schnur, R., Schulzweida, U., Six, K. D.,
4729 Stein, L., Stemmler, I., Stevens, B., von Storch, J.-S., Tian, F., Voigt, A., Vrese, P., Wieners, K.-H., Wilkenskjaeld, S., Winkler, A.,
4730 and Roeckner, E.: Developments in the MPI-M Earth System Model version 1.2 (MPI-ESM1.2) and Its Response to Increasing
4731 CO₂, *Journal of Advances in Modeling Earth Systems*, 11, 998–1038, <https://doi.org/10.1029/2018MS001400>, 2019.
- 4732 McCulloch, M. T., Winter, A., Sherman, C. E., and Trotter, J. A.: 300 years of sclerosponge thermometry shows global warming
4733 has exceeded 1.5 °C, *Nat. Clim. Chang.*, 14, 171–177, <https://doi.org/10.1038/s41558-023-01919-7>, 2024.
- 4734 McNorton, J., Agustí-Panareda, A., Arduini, G., Balsamo, G., Bousseres, N., Boussetta, S., Chericoni, M., Choulga, M., Engelen,
4735 R., and Guevara, M.: An Urban Scheme for the ECMWF Integrated Forecasting System: Global Forecasts and Residential CO₂
4736 Emissions, *Journal of Advances in Modeling Earth Systems*, 15, e2022MS003286, <https://doi.org/10.1029/2022MS003286>, 2023.
- 4737 McNorton, J. R. and Di Giuseppe, F.: A global fuel characteristic model and dataset for wildfire prediction, *Biogeosciences*, 21,
4738 279–300, <https://doi.org/10.5194/bg-21-279-2024>, 2024.
- 4739 McNorton, J. R., Giuseppe, F. D., Pinnington, E. M., Chantry, M., and Barnard, C.: A Global Probability-of-Fire (PoF) Forecast,
4740 <https://doi.org/10.22541/essoar.170542063.30086889/v1>.
- 4741 Meadley, J.: Thailand Enhances Measures Against Forest Fires, Encroachment Increases in Laos, available at:
4742 <https://laotiantimes.com/2024/01/31/thailand-enhances-measures-against-forest-fires-encroachment-increases-in-laos/>, last
4743 access: 2 June 2024, *Laotian Times*, 2024.
- 4744 Mediterranean Center for Environmental Studies: Postfire/Informes de Impacto: Informe sobre el impacto del incendio forestal
4745 de Villanueva de Viver, 2023, available at: [https://www.ceam.es/es/news/postfire-informes-de-impacto-informe-sobre-el-impacto-
4746 del-incendio-forestal-de-villanueva-de-viver-2023/](https://www.ceam.es/es/news/postfire-informes-de-impacto-informe-sobre-el-impacto-del-incendio-forestal-de-villanueva-de-viver-2023/), last access: 2 June 2024, 2023.
- 4747 Meier, S., Elliott, R. J. R., and Strobl, E.: 2023a The regional economic impact of wildfires: Evidence from Southern Europe,
4748 *Journal of Environmental Economics and Management*, 118, 102787, <https://doi.org/10.1016/j.jeem.2023.102787>, 2023a.
- 4749 Meier, S., Strobl, E., Elliott, R. J. R., and Kettridge, N.: 2023b Cross-country risk quantification of extreme wildfires in
4750 Mediterranean Europe, *Risk Analysis*, 43, 1745–1762, <https://doi.org/10.1111/risa.14075>, 2023b.
- 4751 Mengel, M., Treu, S., Lange, S., and Frieler, K.: ATTRICI v1.1 – counterfactual climate for impact attribution, *Geoscientific Model*
4752 *Development*, 14, 5269–5284, <https://doi.org/10.5194/gmd-14-5269-2021>, 2021.
- 4753 Mills, G., Salkin, O., Fearon, M., Harris, S., Brown, T., and Reinbold, H.: Meteorological drivers of the eastern Victorian Black
4754 Summer (2019–2020) fires, *J. South. Hemisph. Earth Syst. Sci.*, 72, 139–163, <https://doi.org/10.1071/ES22011>, 2022.
- 4755 Mindlin, J., Vera, C. S., Shepherd, T. G., and Osman, M.: Plausible Drying and Wetting Scenarios for Summer in Southeastern
4756 South America, *Journal of Climate*, 36, 7973–7991, <https://doi.org/10.1175/JCLI-D-23-0134.1>, 2023.
- 4757 Ministério Público Federal: Procuradoria da República no Amazonas. Reference: PA-PPB nº 1.13.000.001219/2021-55, 2023.



- 4758 Modaresi Rad, A., Abatzoglou, J. T., Kreittler, J., Alizadeh, M. R., AghaKouchak, A., Hudyma, N., Nauslar, N. J., and Sadegh, M.:
4759 Human and infrastructure exposure to large wildfires in the United States, *Nat Sustain*, 6, 1343–1351,
4760 <https://doi.org/10.1038/s41893-023-01163-z>, 2023.
- 4761 Mongabay: Gobierno colombiano declara situación de desastre y calamidad en el país ante el grave impacto de incendios
4762 forestales, available at: [https://es.mongabay.com/2024/01/gobierno-colombiano-declara-situacion-de-desastre-y-calamidad-en-](https://es.mongabay.com/2024/01/gobierno-colombiano-declara-situacion-de-desastre-y-calamidad-en-el-pais-ante-el-grave-impacto-de-incendios-forestales/)
4763 [el-pais-ante-el-grave-impacto-de-incendios-forestales/](https://es.mongabay.com/2024/01/gobierno-colombiano-declara-situacion-de-desastre-y-calamidad-en-el-pais-ante-el-grave-impacto-de-incendios-forestales/), last access: 2 June 2024, *Noticias ambientales*, 2024.
- 4764 Moreira, F., Ascoli, D., Safford, H., Adams, M. A., Moreno, J. M., Pereira, J. M. C., Catry, F. X., Armesto, J., Bond, W., González,
4765 M. E., Curt, T., Koutsias, N., McCaw, L., Price, O., Pausas, J. G., Rigolot, E., Stephens, S., Tavsanoglu, C., Vallejo, V. R., Wilgen,
4766 B. W. V., Xanthopoulos, G., and Fernandes, P. M.: Wildfire management in Mediterranean-type regions: paradigm change
4767 needed, *Environ. Res. Lett.*, 15, 011001, <https://doi.org/10.1088/1748-9326/ab541e>, 2020.
- 4768 Muñoz-Sabater, J., Dutra, E., Agustí-Panareda, A., Albergel, C., Arduini, G., Balsamo, G., Boussetta, S., Choulga, M., Harrigan,
4769 S., Hersbach, H., Martens, B., Miralles, D. G., Piles, M., Rodríguez-Fernández, N. J., Zsoter, E., Buontempo, C., and Thépaut,
4770 J.-N.: ERA5-Land: a state-of-the-art global reanalysis dataset for land applications, *Earth System Science Data*, 13, 4349–4383,
4771 <https://doi.org/10.5194/essd-13-4349-2021>, 2021.
- 4772 Murray, C. J. L., Aravkin, A. Y., Zheng, P., Abbafati, C., Abbas, K. M., Abbasi-Kangevari, M., Abd-Allah, F., Abdelalim, A.,
4773 Abdollahi, M., Abdollahpour, I., Abegaz, K. H., Abolhassani, H., Aboyans, V., Abreu, L. G., Abrigo, M. R. M., Abualhasan, A.,
4774 Abu-Raddad, L. J., Abushouk, A. I., Adabi, M., Adeganmbi, V., Adeoye, A. M., Adetokunboh, O. O., Adham, D., Advani, S. M.,
4775 Agarwal, G., Aghamir, S. M. K., Agrawal, A., Ahmad, T., Ahmadi, K., Ahmadi, M., Ahmadi, H., Ahmed, M. B., Akalu, T. Y.,
4776 Akinyemi, R. O., Akinyemiju, T., Akombi, B., Akunna, C. J., Alahdab, F., Al-Aly, Z., Alam, K., Alam, S., Alam, T., Alanezi, F. M.,
4777 Alanzi, T. M., Alemu, B. wassihun, Alhabib, K. F., Ali, M., Ali, S., Alicandro, G., Alinia, C., Alipour, V., Alizade, H., Aljunid, S. M.,
4778 Alla, F., Allebeck, P., Almasi-Hashiani, A., Al-Mekhlafi, H. M., Alonso, J., Altirkawi, K. A., Amini-Rarani, M., Amiri, F., Amugsi, D.
4779 A., Ancuceanu, R., Anderlini, D., Anderson, J. A., Andrei, C. L., Andrei, T., Angus, C., Anjomshoa, M., Ansari, F., Ansari-
4780 Moghaddam, A., Antonazzo, I. C., Antonio, C. A. T., Antony, C. M., Antriyandarti, E., Anvari, D., Anwer, R., Appiah, S. C. Y.,
4781 Arabloo, J., Arab-Zozani, M., Ariani, F., Armoon, B., Årnlöv, J., Arzani, A., Asadi-Aliabadi, M., Asadi-Pooya, A. A., Ashbaugh, C.,
4782 Assmus, M., Atafar, Z., Atnafu, D. D., Atout, M. M. W., Ausloos, F., Ausloos, M., Quintanilla, B. P. A., Ayano, G., Ayanore, M. A.,
4783 Azari, S., Azarian, G., Azene, Z. N., et al.: Global burden of 87 risk factors in 204 countries and territories, 1990–2019: a
4784 systematic analysis for the Global Burden of Disease Study 2019, *The Lancet*, 396, 1223–1249, [https://doi.org/10.1016/S0140-](https://doi.org/10.1016/S0140-6736(20)30752-2)
4785 [6736\(20\)30752-2](https://doi.org/10.1016/S0140-6736(20)30752-2), 2020.
- 4786 NASA Earth Observatory: Tracking Canada's Extreme 2023 Fire Season, available at:
4787 <https://earthobservatory.nasa.gov/images/151985/tracking-canadas-extreme-2023-fire-season>, last access: 2 June 2024, 2023.
- 4788 NASA Earth Observatory: Fires Rage in Central Chile, available at: [https://earthobservatory.nasa.gov/images/152411/fires-rage-](https://earthobservatory.nasa.gov/images/152411/fires-rage-in-central-chile)
4789 [in-central-chile](https://earthobservatory.nasa.gov/images/152411/fires-rage-in-central-chile), last access: 2 June 2024, 2024.
- 4790 NASA Earth Science Data Systems: MODIS/Aqua+Terra Thermal Anomalies/Fire locations 1km FIRMS V006 and V0061 (Vector
4791 data), available at: <https://www.earthdata.nasa.gov/learn/find-data/near-real-time/firms/mcd14ml>, last access: 2 June 2024, 2020.
- 4792 NASA FIRMS: NASA Fire Information for Resource Management System, available at:
4793 <https://firms.modaps.eosdis.nasa.gov/map/>, last access: 2 June 2024, 2024.
- 4794 National Institute for Space Research: INPE Programa Queimadas - Banco de Dados de Queimadas, available at:
4795 <https://terrabrasilis.dpi.inpe.br/queimadas/portal/>, last access: 2 June 2024, 2024.
- 4796 National Interagency Fire Center: National Interagency Fire Center Situation Report for August 31, 2023, available at:
4797 https://www.nifc.gov/sites/default/files/NICC/1-Incident%20Information/IMSR/2023/August/IMSR_CY23_08_31_23_0.pdf, last
4798 access: 2 June 2024, National Interagency Fire Center, 2023.
- 4799 National Interagency Fire Center: 2024a Statistics - Current National Statistics, available at: [https://www.nifc.gov/fire-](https://www.nifc.gov/fire-information/statistics)
4800 [information/statistics](https://www.nifc.gov/fire-information/statistics), last access: 2 June 2024, 2024a.
- 4801 National Interagency Fire Center: 2024b InciWeb Information, available at: [https://www.nifc.gov/fire-information/pio-bulletin-](https://www.nifc.gov/fire-information/pio-bulletin-board/inciweb)
4802 [board/inciweb](https://www.nifc.gov/fire-information/pio-bulletin-board/inciweb), last access: 2 June 2024, 2024b.



- 4803 National Oceanic and Atmospheric Administration: National Centers for Environmental Information, Monthly Wildfires Report,
4804 available at: <https://www.ncei.noaa.gov/access/monitoring/monthly-report/fire/202308>, last access: 2 June 2024, National
4805 Oceanic and Atmospheric Administration, 2023.
- 4806 National Oceanic and Atmospheric Administration: Fires Rage Across Texas Panhandle, available at:
4807 <https://www.nesdis.noaa.gov/news/fires-rage-across-texas-panhandle>, last access: 2 June 2024, National Environmental
4808 Satellite, Data, and Information Service, 2024.
- 4809 Neris, J., Santin, C., Lew, R., Robichaud, P. R., Elliot, W. J., Lewis, S. A., Sheridan, G., Rohlf, A.-M., Ollivier, Q., Oliveira, L.,
4810 and Doerr, S. H.: Designing tools to predict and mitigate impacts on water quality following the Australian 2019/2020 wildfires:
4811 Insights from Sydney's largest water supply catchment, *Integrated Environmental Assessment and Management*, 17, 1151–1161,
4812 <https://doi.org/10.1002/ieam.4406>, 2021.
- 4813 Nielsen-Pincus, M., Moseley, C., and Gebert, K.: Job growth and loss across sectors and time in the western US: The impact of
4814 large wildfires, *Forest Policy and Economics*, 38, 199–206, <https://doi.org/10.1016/j.forpol.2013.08.010>, 2014.
- 4815 Nikolakis, W., Welham, C., and Greene, G.: Diffusion of indigenous fire management and carbon-credit programs: Opportunities
4816 and challenges for “scaling-up” to temperate ecosystems, *Front. For. Glob. Change*, 5, <https://doi.org/10.3389/ffgc.2022.967653>,
4817 2022.
- 4818 Noble, I. R., Gill, A. M., and Bary, G. a. V.: McArthur's fire-danger meters expressed as equations, *Australian Journal of Ecology*,
4819 5, 201–203, <https://doi.org/10.1111/j.1442-9993.1980.tb01243.x>, 1980.
- 4820 Nolan, R. H., Collins, L., Leigh, A., Ooi, M. K. J., Curran, T. J., Fairman, T. A., Resco de Dios, V., and Bradstock, R.: 2021a Limits
4821 to post-fire vegetation recovery under climate change, *Plant, Cell & Environment*, 44, 3471–3489,
4822 <https://doi.org/10.1111/pce.14176>, 2021a.
- 4823 Nolan, R. H., Bowman, D. M. J. S., Clarke, H., Haynes, K., Ooi, M. K. J., Price, O. F., Williamson, G. J., Whittaker, J., Bedward,
4824 M., Boer, M. M., Cavanagh, V. I., Collins, L., Gibson, R. K., Griebel, A., Jenkins, M. E., Keith, D. A., McIlwee, A. P., Penman, T.
4825 D., Samson, S. A., Tozer, M. G., and Bradstock, R. A.: 2021b What Do the Australian Black Summer Fires Signify for the Global
4826 Fire Crisis?, *Fire*, 4, 97, <https://doi.org/10.3390/fire4040097>, 2021b.
- 4827 Nunes, J. P., Doerr, S. H., Sheridan, G., Neris, J., Santin, C., Emelko, M. B., Silins, U., Robichaud, P. R., Elliot, W. J., and Keizer,
4828 J.: Assessing water contamination risk from vegetation fires: Challenges, opportunities and a framework for progress,
4829 *Hydrological Processes*, 32, 687–694, <https://doi.org/10.1002/hyp.11434>, 2018.
- 4830 Oberholtz, C.: Drone video shows wildfire devastation in Chile as death toll soars to 112 with hundreds still missing, available at:
4831 <https://www.foxweather.com/weather-news/valparaiso-chile-forest-fires-evacuations-damage>, last access: 2 June 2024, FOX
4832 Weather, 2024.
- 4833 O'Dell, K., Ford, B., Fischer, E. V., and Pierce, J. R.: Contribution of Wildland-Fire Smoke to US PM_{2.5} and Its Influence on
4834 Recent Trends, *Environ. Sci. Technol.*, 53, 1797–1804, <https://doi.org/10.1021/acs.est.8b05430>, 2019.
- 4835 OECD: Taming Wildfires in the Context of Climate Change, OECD, <https://doi.org/10.1787/dd00c367-en>, 2023.
- 4836 Oklahoma Department of Emergency Management: April 1 Situation Update 2 Wildfires Impacting State, available at:
4837 <https://oklahoma.gov/oem/emergencies-and-disasters/2023/march-31-wildfire-event/april-1-situation-update-2.html>, last access:
4838 2 June 2024, Oklahoma Department of Emergency Management, 2023.
- 4839 Olson, D. M., Dinerstein, E., Wikramanayake, E. D., Burgess, N. D., Powell, G. V. N., Underwood, E. C., D'amico, J. A., Itoua, I.,
4840 Strand, H. E., Morrison, J. C., Loucks, C. J., Allnutt, T. F., Ricketts, T. H., Kura, Y., Lamoreux, J. F., Wettengel, W. W., Hedao,
4841 P., and Kassem, K. R.: Terrestrial Ecoregions of the World: A New Map of Life on Earth, *BioScience*, 51, 933,
4842 [https://doi.org/10.1641/0006-3568\(2001\)051\[0933:TEOTWA\]2.0.CO;2](https://doi.org/10.1641/0006-3568(2001)051[0933:TEOTWA]2.0.CO;2), 2001.
- 4843 Otón, G., Lizundia-Loiola, J., Pettinari, M. L., and Chuvieco, E.: Development of a consistent global long-term burned area product
4844 (1982–2018) based on AVHRR-LTDR data, *International Journal of Applied Earth Observation and Geoinformation*, 103, 102473,
4845 <https://doi.org/10.1016/j.jag.2021.102473>, 2021.



- 4846 Pai, S. J., Carter, T. S., Heald, C. L., and Kroll, J. H.: Updated World Health Organization Air Quality Guidelines Highlight the
4847 Importance of Non-anthropogenic PM_{2.5}, *Environ. Sci. Technol. Lett.*, 9, 501–506, <https://doi.org/10.1021/acs.estlett.2c00203>,
4848 2022.
- 4849 Palmer, J.: Fire as Medicine: Learning from Native American Fire Stewardship, available at: [http://eos.org/features/fire-as-](http://eos.org/features/fire-as-medicine-learning-from-native-american-fire-stewardship)
4850 [medicine-learning-from-native-american-fire-stewardship](http://eos.org/features/fire-as-medicine-learning-from-native-american-fire-stewardship), last access: 2 June 2024, Eos, 2021.
- 4851 Pan, X., Chin, M., Ichoku, C. M., and Field, R. D.: Connecting Indonesian Fires and Drought With the Type of El Niño and Phase
4852 of the Indian Ocean Dipole During 1979–2016, *Journal of Geophysical Research: Atmospheres*, 123, 7974–7988,
4853 <https://doi.org/10.1029/2018JD028402>, 2018.
- 4854 Pan, X., Ichoku, C., Chin, M., Bian, H., Darnenov, A., Colarco, P., Ellison, L., Kucsera, T., da Silva, A., Wang, J., Oda, T., and
4855 Cui, G.: Six global biomass burning emission datasets: intercomparison and application in one global aerosol model, *Atmospheric*
4856 *Chemistry and Physics*, 20, 969–994, <https://doi.org/10.5194/acp-20-969-2020>, 2020.
- 4857 Perron, M. M. G., Meyerink, S., Corkill, M., Strzelec, M., Proemse, B. C., Gault-Ringold, M., Sanz Rodriguez, E., Chase, Z., and
4858 Bowie, A. R.: Trace elements and nutrients in wildfire plumes to the southeast of Australia, *Atmospheric Research*, 270, 106084,
4859 <https://doi.org/10.1016/j.atmosres.2022.106084>, 2022.
- 4860 Perry, M. C., Vanvyve, E., Betts, R. A., and Palin, E. J.: Past and future trends in fire weather for the UK, *Natural Hazards and*
4861 *Earth System Sciences*, 22, 559–575, <https://doi.org/10.5194/nhess-22-559-2022>, 2022.
- 4862 Polade, S. D., Pierce, D. W., Cayan, D. R., Gershunov, A., and Dettinger, M. D.: The key role of dry days in changing regional
4863 climate and precipitation regimes, *Sci Rep*, 4, 4364, <https://doi.org/10.1038/srep04364>, 2014.
- 4864 Pomeroy, J. W., DeBeer, C. M., Adapa, P., Phare, M. A., Overduin, N., Miltenberger, M., Maas, M., Pentland, R., Brandes, O.
4865 M., and Sandford, R. W.: Water Security for Canadians: Solutions for Canada's Emerging Water Crisis, available at:
4866 <https://landusekn.ca/resource/water-security-canadians-solutions-canada%E2%80%99s-emerging-water-crisis>, last access: 2
4867 June 2024, 2019.
- 4868 Pullabhotla, H., Zahid, M., Heft-Neal, S., Rathi, V., and Burke, M.: Reply to Giglio and Roy: Aggregate infant mortality estimates
4869 robust to choice of burned area product, *Proceedings of the National Academy of Sciences*, 120, e2318188120,
4870 <https://doi.org/10.1073/pnas.2318188120>, 2023.
- 4871 Pyne, S. J.: *Fire in America: A Cultural History of Wildland and Rural Fire*, University of Washington Press, 2017.
- 4872 Rabin, S. S., Melton, J. R., Lasslop, G., Bachelet, D., Forrest, M., Hantson, S., Kaplan, J. O., Li, F., Mangeon, S., Ward, D. S.,
4873 Yue, C., Arora, V. K., Hickler, T., Kloster, S., Knorr, W., Nieradzik, L., Spessa, A., Folberth, G. A., Sheehan, T., Voulgarakis, A.,
4874 Kelley, D. I., Prentice, I. C., Sitch, S., Harrison, S., and Arneth, A.: The Fire Modeling Intercomparison Project (FireMIP), phase
4875 1: experimental and analytical protocols with detailed model descriptions, *Geoscientific Model Development*, 10, 1175–1197,
4876 <https://doi.org/10.5194/gmd-10-1175-2017>, 2017.
- 4877 Radeloff, V. C., Helmers, D. P., Kramer, H. A., Mockrin, M. H., Alexandre, P. M., Bar-Massada, A., Butsic, V., Hawbaker, T. J.,
4878 Martinuzzi, S., Syphard, A. D., and Stewart, S. I.: Rapid growth of the US wildland-urban interface raises wildfire risk, *Proceedings*
4879 *of the National Academy of Sciences*, 115, 3314–3319, <https://doi.org/10.1073/pnas.1718850115>, 2018.
- 4880 Rádio e Televisão de Portugal: Prejuízos dos incêndios no Porto Moniz e Calheta rondam os 3 milhões de euros (áudio), available
4881 at: <https://madeira.rtp.pt/politica/prejuizos-dos-incendios-no-porto-moniz-e-calheta-rondam-os-3-milhoes-de-euros-audio/>, last
4882 access: 2 June 2024, 2023.
- 4883 Reddington, C. L., Spracklen, D. V., Artaxo, P., Ridley, D. A., Rizzo, L. V., and Arana, A.: Analysis of particulate emissions from
4884 tropical biomass burning using a global aerosol model and long-term surface observations, *Atmospheric Chemistry and Physics*,
4885 16, 11083–11106, <https://doi.org/10.5194/acp-16-11083-2016>, 2016.
- 4886 Ren, X., Zhang, L., Cai, W., and Wu, L.: Moderate Indian Ocean Dipole Dominates Spring Fire Weather Conditions in Southern
4887 Australia, *Environ. Res. Lett.*, <https://doi.org/10.1088/1748-9326/ad4fa5>, 2024.



- 4888 Reuters: 2023a Deadly fires rage along Algeria coast, spread to Tunisia, available at:
4889 <https://www.reuters.com/world/africa/deadly-fires-rage-along-algeria-coast-spread-tunisia-2023-07-25/>, last access: 2 June
4890 2024, Reuters, 25th July, 2023a.
- 4891 Reuters: 2023b Syria struggles to contain wildfires as temperatures rise, available at: <https://www.reuters.com/world/middle-east/syria-struggles-contain-wildfires-temperatures-rise-2023-07-18/>, last access: 2 June 2024, Reuters, 18th July, 2023b.
- 4893 Roads, J., Tripp, P., Juang, H., Wang, J., Fujioka, F., and Chen, S.: NCEP-ECPC monthly to seasonal US fire danger forecasts,
4894 *International Journal of Wildland Fire* 19:399–414, 19, 399–414, <https://doi.org/10.1071/WF07079>, 2010.
- 4895 Rodríguez-Trejo, D. A., Ponce-Calderón, L. P., Tchikoué, H., Martínez-Domínguez, R., Martínez-Muñoz, P., and Pulido-Luna, J.
4896 A.: Towards integrated fire management in Mexico's Megalopolis region: a diagnosis, *TFI*, 80–86,
4897 <https://doi.org/10.55515/NWAM8441>, 2022.
- 4898 Román, M. O., Justice, C., Paynter, I., Boucher, P. B., Devadiga, S., Endsley, A., Erb, A., Friedl, M., Gao, H., Giglio, L., Gray, J.
4899 M., Hall, D., Hulley, G., Kimball, J., Knyazikhin, Y., Lyapustin, A., Myneni, R. B., Noojipady, P., Pu, J., Riggs, G., Sarkar, S.,
4900 Schaaf, C., Shah, D., Tran, K. H., Vermote, E., Wang, D., Wang, Z., Wu, A., Ye, Y., Shen, Y., Zhang, S., Zhang, S., Zhang, X.,
4901 Zhao, M., Davidson, C., and Wolfe, R.: Continuity between NASA MODIS Collection 6.1 and VIIRS Collection 2 land products,
4902 *Remote Sensing of Environment*, 302, 113963, <https://doi.org/10.1016/j.rse.2023.113963>, 2024.
- 4903 Romps, D. M.: Evaluating the Future of Lightning in Cloud-Resolving Models, *Geophysical Research Letters*, 46, 14863–14871,
4904 <https://doi.org/10.1029/2019GL085748>, 2019.
- 4905 Rosan, T. M., Sitch, S., Mercado, L. M., Heinrich, V., Friedlingstein, P., and Aragão, L. E. O. C.: Fragmentation-Driven Divergent
4906 Trends in Burned Area in Amazonia and Cerrado, *Front. For. Glob. Change*, 5, <https://doi.org/10.3389/ffgc.2022.801408>, 2022.
- 4907 Roteta, E., Bastarrika, A., Ibisate, A., and Chuvieco, E.: A Preliminary Global Automatic Burned-Area Algorithm at Medium
4908 Resolution in Google Earth Engine, *Remote Sensing*, 13, 4298, <https://doi.org/10.3390/rs13214298>, 2021.
- 4909 Roy, D. P., Boschetti, L., Justice, C. O., and Ju, J.: The collection 5 MODIS burned area product — Global evaluation by
4910 comparison with the MODIS active fire product, *Remote Sensing of Environment*, 112, 3690–3707,
4911 <https://doi.org/10.1016/j.rse.2008.05.013>, 2008.
- 4912 Russell-Smith, J., Yates, C. P., Edwards, A. C., Whitehead, P. J., Murphy, B. P., and Lawes, M. J.: Deriving Multiple Benefits
4913 from Carbon Market-Based Savanna Fire Management: An Australian Example, *PLoS ONE*, 10, e0143426,
4914 <https://doi.org/10.1371/journal.pone.0143426>, 2015.
- 4915 Sabljak, E.: Scotland's wildfires in maps and charts across all councils, available at:
4916 <https://www.heraldsotland.com/news/23498843.scotlands-wildfires-maps-charts-across-councils/>, last access: 2 June 2024,
4917 2023.
- 4918 Safford, H. D., Paulson, A. K., Steel, Z. L., Young, D. J. N., and Wayman, R. B.: The 2020 California fire season: A year like no
4919 other, a return to the past or a harbinger of the future?, *Global Ecol Biogeogr*, 31, 2005–2025, <https://doi.org/10.1111/geb.13498>,
4920 2022.
- 4921 Sánchez-García, C., Santín, C., Neris, J., Sigmund, G., Otero, X. L., Manley, J., González-Rodríguez, G., Belcher, C. M., Cerdà,
4922 A., Marcotte, A. L., Murphy, S. F., Rhoades, C. C., Sheridan, G., Strydom, T., Robichaud, P. R., and Doerr, S. H.: Chemical
4923 characteristics of wildfire ash across the globe and their environmental and socio-economic implications, *Environment
4924 International*, 178, 108065, <https://doi.org/10.1016/j.envint.2023.108065>, 2023.
- 4925 San-Miguel-Ayanz, J., Schulte, E., Schmuck, G., and Camia, A.: The European Forest Fire Information System in the context of
4926 environmental policies of the European Union, *Forest Policy and Economics*, 29, 19–25,
4927 <https://doi.org/10.1016/j.forpol.2011.08.012>, 2013.
- 4928 SantanderMetGroup: ATLAS/reference-regions at main · SantanderMetGroup/ATLAS, available at:
4929 <https://github.com/SantanderMetGroup/ATLAS/tree/main/reference-regions>, last access: 2 June 2024, GitHub, 2021.



- 4930 Santoro, M. and Cartus, O.: ESA Biomass Climate Change Initiative (Biomass_cci): Global datasets of forest above-ground
4931 biomass for the years 2010, 2017 and 2018, v3, <https://doi.org/10.5285/5F331C418E9F4935B8EB1B836F8A91B8>, 2021.
- 4932 Scholten, R. C., Jandt, R., Miller, E. A., Rogers, B. M., and Veraverbeke, S.: Overwintering fires in boreal forests, *Nature*, 593,
4933 399–404, <https://doi.org/10.1038/s41586-021-03437-y>, 2021.
- 4934 Schroeder, W., Oliva, P., Giglio, L., and Csiszar, I. A.: The New VIIRS 375 m active fire detection data product: Algorithm
4935 description and initial assessment, *Remote Sensing of Environment*, 143, 85–96, <https://doi.org/10.1016/j.rse.2013.12.008>, 2014.
- 4936 Schroeder, W., Oliva, P., Giglio, L., Quayle, B., Lorenz, E., and Morelli, F.: Active fire detection using Landsat-8/OLI data, *Remote
4937 Sensing of Environment*, 185, 210–220, <https://doi.org/10.1016/j.rse.2015.08.032>, 2016.
- 4938 Schug, F., Bar-Massada, A., Carlson, A. R., Cox, H., Hawbaker, T. J., Helmers, D., Hostert, P., Kaim, D., Kasraee, N. K.,
4939 Martinuzzi, S., Mockrin, M. H., Pfoch, K. A., and Radeloff, V. C.: The global wildland–urban interface, *Nature*, 621, 94–99,
4940 <https://doi.org/10.1038/s41586-023-06320-0>, 2023.
- 4941 Seddon, N., Chausson, A., Berry, P., Girardin, C. A. J., Smith, A., and Turner, B.: Understanding the value and limits of nature-
4942 based solutions to climate change and other global challenges, *Philosophical Transactions of the Royal Society B: Biological
4943 Sciences*, 375, 20190120, <https://doi.org/10.1098/rstb.2019.0120>, 2020.
- 4944 Seok, M.-W., Ko, Y. H., Park, K.-T., and Kim, T.-W.: Possible enhancement in ocean productivity associated with wildfire-derived
4945 nutrient and black carbon deposition in the Arctic Ocean in 2019–2021, *Marine Pollution Bulletin*, 201, 116149,
4946 <https://doi.org/10.1016/j.marpolbul.2024.116149>, 2024.
- 4947 Sexton, J. O., Noojipady, P., Song, X.-P., Feng, M., Song, D.-X., Kim, D.-H., Anand, A., Huang, C., Channan, S., Pimm, S. L.,
4948 and Townshend, J. R.: Conservation policy and the measurement of forests, *Nature Clim Change*, 6, 192–196,
4949 <https://doi.org/10.1038/nclimate2816>, 2016.
- 4950 Shaddick, G., Thomas, M. L., Amini, H., Broday, D., Cohen, A., Frostad, J., Green, A., Gumy, S., Liu, Y., Martin, R. V., Pruss-
4951 Ustun, A., Simpson, D., van Donkelaar, A., and Brauer, M.: Data Integration for the Assessment of Population Exposure to
4952 Ambient Air Pollution for Global Burden of Disease Assessment, *Environ. Sci. Technol.*, 52, 9069–9078,
4953 <https://doi.org/10.1021/acs.est.8b02864>, 2018.
- 4954 Shakesby, R. A. and Doerr, S. H.: Wildfire as a hydrological and geomorphological agent, *Earth-Science Reviews*, 74, 269–307,
4955 <https://doi.org/10.1016/j.earscirev.2005.10.006>, 2006.
- 4956 Shepherd, T. G., Boyd, E., Calel, R. A., Chapman, S. C., Dessai, S., Dima-West, I. M., Fowler, H. J., James, R., Maraun, D.,
4957 Martius, O., Senior, C. A., Sobel, A. H., Stainforth, D. A., Tett, S. F. B., Trenberth, K. E., van den Hurk, B. J. J. M., Watkins, N.
4958 W., Wilby, R. L., and Zenghelis, D. A.: Storylines: an alternative approach to representing uncertainty in physical aspects of
4959 climate change, *Climatic Change*, 151, 555–571, <https://doi.org/10.1007/s10584-018-2317-9>, 2018.
- 4960 Shingler, B.: It's the middle of winter, and more than 100 wildfires are still smouldering, available at:
4961 <https://www.cbc.ca/news/climate/wildfires-zombie-fires-canada-bc-alberta-1.7119851>, last access: 2 June 2024, CBC News,
4962 21st February, 2024.
- 4963 Shuman, J. K., Balch, J. K., Barnes, R. T., Higuera, P. E., Roos, C. I., Schwilk, D. W., Stavros, E. N., Banerjee, T., Bela, M. M.,
4964 Bendix, J., Bertolino, S., Billign, S., Bladon, K. D., Brando, P., Breidenthal, R. E., Buma, B., Calhoun, D., Carvalho, L. M. V.,
4965 Cattau, M. E., Cawley, K. M., Chandra, S., Chipman, M. L., Cobian-Iñiguez, J., Conlisk, E., Coop, J. D., Cullen, A., Davis, K. T.,
4966 Dayalu, A., De Sales, F., Dolman, M., Ellsworth, L. M., Franklin, S., Guiterman, C. H., Hamilton, M., Hanan, E. J., Hansen, W.
4967 D., Hantson, S., Harvey, B. J., Holz, A., Huang, T., Hurteau, M. D., Ilangakoon, N. T., Jennings, M., Jones, C., Klimaszewski-
4968 Patterson, A., Kobziar, L. N., Kominoski, J., Kosovic, B., Krawchuk, M. A., Laris, P., Leonard, J., Loria-Salazar, S. M., Lucash,
4969 M., Mahmoud, H., Margolis, E., Maxwell, T., McCarty, J. L., McWethy, D. B., Meyer, R. S., Miesel, J. R., Moser, W. K., Nagy, R.
4970 C., Niyogi, D., Palmer, H. M., Pellegrini, A., Poulter, B., Robertson, K., Rocha, A. V., Sadegh, M., Santos, F., Scordo, F., Sexton,
4971 J. O., Sharma, A. S., Smith, A. M. S., Soja, A. J., Still, C., Swetnam, T., Syphard, A. D., Tingley, M. W., Tohid, A., Trugman, A.
4972 T., Turetsky, M., Varner, J. M., Wang, Y., Whitman, T., Yelenik, S., and Zhang, X.: Reimagine fire science for the anthropocene,
4973 *PNAS Nexus*, 1, pgac115, <https://doi.org/10.1093/pnasnexus/pgac115>, 2022.



- 4974 SIC Notícias: Incêndio em Odemira causou prejuízos de sete milhões de euros em habitações, available at:
4975 [https://sicnoticias.pt/especiais/incendios-em-portugal/2023-09-08-incendio-em-odemira-causou-prejuizos-de-sete-milhoes-de-](https://sicnoticias.pt/especiais/incendios-em-portugal/2023-09-08-incendio-em-odemira-causou-prejuizos-de-sete-milhoes-de-euros-em-habitacoes-c3204bcb)
4976 [euros-em-habitacoes-c3204bcb](https://sicnoticias.pt/especiais/incendios-em-portugal/2023-09-08-incendio-em-odemira-causou-prejuizos-de-sete-milhoes-de-euros-em-habitacoes-c3204bcb), last access: 2 June 2024, SIC Notícias, 2023.
- 4977 Silva, C. V. J., Aragão, L. E. O. C., Young, P. J., Espirito-Santo, F., Berenguer, E., Anderson, L. O., Brasil, I., Pontes-Lopes, A.,
4978 Ferreira, J., Withey, K., França, F., Graça, P. M. L. A., Kirsten, L., Xaud, H., Salimon, C., Scaranello, M. A., Castro, B., Seixas,
4979 M., Farias, R., and Barlow, J.: Estimating the multi-decadal carbon deficit of burned Amazonian forests, *Environ. Res. Lett.*, 15,
4980 114023, <https://doi.org/10.1088/1748-9326/abb62c>, 2020.
- 4981 Silva Junior, C. H. L., Pessôa, A. C. M., Carvalho, N. S., Reis, J. B. C., Anderson, L. O., and Aragão, L. E. O. C.: The Brazilian
4982 Amazon deforestation rate in 2020 is the greatest of the decade, *Nat Ecol Evol*, 5, 144–145, [https://doi.org/10.1038/s41559-020-](https://doi.org/10.1038/s41559-020-01368-x)
4983 [01368-x](https://doi.org/10.1038/s41559-020-01368-x), 2021.
- 4984 Silveira, M. V. F., Petri, C. A., Broggio, I. S., Chagas, G. O., Macul, M. S., Leite, C. C. S. S., Ferrari, E. M. M., Amim, C. G. V.,
4985 Freitas, A. L. R., Motta, A. Z. V., Carvalho, L. M. E., Silva Junior, C. H. L., Anderson, L. O., and Aragão, L. E. O. C.: Drivers of
4986 Fire Anomalies in the Brazilian Amazon: Lessons Learned from the 2019 Fire Crisis, *Land*, 9, 516,
4987 <https://doi.org/10.3390/land9120516>, 2020.
- 4988 Skakun, R., Castilla, G., Metsaranta, J., Whitman, E., Rodrigue, S., Little, J., Groenewegen, K., and Coyle, M.: Extending the
4989 National Burned Area Composite Time Series of Wildfires in Canada, *Remote Sensing*, 14, 3050,
4990 <https://doi.org/10.3390/rs14133050>, 2022.
- 4991 Smith, H. G., Sheridan, G. J., Lane, P. N. J., Nyman, P., and Haydon, S.: Wildfire effects on water quality in forest catchments:
4992 A review with implications for water supply, *Journal of Hydrology*, 396, 170–192, <https://doi.org/10.1016/j.jhydrol.2010.10.043>,
4993 2011.
- 4994 Smith, S., Geden, O., Nemet, G., Gidden, M., Lamb, W., Powis, C., Bellamy, R., Callaghan, M., Cowie, A., Cox, E., Fuss, S.,
4995 Gasser, T., Grassi, G., Greene, J., Lueck, S., Mohan, A., Müller-Hansen, F., Peters, G., Pratama, Y., Repke, T., Riahi, K.,
4996 Schenuit, F., Steinhäuser, J., Strefler, J., Valenzuela, J., and Minx, J.: State of Carbon Dioxide Removal - 1st Edition,
4997 <https://doi.org/10.17605/OSF.IO/W3B4Z>, 2023.
- 4998 South African Broadcasting Corporation: 2023b Wildfire scorches 1140 hectares in Simon's Town, available at:
4999 <https://www.sabcnews.com/sabcnews/wildfire-scorches-1140-hectares-in-simons-town/>, last access: 2 June 2024, 2023.
- 5000 South African Broadcasting Corporation News: 2023a Wildfires kill 34 in Algeria as heatwave sweeps north Africa - SABC News
5001 - Breaking news, special reports, world, business, sport coverage of all South African current events. Africa's news leader,
5002 available at: <https://www.sabcnews.com/sabcnews/wildfires-kill-34-in-algeria-as-heatwave-sweeps-north-africa/>, last access: 2
5003 June 2024, 2023.
- 5004 Spessa, A. C., Field, R. D., Pappenberger, F., Langner, A., Englhart, S., Weber, U., Stockdale, T., Siegert, F., Kaiser, J. W., and
5005 Moore, J.: Seasonal forecasting of fire over Kalimantan, Indonesia, *Natural Hazards and Earth System Sciences*, 15, 429–442,
5006 <https://doi.org/10.5194/nhess-15-429-2015>, 2015.
- 5007 Spuler, F. and Wessel, J.: *ibicus v1.0.1*, , <https://doi.org/10.5281/ZENODO.8101898>, 2023.
- 5008 Spuler, F. R., Wessel, J. B., Comyn-Platt, E., Varndell, J., and Cagnazzo, C.: *ibicus: a new open-source Python package and*
5009 *comprehensive interface for statistical bias adjustment and evaluation in climate modelling (v1.0.1)*, *Geoscientific Model*
5010 *Development*, 17, 1249–1269, <https://doi.org/10.5194/gmd-17-1249-2024>, 2024.
- 5011 Staver, A. C., Archibald, S., and Levin, S. A.: The Global Extent and Determinants of Savanna and Forest as Alternative Biome
5012 States, *Science*, 334, 230–232, <https://doi.org/10.1126/science.1210465>, 2011.
- 5013 Sellar, A. A., Jones, C. G., Mulcahy, J. P., Tang, Y., Yool, A., Wiltshire, A., O'Connor, F. M., Stringer, M., Hill, R., Palmieri, J.,
5014 Woodward, S., de Mora, L., Kuhlbrodt, T., Rumbold, S. T., Kelley, D. I., Ellis, R., Johnson, C. E., Walton, J., Abraham, N. L.,
5015 Andrews, M. B., Andrews, T., Archibald, A. T., Berthou, S., Burke, E., Blockley, E., Carslaw, K., Dalvi, M., Edwards, J., Folberth,
5016 G. A., Gedney, N., Griffiths, P. T., Harper, A. B., Hendry, M. A., Hewitt, A. J., Johnson, B., Jones, A., Jones, C. D., Keeble, J.,
5017 Liddicoat, S., Morgenstern, O., Parker, R. J., Predoi, V., Robertson, E., Siahann, A., Smith, R. S., Swaminathan, R., Woodhouse,



- 5018 M. T., Zeng, G., and Zerroukat, M.: UKESM1: Description and Evaluation of the U.K. Earth System Model, *Journal of Advances*
5019 *in Modeling Earth Systems*, 11, 4513–4558, <https://doi.org/10.1029/2019MS001739>, 2019.
- 5020 Stephens, S. L., McIver, J. D., Boerner, R. E. J., Fettig, C. J., Fontaine, J. B., Hartsough, B. R., Kennedy, P. L., and Schwilk, D.
5021 W.: The Effects of Forest Fuel-Reduction Treatments in the United States, *BioScience*, 62, 549–560,
5022 <https://doi.org/10.1525/bio.2012.62.6.6>, 2012.
- 5023 Stephens, S. L., Bernal, A. A., Collins, B. M., Finney, M. A., Lautenberger, C., and Saah, D.: Mass fire behavior created by
5024 extensive tree mortality and high tree density not predicted by operational fire behavior models in the southern Sierra Nevada,
5025 *Forest Ecology and Management*, 518, 120258, <https://doi.org/10.1016/j.foreco.2022.120258>, 2022.
- 5026 Stocks, B. J., Lawson, B. D., Alexander, M. E., Wagner, C. E. V., McAlpine, R. S., Lynham, T. J., and Dubé, D. E.: The Canadian
5027 Forest Fire Danger Rating System: An Overview, *The Forestry Chronicle*, 65, 450–457, <https://doi.org/10.5558/ffc65450-6>, 1989.
- 5028 Stott, P. A., Stone, D. A., and Allen, M. R.: Human contribution to the European heatwave of 2003, *Nature*, 432, 610–614,
5029 <https://doi.org/10.1038/nature03089>, 2004.
- 5030 Sullivan, H. and Tondo, L.: 'Like a blowtorch': Mediterranean on fire as blazes spread across nine countries, available at:
5031 <https://www.theguardian.com/environment/2023/jul/26/northern-hemisphere-heatwaves-mediterranean-fires-croatia-portugal>,
5032 last access: 2 June 2024, *The Guardian*, 26th July, 2023.
- 5033 Swain, D. L., Langenbrunner, B., Neelin, J. D., and Hall, A.: Increasing precipitation volatility in twenty-first-century California,
5034 *Nature Clim Change*, 8, 427–433, <https://doi.org/10.1038/s41558-018-0140-y>, 2018.
- 5035 Synolakis, C. E. and Karagiannis, G. M.: Wildfire risk management in the era of climate change, *PNAS Nexus*, 3, pqae151,
5036 <https://doi.org/10.1093/pnasnexus/pqae151>, 2024.
- 5037 Syphard, A. and Keeley, J.: Factors Associated with Structure Loss in the 2013–2018 California Wildfires, *Fire*, 2, 49,
5038 <https://doi.org/10.3390/fire2030049>, 2019.
- 5039 Tang, W., Lloret, J., Weis, J., Perron, M. M. G., Basart, S., Li, Z., Sathyendranath, S., Jackson, T., Sanz Rodriguez, E., Proemse,
5040 B. C., Bowie, A. R., Schallenberg, C., Strutton, P. G., Matear, R., and Cassar, N.: Widespread phytoplankton blooms triggered
5041 by 2019–2020 Australian wildfires, *Nature*, 597, 370–375, <https://doi.org/10.1038/s41586-021-03805-8>, 2021.
- 5042 Tang, W., He, C., Emmons, L., and Zhang, J.: Global expansion of wildland-urban interface (WUI) and WUI fires: insights from a
5043 multiyear worldwide unified database (WUWUI), *Environ. Res. Lett.*, 19, 044028, <https://doi.org/10.1088/1748-9326/ad31da>,
5044 2024.
- 5045 Tang, Y., Rumbold, S., Ellis, R., Kelley, D., Mulcahy, J., Sellar, A., Walton, J., and Jones, C.: MOHC UKESM1.0-LL model output
5046 prepared for CMIP6 CMIP, 2019.
- 5047 Tiempo: Venezuela se llena de nubes de humos por incendios forestales y una estación muy seca, available at:
5048 <https://www.tiempo.com/ram/venezuela-humos-incendios-forestales.html>, last access: 2 June 2024, *Tiempo.com | Meteored*,
5049 2024.
- 5050 Turco, M., Jerez, S., Doblas-Reyes, F. J., AghaKouchak, A., Llasat, M. C., and Provenzale, A.: Skilful forecasting of global fire
5051 activity using seasonal climate predictions, *Nat Commun*, 9, 2718, <https://doi.org/10.1038/s41467-018-05250-0>, 2018.
- 5052 UC Davis: Global Administrative Regions Data, available at: https://gadm.org/download_world.html, last access: 2 June 2024,
5053 2022.
- 5054 UN Resident Coordinator in Chile: Chile: Incendios forestales, 2024 Sistema de Naciones Unidas, Reporte de Situación No. 3 -
5055 Chile, available at: <https://reliefweb.int/report/chile/chile-incendios-forestales-2024-sistema-de-naciones-unidas-report-de-situacion-no-3>,
5056 last access: 2 June 2024, 2024.
- 5057 UNESCO World Heritage Centre: Landscapes of Dauria, available at: <https://whc.unesco.org/en/list/1448/>, last access: 2 June
5058 2024, UNESCO World Heritage Centre, 2017.



- 5059 United Nations Environment Programme: Global Peatlands Assessment: The State of the World's Peatlands, Nairobi, Kenya,
5060 2022a.
- 5061 United Nations Environment Programme: Spreading like Wildfire – The Rising Threat of Extraordinary Landscape Fires. A UNEP
5062 Rapid Response Assessment, available at: [https://www.unep.org/resources/report/spreading-wildfire-rising-threat-extraordinary-](https://www.unep.org/resources/report/spreading-wildfire-rising-threat-extraordinary-landscape-fires)
5063 [landscape-fires](https://www.unep.org/resources/report/spreading-wildfire-rising-threat-extraordinary-landscape-fires), last access: 2 June 2024, Nairobi, Kenya, 2022b.
- 5064 United Nations Population Division: World Population Prospects 2022, available at: <https://population.un.org/wpp/>, last access: 2
5065 June 2024, 2022.
- 5066 Van Wagner, C. E.: Development and structure of the Canadian Forest Fire Weather Index System, Forestry Technical Report
5067 35, Canadian Forestry Service, Ottawa, 1987.
- 5068 Van Wagtenonk, J. W.: Fire as a Physical Process, in: Fire in California's Ecosystems, edited by: Sugihara, N., University of
5069 California Press, 38–57, <https://doi.org/10.1525/california/9780520246058.003.0003>, 2006.
- 5070 Wang, D., Guan, D., Zhu, S., Kinnon, M. M., Geng, G., Zhang, Q., Zheng, H., Lei, T., Shao, S., Gong, P., and Davis, S. J.:
5071 Economic footprint of California wildfires in 2018, *Nat Sustain*, 4, 252–260, <https://doi.org/10.1038/s41893-020-00646-7>, 2021.
- 5072 Wang, Y., Chen, H.-H., Tang, R., He, D., Lee, Z., Xue, H., Wells, M., Boss, E., and Chai, F.: Australian fire nourishes ocean
5073 phytoplankton bloom, *Science of The Total Environment*, 807, 150775, <https://doi.org/10.1016/j.scitotenv.2021.150775>, 2022.
- 5074 Wang, Z., Wang, Z., Zou, Z., Chen, X., Wu, H., Wang, W., Su, H., Li, F., Xu, W., Liu, Z., and Zhu, J.: Severe Global Environmental
5075 Issues Caused by Canada's Record-Breaking Wildfires in 2023, *Adv. Atmos. Sci.*, 41, 565–571, [https://doi.org/10.1007/s00376-](https://doi.org/10.1007/s00376-023-3241-0)
5076 [023-3241-0](https://doi.org/10.1007/s00376-023-3241-0), 2024.
- 5077 Ward, M., Tulloch, A. I. T., Radford, J. Q., Williams, B. A., Reside, A. E., Macdonald, S. L., Mayfield, H. J., Maron, M., Possingham,
5078 H. P., Vine, S. J., O'Connor, J. L., Massingham, E. J., Greenville, A. C., Woinarski, J. C. Z., Garnett, S. T., Lintermans, M.,
5079 Scheele, B. C., Carwardine, J., Nimmo, D. G., Lindenmayer, D. B., Kooyman, R. M., Simmonds, J. S., Sonter, L. J., and Watson,
5080 J. E. M.: Impact of 2019–2020 mega-fires on Australian fauna habitat, *Nat Ecol Evol*, 4, 1321–1326,
5081 <https://doi.org/10.1038/s41559-020-1251-1>, 2020.
- 5082 van der Werf, G. R., Randerson, J. T., Giglio, L., Collatz, G. J., Kasibhatla, P. S., and Arellano, A. F.: Interannual variability in
5083 global biomass burning emissions from 1997 to 2004, *Atmos. Chem. Phys.*, 6, 3423–3441, [https://doi.org/10.5194/acp-6-3423-](https://doi.org/10.5194/acp-6-3423-2006)
5084 [2006](https://doi.org/10.5194/acp-6-3423-2006), 2006.
- 5085 van der Werf, G. R., Randerson, J. T., Giglio, L., van Leeuwen, T. T., Chen, Y., Rogers, B. M., Mu, M., van Marle, M. J. E.,
5086 Morton, D. C., Collatz, G. J., Yokelson, R. J., and Kasibhatla, P. S.: Global fire emissions estimates during 1997–2016, *Earth*
5087 *Syst. Sci. Data*, 9, 697–720, <https://doi.org/10.5194/essd-9-697-2017>, 2017.
- 5088 Wetterhall, F. and Di Giuseppe, F.: The benefit of seamless forecasts for hydrological predictions over Europe, *Hydrology and*
5089 *Earth System Sciences*, 22, 3409–3420, <https://doi.org/10.5194/hess-22-3409-2018>, 2018.
- 5090 Wigneron, J.-P., Li, X., Frappart, F., Fan, L., Al-Yaari, A., De Lannoy, G., Liu, X., Wang, M., Le Masson, E., and Moisy, C.: SMOS-
5091 IC data record of soil moisture and L-VOD: Historical development, applications and perspectives, *Remote Sensing of*
5092 *Environment*, 254, 112238, <https://doi.org/10.1016/j.rse.2020.112238>, 2021.
- 5093 Wittwer, G. and Waschik, R.: Estimating the economic impacts of the 2017–2019 drought and 2019–2020 bushfires on regional
5094 NSW and the rest of Australia, *Aus J Agri & Res Econ*, 65, 918–936, <https://doi.org/10.1111/1467-8489.12441>, 2021.
- 5095 World Bank: World Bank Policy Note: Managing Wildfires in a Changing Climate, Washington DC, 2020.
- 5096 World Bank: Financially Prepared: The Case for Pre-positioned Finance in European Union Member States and Countries under
5097 EU Civil Protection Mechanism, Washington DC, 2024.
- 5098 World Weather Attribution: Extreme humid heat in South Asia in April 2023, largely driven by climate change, detrimental to
5099 vulnerable and disadvantaged communities – World Weather Attribution, available at:



- 5100 [https://www.worldweatherattribution.org/extreme-humid-heat-in-south-asia-in-april-2023-largely-driven-by-climate-change-](https://www.worldweatherattribution.org/extreme-humid-heat-in-south-asia-in-april-2023-largely-driven-by-climate-change-detrimental-to-vulnerable-and-disadvantaged-communities/)
5101 [detrimental-to-vulnerable-and-disadvantaged-communities/](https://www.worldweatherattribution.org/extreme-humid-heat-in-south-asia-in-april-2023-largely-driven-by-climate-change-detrimental-to-vulnerable-and-disadvantaged-communities/), last access: 2 June 2024, 2023.
- 5102 World Weather Attribution: Climate change, not El Niño, main driver of exceptional drought in highly vulnerable Amazon River
5103 Basin – World Weather Attribution, available at: [https://www.worldweatherattribution.org/climate-change-not-el-nino-main-driver-](https://www.worldweatherattribution.org/climate-change-not-el-nino-main-driver-of-exceptional-drought-in-highly-vulnerable-amazon-river-basin/)
5104 [of-exceptional-drought-in-highly-vulnerable-amazon-river-basin/](https://www.worldweatherattribution.org/climate-change-not-el-nino-main-driver-of-exceptional-drought-in-highly-vulnerable-amazon-river-basin/), last access: 2 June 2024, 2024.
- 5105 Xanthopoulos, G., Zevgoli, E., Kaoukis, K., and Athanasiou, M.: Greece - Lessons not learned, available at:
5106 https://issuu.com/wildfiremagazine-iafw/docs/wildfire_magazine_q4_2023_-_web, last access: 2 June 2024, Wildfire, 2023,
5107 2024.
- 5108 Yebra, M., Dennison, P. E., Chuvieco, E., Riaño, D., Zylstra, P., Hunt, E. R., Danson, F. M., Qi, Y., and Jurdao, S.: A global
5109 review of remote sensing of live fuel moisture content for fire danger assessment: Moving towards operational products, *Remote*
5110 *Sensing of Environment*, 136, 455–468, <https://doi.org/10.1016/j.rse.2013.05.029>, 2013.
- 5111 Yebra, M., Quan, X., Riaño, D., Rozas Larraondo, P., van Dijk, A. I. J. M., and Cary, G. J.: A fuel moisture content and flammability
5112 monitoring methodology for continental Australia based on optical remote sensing, *Remote Sensing of Environment*, 212, 260–
5113 272, <https://doi.org/10.1016/j.rse.2018.04.053>, 2018.
- 5114 Yin, H., Khamzina, A., Pflugmacher, D., and Martius, C.: Forest cover mapping in post-Soviet Central Asia using multi-resolution
5115 remote sensing imagery, *Sci Rep*, 7, 1375, <https://doi.org/10.1038/s41598-017-01582-x>, 2017.
- 5116 Yu, M., Zhang, S., Ning, H., Li, Z., and Zhang, K.: Assessing the 2023 Canadian wildfire smoke impact in Northeastern US: Air
5117 quality, exposure and environmental justice, *Science of The Total Environment*, 926, 171853,
5118 <https://doi.org/10.1016/j.scitotenv.2024.171853>, 2024.
- 5119 Yukimoto, S., Kawai, H., Koshiro, T., Oshima, N., Yoshida, K., Urakawa, S., Tsujino, H., Deushi, M., Tanaka, T., Hosaka, M.,
5120 Yabu, S., Yoshimura, H., Shindo, E., Mizuta, R., Obata, A., Adachi, Y., and Ishii, M.: The Meteorological Research Institute Earth
5121 System Model Version 2.0, MRI-ESM2.0: Description and Basic Evaluation of the Physical Component, *Journal of the*
5122 *Meteorological Society of Japan. Ser. II*, 97, 931–965, <https://doi.org/10.2151/jmsj.2019-051>, 2019.
- 5123 Zachariah, M., Vautard, R., Chandrasekaran, R., Chaithra, S., Kimutai, J., Arulalan, T., AchutaRao, K., Barnes, C., Singh, R.,
5124 Vahlberg, M., Arrgihi, J., Raju, E., Sharma, U., Ogra, A., Vaddhanaphuti, C., Bahinipati, C., Tschakert, P., Pereira Marghidan, C.,
5125 Mondal, A., Schwingshackl, C., Philip, S., and Otto, F.: Extreme humid heat in South Asia in April 2023, largely driven by climate
5126 change, detrimental to vulnerable and disadvantaged communities, Imperial College London, <https://doi.org/10.25561/104092>,
5127 2023.
- 5128 Zheng, B., Ciais, P., Chevallier, F., Chuvieco, E., Chen, Y., and Yang, H.: Increasing forest fire emissions despite the decline in
5129 global burned area, *Science Advances*, 7, eabh2646, <https://doi.org/10.1126/sciadv.abh2646>, 2021.
- 5130 Zheng, B., Ciais, P., Chevallier, F., Yang, H., Canadell, J. G., Chen, Y., Van Der Velde, I. R., Aben, I., Chuvieco, E., Davis, S. J.,
5131 Deeter, M., Hong, C., Kong, Y., Li, H., Li, H., Lin, X., He, K., and Zhang, Q.: Record-high CO₂ emissions from boreal fires in
5132 2021, *Science*, 379, 912–917, <https://doi.org/10.1126/science.ade0805>, 2023.
5133
5134